Imaging right ventricular function to predict outcome in patients treated for pulmonary hypertension

A thesis by

Melanie J Brewis. MBChB, BSc, MRCP

Submitted for the Degree of Doctor of Medicine, University of Glasgow, 2017

Acknowledgement

I would like to thank my supervisor Professor Andrew Peacock for his advice and guidance throughout my period of research and I will always be grateful for the opportunity to work as part of the team at the Scottish Pulmonary Vascular Unit. I would also like to thank my co-supervisor Dr David Welsh for his assistance in writing of this thesis, and Dr Martin Johnson for his advice and support throughout my research.

I am extremely grateful to my colleagues at the Scottish pulmonary vascular unit, Dr Stephen Crawley, Dr Stephen Thomson, Dr Lauren Brash, Dr Colin Church and Dr Neil McGlinchey for both their friendship and assistance with clinical and research work. In addition I would like to thank the team at the cardiac MRI department at the Golden Jubilee hospital and Drs Rebecca Vanderpool and Alessandro Bellofiore from the Department of Biomedical Engineering at Universities of Pittsburgh and San Jose State, without whom this work would not have been possible.

Finally, and most importantly I would like to thank the patients studied in this thesis.

Author's Declaration

The experimental design of the works carried out in this thesis was that of myself and my Supervisor Professor Andrew Peacock. The work reported in this thesis was carried out by myself, with the assistance of several colleagues acknowledged above. All of the data interpretation and statistical analyses herein were performed by me and this manuscript was written solely by me.

Much of this work has been published or submitted to journals for consideration of publication. A list of these papers and other published abstracts relating to this work has been included. This work has not previously been submitted for consideration of a higher degree.

Signed…….

Dr Melanie J Brewis

January 2017

Table of Contents

List of Tables

Chapter 3.

List of Figures

Chapter 1

Chapter 2.

Chapter 3.

List of Abbreviations

ADMA	Asymmetric DiMethylArginine
AoSV	Aortic Stroke Volume
BMPR2	Bone Morphogenetic Protein Receptor type II
BNP	Brain Natriuretic Peptide
BSA	Body Surface Area
CCB	Calcium Channel Blocker
CI	Cardiac Index
cGMP	cyclic Guanosine MonoPhosphate
CHD	Congenital Heart Disease
CMR	Cardiovascular Magnetic Resonance
CO	Cardiac Output
COPD	Chronic Obstructive Pulmonary Disease
CPET	Cardiopulmonary Exercise Testing
CPFE	Combined Pulmonary Fibrosis Emphysema Syndrome
CT	Computed Tomography
CTD	Connective Tissue Disease
CTDPH	Connective Tissue Disease associated Pulmonary arterial Hypertension
CTEPH	Chronic Thromboembolic Pulmonary Hypertension
CXR	Chest Radiograph
DCE	Delayed Contrast Enhancement
DLCO	Diffusion Capacity for Carbon Monoxide
E_a	Effective Arterial Elastance
ECG	Electrocardiogram
ED	End-Diastole
EDV	End-Diastolic Volume
EDVI	End-Diastolic Volume Index
E_{es}	End Systolic Elastance
E_{es}/E_a-P	RV-arterial coupling determined by pressure method
EF	Ejection Fraction
E_{max}	Maximal Ventricular Elastance
eNOS	Endothelial Nitric Oxide Synthase
ETRA	Endothelin Receptor Antagonist
ES	End-Systole
ESP	End Systolic Pressure
ESPVR	End Systolic Pressure Volume Relation
ESV	End-Systolic Volume
ESVI	End-Systolic Volume Index
ET-1	Endothelin-1
FC	Functional Class
FEV1	Forced Expiratory Flow in 1 second
FoV	Field of view
FPAH	Familial/heritable Pulmonary Arterial Hypertension
FVC	Forced Vital Capacity
HLA	Horizontal Long Axis
HPV	Hypoxic Pulmonary Vasoconstriction
ILD	Interstitial Lung Disease
IPAH	Idiopathic Pulmonary Arterial Hypertension
IPF	Idiopathic Pulmonary Fibrosis
IVC	Inferior vena cava

IVS	Interventricular Septum
KM	Kaplan Meier
LTOT	Long Term Oxygen Therapy
LV	Left Ventricle/Ventricular
LVEDV	Left Ventricular End-Diastolic Volume
LVEDVI	Left Ventricular End-Diastolic Volume Index
LVEF	Left Ventricular Ejection Fraction
LVESV	Left Ventricular End-Systolic Volume
LVESVI	Left Ventricular End-Systolic Volume Index
LVH	Left Ventricular Hypertrophy
LVM	Left Ventricular Mass
LVSB	Left Ventricular Septal Bowing
MESA	Multi Ethnic Study of Atherosclerosis
mPAP	Mean Pulmonary Artery Pressure
MRI	Magnetic Resonance Imaging
NO	Nitric Oxide
NTproBNP	N terminal pro B-type Natriuretic Peptide
NYHA	New York Heart Association
P_A	Alveolar Pressure
$Pa0_2$	Partial pressure arterial Oxygen
$PA0_2$	Partial pressure Alveolar Oxygen
PaSV	Pulmonary Artery Stroke Volume
PAH	Pulmonary Arterial Hypertension
PAP	Pulmonary Artery Pressure
PASMCs	Pulmonary Artery Smooth Muscle Cells
PAWP	Pulmonary Artery Wedge Pressure
PDE-5i	Phosphodiesterase V Inhibitor
PDGF	Platelet Derived Growth Factor
PFR_A	Active Peak Filling Rate
PFR_E	Early Peak Filling Rate
PGI2	Prostacyclin
PH	Pulmonary Hypertension
P_{max}	Maximal Pressure point
POPH	Portopulmonary Hypertension
PVH	Pulmonary Venous Hypertension
PVP	Pulmonary Venous Pressure
PVR	Pulmonary Vascular Resistance
PVZ	Pulmonary Artery Impedence
RAC MPA	Relative Area Change of Main Pulmonary Artery
RAP	Right Atrial Pressure
REVEAL	Registry to EValuate EArly and Longterm PAH disease management
RF	Radiofrequency
RHC	Right Heart Catheterisation
RV	Right Ventricle/Ventricular
RVEDD	Right Ventricular End Diastolic Diameter
RVEDV	Right Ventricular End-Diastolic Volume
RVEDVI	Right Ventricular End-Diastolic Volume Index
RVEF	Right Ventricular Ejection Fraction
RVESV	Right Ventricular End-Systolic Volume
RVESVI	Right Ventricular End-Systolic Volume Index
RVH	Right Ventricular Hypertrophy
RVM	Right Ventricular Mass
RVMI	Right Ventricular Mass Index

RVSD	Right Ventricular Systolic Dysfunction
RVSP	Right Ventricular Systolic Pressure
RVSV	Right Ventricular Stroke Volume
RVSVI	Right Ventricular Stroke Volume Index
SA	Short Axis
sGC	soluable Guanylate Cyclase
SLE	Systemic Lupus Erythematosus
SMCs	Smooth Muscle Cells
sPAP	Systolic Pulmonary Artery Pressure
SSc	Systemic Sclerosis
SScPAH	Systemic Sclerosis associated Pulmonary Arterial Hypertension
SSFP	Steady State Free Precession
SV	Stroke Volume
SVI	Stroke Volume Index
SVO2	Mixed Venous Oxygen Saturations
SV/PP	Compliance
T	Tesla
TAPSE	Tricuspid Annular Plane Systolic Excursion
TE	Echo time
TLC	Total Lung Capacity
TR	Repetition time
TRPG	Tricuspid Regurgitant Pressure Gradient
V_0	Volume intercept of ESPVR
VMI	Ventricular Mass Index
VQ	Ventilation Perfusion
WSPH	World Symposium on Pulmonary Hypertension
6MWT	Six Minute Walk Test
6MWD	Six Minute Walk Distance

Publications related to this thesis

Brewis MJ, Church AC, Johnson MK & Peacock AJ. Severe pulmonary hypertension in lung disease; phenotypes and response to treatment. Eur Resp J 2015; 46(5):1378-1389

Brewis MJ, Bellofiore A, Vanderpool R, Chesler N, Johnson MK, Naeije R & Peacock AJ. Imaging right ventricular function to predict outcome in pulmonary arterial hypertension. Int J Cardiol 2016;218: 206-211. *Published online first DOI* 10.1016/j.ijcard.2016.05.015

Abstracts:

Brewis MJ, Church AC, Peacock AJ & Johnson MK. ΔNTproBNP predicts survival and more accurately reflects changing right ventricular structure and function than 6MWD in pulmonary hypertension. Thorax 2014 (suppl2); 69: A146. DOI 10.1136/thoraxjnl-2014-206260.292

Brewis MJ, Naeije R, Bellofiore A, Chesler N & Peacock AJ. Cardiac MRI derived right ventriculo-arterial coupling in pulmonary hypertension as a predictor of survival. Eur Resp J 2014; 44: Suppl 58, P2300

Brewis MJ, Church AC, Peacock MJ & Johnson MK. Severe pulmonary hypertension in patients with emphysema but preserved FEV1: prognosis and response to treatment. Eur Resp J 2013; 42: Suppl 57. P2620

Brewis MJ, Johnson MK & Peacock AJ Indices of right ventricular structure and function assessed by cardiac MRI improves the accuracy of noninvasive detection of "Out of Proportion" pulmonary arterial hypertension in patients with hypoxic lung disease" ARJCCM 2013; 187: A2560.

Summary

Pulmonary arterial hypertension (PAH) is a rare but devastating disorder of the pulmonary vasculature characterised pathologically by progressive intimal obliteration and vascular remodelling leading to increased pulmonary vascular resistance (PVR) and elevation in pulmonary arterial pressure (PAP), and clinically by functional impairment from breathlessness and ultimately death from right ventricular failure. Whilst the initial insult occurs in the pulmonary circulation, it is increasing recognised that survival relates to the ability of the right ventricle (RV) to adapt to this increased afterload. Despite a number of therapeutic advances in recent years, long-term survival remains poor, quality of life impaired by functional limitation and progression to RV failure often inevitable.

In contrast, pulmonary hypertension (PH) related to chronic lung disease is relatively common, but is usually mild in severity with largely preserved RV function. The development of PH is however associated with greater functional impairment and worse survival and at present other than referral for lung transplantation there are no therapeutic options. Severe PH associated with lung disease is relatively rare, but shares many of the characteristics with PAH with more severe RV dysfunction and significant morbidity and mortality. It is also increasingly recognised in data from large PH registries, that increasing overlap exists between the two conditions, and what represents PAH with co-morbid lung disease (and therefore should receive specific PAH therapies) and what is PH secondary to lung disease (and therefore should not) increasingly muddied.

What is clear is the critical role the RV plays in determining outcome in PH, but despite this studies on the impact of current therapies on RV function are few, and improvement or preservation of RV function is not an accepted clinical endpoint in pharmaceutical trials. Current methods of monitoring patient response to therapies are suboptimal, such as the established and commonly employed six minute walk distance (6MWD). The complex anatomy of the RV makes assessment of its function by modalities such as echocardiogram difficult. The development of simple, reproducible measures of RV function will both improve monitoring of PH patients but also facilitate acceptance of routine assessment of RV function in both clinical practice and pharmaceutical trials, and hopefully establish the optimal approach to RV dysfunction in PAH. Cardiac

magnetic resonance imaging (CMR) is particularly suited to interrogating RV function, and has recently been established in the literature to provide prognostic significance in a number of disease states including PAH. At present, however, it is unclear what the optimal method of assessing RV function is, with a number of indices assessed by varying modalities associated with prognosis and therapeutic response in PAH. Recently research interest has developed in the potential utility of RV-arterial coupling in PH. From physiological principles, this metric of RV function has potential superiority over commonly employed indices such as RVEF or right atrial pressure (RAP) as it is less preload dependent. Its clinical use however is limited due to the need for instantaneous pressure-volume loops at varying levels of load in its derivation. It is however possible to estimate non-invasively by CMR. The aim of the work described by this thesis was to provide clarity on the optimal method of determining and monitoring RV dysfunction in PAH patients, and contrast this to patients with severe PH associated with lung disease treated with PAH therapies, where the aetiology of PH differs and utility of CMR to characterise RV function has not been explored.

In chapter 3 PAH therapies given to severe PH/lung disease patients resulted in improvements in 6MWD (average Δ6MWD 24m, p=0.032), and NTproBNP (average ΔNTproBNP -396pg/mL, p=0.008), but to a lesser extent than IPAH patients. CMR imaging demonstrated that RV dysfunction (assessed by RV ejection fraction (RVEF), stroke volume (SV) and increased RV volumes) was prevalent, predicted prognosis in both conditions, and could be used to detect PH in lung disease by either measures of pulmonary vascular stiffness (relative area change of main pulmonary artery – RAC MPA) or RV mass (RVM).

In Chapter 4, invasive pressure (Ees/Ea-P) and non-invasive volume (SV/ESV) estimates of RV-arterial coupling (determined by right heart catheterisation and CMR) were compared to other metrics of RV function in normal subjects, PAH and PH associated with lung disease patients as prognostic variables. Severe PH/lung disease patients displayed impaired RV adaptation in comparison to IPAH subjects, Ees/Ea-P 1.07 versus 1.37mmHg/mL, p=0.020. RV-arterial coupling estimated by the pressure method did not predict survival, but when estimated by the volume method (SV/ESV) did. Both RVEF and SV/ESV were independent predictors of outcome (HR 0.958, p=0.006 and HR 0.329, p=0.002 respectively). Invasive

measures of RV function therefore provided no prognostic advantage over the more patient acceptable CMR.

Finally in chapter 5, improvement in RV-arterial coupling assessed by CMR (SV/ESV) was seen after commencing PAH therapy (0.461 to 0.616, p=0.036). Survival was poorer in those with a fall in either RVEF or SV/ESV during therapy, with no superiority of either method of determining prognosis (Logrank p=0.002 for both). Change in RV function poorly related to change in 6MWD but closely related to change in NTproBNP. ΔNTproBNP but not Δ6MWD was an independent predictor of survival (HR 1.622 p=0.024 and HR 0.995 p=0.129 respectively) and therefore a useful monitoring tool of RV function and therapy response for the clinic.

The results described in this thesis therefore suggest that RV function to predict outcome in patients with PH during treatment follow up is best determined by CMR imaging of RVEF or SV/ESV, with no clear benefit of re-evaluating invasive haemodynamics or pressure estimates of RV-arterial coupling.

Chapter 1 – Introduction

The term Pulmonary Hypertension describes a group of diseases characterised by an elevation in Pulmonary artery pressure (PAP) and Pulmonary vascular resistance (PVR). Clinically, patients develop symptoms of breathlessness, peripheral oedema and exertional syncope with evidence of right ventricular (RV) dysfunction and ultimately die as a result of RV failure. In recent years development of a number of disease specific therapies has led to improvements in morbidity and survival. Despite this, PAH remains a devastating disease with progressive functional limitation, high symptom burden and mortality. Until relatively recently the RV had been less studied than other aspects of PAH, and relatively poorer understanding of the mechanisms of RV failure, prognostic implications of specific changes in RV structure and function or the effects of PAH specific therapy on the RV exists. Furthermore, how best to assess or monitor RV function is unclear with a number of invasive parameters, such as RAP, imaging modalities such as echocardiography or cardiac MRI or biomarkers currently linked to prognosis.

1.1 Structure and function of the normal right heart and pulmonary vasculature

1.1.1 Pulmonary Circulation

The pulmonary circulation is a highly compliant, high flow low pressure system which favours pulmonary gas exchange (1). The low pressures prevent fluid moving out in to the interstitial space and allow the right ventricle to perform at low energy cost. The pulmonary circulation is characterised by an inflow pressure, the pulmonary artery pressure, an outflow pressure, left atrial pressure and pulmonary blood flow which is approximately equal to systemic cardiac output (CO). Mean pulmonary artery pressure (mPAP) is flow dependent and in normal subjects increases by 1mmHg for every 1mmHg increase in Left atrial pressure (LAP). LAP is approximated by wedged pulmonary artery pressure (PAWP) to allow estimation of pulmonary vascular resistance. The normal distribution of vascular resistances is 60% arterial and 40% capillary plus venous resistance (2). In health, the pulmonary arteries exhibit low basal smooth muscle tone and the PVR is only around 1/20 of systemic vascular resistance (3).

The pulsatility of the pulmonary circulation is more significant than that of the systemic circulation, which effects the energy transmission from the right ventricle to pulmonary arteries. Pulmonary arterial pulse pressure, the difference between systolic and diastolic pressures, is in the order of mPAP (in comparison to the systemic circulation where it is less than half the mean), and flow varies across the cardiac cycle from a maximum at mid systole to virtually zero in diastole (1). The distensibility of pulmonary resistive vessels has been shown to approximate to 2% of diameter change per mmHg of distending pressure over a range of species (4). This distensibility coefficient has been shown to decrease with ageing, chronic hypoxic and probably displays gender differences (5-7). The distal arteries and arterioles hold most of the capacitance properties of the pulmonary circulation, with the proximal lung vessels accounting for as little as 20% of total vascular compliance (8). At lower mean pressures the compliance and pulsatile components of the pulmonary circulation constitute a larger fraction of the total afterload of the right ventricle, with some suggesting the pulsatile load may account for between one third and up to 50% of the total (9, 10). The study of the pulmonary arterial circulation as a steady flow system is therefore an oversimplification.

Tight correlation exists between systolic, diastolic and mean pulmonary artery pressure which persists in diseases of the pulmonary vasculature (11). Clinically this is of relevance as it allows the estimation of mPAP from systolic PAP (sPAP) using the formula mPAP = 0.6 x sPAP + 2 (12). sPAP may be calculated using the Bernouilli equation from the tricuspid regurgitant pressure gradient (TRPG) which can be determined non-invasively by echocardiogram (13). The product of PVR by pulmonary artery compliance (SV/PP) remains constant at 0.7 in both health and disease of the pulmonary vasculature which explains this tight relationship (14, 15). The exception to this is proximal pulmonary artery obstruction which may occur in diseases such as proximal chronic thromboembolic pulmonary hypertension (16) or experimentally with pulmonary banding models of pulmonary hypertension (17). This hyperbolic relationship explains why right ventricular afterload may already be markedly increased despite minimal rise in calculated PVR in early pulmonary vascular disease.

The normal value for mPAP derived from a study of 55 healthy young adults is around 13mmHg (range 6-16 mmHg) (18-21). Ageing is associated with an increase

in PVR which is more marked on exercise than at rest and probably relates to an increase in arterial stiffness. The exact limits of normal pulmonary pressure as they relate to age is unknown due to the small number of measurements in older healthy individuals. The slight increase in mPAP but more significant decrease in CO has been shown to lead to a doubling of PVR over five decades of age (22, 23). A more recent review showed a small change in mPAP with age, from 12.8± 3.1 mmHg in healthy subjects <30 years compared to 14.7 ± 4.0 mmHg in those ≥50 (24). Sex has been shown not to influence pulmonary haemodynamics after correction for body dimension.(1, 24)

Pulmonary blood flow increases in an approximate linear fashion from non-dependent to dependent areas of the lung. The vertical height of an average human lung is approximately 30 cm, the difference in pressure of a corresponding vertical column of blood is 23 mmHg which is considerable in the context of the mean pressure of the pulmonary circulation (i.e. 6-16 mmHg quoted earlier) (25). Gravity dependent influences on arterial, venous and alveolar pressures result in the inequality of perfusion distributed from top to bottom of the upright lung reported by West to describe three zones of blood flow in the human lung (25). In zone 1 at the top of the lung, alveolar pressure (P_A) exceeds both venous (PVP) and arterial pressures (PAP). In this zone pulmonary blood flow may occur only in systole or perhaps not at all with resultant poor gas exchange. The extent of zone 1 may extend in conditions of low flow or increased alveolar pressure, such as occurs with mechanical ventilation with positive end expiratory pressures. In zone 2, the midzone of the lung, arterial pressure exceeds alveolar pressure, which in turn is greater than venous pressure (PAP> P_A>PVP). Under these conditions driving pressure for flow is the gradient between PAP and P_A. In zone 3 at the bottom of the lung, PVP exceeds P_A so the driving pressure for pulmonary blood flow is the PAP-PVP gradient. In the supine lung, the lung is almost completely in zone 3, although there is still measurable increase in blood flow from non-dependent to dependent areas.

Active regulatory mechanisms are able to some extent to influence the passive gravity dependent distribution of pulmonary blood flow. Hypoxic pulmonary vasoconstriction (HPV) was first reported by von Euler and Liljestrand (26). The response is found in mammals and birds but with significant inter species and individual variability. The systemic and pulmonary circulations are polar opposites

in their response to hypoxia. In the systemic circulation vasodilation occurs in an attempt to improve tissue oxygenation. In the pulmonary circulation, a decrease in $PA0_2$ causes an increase in vascular tone, resulting in vasoconstriction and diversion of pulmonary blood flow away from underventilated alveoli, to preferentially perfuse well ventilated areas of the lung in an attempt to maintain ventilation-perfusion (VQ) matching and therefore oxygenation of arterial blood. HPV increase in PVR is mainly effected by pre-capillary arterioles although small pulmonary veins also undergo vasoconstriction and contribute to approximately 20-30% of the increase in PVR (27, 28). HPV is enhanced by factors including acidosis, reduced mixed venous $Pa0_2$, repeated hypoxic exposure and decreased lung segment size, and inhibited by alkalosis, hypercapnia, pulmonary vascular and alveolar pressures, nitric oxide and vasodilating prostaglandins and drugs including calcium channel blockers (29). The response is biphasic with vasoconstriction followed by vasodilation in more profound hypoxia. The mechanism of sensing the low $PA0_2$ is not yet identified. It is thought that a decrease in $PA0_2$ inhibits smooth muscle cell voltage gated potassium channels leading to membrane depolarisation, calcium influx and resultant cell shortening (30). In the presence of continued alveolar hypoxia or widespread VQ mismatch, HPV may lead to group 3 PH (secondary to chronic lung disease) or high altitude PH.

In addition to HPV regulation, pulmonary vascular tone is attenuated by mediators including endothelium derived vasodilators nitric oxide and prostacyclin and the vasoconstrictor endothelin. These mediators have been the focus of development of potential therapies for PH. Several other circulating mediators including serotonin, histamine and angiotensin II have been shown to affect vascular tone. Finally, the pulmonary circulation is highly innervated by adrenergic, cholinergic and non-adrenergic non-cholinergic (NANC) nerve endings. However the role played in the regulation of pulmonary circulation appears minor. The innervation is mainly proximal which may suggest a role in proximal vascular compliance (31).

1.1.2 The right ventricle

Until relatively recently the importance of right ventricular function was poorly appreciated. Galen described the right ventricle (RV) as a passive conduit through which part of the circulating volume of blood passes to the lungs for nourishment with the remainder thought to seep through invisible pores in the interventricular septum for the formation of vital spirit (32). In the 13th century Ibn Nafis disputed the existence of these septal pores, instead for the first time suggesting that blood must pass through the lungs from the RV to the LV. 300 years later Michael Severtus came to the same conclusion in his theological treatise Christianismi Restitutio. William Harvey in 1628 has often been accredited with the origins of the role that the RV plays in the pulmonary circulation (33-35). Harvey was the first to develop an experimentally based model of the circulation based on detailed measurements and calculations that allowed him to conclude that the blood recirculated rather than previous speculations of Galen that blood was produced in the liver and consumed by the tissues and organs (3). Even in the 1940s the idea that a functioning RV was not essential to maintain pulmonary circulation was accepted after several studies in dogs showed that cauterisation of the RV did not lead to changes in systemic venous or pulmonary arterial pressures (36, 37). These studies were in open pericardial models and therefore did not explore the influence of ventricular interaction. Studies using RV models between 1950-1980 demonstrated that the RV was necessary for maintenance of pulmonary blood flow (38, 39). However these studies did not achieve widespread acceptance as the models used were met with criticism (35). In 1982 in an animal model with intact pericardium it was demonstrated that RV infarction lead to drop in cardiac output suggesting the importance of RV function (40). Since then the importance of the role the RV plays in both exercising healthy individuals and in many disease states has become well recognised (41-43).

The RV and outflow tracts develop embryologically from the anterior heart field while the remaining chambers of the heart arise from the primary heart field with resultant differences in genetic makeup and cellular physiology (44). The RV is the dominant chamber in the foetus, with equable wall thickness and force generated by RV and the LV in early life. During the first year of life the RV involutes and increases its compliance. The muscle mass of the RV is approximately 1/6 of the LV and under normal loading conditions a 5 mmHg pressure gradient across the

pulmonary circulation is sufficient to maintain cardiac output and therefore minimal RV contractile function is normally required with 1/4th the stroke work of the LV (34). The RV is a thin walled crescent shaped chamber, normally less than 1-3 mm in thickness whose volume is slightly greater than that of the LV. The RV may be divided into an inflow tract, the sinus (body) region with a trabeculated muscular apex and a smooth walled conus or outflow tract. The RV free wall constitutes the anterior border of the RV, lying anterior to the LV and interventricular septum (IVS). Under normal loading conditions, the IVS is concave towards the RV in both systole and diastole. Short axis cross sections through the RV from apex to base vary from a triangular contour at the apex to a crescentric appearance at the base which explains the difficulty with using 2D imaging techniques to interrogate RV size and function in this complex geometric shape. The sinus contains in excess of 80% of total RV volume with different fibre orientation compared to the conus. In addition, timing of contraction differs between the compartments. Contraction occurs sequentially from the apex towards the conus in a peristaltic fashion using predominantly longitudinal fibres in a bellows type movement suited to the low impedence pulmonary circulation (45, 46). In contrast, the longitudinal and circumferential muscle fibres of the LV allow for a more cylindrical contraction. As a result of the larger RV chamber size, under normal conditions, RVEF is lower than LVEF, quoted between 40-76% dependent on imaging modality used (47-49).

The RV largely receives its blood supply from the right coronary artery in approximately 80% of the population. The lateral wall is supplied by the marginal branches with the posterior wall and inferoseptal region supplied by the posterior descending artery. The anterior wall and anteroseptal region are supplied by branches of the left anterior descending artery. Unlike the LV, where myocardial perfusion is largely limited to diastole, the RV intramyocardial pressure remains below aortic root pressure throughout the cardiac cycle and therefore continuous coronary flow occurs (50). The RV displays relative resistance to irreversible ischaemia in comparison to the LV, probably as a consequence of its lower oxygen consumption, more extensive collateral blood supply and ability to increase oxygen extraction.

Both ventricles are encircled by spiralling muscle bundles in a complex interlacing fashion forming a functionally single unit. Ventricular interaction occurs not only

as a series indirect interaction but also directly as a result of the shared IVS, continuity between the muscle fibres and shared pericardium (51). During systole, LV contraction influences pressure development in the RV. Pericardial constraint means that the compliance of each ventricle is influenced by the volume and pressure of the other. Animal models have demonstrated that 20-40% of RV systolic pressure and volume ejected is a result of LV contraction. Models of impaired RV function with scarring of the RV have demonstrated that the septum is able to maintain pulmonary circulation provided that RV dilatation does not occur. Ventricular interaction becomes of significance in disease states such as pulmonary hypertension where LV diastolic filling is impaired by both series effect and the direct effect of leftward septal bowing as a result of RV pressure and volume overload (52).

Right ventricular function is determined by preload, a measure of RV filling, afterload and contractility. Under normal filling conditions, an increase in preload results in increased contractility and cardiac output (53). In addition to chamber compliance, heart rate and the afore mentioned LV filling and pericardial factors, RV filling is influenced by negative pressure of respiration to a greater degree than the LV because of its thin free wall and connection to systemic veins (21). The RV has a limited ability to compensate for increased afterload, acutely the normal RV is unable to generate pressures that exceed 40-60 mmHg (54). Right ventricular response to an increase in filling is the Frank-Starling mechanism. Increasing ventricular end diastolic volumes with greater sarcomere length at the beginning of contraction, results in a greater force of contraction due to alteration in myofilamental sensitivity to calcium as a result of stretch (55). Consequently stroke volume increases in response to increased venous return. Similarly an acute increase in RV afterload in pathology such as pulmonary embolism which results in an increase in RVEDV in an attempt to compensate and maintain stroke volume through the same mechanism, sometimes called heterometric adaptation. In addition, other compensatory mechanisms exist to maintain SV to a certain extent in the face of an increase in afterload. An increase in myocardial contractility (inotropy) occurs in the acute setting by activation of the sympathetic nervous system. B-adrenergic receptor stimulation, located on the cardiac myocytes leads to increased contractility through an increase in intracellular free calcium. Additionally, sympathetic activation enhances rate of lusitropy (relaxation) as a

result of faster re-uptake of calcium ions by the sarcoplasmic reticulum and a resultant quicker release of calcium from the myofilaments (35). The RV also adapts through a continued progressive increase in cardiomyocyte contractile force over the 10-15 minutes following the acute rise in contractility as a result of the Frank-Starling mechanism, known as the Anrep phenomenon. This mechanism involves stretch related release of angiotensin II and endothelin (56) and results in a progressive decline of RVEDV and pressure after the initial increase in response to afterload, so called homeometric autoregulation.

1.1.3 Cardiac MRI in the normal right ventricle

The role of Cardiac magnetic resonance (CMR) imaging is well established in the evaluation of wide range of cardiovascular diseases, both acquired and congenital. It is non-invasive, does not involve the use of ionizing radiation and assessment of ventricular volumes and function can be obtained without the need for contrast administration. Over the last two decades it has become recognised as the gold standard for assessing left and right ventricular structure and function with accuracy demonstrated in broad range of diseases (57-62). It is particularly suited to the morphology of the right ventricle (RV) the complex structure and contractile pattern of which makes accurate assessment by 2D methods such as echocardiogram more difficult. The high resolution, 3 dimensional images obtainable by CMR avoid the need for any geometrical assumptions and have been shown to have superior interstudy reproducibility for right ventricular volume and mass in comparison to echocardiography, making CMR an attractive modality for monitoring ventricular function (63-65). CMR is not without limitation. It is less suitable for haemodynamic measurements than echocardiography due to more limited temporal resolution. It is expensive and less widely available in clinical practice. Incompatibilities with some ferrous implants such as cardiac pacemakers or aneurysm clips exist (66). Claustrophobia, body habitus, long scan times and need for repetitive breath-holds for acquisition of images to reduce respiratory motion artefact may limit tolerance in some patients. However with advancing technology it is now possible to perform single breath-hold and real-time acquisitions with adequate resolution (67, 68).

1.1.3.1 MRI theory

Magnetic resonance imaging relies on the physical properties of hydrogen nuclei (protons). Protons have an intrinsic spin which when the human body is brought into a high strength magnetic field align with the direction of this field. Application of a radiofrequency (RF) pulse can excite these spins and perturb their alignment, with vector components in line with the magnetic field (longitudinal magnetisation) and perpendicular to the field (transverse magnetisation). These spins gradually return to their resting state (relaxation) and in the process create RF signals that are used to create an image.

1.1.3.1.1 MR system components

An MRI system consists of a main magnet, three gradients coils and an integral RF transmitter. These components each generate a different type of magnetic field which when applied to a patient in combination produce spatially encoded MR signals that are used to firm images. The scanner itself is composed of a superconducting resistive electromagnet (made of niobium, low resistance wire) bathed within supercooled (around -250^0) liquid helium. The main magnet generates a strong constant magnetic field. The patient is positioned within the bore of the magnet where the strength of the field, B_o, defines the normal operating field strength of this particular MRI system. B_o is measured in units of Tesla (T) with 1T equal to approximately 20,000 times the earth's magnetic field. Typically a field strength of 1.5T is employed in CMR. A reference co-ordinate system of three orthogonal axes, x, y and z are used to define the magnetic field direction, with the z axis parallel to the direction of B_o (69).

Smaller gradient coils are housed in the inner circumference of the main magnet. A gradient magnetic field that can be rapidly switched on and off is generated by each of the three coils. Each coil generates a magnetic field in the same direction as B_o but with a strength that changes with position along the x, y or z direction according to which coil is applied. This gradient field is super-imposed onto B_o so that its strength increases (or decreases) along the direction of the gradient field.

A RF magnetic field is generated by the RF transmitter coil mounted inside the gradient coil closest to the patient. It has a smaller amplitude than the other

magnetic fields but oscillates at a characteristic frequency in the megahertz range which is determined by the field strength of the main magnet.

The static magnetic field and the RF field combine to generate MR signals that are spatially localised and encoded by the gradient magnetic fields to create an MR image.

The machine is housed within a copper lined room to deflect external radiowaves that would interfere with process and external RF sources which create artefact in the image.

For cardiac imaging, the MR signal is received by the phased array chest coil. This separate RF receiver coil is placed on top of the patient's chest. Several component coils within are arranged to maximise MR signal strength whilst minimising interference i.e. aimed to optimise signal to noise ratio.

1.1.3.1.2 Origin of MR signal

The origin of the MR signal used to generate images is from water or fat within patients' tissues, or more specifically hydrogen nuclei (consisting of a single proton) within free water or lipid molecules. Protons possess an intrinsic property known as nuclear spin that gives rise to a small magnetic field for each proton. Under normal circumstances the spins are randomly orientated. When the externally applied B_o field is applied, protons align either towards or against the direction of the field. The majority of proton spins align in the same direction as B_o as this is more energetically favourable direction of alignment. This excess combines to form a net magnetisation which is a key determinant of maximal signal intensity that can be generated and used to create images. The greater the applied field strength B_o the greater the size of net magnetisation.

Generation of a MR signal from the net magnetisation is achieved by the application of the RF transmitter coil described earlier to create RF magnetic field and delivery energy to the population of protons. This field is applied at a specific frequency, known as the Larmor frequency (w_o) determined by the equation $w_o = \gamma \times B_o$. The constant γ is the gyromagnetic ratio which has a value of 42.6MHz/Tesla for the proton. At 1.5T, the Larmor frequency is approximately 64MHz. This is also known as the resonant frequency as protons only absorb energy

(or resonate) at this characteristic frequency, or precession frequency. The RF field is normally applied as short pulses, known as a RF pulse.

1.1.3.1.3 Radiofrequency pulses

By applying a RF pulse at the precession frequency protons are made to absorb energy and alter net tissue magnetisation, a process known as excitation. When the RF pulse is switched off protons will relax back to a low energy state (and orientate with B_o), emitting detectable RF energy which can be used to construct MR images. However, as net magnetisation is in the longitudinal plane (aligned with the main magnetic field), changes is proton alignment cannot be detected. MR systems overcome this by producing magnetisation in tissue protons in the transverse plane.

Before the RF pulse is applied, net magnetisation is aligned along the z axis in direction of B_o. When RF pulse is switched on, net magnetisation moves away from alignment with B_o field and rotates around it. This oscillating field is applied as a rotating field at right angles to B_o in x and y vectors, rotates at same frequency as Larmor frequency and therefore appears as additional static field. As a result net magnetisation follows a spiral path from alignment with B_o (z axis) towards rotational motion in x and Y axes. The greater the amount of energy applied by the RF pulse, the greater the angle net magnetisation makes with B_o field (z axis). This angle of precession is known as the flip angle and is dependent on both amplitude and duration of the RF pulse. A 90^0 pulse will convert all longitudinal magnetisation into detectable transverse magnetisation and is therefore referred to as the saturation pulse. This pulse is used to initiate spin echo-based pulse sequences described in section 1.1.3.1.8. Low flip angle RF pulses are those $<90^0$, with a proportion of net magnetisation transferred from z axis to xy plane. This produces a lower MR signal, but can be repeated more rapidly as some of the magnetisation remains along the x axis immediately after the pulse. This is the pulse used to generate signal in gradient echo pulse sequences. A 180^0 pulse is known as an inversion pulse and are used to prepare net magnetisation before application of excitation pulse and in black blood pulse sequences. They are applied when magnetisation is at close to equilibrium and converts excess population of proton spins from aligned to ant-aligned with the B_o field. Because

the net magnetisation remains in longitudinal phase this pulse does not result in detectable signal.

1.1.3.1.4 Relaxation

Once the RF pulse is turned off the tissue magnetisation vector drifts back from transverse plane into longitudinal under the influence of the main magnetic field. This process is relaxation. During relaxation RF energy is released and detected as a MR signal in the transverse receiver coil. There are two distinct relaxation processes that relate to the two components of net magnetisation described above, longitudinal (z) and transverse (xy) components. T1 relaxation describes recovery of the z component along its longitudinal axis to original equilibrium state. Transverse relaxation (T2) is responsible for the decay of the xy component as it rotates about the z axis, causing a corresponding decay of the observed MR signal. Both occur at the same time but in human tissues T2 relaxation is typically a faster process.

The rate of relaxation is an important determinant of tissue contrast. Relaxation is rapid in tissues containing large amounts of bound water. These water molecules are in close proximity to macromolecules such as proteins which restrict movement of the smaller water molecules where their association makes energy transfer more efficient.

Relaxation is slower in free water solutions containing randomly orientated and rapidly tumbling water molecules where energy transfer is less efficient due to the less structured environment. The molecular environment of the water protons undergoing excitation therefore has significant influence on rate of RF energy release and therefore the MR signal receive from different tissues.

T1 relaxation (sometimes referred to as T1 recovery) describes the recovery of longitudinal magnetisation after RF pulse. T1 relaxation time is a constant for a given tissue within a given MR field strength. The time taken for T1 relaxation is dependent on the efficiency with which RF energy can be dissipated from the excited protons to the surrounding tissues, and the strength of the main magnetic field. The rate at which energy is released to surrounding molecular structure is related to the size of the molecule that contains the hydrogen nuclei and rate of

molecular motion known as the tumbling rate. As molecules tumble or rotate they give rise to a fluctuating magnetic field which is experienced by the protons of adjacent molecules. When this fluctuating field is close to Larmor frequency, energy exchange is more favourable. Lipid molecules are of a size that have a favourable tumbling rate close to this frequency and therefore adipose tissue has one of the fastest relaxation rates and shortest T1 relaxation time of body tissues (~260msec in 1.5T field). Larger molecules have slower tumbling rates unfavourable for energy exchange leading to longer relaxation times. Free water smaller molecular size has a fast tumbling rate which is also unfavourable and has a longer T1 relaxation time (around 3 seconds). It therefore takes a relatively long time to receive adequate MR signal back from pure water solution. Most MR sequences aim to detect signals in under 1 second and therefore free water solutions (such as CSF) appear dark and adipose tissues appear bright on images that rely on T1 contrast.

Muscle, liver, brain and viscous fluids such as pus contain variable proportions of free water and larger macromolecules. The tumbling rates of water molecules adjacent to large macromolecules are slowed down towards Larmor frequency shortening the T1 time. Therefore characteristic T1 relaxation times of these tissue lie in the spectrum between free water and adipose tissue. Conversely when free water content of these tissues increases for example by inflammation, T1 time increases.

T2 relaxation describes the decay (or dephasing) of transverse magnetisation produced by the RF pulse. Net magnetisation is a result of sum of whole population proton spins. Immediately following an RF pulse, spins rotate together in a coherent fashion so as they rotate they continuously point in the same direction in the xy plane. The angle they point is known as the phase angle and at this stage are described as being ‘in phase’. Over time, the phase angles spread out, there is loss of coherence and spins no longer rotate together and are said to move out of phase. The net magnetisation is therefore reduced and the signal the receiver coil detects gradually decays. There are two causes of loss of coherence. Interactions between neighbouring protons cause a loss of coherence described by T2 relaxation. While the applied magnetic field B_o is constant, the magnetic moment of one proton is able to slightly modify the magnetic field experienced by its neighbour. As protons are moving rapidly and randomly the effects are

transient and random. The Larmor frequency of individual protons therefore fluctuates in a random fashion leading to loss of coherence of the proton population which is known as de-phasing. T2 relaxation therefore relates to the amount of spin-spin interaction that takes place.

If T2 decay was automatically translated in to T1 recovery the use of individual terms would be unnecessary. However, rate at which transverse magnetisation is lost (T2 relaxation) is greater than rate at which longitudinal magnetisation returns (T1 relaxation) in most tissues. T1 and T2 relaxation times for pure water are similar. Free water contains small molecules relatively far apart and moving rapidly and therefore spin-spin interactions are infrequent leading to long T2 relaxation times. Water molecules bound to large macromolecules are slowed down and more likely to interact so water based tissues with high macromolecular content such as muscle tend to have shorter T2 times. Lipid molecules are of an intermediate size but interactions between hydrogen nuclei on long carbon chains (J-coupling) causes a reduction of T2 relaxation to an intermediate value. Rapidly repeated RF pulses used in turbo or fast spin echo sequences can reduce J-coupling resulting in increased signal intensity from fat as a consequence of the increase in T2 relaxation time.

Additional decay (or loss of coherence) occurs if there is inhomogeneity in the magnetic field which are constant in time, due to either inconsistences in the structure of the electromagnet or paramagnetic material in the imaged tissues such as ferrous joint replacements or foreign bodies. If the field varies between locations then so does the Larmor frequency. Protons at different spatial locations will rotate at different rates causing further dephasing so that the MR signal decays more rapidly. T2* relaxation describes the total decay of transverse relaxation as result of T2 relaxation and these inhomogeneities.

1.1.3.1.5 MR echoes

Most MR imaging measures the MR signal in the form of an echo as the gradient fields employed to localise and spatially encode the MR signals causes additional de-phasing that disrupts free induction decay. Gradient echoes are generated by application of magnetic field gradients to produce a change in field strength along a particular axis. This causes rapid dephasing of proton spins along the direction

of the gradient and transverse magnetisation rapidly drops to zero. A second gradient with a slop of equal magnitude but applied in the opposite direction reverses the amount of de-phasing resulting in recovery of FID signal to generate the gradient echo at the echo time TE. If the second gradient continues to be applied the FID signal de-phases and disappears.

Spin echos are generated by application of 180^0 refocusing pulse after the 90^0 excitation pulse. This has the effect of causing proton spins that have de-phased as a result of magnetic field inhomogeneities to come back in to phase causing FID to increase and therefore increased signal intensity reaching a maximum at TE. Imaging based on spin echo is therefore less effected by field inhomogeneities caused by metallic artefacts.

A

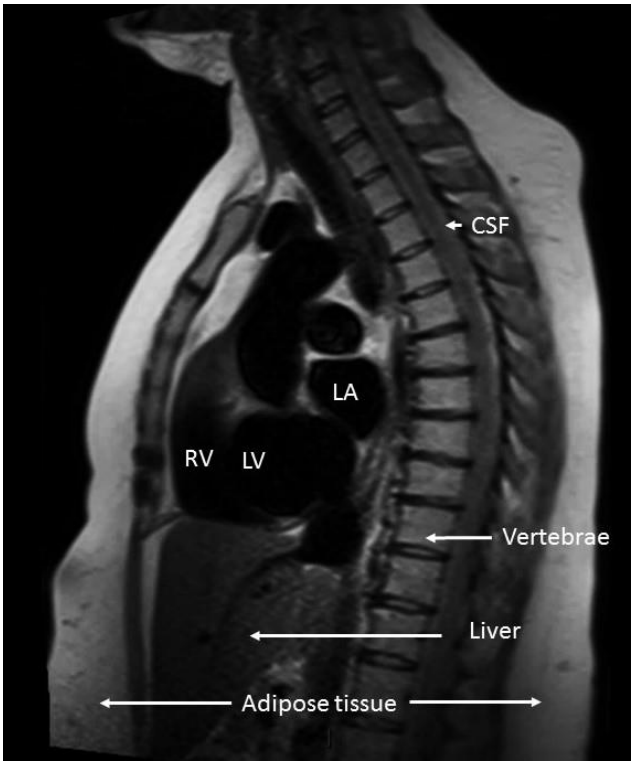

B

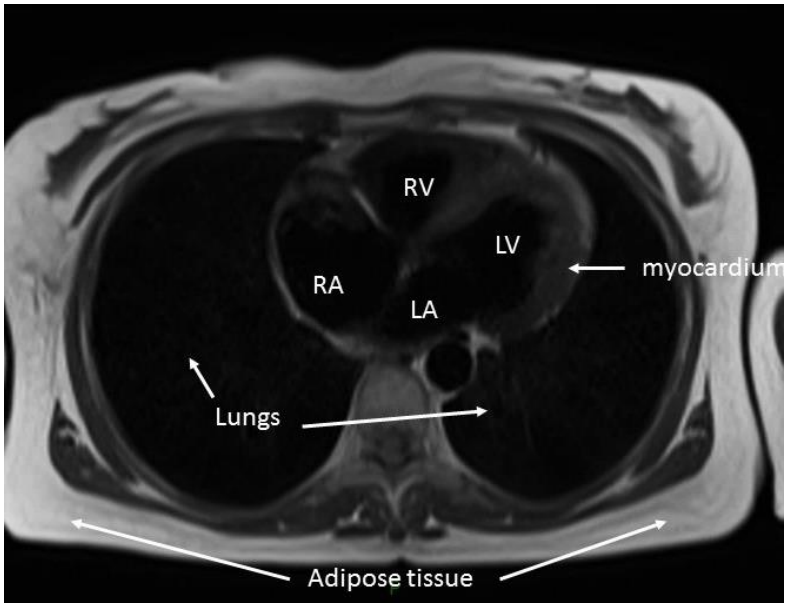

Figure 1.1 Black Blood contrast images
A Sagittal and B Axial images commonly employed for cardiac morphology using fast spin echo sequences with black blood double inversion preparation pulses. Images have intrinsic black blood contrast due to blood flow through the image slice and bright appearance from tissues (when T1 weighted). Adipose tissue as shown above particularly bright due to very short T1 relaxation time.

1.1.3.1.6 Magnetic field gradients and spatial localisation

The MR signal produced by the tissues as described can then be localised and encoded by applying three magnetic field gradients to produce an image. The applied magnetic field gradient causes the strength of the magnetic field and therefore the Larmor frequency to depend on position along that gradient field direction. Protons at the stronger end of the magnetic field gradient will therefore spin faster than those at the weaker end.

Slice selection gradients (G_S) are first used to identify the slice of tissue to undergo excitation by the RF pulse. A magnetic field gradient is applied at the same time as the RF pulse to alter the procession frequency along a section of tissue protons. The frequency of the RF pulse corresponds to a Larmor frequency at a chosen point along the direction of the applied gradient. This causes resonance only in protons that cuts through that point effectively defining a slice of tissue. The orientation of the slice is determined by the direction of the applied gradient. The transmitted RF pulse compromises a small range of frequencies rather than just a single frequency which determines slice thickness.

Following slice selection a phase encoding gradient (G_P) is applied which induces protons to rotate at different frequencies according to their relative position along the gradient. Where the gradient increases magnetic field strength the protons acquire a higher frequency of procession and where the gradient decrease the magnetic field a lower frequency. The protons also change their relative phase according to position along this gradient. When the gradient is switched off the protons will have changed their relative phase by an amount determined by their position along the gradient and can therefore determine their location within the tissue slice. This is known as phase encoding and direction of the gradient as phase encoding direction.

Following G_P the frequency encoding gradient (G_F) is applied in a direction at right angles to it and similarly causes protons to rotate at different frequencies depending on their position along the direction gradient. G_F is applied for a longer period and at the same time the signal is measured. The signal is comprised of a range of frequencies corresponding to Larmor frequencies of proton spins at different locations along the gradient.

These separate magnetic field gradients are therefore applied in a three step process to localise the MR signal in three dimensions. Slice orientations are determined by re-assigning each of the gradients to a different axis, for example images obtained in a trans-axial plane occur when G_S is applied along the z axis, G_P along the y axis and G_F along the x axis as shown in figure 1.1B. Angled slices can be obtained by combining gradients along two or more axis to perform each of the localisation tasks. This ability of MRI to define slice orientation along any axis is a key strength in obtaining functional imaging of cardiac structures.

1.1.3.1.7 Image reconstruction

This frequency encoded signal must then be reconstructed to produce images. The Fourier transform is a mathematical tool that analyses the time dependent MR signal and transforms it into its different frequency components. The amplitude of each frequency component can be mapped onto a location along the frequency encoding gradient to determine the relative amount of signal at each location. The field of view (FOV) in the frequency encoding direction is defined by the operator.

The phase changes cannot be decoded by this process. The Fourier transform can only analyse a signal that changes over time. To enable this multiple signal echos are generated by repeating the three step gradient field process, each time applying the same slice selection and frequency encoding gradient, but a different amount of phase encoding by increasing the slope (or strength) of G_P for each repetition by equal increments or steps. For each step the signal echo is measured, digitised and stored in a raw data matrix. The time interval between each repetition is called the repetition time TR. Once all the signals for a defined number of phase encoding steps are complete they can be analysed together by Fourier transform to decode both frequency and phase information.

TR is set by the operator and determines how fast MR images are acquired but also affects image contrast. The spatial resolution and number of pixels in the reconstructed image is determined by the number of phase encoding steps used. The greater the number of repetitions however the longer the image acquisition time.

The MR signals derived from each phase encoding step are stored in a raw data matrix known as K space. Just as each pixel occupies a unique location in an image, each point of an MR signal belongs to a particular location in k space which is represented by a 2D grid of points of which x axis represents frequency encoding direction and y axis phase encoding direction. There is an inverse relationship between image space and K space whereby if coordinates of the image represent spatial position x and y, the c-ordinates of K space represent 1/x and 1/y. Data points at the centre of K space (low spatial frequency) contribute mostly to signal intensity and image contrast while those arising from points near the edge of K space (high spatial frequency) to fine detail or edges and define spatial resolution of the image. To reconstruct an image that is accurate representation of the imaged subject it is important that the whole range of spatial frequencies is acquired and whole of K space filled. For standard CMR protocols this is done by filling k space with equally spaced parallel lines of signal data, line by line known as Cartesian acquisition. Each line represents a separately sampled MR signal during a phase encoding step. Once K space has been filled the Fourier transform analyses the digitised information and reconstructs this into a MR image.

1.1.3.1.8 Pulse sequences and image contrast

Pulse sequence is a timed series of RF pulses and magnetic field gradients which provides raw data to fill k-space – the "echo". The two broad families of pulse sequences are spin-echo and gradient echo.

In Spin echo sequences, a 90^0 RF pulse is applied to the selected slice so that resting longitudinal (z) magnetisation is entirely flipped to the transverse (XY) plane. The transverse magnetisation begins to de-phase when a 180^0 RF pulse is applied. This causes transverse magnetisation to partially rephrase and produces a spin echo, filling one line of K-space. This rephrasing 180^0 pulse can be repeated multiple times to acquire multiple lines of K-space, known as fast or turbo-spin echo. Image quality for this sequence is high at the expense of long acquisition time to fill K-space. The excitation angle is fixed at 90^0 and therefore TR and TE control the influence of tissue's T1 and T2 relaxation times. T1 weighted spin echo sequences have a short TR and short TE and characterised by bright fat signal and low fluid signal. They are useful for anatomical imaging where contrast is high between fat, muscle and fluid. In cardiac imaging, TR is determined by subject

heart rate and set to one RR interval and TE is short to minimise T2 weighting. T2 weighted spin echo sequences are characterised by long TR and TE. Long TR allows z magnetisation to recover to equilibrium for most tissues reduce influence of differences in T1 relaxation. Longer TE however allows more decay of xy component leads to differential signal between short T2 tissues such as muscle and those with long T2 such as fluid. These images are characterised by bright fluid and useful for characterisation of fluid collections or oedema.

The two main types of gradient echo pulse sequence used in cardiac imaging are spoiled gradient echo and balanced steady state free precession (SSFP).

Gradient echo pulse sequences use a smaller initial RF pulse typically between 10-90^0 and then apply magnetic field gradients to rephrase net magnetisation. TR, TE and flip angle control the influence of T1 and T2* relaxation times on the signal. The main advantage is that gradient echoes can be produced very quickly with short scan times but at the disadvantage of increased susceptibility to artefacts. Gradient echo sequences have very short TR values which is attractive for cardiac imaging as gives rise to short acquisition times. The TR values are much shorter however than T2 relaxation times of blood and myocardium. Transverse magnetisation therefore would still exist when the next RF pulse is applied and contribute to the signal during the subsequent TR unless destroyed.

Spoiled gradient echo sequences (Siemens FLASH - Fast Low Angle Shot) incorporate an additional “spoiler” gradient at the end of each TR period to destroy any residual transverse magnetisation prior to the next RF pulse (70, 71). These are used in both T1 weighted and T2* sequences.

SSFP gradient echo sequences rather than spoiling transverse magnetisation instead ensure it is brought back in to phase at the end of each TR period when the next RF pulse is applied. This is then superimposed onto transverse magnetisation generated by that RF pulse. After a number of repetitions this combines to give a greater signal and results in images with both T1 and T2 contrast with tissues appearing bright and contrast depending on T2/T1 ratio (72). Fluid and fat have highest signal on T2/T1 weighted images with all other tissues showing intermediate signal. The increased signal allows for shorter TR and TE compared to spoiled sequences but is prone to dark banding artefacts due to field

inhomogeneities. The Siemens “unspoiled” gradient echo sequence used in this thesis is known as TrueFISP (Fast Imaging with Steady state Procession).

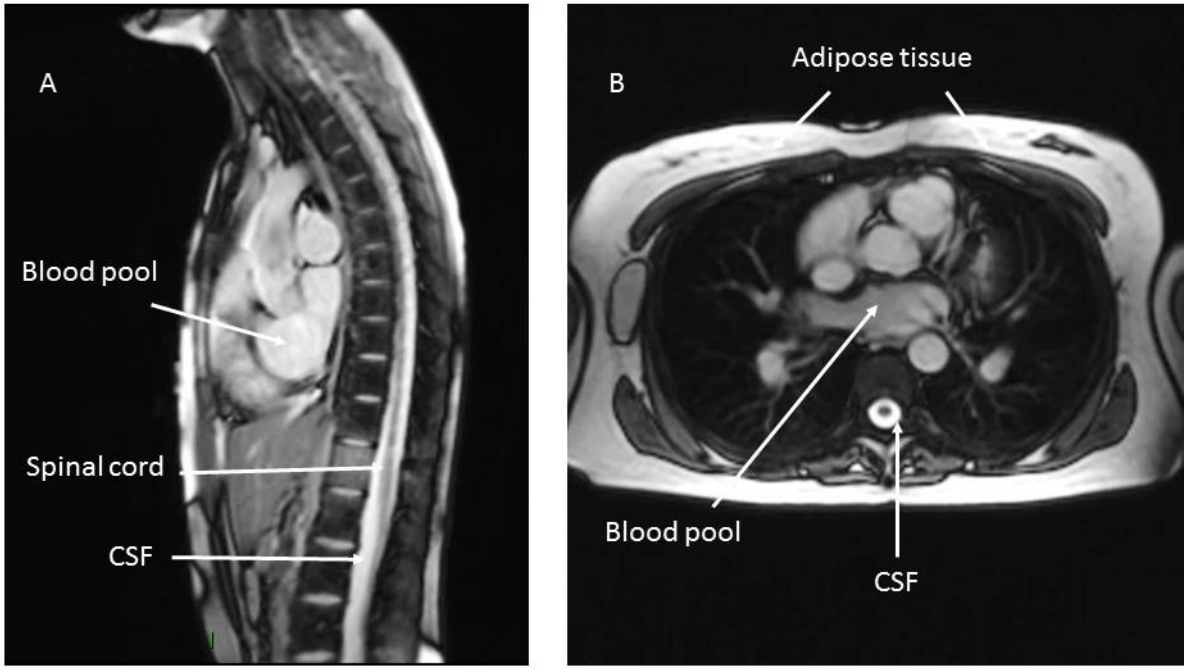

Figure 1.2 'Bright blood ' cine steady-state free procession images
Examples of b-SSFP sequences images used in assessment of cardiac function. A. Sagital view B. Axial from single-phase scout localiser images. In contrast to figure 1.1 blood pool (and CSF) appears bright. Images are not T1 or T2 weighted, but signal depends on ratio of T2/T1 in addition to flow. Blood, water and fat therefore all appear bright. In this thesis sequence is known as TrueFISP.

1.1.3.2 Cardiac MRI sequences

To acquire an image of the heart unaffected by motion requires an image acquisition period of just a few tens of milliseconds. This means limiting both the number of phase encoding steps (and therefore spatial resolution) and a short TR time. This is achieved at the cost of reduced image quality, but in order to achieve acceptable images the acquisition time becomes too long to 'freeze' cardiac motion. For CMR therefore the MR signals are acquired over multiple heart beats synchronising the pulse sequence and therefore signal acquisition to a particular time point in the cardiac cycle.

1.1.3.2.1 Fast imaging techniques

As described in section 1.1.3.1.8 the attributes of spin echo and gradient echo sequences are employed in CMR dependent on the goal of imaging. Spin echo technique is ideally suited when goal is to achieve images with a high signal to noise ratio and reduce sensitivity to artefacts caused by magnetic field inhomogeniety. Fast gradient echo pulse sequences are used where imaging speed is of more importance than imaging quality. Flowing blood appears differently between the two sequences with spin echo giving intrinsic black blood appearance employed in anatomical imaging (see figure 1.1) (73) and gradient echo pulses intrinsic bright blood appearance employed in fast cine imaging (see figure 1.2). Balanced steady state free procession (b-SSFP) sequences are commonly employed for functional assessment (74, 75). Conventional imaging techniques acquire only one phase encoding step and therefore one line of k space per heartbeat. TR is defined by patients' heart rate and equal to the R-R interval. It would therefore take several minutes to acquire an anatomical dataset. Fast imaging techniques acquire more than one line of k space per heart beat leading to shorter acquisition times and are known as turbo or fast pulse sequences (76). These sequences generate multiple echoes by applying multiple 180^0 pulses after the initial 90^0 pulse. Turbofactor describes the number of lines of k space filled per heart beat. Sequences with very high turbofactor such as that employed in real time or single shot acquisitions shortens acquisition time but at the expense of reducing the number of cardiac phases within the cardiac cycle and therefore the cine frame rate. Imaging therefore suffers from poor temporal and spatial resolution.

CMR data acquisition is synchronised to cardiac motion using the electrical activity of the heart (77). The magnetic field exerts a significant effect on the ECG, resulting in voltage artefact in the ST segment on the ECG. Reliable r wave detection is possible using a vector cardiogram (VCG), but reliable ST/T wave monitoring is not possible. The VCG can be used for either prospective or retrospective gating.

Prospective triggering is typically used for single phase acquisitions such as static image of the heart at a single point in cardiac cycle. Information is acquired at a specific interval after the r wave, usually to coincide with diastole when heart relatively still. This still imaging approach is typically used in combination with turbo or fast spin echo pulse sequence to acquire black blood anatomical images shown in figure 1.1.

Multiphase acquisitions are used to acquire dynamic information such as cine MRI. Data is acquired throughout the cardiac cycle and reconstructed with retrospective reference to the VCG (78). Typically the cardiac cycle is divided in to 20-30 phases with one image reconstructed for each phase and displayed as a cine loop. Retrospective gating in combination with a turbo or fast gradient echo method is most common approach to bright blood functional cine imaging shown in figure 1.2. Most CMR images are obtained during breath holds, typically of 10-15s duration to minimise image degradation caused by respiratory motion. End-inspiratory breath hold is more comfortable and tolerate for longer periods. However breath hold at end of gentle expiration is usually more consistent (minimising slice misregistration) and less likely to provoke ectopic beats.

Real-time cine MRI can also be acquired by increasing the parallel imaging factor and reducing spatial resolution. When applied it is possible to obtain diagnostic images in those with very irregular heart rhythms or in patients who are unable to breath hold (79, 80).

In this thesis pulse sequence is known as TrueFISP (Siemens). Resultant images are not T1 or T2 weighted, but signal intensity depends on ratio of T2/T1 in addition to flow. Blood, water and fat therefore all appear bright.

Ventricular volume is determined using a “stack” of contiguous short axis slices 5-10 mm thick acquired during breath-hold (typically in region of 5-18 seconds), ECG-gated cine “bright” blood sequences. This sequence gives good blood-myocardial contrast to allow tracing of endocardial and epicardial contours on end-diastolic and end-systolic frames. Ventricular volume is calculated as sum of individual slice volumes (Simpson’s rule). Ventricular mass is determined by multiplying myocardial volume by the muscle-specific density for myocardial tissue (1.05g/cm^3). Inclusion or exclusion of the RV trabeculations as either mass or volume is source of interstudy variability (81).

1.1.3.2.2 Velocity encoding and phase contrast MRI

Velocity encoded CMR, also known as phase contrast, is a fast and simple method of measuring blood flow (82-84). As proton spins flow along a magnetic field gradient they acquire a shift in transverse (xy) magnetisation which is proportional to the strength of the magnetic field gradient and to flow velocity, which can then be determined. Phase maps are generated to enable quantification of flow where pixel intensity depends on phase of transverse magnetisation rather than its magnitude. First the image is prescribed perpendicular to flow direction through the vessel. More than 15^0 of variation from the true perpendicular will significantly underestimate the flow. Secondly an appropriate encoding velocity (VENC) is selected. This must be greater than the highest velocity in the flow otherwise aliasing artefact (see section 1.1.3.3) will make data unreliable. Typical VENC in normal systemic flow ~150cm/s and in right sided flow ~100cm/s but may need adjusted in pathological situations, for example severe valve stenosis may require VENC set in region of 400cm/s by the operator (85) . Selection of too high a value results in underestimation of velocity. Adequate temporal resolution typically requires 30 phases in free breathing acquisitions or 20-25 in breath hold. Velocity maps are generally displayed using a gray scale (example is shown in figure 1.4) with stationary tissue appearing gray, velocities in forward (positive) and reverse (negative) directions represented as higher (white) and lower (towards black) pixel intensities. Volumetric flow (ml/s) is determined in each time frame by multiplying spatial mean velocity (cm/s) of blood flow with the cross sectional area of the vessel (cm^2) delineated by a region of interest (ROI) drawn by the operator at time of post acquisition analysis.

By multiplying blood velocity by the cross sectional area of chosen vessel, such as the main pulmonary artery, SV can be calculated (86). In addition this can be used to quantify intracardiac shunt by comparing aortic and pulmonary arterial flow (87). Flow assessment by CMR has the advantage over echocardiography as it can be conducted in any orientation or plane whilst accurate echocardiographic assessment requires the flow to be parallel to the echocardiographic plane. Phase contrast flow is less accurate in the presence of cardiac arrhythmia or turbulent blood flow.

1.1.3.3 MRI artefacts

Artefacts can degrade image quality and may cause measurements in functional imaging to be unreliable (88). Most can only be corrected during image acquisition and therefore artefact recognition and adaptation of acquisition protocol where possible to resolve.

Aliasing occurs when the FOV does not enclose all of the region of interest being imaged. The region outside the FOV wraps around and is projected at the opposite side of the image as shown in figure 1.3. This projected image may cover the region of interest. Increasing the FOV or number of phase encoding steps (oversampling) often resolves this. Alternatively frequency and phase encoding directions can be swapped. In velocity encoded sequences any velocity greater or smaller than the defined VENC causes aliasing. Here aliasing appears as black holes in the flow sequence and will lead to over or underestimation of the true velocity. Correction of the VENC until the velocity encoded slightly exceeds that of the flow will eliminate the artefact.

RF artefact is caused by distortion of the magnetic field by an external RF source and characterised by regular striped pattern (sometimes known as zipper artefact) across all images irrespective of the MR sequence. This may arise when the door to the MRI room is not closed or the isolation of the room damaged.

Chemical shift artefacts appear at the interface between fat and water based tissues. Misregistration of signal as result of difference in frequency resonance between fat and water protons in same voxel along the frequency encoding direction causes a separation (pixel shift) in the reconstructed image. Dephasing

of fat and water protons can cause signal cancellation and also cause chemical shift artefact. Increasing the bandwidth reduces the difference between the frequency of fat and water protons in one voxel and can diminish this artefact. Fat suppression sequences can also be used.

Dark rim artefacts can be seen in any CMR image at the interface of bright blood pool and darker (myocardial) signal. In CMR perfusion imaging this may be difficult to differentiate from subendocardial perfusion defects. This can be reduced by increasing spatial resolution.

Inhomogeneity artefacts may arise from presence of implanted metallic foreign bodies such as coronary stents, sternal wires or devices. Due to different magnetic properties of most tissues the applied field is slightly inhomogenous. This causes regional dephasing of protons at boundaries between different tissues. Metallic susceptibility artefacts tend to worsen at higher field strengths and limited field strengths 1.5T advisable. Intermittent use of a 180^0 refocusing pulse may rephrase the protons and therefore spin echo sequences are less sensitive to susceptibility artefact than gradient echo sequences. A saturation band may also be employed to suppress signal from the implant.

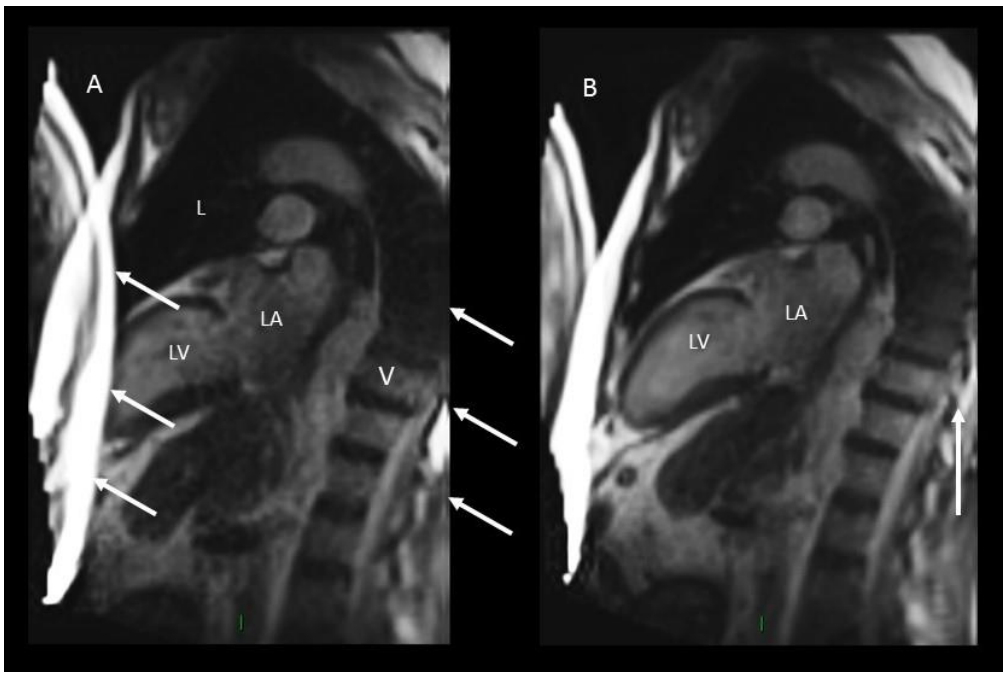

Figure 1.3. 2 chamber view demonstrating aliasing artefact
Sagittal imaging of 2 chamber view with left atrium (LA) and ventricle (LV) shown, vertebrae indicated by V. Region outside the field of view (FOV) shown by arrows in panel A wraps around and is projected at the other side of the image, causing interference with the image of the LV. In panel B FOV is increased (white arrow) so less wrap occurs and LV can now be seen clearly.

1.1.3.3.1 Motion artefacts.

Ghosting refers to appearance of parallel lines or double contours in the image usually as a result of respiratory motion during acquisition. An example is shown in Figure 1.4. Coaching of the subject to control breathing will eliminate ghosting, if patients struggle with breath-holds in expiration, inspiratory breath-hold can be employed or shortened acquisition times to decrease breath-hold duration at expense of reduced spatial resolution.

Trigger artefact causes myocardial borders to become less defined or blurry. An example is shown in figure 1.5. Cardiac data acquisition is synchronised to the R wave and data collected throughout the cardiac cycle and retrospectively assigned to specific phases. As a result the presence of a poor ECG signal or arrhythmia impairs data acquisition. The image quality may decline and render the image non diagnostic due to difficulty delineating endo and epicardial borders and hence calculations of volume or mass unreliable. Arrhythmia rejection software can be applied so images obtained during irregular R-R intervals are rejected. Prospective triggering can also be used to acquire data during a predefined period of the cardiac cycle but as this does not cover the complete R-R interval SV may be underestimated. In severe arrhythmia real time imaging can be used with limitations as described above.

Blood flow artefact occurs as a result of protons moving at high velocity near or in the selected imaging slice, usually close to outflow tracts or large arteries, which can disturb the homogenous steady state magnetisation. This can be overcome by improvement (shimming) locally of the homogeneity of the main magnetic field. Reducing TR or TE results in a sequence less susceptible for turbulent flow artefacts. Alternatively slice selection can be adjusted or the signal from passing protons inverted by application of a saturation band across the outflow tract.

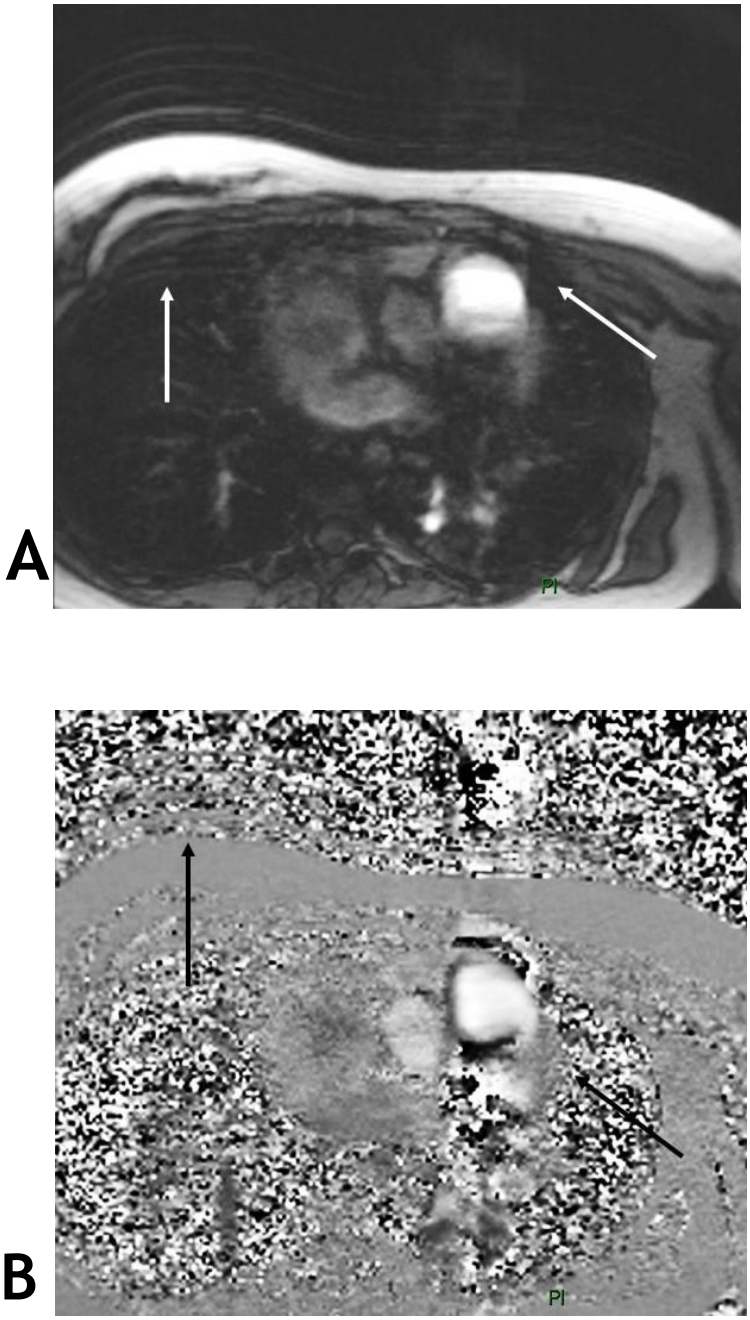

Figure 1.4 Ghosting Artefact
Example of ghosting artefact caused by respiratory motion during acquisition. Panel A shows the axial view with parallel lines caused by multiple contours indicated by arrow. And B corresponding phase velocity map which would have been used to determine flow in pulmonary artery (arrow) which will be inaccurate due to motion artefact.

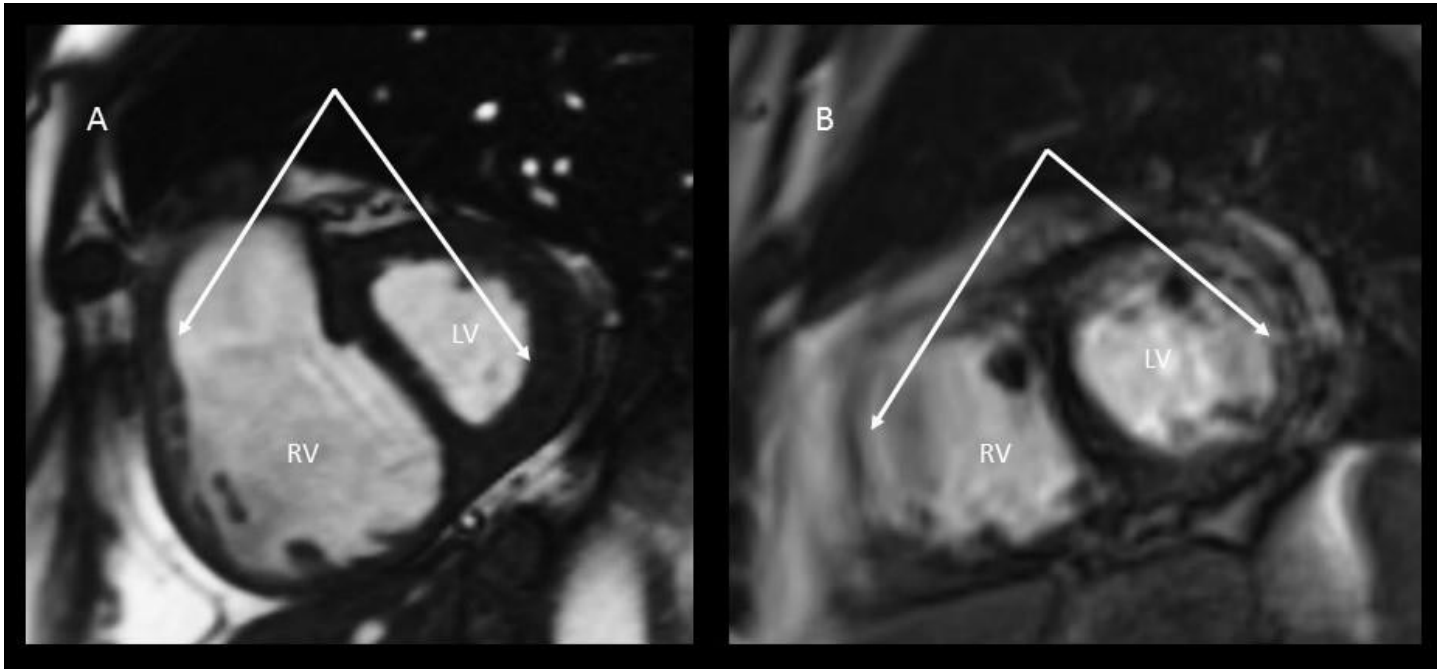

Figure 1.5. Trigger artefact caused by arrhythmia.
Short access views of right and left ventricle used to delineate endocardial and epicardial borders in the analysis of ventricular mass, volume and function. Panel A shows clear delineation between myocardium and blood pool. In Panel B, myocardial borders are poorly defined and image blurry as the result of arrhythmia and trigger artefact. This can be overcome by use of arrhythmia rejection software or real-time image acquisition.

1.1.3.4 Normal Variants in right ventricular structure and function

LV mass and volumes are known to vary by age, sex and race and are typically adjusted for body surface area (BSA) (89-91). Echocardiography and autopsy studies have demonstrated significant age and gender related differences in both cardiac function and mass in healthy subjects (92-94). Autopsy study has also shown subject weight, height and BSA to relate to cardiac mass (94, 95). Over the last decade a number of studies have reported normal values for right ventricular structure and function but have been limited by small sample size over a narrow age range with varying acquisition techniques (47, 64, 96, 97). More recently, the multi-ethnic study of atherosclerosis (MESA)-right ventricle study, a multicentre prospective cohort study of over 4000 participants without evidence of clinical cardiovascular disease at baseline (98), have evaluated a number of patient demographics that influence CMR value interpretation.

Conventional cardiovascular scaling approach uses ratiometric method of dividing indices such as RV mass by a measure of body size such as height or BSA. Body composition has significant effects on relationship between body mass, surface area and cardiac structure as large volumes of adipose tissue in the obese or extravascular fluid in heart failure patients are not adjusted for, which have little metabolic demand and therefore are unlikely to influence cardiac adaptation whose function is to provide efficient circulatory supply of metabolic substrates. Fat free mass or lean body mass has been proposed as more appropriate method of scaling to body size, however clinical use is limited as accurate measurement requires assessment of body composition using dual-energy x-ray absorptiometry (DEXA) or hydrodensitometry (99). Superiority of height indexed over BSA indexed LV mass has been demonstrated (100). Height may be preferable to index RV parameters to over BSA as it is not affected by volume of adipose tissue. However autopsy study has shown weight or BSA to be superior to height in predicting cardiac mass (94) and CMR study has shown worse correlation coefficients in healthy subjects between RV mass, volumes and height than weight or BSA, although this appears population dependent (47). Fat free mass may also vary considerably for subjects of identical height. It is therefore current clinical practice to adjust RV parameters for BSA.

1.1.3.4.1 Ageing and the right ventricle

Increasing age in autopsy studies is associated with myocyte loss and decreases in LV mass and volume in males but not females (95). Remodelling may occur due to age-related hormonal change such as reduced testosterone levels in males, or as a result of decreasing levels of physical activity. Absolute and indexed CMR derived RV mass and volumes have also been shown to be lower with increasing age (101-104). Larger effects are observed in males than females, but significant changes have been reported in both albeit not consistently. An approximate 5% lower RV mass per decade of increasing age has been reported. Age related increase in right ventricular ejection fraction is also seen (about 1% per decade) and changes in RV diastolic function defined by decreased early peak filling rate (PFR_E) and increased active peak filling rate (PFR_A) are also reported, reflecting a degree of ventricular stiffening with age (104).

1.1.3.4.2 Sex differences in right ventricular morphology

Absolute right ventricular volumes are greater in men than women (101, 105). Differences in RV mass have been reported variably (47, 96, 101, 102, 104, 106) but in larger cohort studies seems to be higher in males. RV mass has been reported as up to 8-15 % lower in females and RV volumes 10-25% lower (101, 102). These differences have been shown to persist despite adjustment for BSA (104). As previously mentioned, greater age related decline in RV mass and volume is seen in men and one study has reported restriction of this decline to the male sex (102). In general no gender differences have been reported in RVEF, with the exception of the larger MESA-RV study where males had 4% lower RVEF after adjustment for age and ethnicity (101). These gender differences are potentially hormone related (107, 108). Higher levels of estradiol are associated with better RV systolic function in healthy postmenopausal woman taking hormone replacement and higher levels of androgens in both males and postmenopausal women are associated with greater RV mass, higher stroke volume and larger RV volumes (109).

1.1.3.4.3 Ethnicity and RV structure

The influence of ethnicity has been less well studied. Lower RV mass in African Americans and higher RV mass in Hispanics in comparison to Caucasians has been reported (101). After adjustment for LV mass, lower RV mass in African Americans remained significant suggesting a RV specific effect. In the same study, Hispanics had larger RVEDV and RVSV, and African-American men had lower RVEDV despite adjustment for age and sex. Chinese ethnicity has also been shown to have lower RV volumes after adjusting for BSA than Caucasians, although mass was not reported in this study (105).

1.1.3.4.4 Influence of physical activity on RV structure

Long term high intensity exercise in elite athletes is well documented to cause adaptive changes in cardiac structure characterised by increases in LV mass, volume and wall thickness with a small number of CMR studies showing increases in RV mass and volume, the so called “athlete’s heart”(110-113). Levels of physical activity in non-athletes however have also been shown to influence RV mass and volumes. The MESA-RV cohort has been used to interrogate levels and intensity of activity from household chores to sports and leisure activities (114). Higher levels of moderate and vigorous physical activity were associated with greater RV mass and volumes after age, body size and gender adjustment, although the absolute value was low (1g of RV mass from lowest to highest quintile of activity, and 7% increase in RVEDV) which remained significant after adjusting for LV size.

1.1.3.4.5 Obesity

Obesity is independently associated with increased cardiovascular morbidity and mortality and is a growing health problem in the western world. Obesity is associated with increases in blood volume, cardiac output and direct infiltration of fat in the myocardium, termed the cardiomyopathy of obesity (115, 116). RV mass and volumes determined by CMR are higher in obese individuals even after adjustment for LV parameters and demographic variables. Chahal et al demonstrated a 14 % absolute and 8 % LV adjusted higher RV mass, 16 % higher

RVSV, larger RVEDV and slightly lower RVEF in healthy obese individuals without reported symptoms suggestive of a sleep disorder (117). Adjustment for LV parameters and height suggests these increases could not be attributed to increased body size alone. Again, these effects were relatively small, a 5kg/m^2 increase in BMI was associated with 1.3g higher RVM, 8.65ml greater RVEDV and 0.5% lower RVEF. The BMI related increase in RVM was out of proportion to RVEDV suggesting remodelling rather than simply increase in cardiac size. Earlier CMR studies in the obese have also shown higher RV mass and volumes but preserved RVEF (97). These studies potentially could be limited as subclinical sleep disorder was not excluded where nocturnal hypoxic vasoconstriction could result in increased RV afterload or directly affect the RV (118). It is however thought obesity-related increase in blood volume impacts on cardiac output and ultimately adaptive change in RV morphology (119). Additionally obesity results in changes in adipokine levels which have effects on RV morphology along with fatty infiltration of myocardium and increased mass (120, 121).

Several large cohort studies have now published age and gender specific CMR right ventricular reference ranges for mass, volume and function (101, 102, 104).

1.1.4 Right Ventricular - arterial coupling

Isolated RV failure can arise as a consequence of intrinsic RV pathology such as infarction, but typically occurs as a consequence of pathology of its adjoining circuit, either impedence of the pulmonary circulation or disease of the left heart. It is therefore intuitive when considering RV dysfunction in PAH, where the primary disease is in the pulmonary circulation but the capacity of the right heart to adapt to this increased afterload that ultimately dictates outcome and functional capacity, to consider the RV-pulmonary artery circuit as a unit. RV-arterial coupling considers the extent of RV adaptation in context of its afterload, represented as a ratio of elastances, contractility (or end systolic elastance - E_{es}) with effective arterial elastance (E_a).

1.1.4.1 Right ventricular contractility

RVEF is the most commonly used measure of RV function and by inference RV contractility. Ideally however indices of RV contractility should be independent of preload and afterload in addition to being sensitive to change in inotropy and independent of cardiac mass. SV is the net result of RV contraction, however it too is determined by RV filling (preload) and in addition to myocardial function by the afterload that the ventricle contracts against i.e. arterial resistance. Ventricular pressure-volume loops allow derivation of load independent measures of RV contractility, known as maximum ventricular elastance (E_{max}), which is regarded by many as the gold standard measurement of RV function (122). A single pressure volume loop describes the changes in ventricular pressure and volume through a cardiac cycle. Unlike the rectangular shape observed in the LV, the RV pressure-volume loop is more triangular in a normal RV-pulmonary circulation. The cycle can be divided in to four phases; (1) the filling phase, which in the RV is described by significant increase in volume with only slight increase in pressure as a result of high RV distensibility, (2) isovolumetric contraction which is short due to low PA pressures, (3) RV ejection with an early peak in pressure and subsequent rapid decline, (4) isovolumetric relaxation from pulmonary valve closure until pressure falls to baseline. Multiple pressure-volume loops under different loading conditions, such as preload reduction generated in models of isolated RV by IVC occlusion, allow identification of end-systolic pressure-volume points of each pressure-volume loop. The end-systolic pressure-volume points can be connected by a linear line, the end-systolic pressure-volume relation (ESPVR). The gradient of this line is the end-systolic elastance (E_{es}) (123) which approximates E_{max}. Figure 1.6 describes derivation of E_{es} from PV-loop analysis.

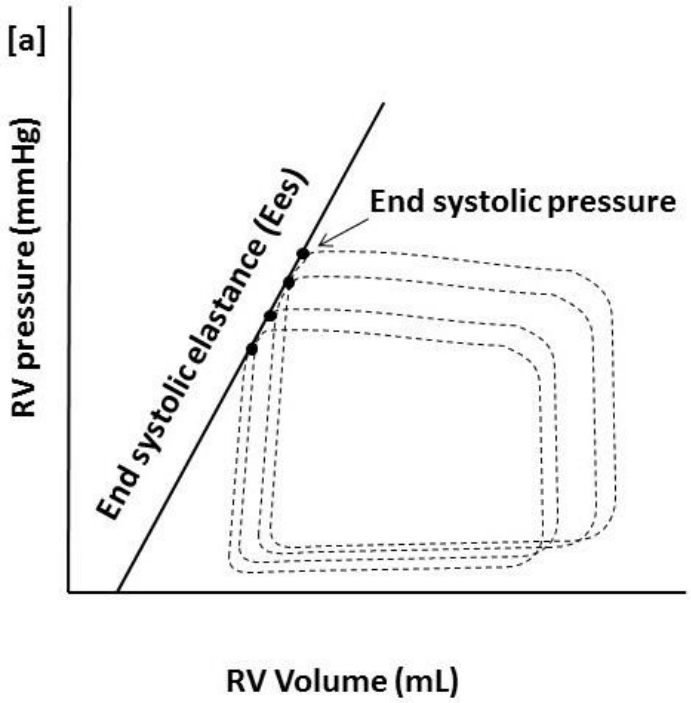

Figure 1.6. Derivation of Ees from multiple pressure-volume loop

Pressure volume loops at decreasing levels of venous return are obtained by instantaneous pressure and volume measurement, usually by IVC occlusion. End systolic pressure points are then determined as shown, and Ees is the slope of the gradient line connecting these points, the end systolic pressure volume relation.

E_{es} is therefore a load independent measure of ventricular contractility and has been shown to increase in response to inotropic agents. A shift in the ESPVR may occur with changes in ventricular mass and configuration.

The generation of multiple pressure-volume loops requires the use of conductance catheters which are expensive, is time consuming requiring simultaneous measure of pressure and volume, and alteration of loading conditions (i.e. venous return to the heart) which may not be safe in unwell patients. It is therefore not an attractive modality for clinical use. Single beat methods have been developed, initially in the LV but more recently translated to the RV (124, 125). The single beat method relies on the derivation of the maximal pressure that the RV could generate if isovolumetric contraction occurred, known as P_{max}. This point is derived by the nonlinear extrapolation of the early and late portions of the RV pressure time curve for a single ventricular contraction obtained by standard right heart catheterisation. P_{max} is then plotted on the pressure-volume plot at end diastolic volume. E_{es} can then be determined as the slope of the line from P_{max} to ESP. Figure 1.7 describes the derivation of E_{es}, E_a and P_{max} using single beat method.

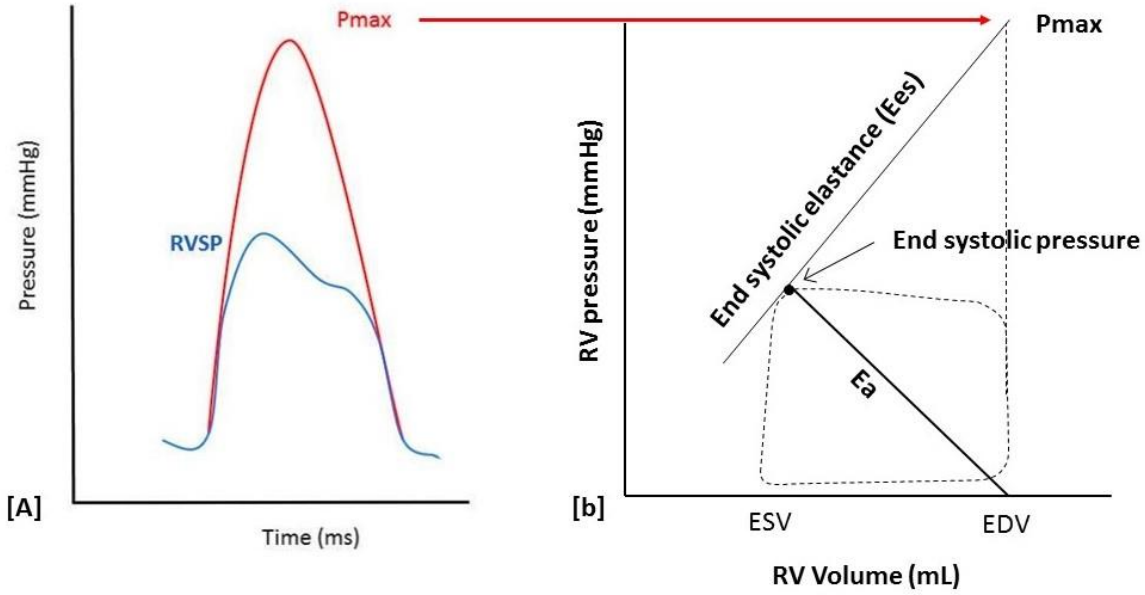

Figure 1.7. Derivation of Ees using single beat method.

Panel A shows a RV pressure/time trace over a single cardiac cycle obtained at right heart cathetersation. Pmax is calculated from the non linear extrapolation of the early systolic and diastolic portions of the pressure curve. Panel b shows a RV pressure/volume trace for a cardiac cycle. Ees can be determined by the slope of the ESPVR between Pmax plotted at end-diastolic volume and ESP at end-systolic volume.

1.1.4.2 Right Ventricular afterload

The afterload faced by the RV is determined by several components; the steady state mean resistance to blood flow, compliance of the system, arterial wave reflections that arise as a result of the pulsatile nature of flow, and inertance of blood during ejection (126). Clinical measures commonly derived from right heart catheterisation such as PVR are therefore not ideal measures of RV afterload. Afterload can be defined by RV wall stress that arises during RV ejection. This can be approximated by the maximum product of volume and pressure divided by wall thickness, by Laplace's law. This is however problematic in the RV as there is considerable variation in RV internal radius due to its complex shape and it is not in essence the true sphere to which this law applies (127). Pulmonary artery impedence (PVZ) is the ratio of pressure to flow oscillations which can be calculated by spectral analysis of pressure and flow waves. Whilst this method does provide a comprehensive description of all aspects of RV vascular load, it is both difficult to measure and interpret (128). Effective arterial elastance (E_a) is a simpler approach to describing the load faced by the RV and incorporates both resistive and pulsatile components (129). It is graphically determined on a pressure volume loop by dividing the pressure at ESP by stroke volume. This method allows matching of afterload to RV contractility (E_{es}). As contractility should be homeometrically adjusted to match its afterload, the adequacy of this adaptation can be assessed by the ratio of E_{es}/E_a, which defines ventricular-arterial coupling.

1.1.4.3 Simplified methods for the assessment of right ventricular-arterial coupling.

RV-arterial coupling as a ratio of elastances represents optimal transfer of energy from the RV to pulmonary circulation at ratios of 1.5-2 (130). It is, however, also possible to determine coupling by a ratio of volumes. E_{es} can be approximated by the formula;

$$E_{es} = ESP / (ESV - V_0)$$

Where ESP is the end systolic pressure, ESV the end systolic volume and V_0 is the volume intercept of the ESPVR line, and approximates to the theoretical volume of the unloaded ventricle.

And E_a can be approximated by

$E_a = ESP/SV$.

RV-arterial coupling (E_{es}/E_a) therefore can be determined by ratio of volumes, SV/ESV, if V_0 is regarded as negligible.

There are several limitations to using SV/ESV. The first is that ESP-ESV relationship is linear and crosses the origin. This is incorrect as the ventricular volume at zero filling (ie V_0) has to be positive and therefore this method leads to an underestimation of E_{es}. In addition, we assume that E_{es} coincides with E_{max} which may not be correct (131). SV/ESV however offers a measure of RV function in a similar manner to RVEF (SV/EDV) however in a less preload dependent manner.

Additionally, RV-A coupling can be approximated by pressure measurement obtained at RHC and RV volume measurement by CMR (132). P_{max} is derived as previously mentioned from extrapolation of the RV pressure curve, however ESP is approximated by mPAP. E_{es} is therefore calculated as;

$E_{es} = (P_{max} - mPAP)/SV$

or by further simplification if $V_0 = 0$, $E_{es} = mPAP/ESV$.

Trip et al demonstrated that V_0 may vary from-8 to 171 ml, and correlated with ventricular volume and therefore could not be regarded as negligible, nor could the calculated E_{es} be preload independent. However, this method has a number of limitations raised by the use of surrogate pressures and volumes in addition to reliance on a linear extrapolation from the slightly curvilinear ESPVR which may result in markedly different pressure or volume intercepts (122).

1.2 The right heart and pulmonary vasculature in pulmonary hypertension

1.2.1 Aetiology

Pulmonary arterial “sclerosis” was first described by Ernst von Romberg in 1891 but it wasn’t until 1951 that a larger study reported the characteristics of 39 patients with PAH of unknown aetiology and the term ‘primary pulmonary hypertension’ was coined (133, 134). The WHO presented the first definition of the disease in 1973 in Geneva, classifying the disease by primary, secondary and associated PH (135). Since then, four further world symposia have developed a more comprehensive clinical classification system based on 5 main groups of pulmonary hypertensive disease initially proposed in Evian France in 1998 (136-138). The most recent clinical classification from the fifth WSPH held in Nice, France in 2013 is shown in table 1-1

Table 1-1 Clinical classification of Pulmonary Hypertension (Nice 2013)

1. Pulmonary arterial hypertension (PAH)

1.1 Idiopathic (IPAH)
1.2 Heritable PAH
1.2.1 BMPR2
1.2.2 ALK1, ENG, SMAD9, CAV1, KCN K3
1.2.3 Unknown
1.3 Drug and toxin induced
1.4 Associated with:
1.4.1 Connective tissue disease
1.4.2 HIV Infection
1.4.3 Portal hypertension
1.4.4 Congenital heart disease
1.4.5 Schistosomiasis
1′ Pulmonary veno-occlusive disease and/or pulmonary capillary hemangiomatosis
1″ Persistent pulmonary hypertension of the newborn (PPHN)

2. Pulmonary hypertension due to left heart disease

2.1 Left ventricular systolic dysfunction
2.2 Left ventricular diastolic dysfunction
2.3 Valvular disease
2.4 Congenital/acquired left heart inflow/outflow tract obstruction and congenital cardiomyopathies

3. Pulmonary hypertension due to lung diseases and/or hypoxia

3.1 Chronic obstructive pulmonary disease
3.2 Interstitial lung disease
3.3 Other pulmonary diseases with mixed restrictive and obstructive pattern
3.4 Sleep disordered breathing
3.5 Alveolar hypoventilation disorders
3.6 Chronic exposure to high altitude
3.7 Developmental lung diseases

4. Chronic thromboembolic pulmonary hypertension (CTEPH)

5. Pulmonary hypertension with unclear multifactorial mechanisms

5.1 Haematological disorders: chronic haemolytic anaemia, myeloproliferative disorders, splenectomy
5.2 Systemic disorders: Sarcoidosis, pulmonary histiocytosis, lymphangioleiomyomatosis
5.3 Others: tumour obstruction, fibrosing mediastinitis, chronic renal failure, segmental PH

1.2.2 WHO group I pulmonary arterial hypertension

The global burden of PAH is difficult to estimate as accurate diagnosis requires access to healthcare and specialist diagnostic tools including RHC which is limited in many developing countries. The incidence and prevalence from France is estimated at 2.4 cases/million annually and 15 cases per million respectively (139). In the UK, national audit data from 2013 reports prevalence rates of 49.2/million and 51.8/million in England and Scotland respectively (140). Historical data from Scotland suggests annual incidence of 7.6/million population (141). Information regarding the prognosis of idiopathic and familial PAH were derived from the National Institute of health (NIH) supported US registry in the 1980s, based on both prevalent and incident cases, in an era which predated PAH therapies. Based on this registry, very poor median survival of 2.8 years from diagnosis has been quoted (142, 143). Since that time a number of PAH therapies have been developed, and several large national registries have been established and reported improved survival in PAH. In the US REVEAL registry 1, 3 and 5 year survival rates of 85%, 68% and 57% respectively were observed, with a median survival of 7 years (144, 145). This registry is however in a cohort of predominantly prevalent patients, which may create survival bias. Data from France and the UK of incident PAH cases report similar 1 year survival rates of 88%.

Prognosis varies depending on the aetiology of PAH and comorbid conditions. Prognosis in PAH associated with CHD tends to be better than IPAH, while historically CTD associated PAH carried a significantly worse prognosis than IPAH prior to availability of therapeutic options. In the 2013 national audit data from the UK similar 1 year survival rates of incident cases of CTDPH vs IPAH of 89 vs 88% were observed. In Ssc associated CTDPH, 1 and 3 year survival rates 78% and 47% have been reported in comparison to 1 and 3 year survival rates of 92.7% and 73.3% in IPAH, familial and anorexigen associated disease, both from incident cohorts albeit different UK registries (146, 147). In SLE associated disease 1 and 3 year survival rates were 78 and 74% respectively, and 83% and 66% for rheumatoid arthritis, suggesting the aetiology of the CTD also has some influence on outcome. PAH is therefore a rare disease but one of significant mortality.

1.2.2.1 Pathophysiology

PAH is a syndrome characterised by progressive pulmonary arterial obstruction and remodelling as a consequence of excessive cell proliferation and impaired apoptosis, leading to an increase PVR and RV afterload. Remodelling mostly occurs in small to medium sized pulmonary arterioles <500μm and involves all three layers of the vessel wall. Endothelial dysfunction leads to an imbalance that favours vasoconstriction, in situ thrombosis and mitogenesis. Histological appearances are of muscularisation of distal and medial pre-capillary arteries, neointimal formation, infiltration of inflammatory and progenitor cells, thrombosis in situ and formation of complex lesions called plexiform lesions (148). Endothelial cells and PASMCs from patients with PAH display a pro-proliferative anti-apoptotic phenotype and a glycolytic shift in metabolism which has led to some analogies with cancer cells (149).

A number of growth factors act as mitogens and chemoattractants for SMCs, fibroblasts and endothelial cells including FGF-2 and PDGF (150). Levels of cytokines and chemokines such as IL-6, TNF and IL-1β are raised in PAH and may correlate with severity of disease (151). Monocytes, macrophages, T and B lymphocytes are found in plexiform lesions and autoantibodies to endothelial cells and fibroblasts have been isolated from the lungs of PAH patients. Inflammation therefore is thought to be an important contributor to progression of vascular remodelling and may be implicated as a triggering factor in PAH (152).

Perturbed angiogenesis is suggested by the development of plexiform lesions and altered levels of circulating pro-angiogenic progenitor cells in patients with IPAH. The precise role that disordered angiogenesis plays however is uncertain (153, 154). Alterations in the function of K^+ and Ca^{2+} channels have been linked to dysregulation of cellular homeostasis, promotion of SMC proliferation and alterations in pulmonary vascular tone. In PAH, reduced expression of voltage gated K^+ channels, specifically Kv1.5 is linked to induction of muscle contraction and vascular remodelling due to an imbalance in apoptosis and proliferation (155). Finally, roles for insulin resistance, obesity and sex hormones have been linked to development of PAH (156, 157). Both idiopathic and familial disease is more common in females, however animal studies suggest a protective effect of

oestrogens. Further study is required to better understand potential links with development of PAH.

1.2.2.1.1 Endothelial dysfunction

Endothelial dysfunction is reflected by reduced production of the vasodilators/growth inhibitors nitric oxide (NO) and prostacyclin (PGI2), and increased production of vasoconstrictor/co-mitogens, such as endothelin-1 and thromboxane A2 (158).

NO is produced in the endothelium by the action of endothelial NO synthase (eNOS). In PASMC NO stimulates soluable guanylate cyclase (sGC) to produce cyclic GMP (cGMP) which has antiproliferative properties in addition to causing vasodilatation. In the pulmonary circulation, the eNOS/NO/sGC/cGMP pathway is the principle driver of endothelium mediated vasodilation and focus of therapeutic targeting in PAH (159). In PAH, reduced NO bioavailability arises as a result of reduced NOS expression, consumption of NO by overproduction of free radicals by oxidative stress, and inhibition of NO synthesis (160-162). Additionally elevated levels of asymmetric dimethylarginine (ADMA) which is a competitive inhibitor of NOS have been found in patients with IPAH. Increased expression of phosphodiesterase type 5 (PDE-5) has been shown in both PASMC and the right ventricle, which is the enzyme responsible for cGMP degradation (163). PDE5 inhibition has also been exploited as a therapeutic target in PAH.

ET-1 regulates vascular tone causing vasoconstriction and inducing cell proliferation via ETA and ETB receptors located on PASMCs. ET-1 levels have been shown to be elevated in PAH as well as patients with heart failure and COPD (164, 165). Endothelial cells also express ETB receptor which is involved in release of NO and prostacyclin. ET-1 also interacts with matrix metalloproteinases (MMPs) causing fibrogenesis. Both selective (against ETA) and nonselective ETRAs have been developed as treatments in PAH.

Overproduction of serotonin by pulmonary artery endothelial cells has also been shown in PAH which acts on SMC and fibroblasts to cause vasoconstriction and remodelling (166). Abnormal cross-talk between endothelial cells and SMC in IPAH

has been linked to enhanced paracrine overproduction of serotonin and other pro-migratory pro-proliferative mediators (167).

1.2.2.1.2 Genetic mechanisms

PAH has a genetic component. Mutations in bone morphogenetic protein type II receptor (BMPR2) have been reported in >70% patients with one or more affected relatives (heritable PAH) but also 11-40% of those with sporadic IPAH (168-170).Penetrance is low with only ~25% of carriers developing PAH (171). Most cases of familial PAH have loss of function mutations in BMPR2 that promote cell proliferation. Modifier genes such as SERT may in part explain the variable penetrance, however it seems likely that aberrant BMPR2 function alone is insufficient to explain the subsequent development of PAH and lead to second hit hypothesis from environmental or comorbid conditions. Mutations in several other genes have been discovered, including ALK1 (172), the endoglin gene (173), SMAD9 (174), Caveolin-1 (175) and K+ channel subfamily K KCNK3 (176). Patients with BMPR2 and ALK1 mutations present with higher PVR, and present and die at younger age than those without (177, 178).

1.2.2.2 Diagnosis

Echocardiography is employed to detect suspected PH in symptomatic individuals with breathlessness or signs of RV dysfunction, or as a screening tool in at risk populations such as scleroderma. Doppler derived measurements of the peak velocity of blood crossing tricuspid or pulmonic valves allow estimation of the pressure gradient using a simplified Bernoulli's equation

$$PG = 4x\ (peak\ velocity)^2$$

Tricuspid valve regurgitant jets are more readily acquired and used for this purpose. Systolic PAP can then be estimated, as the sum of tricuspid valve regurgitant pressure gradient (TRPG) + estimated RAP. The presence of tricuspid regurgitation increases as sPAP increases and regurgitant jets are visualised by echocardiogram in the majority of PH patients. One study demonstrated TR in 74% of patients with PH (179), whilst another has reported appreciable TR jets in 80% patients with a sPAP above 35mmHg rising to 96% of those with sPAP >50mmHg

(180). RAP can be estimated from inferior vena cava collapsibility index by echocardiogram or clinically from assessing the extent of jugular venous pressure elevation. Impressive correlation with invasively measured sPAP has been demonstrated, with r = 0.89-0.97. There are however a number of limitations, reliance on the presence of tricuspid regurgitant jet, operator dependence and relatively high standard errors of estimation. Therefore, whilst echocardiography has been established as the imaging modality of choice in screening for PH it is not sufficient to diagnose PH.

Right heart catheterisation (RHC) is the gold standard for both diagnosis and haemodynamic assessment of patients with suspected PH. For standardisation of measurements the pressure transducer is zero levelled at the midthoracic line in the supine patient, halfway between the anterior sternum and table surface, which represents the level of the left atrium. PH is defined by the presence of mPAP ≥25mmHg at rest, however for a diagnosis of PAH, additional haemodynamic measurements are required;

1. Cardiac output (CO) must be normal or low. This is commonly measured using the thermodilution method which has been shown to provide reliable measurements in patients with very low CO or with severe tricuspid regurgitation.

2. Pulmonary artery wedge pressure (PAWP) < 15mmHg. PAWP provides an approximation of left atrial pressure by recording pressure measurements with a balloon-tipped pulmonary artery catheter wedged, with the balloon inflated, within a branch pulmonary artery. Measurement at end of normal expiration minimises the effect of swings in intrathoracic pressure with respiration. A PAWP >15mmHg suggests PH secondary to left heart disease (group 2 disease).

3. Raised pulmonary vascular resistance (PVR) ≥ 3 wood units. PVR is calculated by (mPAP – PAWP) / CO.

Additional haemodynamics measurements that are assessed include RAP, pulmonary artery or mixed venous oxygen saturations (SVO2) which have been shown to have prognostic significance in PH.

A resting mPAP ≥25mmHg is required for a diagnosis of PH. As discussed in section 1.1.1 mPAP increases with ageing, with the upper limit of normal of 20mmHg (24). It is unclear how to classify and manage patients with mPAP 21-24mmHg as most epidemiological and therapeutic studies have used mPAP ≥25mmHg as threshold for inclusion. These modest elevations in mPAP could represent early pulmonary vascular disease particularly if the TPG or PVR is high. Whether these patients go on to develop more significant pulmonary vascular remodelling and meet current diagnostic criteria for PAH is unknown as the natural history of such a group has not been widely studied. The exception to this is in scleroderma where screening for PH is widely carried out due to the lifetime risk of development of PAH. The presence of borderline mPAP is associated with higher risk of developing clinically significant PAH (181) and associated with poorer prognosis when raised TPG is also present. The consequence of delaying therapeutic intervention until PAH manifests is unknown. Current guidelines recommend close monitoring of patients with mPAP 21-24mmHg, particularly if they have an additional risk factor associated with PAH.

Before the 4th WSPH, PH was also defined by the presence of mPAP which rose to >30mmHg on exercise in the absence of resting PH. This has subsequently been removed from the updated diagnostic criteria. Exercise related mPAP rises with age as part of normal age related increase in vascular stiffness. Previous studies have not standardised the level, type and posture of exercise and it is therefore uncertain what represents a normal valve of exercise mPAP. Additionally, the prognostic and therapeutic significance of exercise induced PH with normal resting haemodynamics is unknown and further study in this area is required.

Despite increased awareness of the disease there is often considerable delay between the onset of symptoms and the diagnosis. The majority of patients are diagnosed with NYHA FC III-IV disease which has been shown to predict poorer survival. Data from the REVEAL registry found that 21% of patients had symptoms for more than 2 years before diagnosis, and so interest has focussed on striving to identify patients with PAH at an earlier stage and commence treatment before the development of RV failure. Due to the variable penetrance of mutations associated with FPAH, the benefit of genetic screening of asymptomatic relatives is uncertain. Furthermore, a monitoring strategy for mutation carriers has not been agreed, with some suggesting annual echocardiogram, and others advocating

investigating symptomatic relatives only due to lack of evidence for treating asymptomatic individuals. In scleroderma, annual screening of asymptomatic patients using modalities such as DLCO, biomarkers, echocardiography and RHC in those with positive findings or clinical signs is already underway. Focussed screening of at risk groups is suggested, but the majority of cases arise in sporadic patients in wider populations. Earlier diagnosis therefore relies on increasing awareness and education of clinicians who patients are likely to present to, such as cardiorespiratory physicians and rheumatologists.

1.2.2.3 Treatment

Over the past two decades the three major pathways underlying the development of PAH, the prostacyclin, nitric oxide and endothelin pathways, have been targeted for the development of PAH specific therapies. At the time of the 2nd WSPH in 1998, only epoprostenol, an intravenous prostacyclin analogue in addition to calcium channel blockers were known therapies. 15 years later at the time of the 5th WSPH, the therapeutic options have expanded considerably with 7 compounds approved, different modalities of administration available and a number of drugs under development. These pharmacological discoveries have led to considerable reduction in mortality and morbidity (182). Additionally, therapies from all three drug classes, prostacyclin analogues, phosphodiesterase-5 inhibitors (PDE-5i) and endothelial receptor antagonists (ETRA) have been shown to improve exercise capacity, functional status, symptoms and haemodynamics. Whilst some have been shown to delay time to clinical worsening, only Epoprostenol is proven to improve survival. Newer therapies Macitentan and Selexipag which have completed phase III studies in the last 3 years have also shown improvement in composite endpoint of morbidity and mortality. Table 1-2 displays current drug therapies licensed for use in PAH.

In addition to vasodilatory effects, ETRAs have been shown to improve pulmonary vascular endothelial function and beneficial remodelling in pre-clinical studies (183). PDE-5 inhibition has antiproliferative effects and in PAH models enhances myocardial contractility as a result of the pressure overloaded RV myocytes expression of PDE5 (184). As discussed above, the pathogenesis of PAH is complex and in addition to focusing drug development on overcoming vasoconstrictive

components, recent interest has arisen in targeting other components of pulmonary vascular remodelling, including inflammatory mediators, growth factors, BMPR2 mutations, metabolic dysfunction and calcium signalling. Preclinical studies into utility of Tocilizumab (an anti-IL-6 monoclonal antibody), Rapamycin (HDAC1 inhibitor), Apelin, PPARγ agonists and Rho kinase inhibitors such as Fasudil respectively targeting these pathways may provide novel therapeutic agents in the future (185).

Combination therapy because of the 3 signalling pathways involved is an attractive prospect for management of PAH. Recent meta-analysis has suggested combination therapy reduces time to clinical worsening, and improves haemodynamics and exercise tolerance (186). It is unknown if combination therapy upfront is of benefit. Current guidance recommends sequential combination therapy in those with unsatisfactory clinical response. The suggested initial therapy is based on NYHA functional class, with those in FC II treated with an oral agent and Epoprostenol reserved for those in FC IV (187).

Table 1-2. Drugs approved or completing phase III studies for treatment of PAH in UK.

Drug	route	Study	Outcome Measure					Reference
			6MWD	FC	Haemodynamics	TTCW	Survival	
Endothelin Pathway								
Endothelin receptor antagonists (ETRA)								
Bosentan	Oral	BREATHE 1 and 2	+ (44)	+	+	+	NT	(188)
Ambrisentan	Oral	ARIES 1 and 2	+ (51.4)	+	+	+	NT	(189)
Macitentan	Oral	SERAPHIN	+	+	+	NT	+*	(190)
NO Pathway								
PDE-5 inhibitors								
Sildenafil	Oral	SUPER-1	+ (45)	+	+	-	NT	(191)
Tadalafil	Oral	PHIRST	+	-	+	+	NT	(192)
Soluable guanylate cyclase stimulator								
Riociguat	Oral	PATENT 1 and 2	+ (35.8,51)	+	+	+	NT	(193, 194)
Prostacyclin Pathway								
Prostacyclin analogues								
Epoprostenol	IV		+	+	+	NT	+	(195, 196)
Iloprost	Inhaled	AIR	+	+	+	+	NT	(197)
Prostaglandin Receptor Agonist								
Selexipag	Oral	GRIPHON					+*	(198)

1.2.3 WHO group 3 PH associated with hypoxic lung disease

Pulmonary hypertension associated with chronic lung disease is one of the most common forms of PH. The true prevalence is unknown as echocardiography is known to be unreliable in lung disease patients making accurate noninvasive diagnosis difficult in large population based studies (199). It is known, however, that the prevalence of PH varies with both the underlying aetiology and severity of lung disease, and its development is associated with both exercise limitation and worse prognosis. Unlike group I PAH, where development of pharmacological therapies has substantially progressed in the last decade, with the exception of provision of oxygen therapy there are no proven therapeutic options.

1.2.3.1 Epidemiology

1.2.3.1.1 Chronic obstructive pulmonary disease

Studies in patients with advanced COPD have shown a high prevalence of PH with up to 90% having a mPAP >20mmHg. The reported prevalence however varies widely, dependent on the definition of PH, methods used to determine pulmonary pressures and the population studied. The absence of large epidemiological studies means the true prevalence of PH in mild to moderate COPD is unknown. Relative to other forms of PH, COPD largely causes modest haemodynamic changes at rest with mPAP typically in range 20-35mmHg. However, even moderate levels of exercise have been shown to cause further rapid rise in mPAP likely as result of impaired vascular distensibility and recruitment (200). The presence of mild PH, with mPAP >18mmHg is associated with increased risk of hospitalisation with exacerbations (201). During episodes of acute respiratory failure mPAP may rise by as much as 20mmHg but return to baseline following recovery of the exacerbation (202). The rate of PH progression is normally slow, typically in the range of 1-3mmHg/year in small studies with serial RHC in COPD patients (203).

There have been a number of RHC studies in patients with severe COPD undergoing evaluation for lung volume reduction surgery (LVRS) or lung transplantation. Scharf et al reported the RHC results of 120 patients with severe emphysema screened for participation in the National emphysema treatment trial (NETT) (204). 91% had an mPAP >20mmHg with a mean mPAP 26.3 ± 5.2mmHg. Vizza et

al observed similar results in 168 patients listed for lung transplantation with mean mPAP 25.6mmHg (205). Thabut et al reported a retrospective review of 215 patients with severe COPD (mean FEV1 23.9% predicted) whom underwent RHC as part of evaluation for LVRS or transplantation and found PH was present (using traditional definition of mPAP >25mmHg) in 50.2% with mean mPAP of 26.9mmHg (206). Cuttica et al found remarkably similar prevalence with a retrospective review of 4930 COPD patients listed for transplantation (207). Whilst 48% had mPAP ≥25mmHg, 30% had both mPAP ≥25mmHg and PAWP ≤15mmHg highlighting prevalence of coexistent pulmonary venous hypertension. Finally, in a large study of 998 COPD patients with less severe airflow limitation (mean FEV1 33%) and hypoxaemia, mPAP was 20.3mmHg, with a prevalence of PH (defined as mPAP >20mmHg) in approximately 50% of patients hospitalised for COPD (208).

The development of PH in COPD has been shown to have significant prognostic relevance, with inverse correlation between mPAP or PVR with survival (209, 210). It is suspected that the improved survival of hypoxaemic COPD patients with LTOT relates to improvement of pulmonary haemodynamics, although mPAP remains a prognostic variable in LTOT treated patients. In recent study, the 5 year survival of COPD patients with mPAP >25mmHg was 36.3% in comparison to 62.2% without PH. Pulmonary haemodynamics were stronger prognostic variable than either FEV1 or gas exchange variables (210).

1.2.3.1.2 Interstitial lung disease

Idiopathic pulmonary fibrosis (IPF) is a progressive fibrosing interstitial lung disease of unknown aetiology with a median survival of 2.5 to 5 years (211, 212). PH has been reported in 8.1% and 14.9% of patients at time of diagnosis (213, 214), rising to 20-50% in advanced disease at time of evaluation for transplant and >60% with end stage IPF (215-217). Serial RHC has shown progressive PH from a prevalence of 38.6% at time of transplant evaluation to 86.4% at time of transplantation. Rapid progression of PH has also been reported. Like COPD, the PH is usually mild, in a retrospective study of 135 patients, mean mPAP was 31±6mmHg (218). Shorr et al reported on 2,525 IPF patients listed for transplantation (219). Of the 46.1% whom had PH, mean mPAP was 34.2±9.9mmHg, although 18% had a PAWP >15mmHg suggesting co-existent

pulmonary venous hypertension. Poor or even no correlation between lung function (219, 220) or HRCT fibrosis score (221) and severity of PH has been reported. The development of PH has been associated with more pronounced exercise capacity limitation due to circulatory impairment in comparison to IPF patients without PH but similar lung function (216, 222). The presence of PH is associated with an almost 3 fold increase in the risk of death (220, 223). Both echocardiography defined PH (sPAP >50mmHg) and RHC (with even trivial increase to an mPAP of >17mmHg) has been associated with poorer survival (213, 220). In one study, the 1 year mortality in those with PH IPF was 28% compared to 5.5% in those without (220).

1.2.3.1.3 Combined pulmonary fibrosis and emphysema syndrome

PH is particularly prevalent in combined pulmonary fibrosis and emphysema (CPFE) syndrome with estimates approaching 30-50% of patients. CPFE is characterised by predominantly upper lobe emphysema with lower lobe fibrosis in association with marked impairment of gas exchange demonstrated by low DLCO (224). The incidence is unknown but case series suggest it may compromise up to 35% of patients with IPF (225). Prognosis is poor, with a 5 year survival of 55% (226). Unlike COPD and IPF, often severe PH is seen with markedly reduced DLCO but largely preserved lung volumes. At RHC, mPAP >35mmHg occur in 68% and >40mmHg in 48% of patients (227). The development of PH is associated with poor survival (228) with reduced CI being a strong prognostic determinant. 1 year survival of only 60% has been reported (227).

1.2.3.2 Pathophysiology

The pathophysiology of PH in patients with lung disease is complex and likely arises due to a combination of HPV, vascular inflammation and remodelling, and loss of the vascular bed as a result of parenchymal destruction. Chronic effects of hypoxia on the pulmonary circulation is the basis of many animal models used in the study of pulmonary hypertension therapies. Chronic alveolar hypoxia results in a sustained elevation in pulmonary vascular resistance due to vasoconstriction and induces vascular remodelling. Whilst undoubtedly one of the initiating factors in development of PH in lung disease, the failure of oxygen therapy to

subsequently reverse PH suggests the resultant structural changes in the pulmonary circulation are the major factor.

In COPD, autopsy specimens from patients with severe disease have demonstrated muscularisation of pulmonary arterioles which can extend to the periphery of the lung in precapillary vessels as little as 20μm in diameter (229, 230). Muscularisation can also be seen in post capillary veins and venules. Intimal hyperplasia has been observed in both mild and endstage COPD. Complex plexiform lesions of PAH have not been demonstrated, but reduction in total number of pulmonary vessels has been shown in both angiographic and autopsy studies (231, 232). The changes in vessel structure are accompanied by endothelial dysfunction and alteration in expression of growth factors and antiproliferative mediators that favour cell proliferation and vascular contraction. Whilst the severity of hypoxaemia has been related to the increase in both PAP and PVR, pulmonary vascular remodelling also occurs in non-hypoxaemic mild COPD patients (233, 234). Regional hypoxia in under ventilated areas of the lung in absence of systemic hypoxaemia may be present in COPD and therefore regional remodelling related to HPV may still occur. Tobacco smoke exposure is thought to play an important role in development of pulmonary vasculopathy (235). “Healthy” smokers without demonstrable airflow obstruction have been shown to have intimal hyperplasia, reduced eNOS expression, increased VEGF and inflammatory cell infiltrate in pulmonary arteries at a similar level to COPD patients (234, 236-238). In experimental models, cigarette smoke is known to cause endothelial dysfunction, and when exposed to both cigarette smoke and hypoxia, animal models are seen to develop more severe pulmonary hypertension and remodelling, suggesting a possible synergistic effect (239, 240). This has led to some to postulate that smokers are perhaps more susceptible to effects of hypoxia on the pulmonary vasculature as a result of pulmonary vascular dysfunction initiated by cigarette smoke. The role inflammation plays in the development of PH is poorly understood. It is known that systemic inflammation appears to be a risk factor for development of PH, with some studies showing a correlation between pro-inflammatory cytokines such as IL6 and c-reactive protein and PAP (241, 242). Additionally hyperviscosity from polycythaemia, compression of the alveolar vessels from hyperinflated emphysematous lungs, hypercapnic acidosis related

vasoconstriction and increase in PAWP as result of dynamic hyperinflation may play a role (243).

In IPF, vascular remodelling with intimal proliferation and medial thickening in both muscularised pulmonary arterioles and veins have been demonstrated in pathological specimens consistent with those seen in other hypoxic lung diseases (244). In addition to vessel ablation in dense areas of fibrosis, occlusive venopathy and vascular remodelling is present in non-fibrotic areas suggesting a potential role for other mechanisms (245). Overexpression of inflammatory cytokines and growth factors including PDGF and fibroblast growth factor are implicated in the pathogenesis of IPF (246, 247). Decreased levels of prostaglandin E2 (PGE2) which opposes fibrotic response and may increase expression of TGF-β, has been found in bronchoalveolar lavage in IPF patients (247). Additionally ET1, a potent vasoconstrictor and smooth muscle mitogen found in increased levels in IPAH, has been found in elevated concentrations of IPF patients both with and without PH (248, 249). Arterial levels of ET-1 have been shown to correlate inversely with $Pa0_2$ and directly with PAP in IPF patients (250). PDGF, TGF-β, and fibroblast growth factor have been implicated in the pathogenesis of both IPAH and hypoxia induced PH suggesting the possibility of common inflammatory pathways in parenchymal and vascular remodelling seen in IPF PH and potentially a shared therapeutic target (246).

1.2.3.3 Severe pulmonary hypertension in hypoxic lung disease

Whilst mild PH in chronic lung disease may be prevalent, severe PH, defined as mPAP ≥35mmHg is rare occurring in only 3-5% of COPD patients. These patients typically display less severe respiratory function compromise and the PH is therefore regarded as disproportionate. Haemodynamic or CMR evidence of RV dysfunction more commonly seen in PAH patients is often seen. Severe PH is postulated to occur in individuals with excessive HPV response, including those with genetic polymorphisms of the serotonin (5HT) transporter gene (251). Whether these patients should be managed as Group 3 disease or possibly regarded as having co-existent Group I disease is uncertain. Recent data from large national PH registries has reported on increasing prevalence of comorbid disease in PAH diagnoses with up to 17% having COPD (252). Previous literature on “out of proportion” PH in lung disease has been clouded by use of differing levels of mPAP

between 35-40mmHg, and varying degrees of lung function impairment in its definition. The most recent world congress has suggested classification system in efforts to standardise therapeutic trials and also to address the issue of what represents comorbid lung disease or group 3 disease (253). A level of mPAP ≥35mmHg is suggested to define severe PH in lung disease.

Cuttica et al reported <1% of COPD patients listed for transplant had a mPAP >35mmHg at RHC (207). Severe PH was found in 5% of emphysema patients from the NETT trial (254), although this is probably an underestimate as severe PH was one of the exclusion criteria for the study. In the studies from France, Thabut et al found 13.5% of patients with advanced COPD had severe PH (206), whilst Chaout et al reported a prevalence of 5.8% with mPAP >35mmHg and 2.7% mPAP >40mmHg (208). The majority however had an alternate cause for PH. In the remaining 1.1%, clinically these patients displayed less severe airflow obstruction but more severe hypoxaemia, hypocapnia and grossly impaired DLCO. Those with a mPAP >40mmHg had worse survival than both those with no PH (mPAP <20mmHg) and those with mild-moderate PH (mPAP 20-40mmHg).

Data on the prevalence of severe PH in IPF studies is limited. Shorr et al reported 9% of IPF patients had an mPAP>40mmHg (219). Letteri et al whilst not specifically reporting on frequency of severe PH, found mPAP ranging up to 46mmHg in the cohort with a linear correlation between mPAP and outcome, suggesting greater risk of mortality in those with severe PH similar to COPD patients (220). Severe PH associated with CPFE is thought to be relatively more common, reported in 68% at RHC and 72% by echocardiogram in two small case series (227, 228).

Severe PH associated with lung disease whilst rare, is therefore a disease with severe morbidity and mortality, with some features, such as relative preservation of lung function, greater degree of RV dysfunction and haemodynamic compromise, that have generated interest in the potential for use of pulmonary vasodilator therapies.

1.2.3.4 Treatment

Unlike PAH, there are no studies to support the use of pulmonary vasodilator therapy in patients with hypoxic lung disease PH. Clinical studies examining the

effect of PAH therapies in group 3 disease have however been in small population sizes, with poorly defined levels of PH often using echocardiography alone to diagnose PH or using mixed populations of lung disease patients with and without PH. Management therefore focuses on treating the underlying lung disease, excluding an additional aetiology for the PH such as thromboembolic disease and consideration of lung transplantation. In COPD, in addition to improving mortality LTOT has been demonstrated to stabilise or even slightly improve mPAP. In the MRC trial, at 5 years mPAP increased by 2.7mmHg/year in the no oxygen group whilst remained unchanged in the oxygen therapy group (255). In the NOTT study, mortality was 11.9% in the continuous oxygen group versus 20.6% in the nocturnal oxygen group at 1 year (256). In the 117 patients whom underwent haemodynamic evaluation at 6 months, mPAP showed a slight rise in the nocturnal oxygen group whereas an average decrease of 3 mmHg/year was seen in the continuous therapy group. PVR also fell by 11.1% in the continuous oxygen group and rose by 6.5% in the nocturnal oxygen patients. Smaller studies have also shown fall in mPAP of 2.1mmHg per year after initiation of oxygen therapy and long term stabilisation of PH in COPD patients receiving LTOT (257, 258). In severe PH with lung disease however results are less encouraging. In the NOTT study, those patients with high PVR did not demonstrate a survival benefit with continuous oxygen therapy whereas low PVR patients did. Additionally autopsy studies show no significant difference in structural pulmonary vascular remodelling in those receiving LTOT and those not (259). Therefore it would seem that LTOT has the potential to stabilise pulmonary haemodynamics, but does not lead to a normalisation of haemodynamics or reversal of vascular remodelling. In ILD, there is limited data on the use of LTOT and similar benefit has therefore not been demonstrated. The use of LTOT is recommended to maintain arterial saturations above 90% as HPV is known to play a role in the pathogenesis.

1.2.4 The right ventricle in pulmonary hypertension

Right ventricular failure is the major cause of death in patients with PAH, and it is increasingly recognised that both survival and functional status relate to the ability of the RV to adapt to the increasing levels of afterload that occur as the disease progresses. As a result of sustained elevation in PVR and reduction in compliance of the pulmonary circulation that slowly develops in PAH, the RV initially undergoes homeometric adaptation characterised by concentric remodelling and preservation of systolic and diastolic function. Eventually as the disease progresses, the RV cannot maintain adaptive hypertrophy to match its afterload, and RV dilates in an effort to maintain SV and maladaptive remodelling associated with eccentric hypertrophy and impaired function occurs (260). At this point there is no further increase in contractility, or even a decrease may occur despite continued elevation in load, and "uncoupling" of the RV from the pulmonary circulation. RV dilatation increases wall tension which in turn increases myocardial oxygen demand whilst decreasing RV perfusion leading to ongoing cycle of further compromised RV contractility and dilatation. Additionally, due to ventricular interaction, RV enlargement decreases LV filling due to pericardial constraint, which further decreases SV and therefore systemic blood pressure, which may add to RV ischaemia from reduced coronary perfusion pressure. Prolongation of RV contraction occurs as RV function declines, with resultant ventricular asynchrony. The RV free wall continues to contract whilst the LV has already relaxed in its early diastolic phase, leading to left ward septal bowing which further impairs LV filling (261). This, together with systolic and diastolic RV dysfunction and fall in RV SV culminate in the marked fall in CO seen in severe PAH. Chronic neurohormonal activation (adrenergic and angiotensin pathways), oxidative stress, immune activation and cardiomyocyte apoptosis have also been implicated in the progression of RV failure and deterioration in contractility in PAH (262-264). Increases in RV volumes leads to functional tricuspid regurgitation as a result of annular dilatation which in turn causes RV volume overload, and further RV remodelling and annular dilatation. Therefore, once the onset of RV functional decline is initiated, a cycle of events is triggered which spirals towards RV failure. In comparison to the LV, ventricular enlargement occurs earlier in PAH then in the pressure overloaded LV as a result of greater wall stress experienced by the thin walled RV. However, significantly less fibrosis occurs often limited to the RV septal insertion points and constitutes <10% of the ventricular volume (265,

266). This explains why patients whom undergo lung transplantation restore RV function despite severe RV impairment prior to transplantation (267, 268).

1.2.5 Monitoring and prognosis in pulmonary hypertension

Although remodelling of the pulmonary circulation is the cause of PAH, symptom severity and survival have been shown to relate to RV function. A number of prognostic indices have been identified from both large cohorts from National registries and smaller imaging modality studies. Most reflect right ventricular function, such as right atrial pressure and cardiac index from haemodynamic studies (142, 269), or Tei index and tricuspid annular plane systolic excursion (TAPSE) from echocardiographic studies (270-272). Traditional prognostic measures for evaluating both severity of disease and treatment response however have a number of limitations reflecting the complexity of the geometry of the RV with the use of non-invasive tools.

1.2.5.1 Echocardiography

Echocardiography, being cheap, portable and widely available is readily employed to assess RV function and its use as a prognostic tool in PH has been extensively studied. There are however a number of important limitations. The complex anatomy of the RV means that accurate measurement of size and volume using 2D imaging modality is difficult, and measurements that rely on geometric assumptions can be complicated to adopt for RV evaluation by echo. The technique is highly operator dependent and hampered by poor acoustic windows due to body habitus or in some clinical conditions such as emphysema. Inaccuracies and variability may arise from other factors such as patient or probe position, image quality or phase of respiration. There is a lack of standardised models for calculation of RV volumes and function. Additional, when using echo as a monitoring tool, as progressive RV dilatation occurs changes in heart position and orientation can be seen that could influence serial measurements (273).

The most reported prognostic echo parameter of RV function associated with mortality is the presence of pericardial effusion. Increased right atrial pressure impairs venous and lymphatic drainage of the myocardial and presence of pericardial effusion is therefore a reflection of RV dysfunction. Pericardial

effusion has been reported in 54% of severe IPAH cases, with larger effusion associated with RHF, impaired exercise tolerance and poor 1 year survival (274). In prospective study, presence of pericardial effusion was the strongest predictor of mortality (270) which has been confirmed by recent data from the REVEAL registry (144). However, the studies give no diagnostic criteria and therefore what size of pericardial effusion should be considered significant needs further study.

TAPSE is a measure of the longitudinal movement of the lateral tricuspid annulus towards the RV apex and is used to reflect RV systolic function. In the normal RV, longitudinal shortening accounts for the greater proportion of RV volume change during ejection. TAPSE has been shown to correlate with RVEF (275). In PAH TAPSE <1.8cm shown to be associated with RV dysfunction and reduced survival (272). TAPSE is influenced by coexistent LV dysfunction (276) and its relationship to RV function is less accurate in those with significant tricuspid regurgitation (277).

The myocardial performance or Tei index is an echocardiography derived measure of global RV function (271). It has been shown to have prognostic significance in PAH (278), however is influenced by volume loading of the patient, is less reliable during tachycardia and interpretation is highly operator dependent. Other echo parameters known to have prognostic significance in PH include greater RV diameter (279), eccentricity index (270) and right ventricular dysynchrony (280).

Some RCTs of PH targeted therapies have reported changes in echocardiography derived indices in small subsets of patients. Chronic epoprostenol therapy improved RV end diastolic area, left ventricular eccentricity index and maximum tricuspid regurgitant velocity (281). Bosentan improved ratio of RV to LV end-diastolic area, left ventricular eccentricity index, Tei index, RV ejection time, SV and severity of pericardial effusion in 56 PAH patients after 16 weeks of therapy (282).

1.2.5.2 Right heart Catheterisation

As previously discussed in section 1.2.2.2 RHC is the gold standard for diagnosis of PH. Haemodynamic studies have identified RAP, SVO2, CO and CI, all indices reflecting RV function, to be significant predictors of survival (142, 144, 269, 283). In addition, mPAP at diagnosis was predictive of survival in the IPAH cohort from

the NIH registry in patients before the availability of PAH specific therapies. However, as mPAP is a product of both PVR and RV function, rise in mPAP is subsequently followed by fall in late disease as the RV fails, and therefore relationship between mPAP and survival is lost. It has been demonstrated that RV power is distributed approximately 77% for steady state resistance (PVR) and 23% pulsatile component (compliance SV/PP) (284). It is known that resistance and compliance are inversely related to each other in the pulmonary circulation, and therefore in early disease large decreases in compliance are seen for small increases in PVR. It is not therefore surprising that measurements of compliance at RHC, SV/PP, in patients with IPAH is an independent predictor of mortality (285).

Current management guidelines recommend repeat haemodynamic measurements at 3-4 months following addition of new PAH therapy, or at times of clinical worsening. Improved survival has been reported in patients with fall in total pulmonary vascular resistance of at least 30% (286), or improved CI and mPAP (287). However, recent study has shown continued progression in RV failure and worse survival in this subset despite improvement in PVR at RHC (288). Additionally, RHC is invasive and needs to be performed in centres with appropriate expertise. RHC is associated with small risk of morbidity such as pneumothorax or cardiac arrhythmia and mortality. A multicentre review of over 7000 RHC procedures carried out in experienced PH centres reported serious adverse events in 1.1%, and mortality rate of 0.055% (289). It is therefore not practical or acceptable to patients as a methodology for regular monitoring of disease progression and therapeutic response. Research therefore is driven by the need for simple, reproducible noninvasive measures of RV function to improve management of patients with PAH and explore optimal therapeutic approach to treat both the pulmonary circulation and RV as a unit.

1.2.5.3 Six minute walk test

Exercise testing in the form of either a walking test or cardiopulmonary exercise test in addition to assessing the patient's functional capacity can provide a measure of RV function due to the relationship between cardiac output, oxygen delivery and consumption. The 6MWT is commonly employed as it is easy to perform, is the commonly accepted end point for studies evaluating treatment

effect in PAH, and has been shown to correlate to peak oxygen pulse (which in itself correlates to SV), CO, total pulmonary resistance and to fall in proportion to worsening FC (290). Absolute 6MWD has been demonstrated to be a strong prognostic variable both at diagnosis and whilst on therapy. At baseline, 6MWD less than 332m, or <250m with associated drop in oxygen saturations of >10% have been shown to predict poor survival (286, 290). Improvement in absolute 6MWD to >380m after 3 months of therapy has been shown to confer improved survival. However, change in 6MWD does not seem to predict survival benefit, and what constitutes a relevant change in order to confer survival advantage is unknown. A pooled analysis of 10 placebo controlled drug trials in PAH found that Δ6MWD accounted for only 22.1% of the treatment effect and may therefore not be a sufficient surrogate end point (291). An average Δ6MWD of 22.4m favouring active treatment over placebo was seen across the studies, with a calculated minimum of 41.8m corresponding to a significant reduction in clinical events. These studies however are confounded by select population for trial entry including a threshold minimum distance walked.

Additionally, 6MWD is influenced by a number of confounders including patient motivation, age, weight and comorbidity such as musculoskeletal disease. Recent study looking at utility of exercise variables including 6MWT to predict outcome in IPAH versus associated PAH found no variable independently predicted survival or time to worsening in the associated PAH group, whilst distance walked was of significance in those with IPAH (292). Expressing 6MWD as a percent of predicted which would take into account confounders such as age and sex confers no advantage over absolute distance walked in relation to outcome and therefore raises concerns over the reliability of the test as an outcome measure (293). In those with IPAH, exercise and respiratory training resulted in mean increase of 111m in 6MWD compared with controls without any measurable effect on RV function (294). Additionally, a ceiling effect may occur whereby in those with increasing baseline walk distance treatments that improve haemodynamics and symptoms may not translate into further additional significant increment in distance walked. This has been demonstrated suggesting reduced sensitivity of the 6MWD in those PAH patients walking >450m (295). Current guidelines recommend treatment goal of achieving 6MWD above 500m, however in practice few patients

will achieve this and better indirect measures of RV function for monitoring therapeutic response are needed.

1.2.5.4 NTproBNP

BNP is secreted by ventricular cardiomyocytes in response to increased stretch as a result of an increase in cardiac wall stress and play important roles in regulation of blood pressure, volume and sodium homeostasis. The BNP precursor is split into biologically active peptide and the more stable N terminal fragment NTproBNP (296). Levels of NTproBNP (and BNP) have been shown to reflect severity of RV dysfunction with inverse correlations demonstrated with RVEF and cardiac output, and correlates with haemodynamics measurements of mPAP, RAP and total pulmonary vascular resistance in PAH (297, 298). Changes in levels have been shown to parallel haemodynamics and functional status of PAH patients during treatment, and relative change in NTproBNP reflects changes in CMR indices of RV structure and systolic function. High NTproBNP levels or in particular increasing levels during follow up have been shown to be independent predictors of mortality (299-301). There are however no validated cut off levels of NTproBNP and its value lies in a change in level on an individual patient basis as an indication of a decline in RV function but not the extent of deterioration.

1.3 Cardiac MRI in pulmonary Hypertension

CMR offers the opportunity of a more comprehensive approach to the non invasive assessment of patents with PH, simultaneously evaluating RV status, vascular stiffness, pulmonary blood flow and potentially coupling of the RV-PA circuit. Quantification of RV volumes or ejection fraction reflects cardiovascular adaptation to chronic pressure overload, however investigation of the RV-PA circuit as a whole and coupling of RV contractility to arterial load may provide insights into the discrepancy seen in progression of RV dysfunction despite improvements in PVR with PH therapies. The high accuracy and interstudy reproducibility of CMR derived indices of ventricular structure and function have demonstrated superiority over 2D echo, although the interstudy reproducibility of RV parameters is lower than that of the LV due to the heavy trabeculation seen (64). CMR is therefore ideally suited to non invasive serial monitoring of PAH patients in assessing treatment response.

1.3.1 Ventricular mass, volume and function

A number of studies in PAH have demonstrated significantly raised RV end diastolic (RVEDV) and end systolic (RVESV) volumes, with impaired systolic function determined by reduced RVEF, CO and SV in comparison to normal subjects (58, 302, 303). Figure 1.1 shows transverse and sagittal MRI images of the RV in a normal subject in comparison to a patient with IPAH.

Increasing RVM has been shown to correlate with mPAP (r=0.75) in IPAH (57). RV hypertrophy as previously discussed is an adaptive response to the increased afterload in PH. It is perhaps not surprisingly that RVM is not a strong predictor of mortality however, as RV failure in late disease is more characterised by progressive RV dilatation with reduced contractility. Reduced LVEDV and LV peak filling rate but similar LVM have been demonstrated by CMR in patients with PH in comparison to healthy controls (304). Using tagged MRI, a non invasive technique for interrogating 3D motion and deformation of myocardium, demonstrated interventricular asynchrony with prolonged RV contraction in comparison to LV (261). This asynchrony led to decreased LV diastolic filling, septal bowing and reduced LVEDV. A low baseline SV, RV dilatation (increased RVEDVI) and impaired LV filling (reduced LVEDVI) measured by CMR independently predicted mortality in 64 patients followed up for 32 months (41). RVM did not have a significant relationship to mortality. Mauritz et al demonstrated that progressive RV functional decline is characterised by both reduction in longitudinal and transverse shortening until a plateau is seen in longitudinal shortening (305). Further progressive decline in RV function characterised by reduced transverse shortening related to increased LVSB was seen in subsequent nonsurvivors at 4 years. Transverse shortening is therefore a CMR index that can be used to monitor RV functional decline in end stage PAH, which is not assessed by TAPSE at echocardiogram.

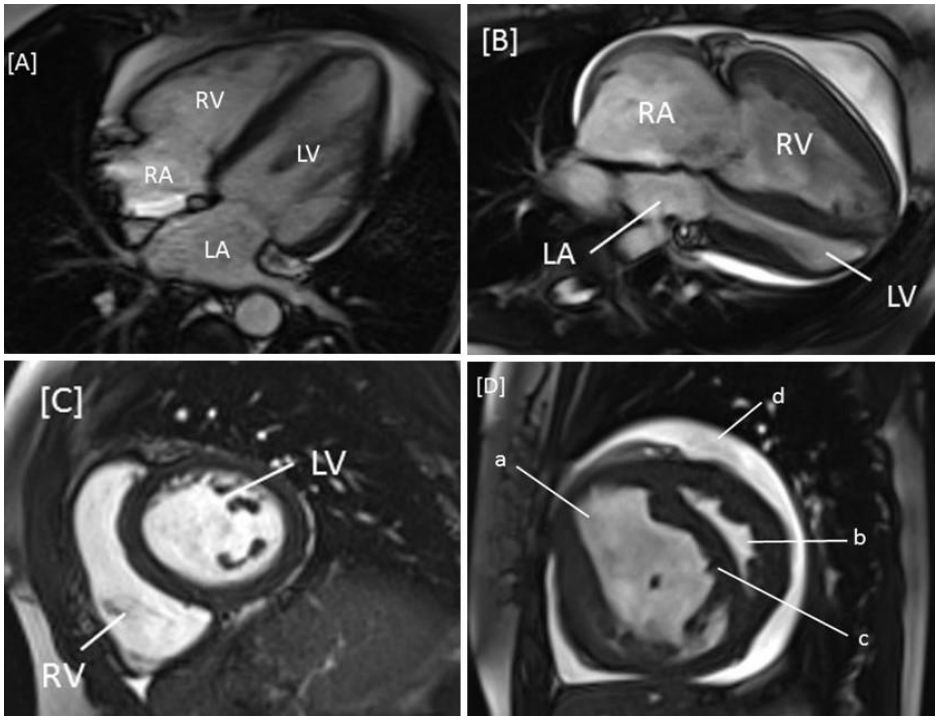

Figure 1.8 Cardiac MRI images of a normal subject in comparison to patient with pulmonary arterial hypertension.

Panels A and C display transverse and short axis views in a normal subject whilst panels B and D show IPAH patient. In Panel B, gross enlargement of right atrium (RA) and ventricle (RV) is seen, with compression of left sided chambers (LA, LV). In Panel D, note enlarged RV (a), small underfilled D shaped LV (b), septal bowing (c) and pericardial effusion (d).

1.3.2 Pulmonary blood flow and vascular stiffness

As previously discussed in section 1.1.3, phase contrast velocity mapping is a MRI sequence that allows measurement of velocity and flow, or interrogation of flow profiles, across valves or within blood vessels. It has advantages over thermodilution measures of SV or CO as it is both noninvasive, and, as it is averaged over a number of cardiac cycles, also less influenced by changes in SV between cardiac cycles and when measured at level of aorta or pulmonary artery, not affected by TR. Volumetric RVSV tends to overestimate actual SV in presence of considerable TR which can occur in PH patients with RV failure as it is impossible to determine what proportion of flow moves back through the tricuspid valve in preference to ventricular ejection. In PH however, aortic blood flow or LVSV has been shown to more accurately reflect actual SV measured at RHC (306). Phase contrast MR flow is known to be less accurate in presence of turbulent blood flow which occurs in pulmonary artery in PH patients. Figure 1.2 shows cross section view through the main pulmonary artery in a patient with IPAH with demonstrable turbulent PA flow. For SV determined by PA flow versus invasive SV determined by Fick principle, correlation co-efficients were r=0.71 (mean difference -4.2ml, limits of agreement 26.8 and -18.3ml) and for RVSV r=0.73, in comparison to SV by LV volumes vs Fick, r=0.95 (mean -0.8ml, limits of agreement 8.7 and -10.4ml). In the absence of intracardiac shunt, aortic flow or LV volumes is therefore the preferred method for assessing stroke volume in PAH.

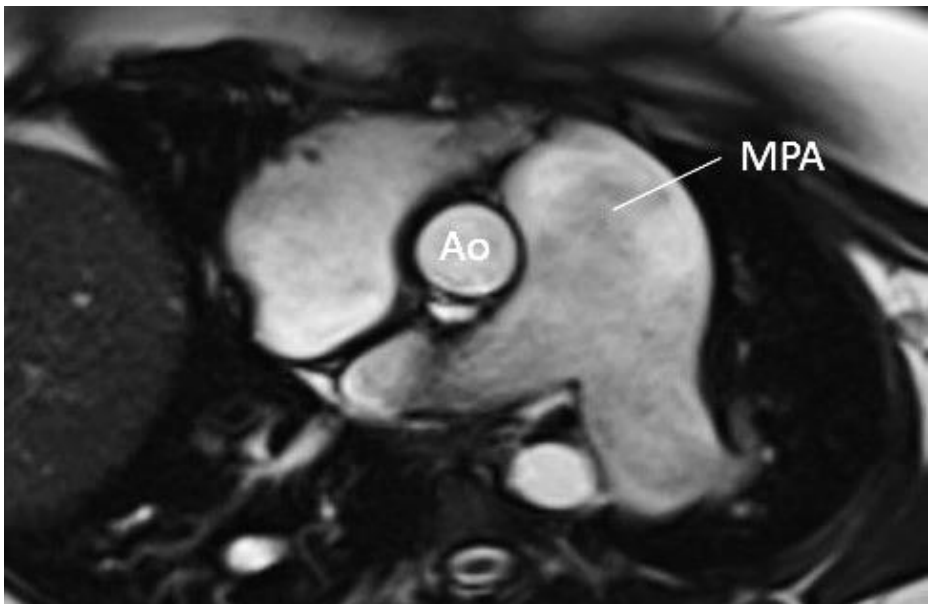

Figure 1.9 Cross sectional image of dilated pulmonary artery in patient with IPAH.

Turbulent blood flow clearly seen in enlarged main pulmonary artery (MPA) in comparison to aorta (Ao).

CMR has shown reduced peak systolic velocity and greater retrograde flow in pulmonary arteries of PAH patients. Retrograde flow was proportional to resistance and inversely to flow volume (307). PA flow, peak velocity and distensibility were significantly lower in 25 PAH patients in comparison to matched controls (308). Strong correlations between average velocity of pulmonary blood flow and mPAP and PVRI have been demonstrated (r= -0.86), suggesting a possible role in non invasive diagnosis of PAH (309).

As previously discussed, it has been shown that an inverse curvilinear relationship exists between compliance and mPAP, so large changes in compliance occur at small increases of mPAP in early PAH. At a level of a mPAP of 40mmHg little further decrease in compliance occurs, i.e. vessels become stiff and indistensible (310). Increased stiffness (reduced compliance) causes higher RV pulsatile workload, decreased contractile performance and enhanced energy transmission to smaller vessels increasing vascular damage. Invasive haemodynamic studies in patients with PAH have shown that those with lower SV/PP of <0.81 ml/mmHg, had a less than 40% 4 year survival compared with 100% 4 year survival in those with value above 2 (285). CMR derived relative area change (RAC) of the proximal pulmonary artery can be used to approximate compliance of the proximal pulmonary circulation. Vessel wall stiffness can be approximated by

$$\text{Ln (sPAP/dPAP)/(}\Delta\text{ 2A/A)}$$

where sPAP/dPAP is the pulmonary artery pulse pressure, and A is the area of the vessel (311).

It has been shown that in pulmonary hypertension, sPAP/dPAP is a linear relationship through a wide range of PA pressures, implying ratio is constant (11). Therefore, ΔA/A (RAC) is inversely proportional to stiffness (and a measure of compliance of PA circulation).

RAC (by CMR) = (max PA area – min PA area)/min PA area *100% (312, 313)

Gan et al reported a decrease in RAC (20% vs. 58% in controls) in 70 patients with PAH, and the same inverse curvilinear relationship between RAC and mPAP was demonstrated (314). Both reduced RAC and SV/PP were predictive of increased

mortality. RAC has also been demonstrated to correlate with 6MWD (r^2 = 0.61) and RAC <20% predicted poor functional status (defined as 6MWT <400m) with sensitivity and specificity of 82% and 94% respectively (315). Reduction in RAC has been proposed as a marker for early pulmonary vascular disease in a recent study by Sanz et al (310). 75 patients with PH were compared to 13 patients without resting PH but exercise induced rise in PA pressure (EIPH), and 13 normals. In EIPH, despite normal PA size, reduced compliance and capacitance was observed. A RAC of <40% had a sensitivity of 93% and specificity of 63% for presence of PH.

Whilst there is evidence that treatment causes a reduction in PVR, it is unknown how disease targeted therapies affect compliance and whether this is a useful measure of treatment efficacy. Furthermore, in hypoxic lung disease associated with pulmonary hypertension, whilst evidence is growing on cardiovascular risk and increased peripheral arterial stiffness in COPD (316), whether the use of RAC and measures of compliance in this population is of clinical benefit.

1.3.3 Diagnosing pulmonary hypertension

At present the utility of CMR in the diagnosis of PH is lacking, with somewhat contradictory studies. Correlations between mPAP or sPAP and CMR derived RVM, pulmonary blood flow average velocity and septal curvature have been reported (317). One study in 26 PAH patients found superiority of calculated ventricular mass index, (VMI - ratio of RVM to LVM), over echocardiography estimated mPAP (318). Correlations between VMI and mPAP were stronger with narrower CI than for echo. Sensitivity and specificity of VMI using >0.6 as a diagnostic threshold were 84% and 71% in comparison to 89% and 57% for echo. Laffon et al applied a computerised algorithm to estimate mPAP in 31 patients based on MRI indices including blood flow velocity and PA cross-sectional area with patient characteristic such as height and found strong correlation with RHC values (r=0.92) (319). In contrast, poor correlation between mPAP and 5 MRI indices including pulmonary artery acceleration time and the Laffon algorithm was shown in a study of 44 PAH patients (320). Significant, if weaker, correlation was still seen for VMI (r=0.56) but using the previous threshold of VMI >0.6 resulted in missed diagnosis in 9 of the 44, and false negative rate of 20%.

1.3.4 Monitoring treatment response

There are few completed studies of PAH therapies that have used CMR indices as endpoints despite clear evidence that RV function rather than degree of PAP strongly predicts survival. Reverse remodelling and improvements in RV function and pulmonary flow has been demonstrated in CMR studies following lung transplantation (321, 322) and endarterectomy for treatment of CTEPH (323). Substudies of pharmacological RCTs or small, single centre studies in PAH have reported on associated changes in CMR indices. In a small study of 5 patients, 3 months of Sildenafil decreased RVM, improved RVSV and reversed IVS shift (324). In another blinded RCT, sildenafil but not Bosentan lead to a reduction in RVM despite similar decreases in PAP, suggestion the possibility of a direct effect on the RV by Sildenafil (325). Two studies using the ETRAs Bosentan and Ambrisentan in PAH found no improvement in RV ejection fraction, or volumes at 12 months (326, 327). CMR was used to assess response to Epoprostenol in 11 IPAH patients treated for 1 year. RVSV increased from 34±11 ml to 41±11 ml, $p<0.05$ with no change in RV mass or volumes (302). Change in RVSV related to improvement in 6MWT suggesting this resulted in functional improvement, a correlation which has not been demonstrated with invasive haemodynamic parameters. In 18 systemic sclerosis patients treated with Bosentan, CMR has been utilised to demonstrate improvement in myocardial perfusion, although these patients did not have PH (328). Finally, Van Wolferen et al demonstrated the addition of Sildenafil to Bosentan therapy resulted in significant increase in RVEF and CI in comparison to baseline in 15 PAH patients (329).

Increasing RVEDVI or a further decrease in SV or LVEDV at 1 year of follow-up were the strongest predictors of mortality and treatment failure in longitudinal CMR study in 54 patients with IPAH (41). Significant increases in RVEF, SVI, CI and LVEDVI and improvement in RVEDVI were demonstrated at 1 year. Change in RVM has not been shown to have prognostic significance, presumably as a result of the ambiguous nature of an increase in mass, which could arise as both a consequence of concentric hypertrophy representing successful adaptation to afterload or eccentric hypertrophy that occurs with RV failure and dilatation. In comparison with follow up haemodynamic data at right heart catheterisation, recent study has shown that despite haemodynamic improvements with treatment in PVR and CI, and stability of 6MWD at 1 year, progressive right ventricular dysfunction was

demonstrated by CMR, and the deterioration of RV function was associated with poorer outcome regardless of the change in PVR (288). Change in RVEF was associated with survival, but change in PVR was not. Therefore it would seem reasonable to propose that CMR is a better tool for follow up and monitoring of patients with PAH.

Van wolferen et al have determined by correlation of SV with 6MWD during therapy that a > 10ml change in stroke volume is of clinical relevance in PAH (330). This could be potential endpoint for future studies in PAH.

1.4 Thesis outline

It is apparent that although PAH specific therapy improves PVR, this does not necessarily translate into improvements in functional status and mortality unless accompanied by a parallel improvement in RV function. In a recent meta analysis of studies undertaken to evaluate PAH therapies, treatment was associated with a reduction in PVR mediated by reduction in mPAP and increase in SV, but without improved contractility, suggesting current therapies have vasodilating effects with limited cardiac specific effect (331). Studies have demonstrated that despite a reduction in PVR with therapy, progressive RV dysfunction continues. Reduction in PVR as a result of PAH therapy in severe PH leads to an increase in CO without appreciable change in mPAP and therefore unchanged RV power output which perhaps explains this continued spiral of deterioration. This highlights the need to evaluate the RV-PA circuit as a whole and CMR offers the unique opportunity to study this. RV systolic function traditionally has been evaluated by RVEF, however this is preload dependent and gold standard evaluation of RV contractility from derived PV loops is invasive, time consuming and not suitable to serial monitoring of patients. SV/ESV is a volumetric measure of RV coupling that can be easily determined by CMR and is a less preload dependent measure of RV systolic function. It is unknown whether this has superior prognostic significance in PAH over traditional methods of assessing RV function, and how PH specific therapies alter it.

Whilst response to PH specific therapy in PAH and relationship to prognosis has been extensively studied by both functional and biomarker outcomes in addition to CMR indices of RV function, there is limited data on treatment of severe PH

associated with lung disease where the pathophysiology, whilst sharing some common mechanisms described earlier in this chapter, is different. The prognostic significance of CMR indices of pulmonary vascular stiffness, RV function and coupling to the pulmonary circulation in the latter and its comparison to those with PH “in proportion” to lung disease may provide mechanistic insights as to why a small subgroup develop severe PH and whether they would benefit from PH therapies.

The aim of this thesis was the explore the utility of CMR to interrogate RV function, vascular stiffness and RV-arterial coupling by SV/ESV in patients with PAH and contrast this to patients with PH associated with lung disease in whom the pathophysiology is different. The thesis is therefore divided into three separate but complementary studies described in chapters 3, 4 and 5.

In chapter 3, I aim to describe the right ventricular characteristics of patients with severe PH associated with lung disease in comparison to IPAH (where utility of common metrics of RV dysfunction is already established) and PH “in proportion” to lung disease, and how CMR may be employed to detect PH, determine prognosis and response to PH therapies.

In chapter 4 I aim to compare invasive and CMR estimates of RV-arterial coupling in PAH in comparison to normal subjects and PH associated with lung disease. In addition, to determine if CMR estimates of RV-arterial coupling is a superior prognostic variable in comparison to commonly implemented metrics of RV function in PAH such as RV ejection fraction.

Finally, in chapter 5 I aim to assess the impact of PAH therapies on RV-arterial coupling assessed by CMR, in comparison to other indices of RV function and clinical endpoints (such as 6MWD or NTproBNP) and relate this change to survival, to determine the optimal method for monitoring the right ventricle in patients undergoing PAH therapy.

Chapter 2 - Materials and Methods

2.1 Patient recruitment

The patients involved in the studies for this thesis were retrospectively identified and included following inpatient diagnostic assessment for the evaluation of clinically suspected PH between January 2000 and March 2014 at the Scottish Pulmonary Vascular Unit, Glasgow. In total, 325 patients were included across the 3 studies, 206 underwent CMR and RV pressures traces were available for analysis in 125. A flow chart describing patients included in the studies is shown in figure 2.1. Inclusion criteria thus compromised a diagnosis of PH of either group 1 or 3 disease after diagnostic assessment according to ESC guidelines. All were incident cases and treatment naive. A control group without PH (defined as mPAP <25mmHg) whom had undergone diagnostic assessment due to the suspicion of PH were also included. Additional specific exclusion criteria were applied for each study. These will be discussed in the relevant chapter and a demographic description of each study population will be shown. For all studies identical CMR exclusion criteria applied. These include ferrous implant such as cardiac pacemaker, pregnancy, claustrophobia or tolerability relating to breathlessness.

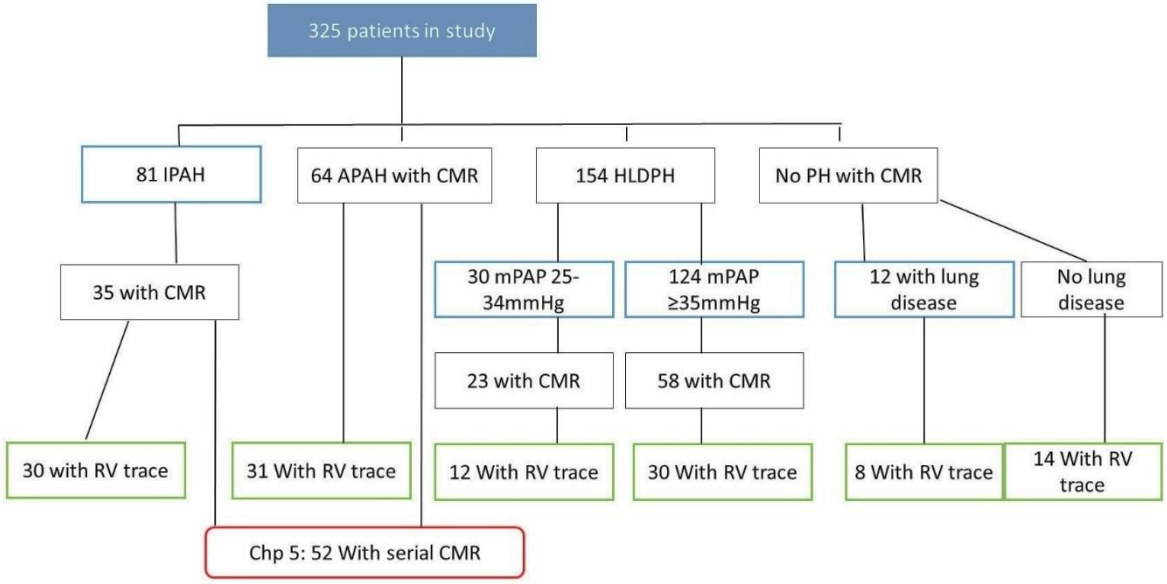

Figure 2.1 Flow chart describing study population for each chapter.

Patients included in Chapter 3 indicated by blue, Chapter 4 in green and Chapter 5 in red. Specific inclusion and exclusion criteria will be discussed in methods of each chapter.

In Chapter 3 clinical characteristics, survival and treatment outcomes of 81 IPAH patients will be compared to 124 severe PH/lung disease patients. RV characteristics of 30 mild/mod PH and 12 no PH lung disease patients included for comparison.

In Chapter 4, RV-arterial coupling values will be estimated by invasive pressure and non invasive volume methods for 30 IPAH patients, 31 APAH, 42 hypoxic lung disease PH (30 with severe PH) and 22 subjects without PH (8 with lung disease).

In Chapter 5, 52 PAH patients with serial CMR included to examine change in RV function and RV-arterial coupling with PH therapy.

2.1.1 Diagnostic assessment

During 4 day admission all patients underwent a series of investigations following standard diagnostic algorithm for PH (332). These included blood investigations, including HIV serology, thyroid function, connective tissue serology and NTproBNP, lung function and 6MWT, transthoracic echocardiogram, arterial blood gases and CT imaging of thorax. CMR and right heart catheterisation were carried out within 72 hours.

Right heart catheterisation was performed using a 7F triple-channel thermodilution Swan Ganz catheter (Baxter Healthcare, Irvine, California, USA). All measurements were recorded with the patient in a supine position, at rest, breathing room air or with supplementary oxygen to obtain peripheral saturations above 90%. Measurements carried out included mean right atrial pressure (RAP), right ventricular pressure and systolic, mean and diastolic pulmonary artery pressures (PAP) and pulmonary artery wedge pressure. Cardiac output (CO) was determined by thermodilution, allowing the determination of pulmonary vascular resistance (PVR) by the following: (mPAP – PAWP)/CO. Cardiac index was determined as CO/body surface area and compliance as SV/ (sPAP-dPAP). Mixed venous oxygen saturations were determined from a sample drawn from the pulmonary outflow tract.

2.2 Cardiovascular Magnetic Resonance imaging

CMR was performed as part of patient's routine diagnostic assessment. Follow up scans were performed as part of two longitudinal studies approved by the West Glasgow Hospitals University NHS Trust (as part of EURO-MR project) and West of Scotland REC 4 ethics committee, to which patients gave written consent. All scans were performed on a 1.5 T MRI scanner (Sonata Magnetum, Siemens, Germany) using a previously described protocol (304). Fast cine imaging with SSFP sequences (TrueFISP Siemens) was used for functional imaging. Initial scout images (shown in Figure 2.2) were obtained to localise the heart within the thorax and plan subsequent cine images. All cines were acquired during a breath hold typically lasting 5-8s. Total scan time was approximately 40-50 minutes.

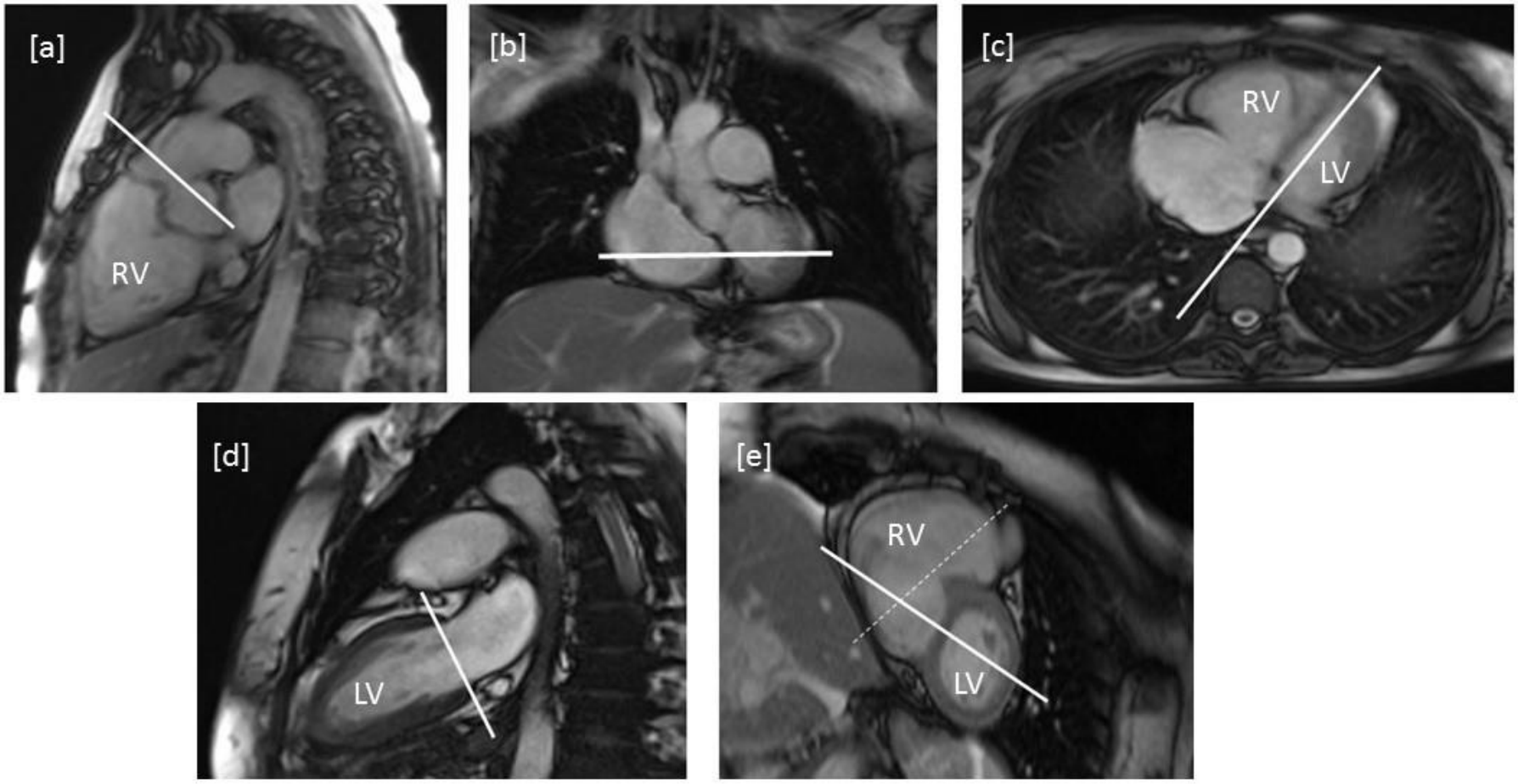

Figure 2.2. Initial localiser images in the planning of stack of short axis cines.

The white lines indicate the projection lines to plan the next step in localising. [a] Sagittal view of RV outflow tract. Planning for cross section of PA shown. [b] Coronal view, [c] transverse view, [d] vertical long axis view, and [e] short axis view. The line on the coronal view defines the transverse view, and similarly progression to next views are displayed.

Horizontal long axis (HLA) cines were then planned and acquired using these scout images. A series of short axis "stack" of images was then obtained from the HLA view from the base of the atrioventricular valve to the cardiac apex covering both ventricles with 8-mm SA imaging slices, separated by a 2-mm inter-slice gap as shown in Figure 2.3. Imaging parameters were standardised for all subjects, TR/TE/flip angle/voxel size/FOV = 3.14ms/1.6ms/60^0/2.2 x 1.3 x 8.0 mm/340mm.

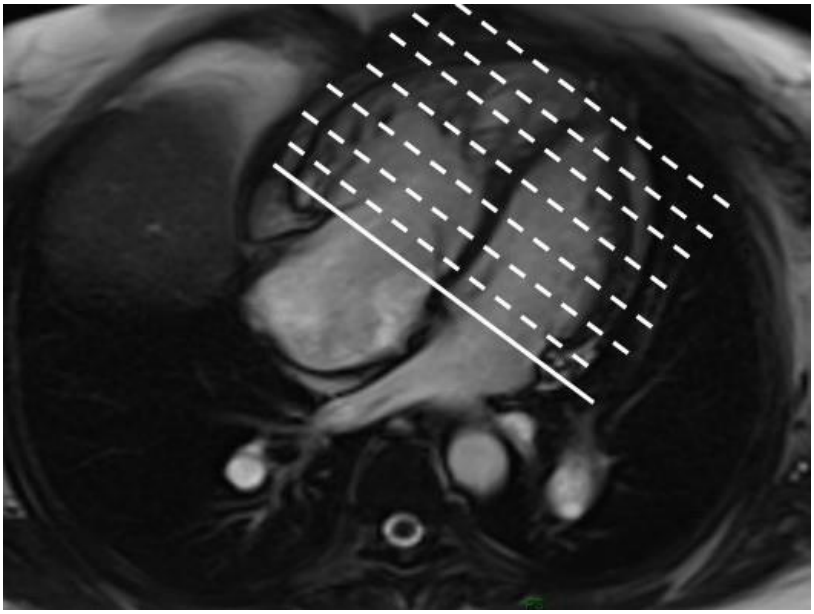

Figure 2.3. Horizontal long axis view (HLA) acquired in a patient with PH

Note the dilated RA and RV with regurgitant flow visible in the RA. The solid white line denotes the planned first short axis image intersecting base of the atrioventricular valve. Subsequent dashed white lines indicate the propagation of the SA imaging plane towards the apex at 2mm intervals to create a stack of images through both ventricles.

2.2.1 Volumes and mass

All CMR images were analysed using Argus analysis software (Siemens, Germany). Right and left ventricular volumes and mass were determined by manual delineation of endocardial and epicardial borders of end diastolic and end systolic images at each slice position on the short axis cines. This method of manual planimetry has been well described previously and is regarded as standard method for analysis of ventricular volumes and mass. An example of an analysed series of images is shown in figure 2.4. By multiplying the individual slice areas by slice thickness (8 mm) plus the inter-slice gap (2mm) and applying Simpson's rule, the software calculates ventricular end diastolic and end systolic volumes (RVEDV, RVESV, LVEDV and LVESV). Stroke volumes (RVSV & LVSV) are also calculated by EDV-ESV. Right and left ventricular mass (RVM and LVM) were determined as the product of myocardial volume for each ventricle and the quoted density of cardiac muscle (1.05 g/cm3). RV mass was determined as RV free wall mass, while the Interventricular Septum (IVS) considered part of the LV in accordance with accepted practice (47). For the purpose of this analysis, trabeculations were considered part of ventricular volume. All indices of mass and volume were indexed to the patients' body surface area (BSA) and when considered for survival analysis adjusted for patient age.

Imaging was reviewed during acquisition for artefacts described in Section 1.1.3.3 and adjustments made where possible to rectify, such as patient coaching for breath-holding or end inspiratory breath-holds in presence of motion artefact, arrhythmia rejection software in presence of image blurring due to arrhythmia, alteration of FOV if wrap artefact interfered with region of interest or alteration of VENC settings in phase velocity map sequences if aliasing noted. Scans were abandoned if patients were unable to breath-hold or in presence of significant arrhythmia, or converted to real-time acquisition if CMR imaging was of clinical benefit. At time of functional analysis, scans were excluded if real-time sequences were used, or if image quality was poor with blurring of myocardial borders.

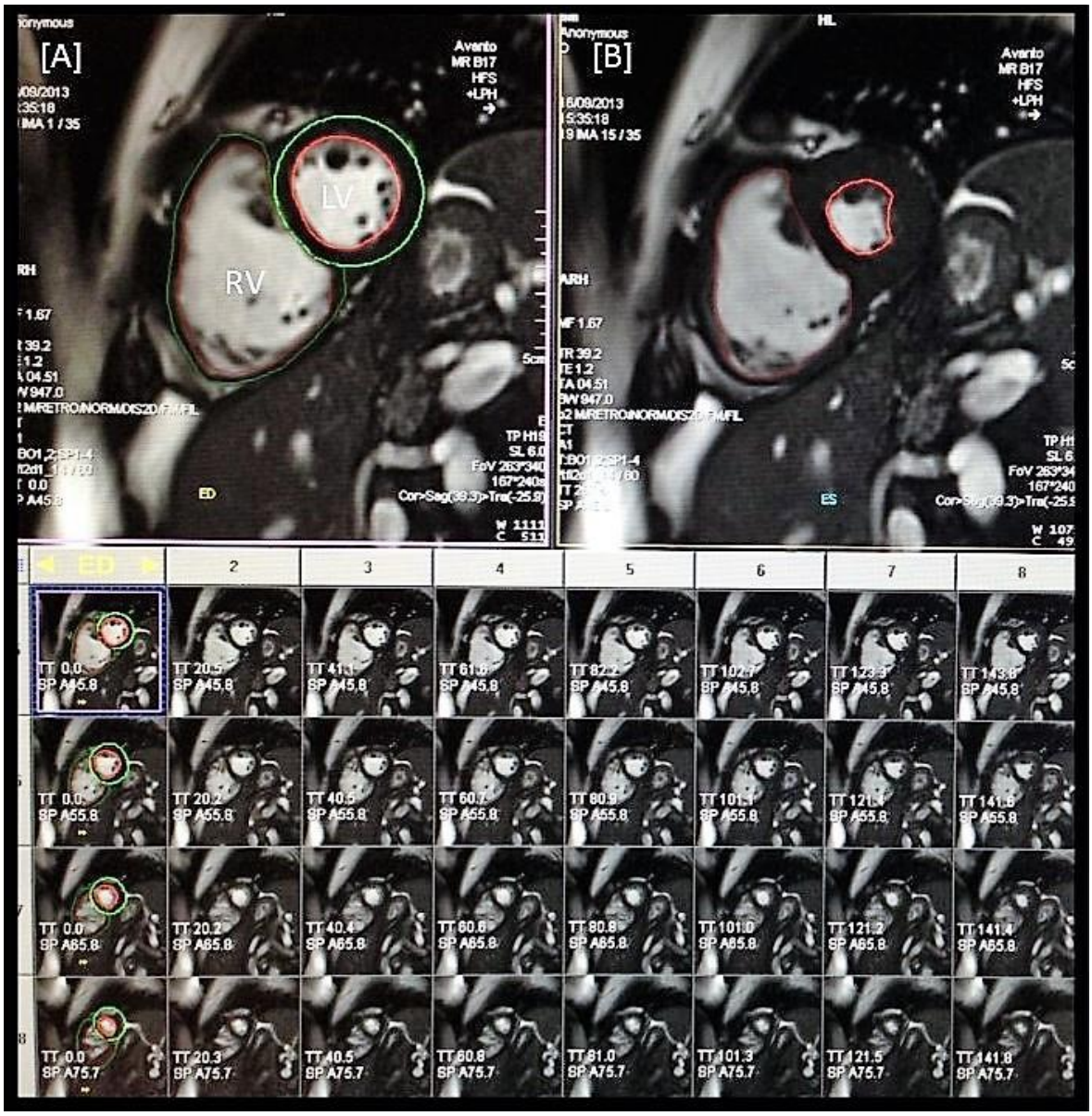

Figure 2.4. An example of planimetry analysis of right and left ventricular volumes and mass in a PH patient.

Note the dilated thin walled RV in comparison to the LV. Each row of short axis images represents a loop of cine images acquired during one cardiac cycle at consecutive slice positions, beginning at the base of the heart, moving apically to cover both ventricles. The first images within each row (or slice position) are the end-diastolic images (indicated by the yellow ED at the top of the left-hand column) [A] shows one enlarged end diastolic image with endocardial borders delineated in red and epicardial in green. [B] indicates the end systolic image at the same slice position with endocardial borders shown.

2.2.2 Function

Ejection fraction (RVEF and LVEF) was determined as a percentage (%) using this planimetry derived stroke volume measurement. RVEF = RVSV/RVEDV x100 and LVEF as LVSV/LVEDV x100.

2.2.3 Flow mapping

As described in section 1.1.3.2.2, two Image acquisitions was prescribed perpendicular to flow direction through the great vessels (MPA and aorta) with image plane just distal to valve leaflet tips. Direction of flow was set (R-L, F-H) to determine forward velocity from ejecting heart. Appropriate VENC was set, typically 100 - 120 cm/s for MPA and ~150cm/s Aorta with adjustment for aliasing/valvular pathology. Image acquisition performed during free breathing. A region of interest (ROI) was drawn around the interior surface of the target vessel, either cross section of aorta or pulmonary artery, on the first anatomical image. This ROI was propagated throughout the anatomical images using a semi-automatic function within the Argus software. These were then checked visually and modified within Argus to approximate the interior surface of the target vessel throughout the cardiac cycle. These modifications were then copied onto the corresponding velocity images. A second, reference, ROI was then drawn within the soft tissue of the chest wall as close as possible to the target vessel and propagated throughout the cycle. This was applied for phase correction, to correct for background movement of the thoracic contents through the imaging plane during respiration. An example of flow map analysis is shown in figure 2.5.

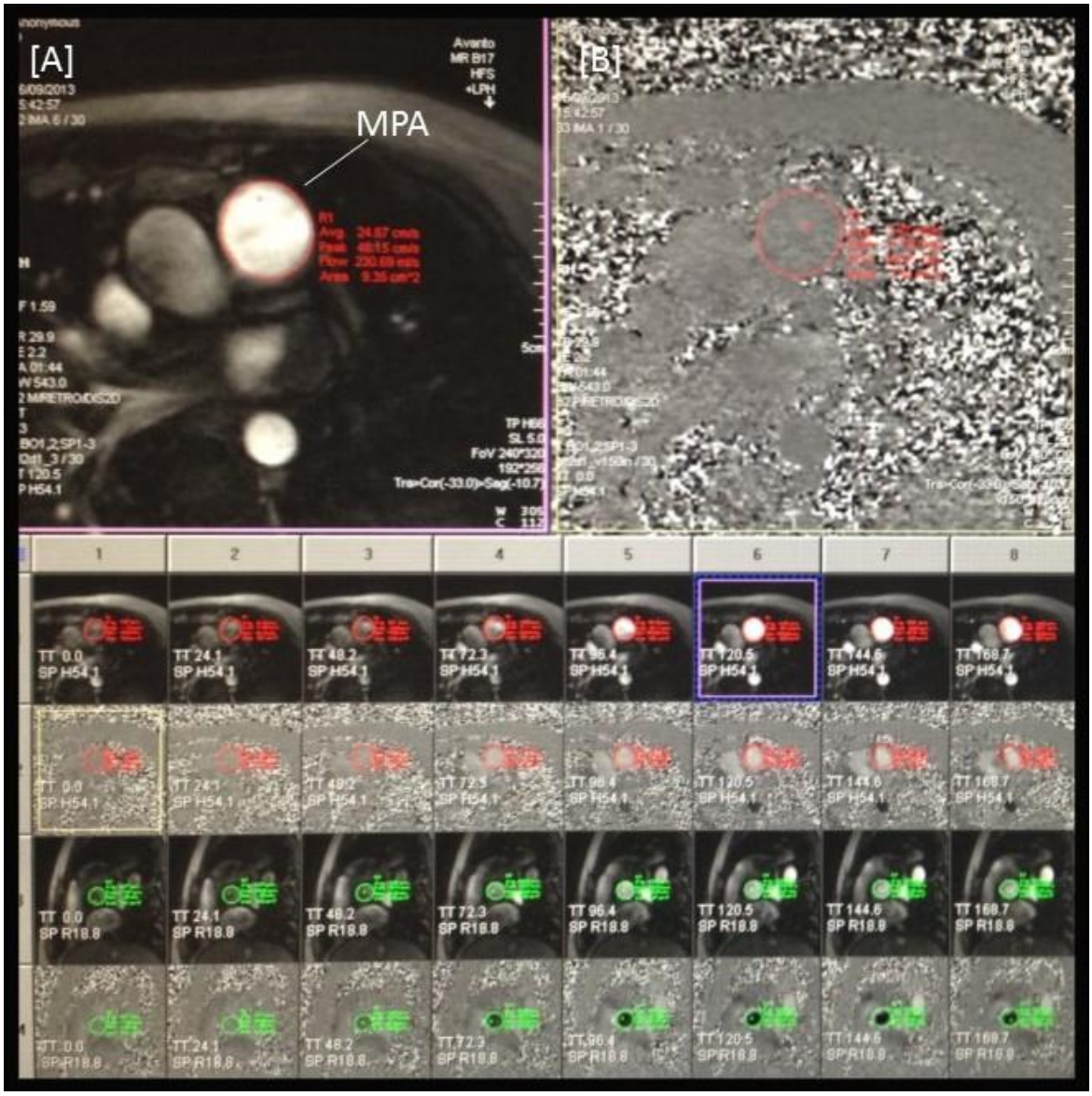

Figure 2.5. Magnetic resonance phase contrast flow quantification.

[A] Anatomy image of main pulmonary artery with ROI drawn around the interior surface of the vessel. [B] corresponding velocity encoded image. Pulmonary flow images denoted in red and aortic in green.

Six SV results were therefore obtained by CMR for each patient, RVSV and LVSV from planimetry, and Aortic SV (AoSV) and pulmonary artery SV (PaSV) both with and without phase correction. It has previously been shown that in PH, LVSV and AoSV (the latter with phase correction) is a more accurate reflection of invasively determined SV at RHC than right sided SV (306). This relates to difficulties in delineation of endocardial contours in the heavily trabeculated RV, and turbulent flow observed in the PA of PAH patients with reverse flow occurring during RV ejection. An initial analysis was performed correlating the 6 SV determined by CMR with invasive thermodilution determined SV in 134 patients. In our centre thermodilution CO is employed whereas most regard Fick method as the gold standard invasive measure of CO. This however requires simultaneous arterial sampling of $Pa0_2$ with an arterial line. The correlations shown here are therefore with thermodilution CO, whilst previous published data by Mauritz et al employed Fick CO. The use of phase correction resulted in poorer correlations, presumably as this is not a true phantom (i.e. motionless) as used in CMR theory where stationary objects were used for phase correction. AoSV and LVSV demonstrated superiority over RVSV and PaSV. Correlations are shown in figures 2.6 – 2.8. AoSVI therefore will be quoted throughout (without phase correction) for SVI. RVEF however is generated by the use of RVSV and in order to directly compare the superiority of SV/ESV as a measure of systolic function in PH, RVSV will be applied in this calculation.

CMR derived measures of vascular stiffness was determined by the relative area change (RAC) of the cross sectional area of both the PA and proximal Aorta. RAC was calculated as the difference between maximum and minimum vessel area / minimum area and multiplied by 100% (312, 313).

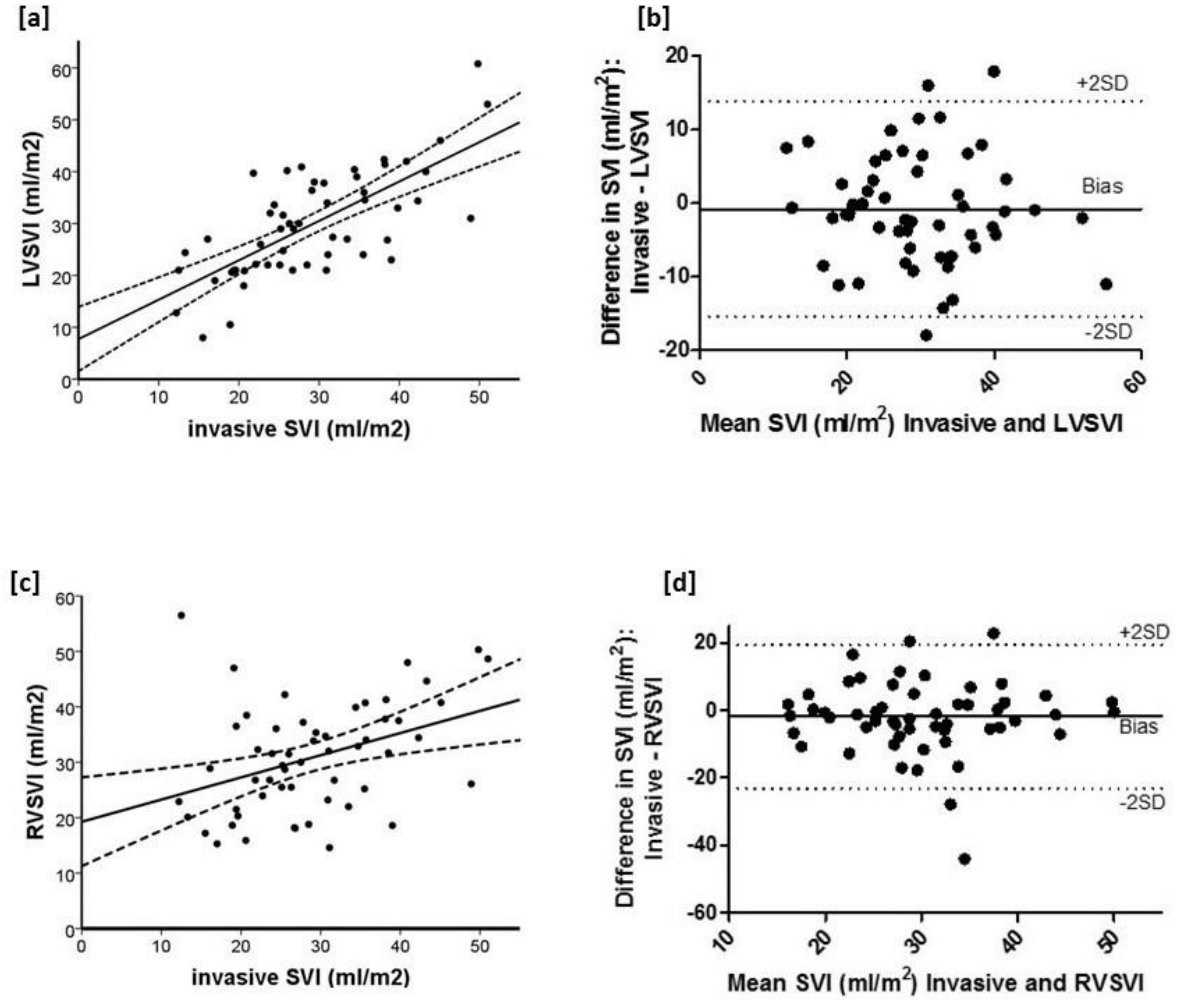

Figure 2.6 Correlation of invasive measured stroke volume with cardiac MRI values determined by ventricular planimetry.

Stroke volumes determine by left and right ventricular planimetry (LVSVI and RVSVI). Panels a & c display correlations between CMR measured and invasive stroke volume index and Panels b & d Bland-Altman analysis of difference versus mean (limits of agreement indicated by dashed line and mean difference by solid line). Correlation of LVSVI with invasive SVI was superior to RVSVI, r^2 = 0.51, $p<0.0001$ and r^2 = 0.15, p = 0.004 respectively.

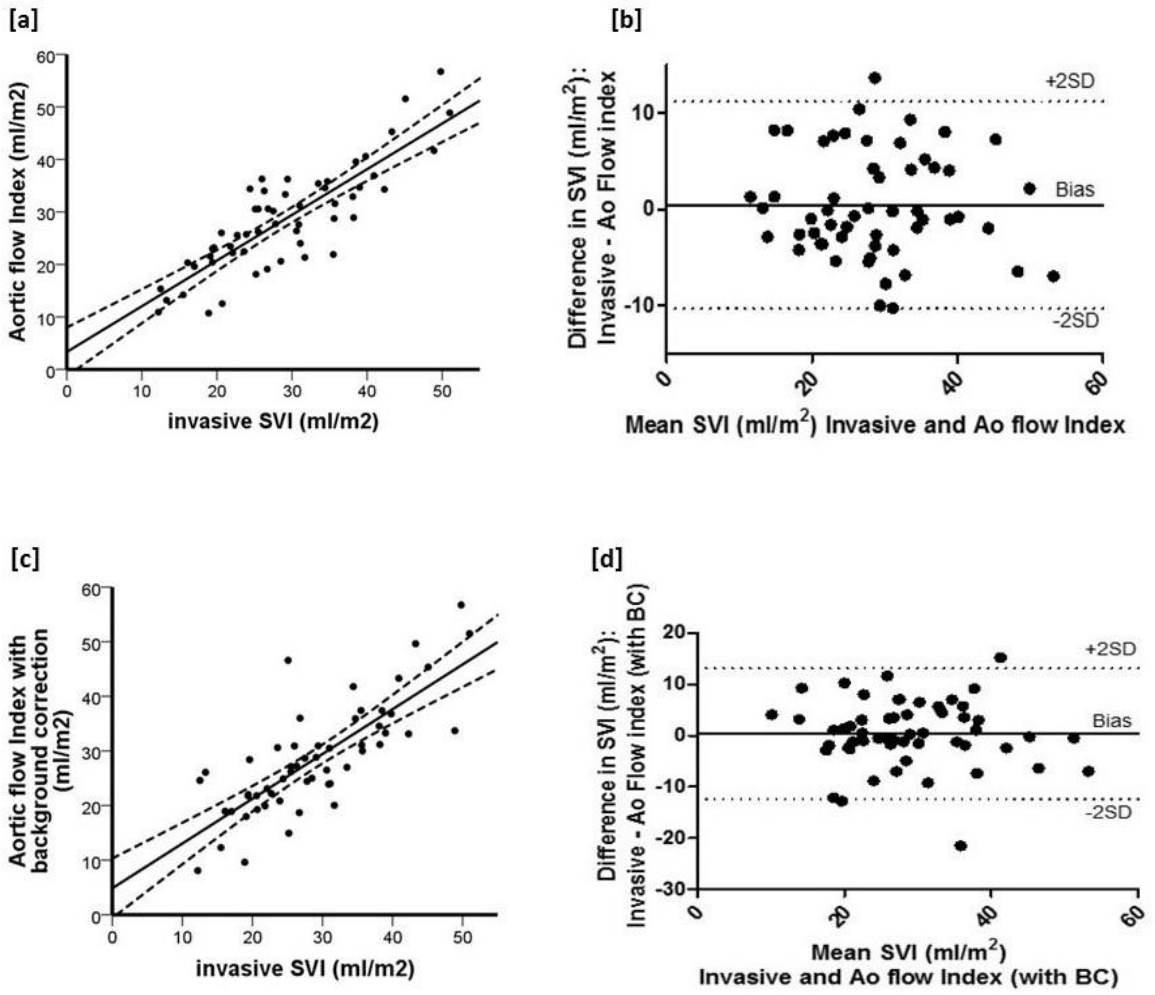

Figure 2.7 Correlation on invasive Stroke volume with CMR stroke volume determined by Aortic flow mapping

Stroke volume determined by flow mapping of the proximal aorta (AoSVI) without (panel a) and with (panel c) phase correction shown. Panels b & d Bland-Altman analysis of difference versus mean (limits of agreement indicated by dashed line and mean difference by solid line).

Correlation with invasive SVI for AoSVI without and with phase correction was $r^2 = 0.71$ and $r^2 = 0.61$ respectively, both $p<0.0001$. Closest agreement between AoSVI without phase correction and invasive SVI was determined.

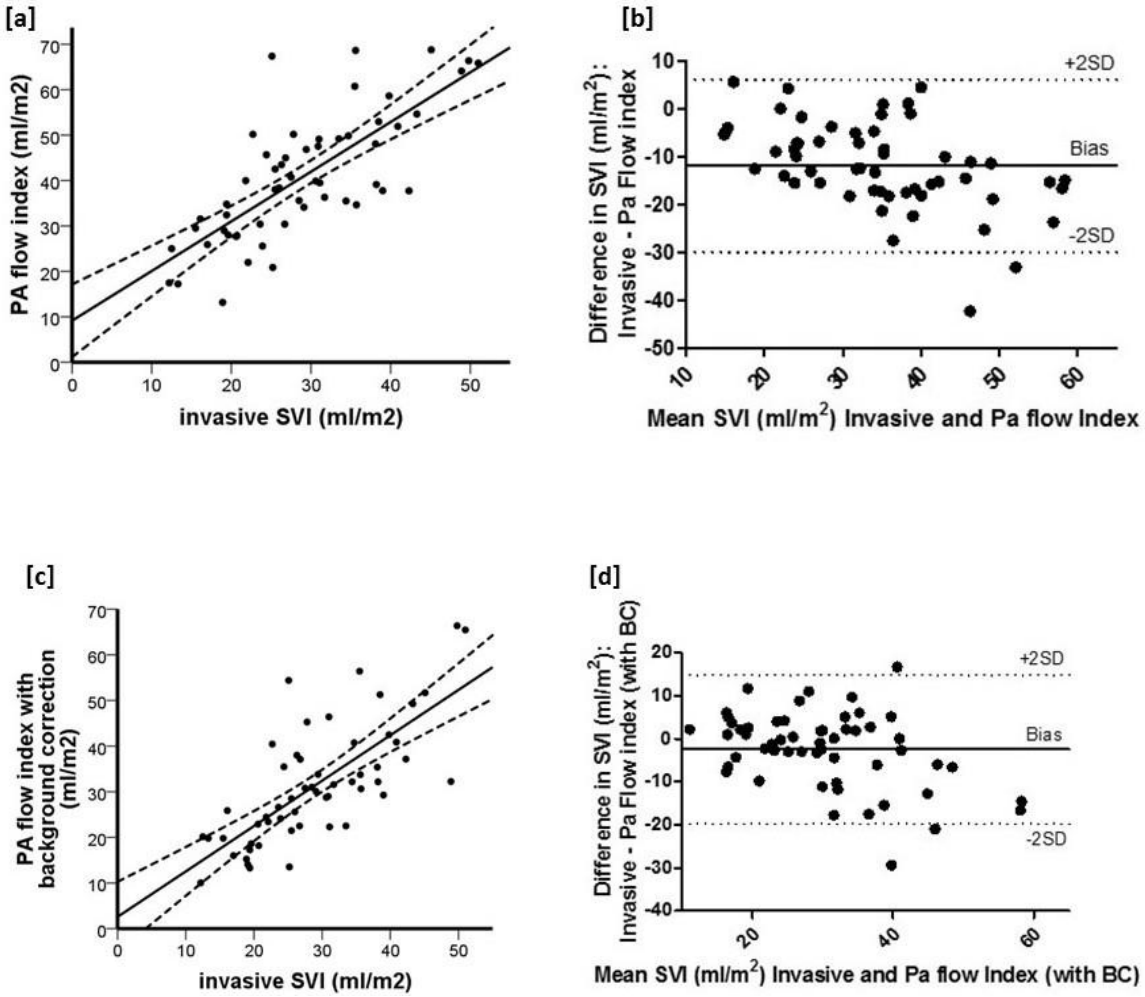

Figure 2.8 Correlation of invasive stroke volume with CMR stroke volume determined by Pulmonary artery flow mapping.

Stroke volume determined by flow mapping of the main pulmonary artery (PaSVI) without (panel a) and with (panel c) phase correction shown. Panels b & d Bland-Altman analysis of difference versus mean (limits of agreement indicated by dashed line and mean difference by solid line).

Correlation of both methods with invasive SVI similar, $r^2 = 0.57$ and $r^2 = 0.54$ without and with phase correction respectively, both $p<0.0001$.

2.3 Statistical Analysis

Statistical analysis was performed using SPSS 21 (SPSS Inc, Chicago, IL) and Graphpad Prism Version 5.00 (Graphpad Software, California, USA). Continuous variables were tested for normality using D'Agostino and Pearson omnibus normality test. Normally distributed variables are shown as mean ± standard deviation and non-normally distributed variables as median (IQR). Categorical variables are described by percentages (number) unless otherwise stated. Comparison of characteristics was made using unpaired t-test or Mann-Whitney U test depending on data distribution. Comparison of several groups was performed using ANOVA or Kruskal-Wallis test with post hoc analysis using Tukey's or Dunn's multiple comparison test. Comparison between baseline and follow up investigations was made by paired t-test or Wilcoxon signed rank test. Comparison between categorical variables was made using X^2.

Survival was from date of diagnostic right heart catheter and endpoint as either date of death, lung transplantation or censoring. Patients were censored if they were lost to follow up or alive at last day of study (05/08/2014). All cause mortality was used for survival analysis. Survival predictors were determined using Cox proportional hazards regression analysis. Variables with a p-value ≤0.2 were considered for multivariate analysis. Indicator variable coding for missing data was used for multivariate analysis. A P value <0.05 was considered statistically significant throughout.

Chapter 3 - Right ventricular dysfunction and response to PH specific therapy in severe pulmonary hypertension associated with lung disease

3.1 Introduction

As discussed in chapter one mild to moderate PH is relatively common in patients with hypoxic lung disease although the prevalence varies depending on the aetiology and severity of the underlying lung disease (204, 207, 219, 220). Hypoxaemia has been shown in clinical studies to be the major determinant in the development of PH, with patients with relatively normal $Pa0_2$ rarely displaying pulmonary hypertension at rest even in the presence of severe ventilatory impairment (333, 334). Severe PH, defined by a mPAP ≥ 35mmHg, in contrast is rare, occurring in 5 -13% of patients and is characterised by relatively preserved lung function, gross hypoxaemia and impaired DLCO, and greater RV dysfunction (206, 208). The level of PH has therefore often been described in the literature as "disproportionate". Regardless, the development of PH is associated with poor prognosis (208, 223, 335), greater functional limitation with little or no therapeutic options.

In contrast to patients with group I PAH where large increases in PVR and right ventricular dysfunction is observed, PH associated with COPD is usually mild to moderate and right ventricular function and cardiac output are usually in the normal range (243). COPD patients with moderate to severe disease but without hypoxaemia have been shown to have preserved RV systolic function at rest. In a small study of 25 COPD patients with FEV1 41±15% but a $Pa0_2$ 10.9 ±1.3KPa, RVEF was 53±12% in comparison to 53±7% in normal controls (336). During acute exacerbations with evidence of peripheral oedema, decreased RV contractility has been demonstrated but only in these circumstances (337). In contrast, in 158 patients undergoing lung transplantation evaluation, RV dysfunction was present in 59%, and in 120 patients with severe emphysema, mean RVEF was reduced at 34±8% (204, 205) suggesting a greater degree of RV dysfunction in those with end stage disease. In the latter study, mPAP and $Pa0_2$ were shown to predict RVEF, but only explained 13% of the variance, which is perhaps not surprising as RVEF is product of complex interaction between preload, afterload and contractility which were not evaluated.

3.1.1 Prognosis

The prognostic implications of the presence of PH highlights the clinical importance of detection. However, echocardiography, the accepted screening tool for PH in the general population has been shown to be less accurate in those with lung disease. The accuracy of echocardiography estimated PAP was compared to RHC measurement in 374 patients undergoing evaluation for lung transplantation, the majority of whom had COPD (199). PH was present in 25% of the population, 18% of those with obstructive lung disease and 59% of those with ILD. It was not possible to estimate sPAP by echo in 56% of subjects. In 52% of cases estimated sPAP was inaccurate (varied by >10mmHg), 48% were misclassified as having PH by echo and 13% were missed. The sensitivity and specificity of echocardiography for the presence of PH in this population was therefore 85% and 55% respectively, demonstrating the need for better non invasive screening tools in lung disease patients.

3.1.2 Therapy

Long term oxygen therapy (LTOT) has been demonstrated to stabilise or decrease mPAP in COPD with mild to moderate PH (256-258). However, in those with severe PH results are less encouraging (257, 338). The role of PH specific medication in those with severe PH is uncertain. Features such as greater haemodynamic compromise and RV dysfunction in this subgroup may suggest a role for PH specific therapy. Studies to date have been of small sample size, used echocardiography to diagnose PH and included those with both mild and severe or even no PH (339-342). Acute vasodilator studies in COPD patients have raised the possibility of worsening hypoxaemia. Blanco et al administered Sildenafil, a PDE-5i to 20 patients with severe or very severe COPD, 17 of whom had PH at rest with an average mPAP of 27 mmHg (range 21 -61 mmHg) at RHC (343). Whilst a fall in mPAP was demonstrated, CO was unchanged and increased hypoxaemia occurred from increase in VQ mismatch. Acute inhalation of nebulised iloprost in 16 PH-COPD patients also demonstrated worsening hypoxaemia, although 6 of the 16 had PCWP >15mmHg at rest indicating pulmonary venous disease and potential of pulmonary oedema as an explanation for increased hypoxaemia (344). Alp et al demonstrated a 42% fall in PVR at 1 hour after IV Sildenafil administrated in 6 patients with severe COPD and PH, and fall in mPAP from 30mmHg to 22mmHg

($p<0.001$) (345). These studies suggest that PH even when mild in COPD is vasoresponsive, however how these haemodynamic effects translate into functional or symptomatic benefit is less clear, particularly given concerns regarding possible worsening of VQ mismatch in those already compromised by chronic lung disease.

Several studies in COPD with either only a mild elevation in PAP or without PH suggest no role for vasodilator therapy with no change in quality of life scores or 6MWD and varying effects on haemodynamics and oxygenation. Patients with COPD have been shown to have impaired resting stroke volume and blunted SV response to exercise, with evidence of RV dysfunction and disproportionate rise in PAP on exercise (346, 347). In a small study of 18 patients with COPD, 5 with PH at rest and 6 with exercise induced PH, Sildenafil administration resulted in attenuation of exercise related increase in PAP (348). Rietema et al showed no improvement in SV response after sildenafil administration in 15 COPD patients (9/15 had PH, average mPAP 22 mmHg) (340). Bosentan therapy for 3 months led to no improvement in 6MWD or sPAP but demonstrated a drop in arterial oxygen pressure when given to 20 patients with severe and moderate PH (echocardiogram estimated sPAP 32 mmHg) (342). In a larger study of 63 patients with severe COPD and modest PH on echocardiogram (sPAP 42 ± 10 mmHg) Sildenafil therapy resulted in no additional benefit over pulmonary rehabilitation in incremental exercise but no deterioration in oxygenation was seen (349). In contrast, Iloprost (an inhaled prostacyclin analogue) therapy given to 10 COPD patients with echocardiogram evidence of mild PAP elevation increased 6MWD by an average 49.8m with no deterioration in VQ mismatch (341). In the study described earlier by Alp et al, after 3 months of Sildenafil 6MWD increased (from an average of 351 to 433m) and mPAP fell (from 30 to 25mmHg) but observations were based on only 5 patients (345).

Similar lack of clarity exists in the literature on the role of pulmonary vasodilators in interstitial lung disease associated PH. As discussed in section 1.2.3.2 similar cytokines are implicated in both the pathogenesis of IPF and pulmonary arterial disease and the use of ETRAs in particular would seem intuitive. The BUILD1 (Bosentan Use In Interstitial Lung Disease) study demonstrated no change in 6MWD in comparison to placebo in the 49/74 IPF patients completing 12 months of Bosentan, but a trend towards prolongation of time to disease progression or death

was perhaps suggested (350).There was no controlling for PH between the placebo or therapy groups, and patients with sPAP > 50 mmHg on echocardiogram were excluded so it is not possible to apply the findings to an ILD PH population. A randomised placebo controlled trial of the ETRA Ambrisentan in nearly 500 IPF patients (of which 10% had associated PH) was terminated early as interim analysis not only suggested a lack of efficacy, but the possibility of increased risk of disease progression and hospitalisation related to respiratory exacerbation in the Ambrisentan arm (351).

In 2014 Corte et al reported on 40 IPF patients with associated PH (352). After 16 weeks of Bosentan no change occurred in 6MWD, mPAP or QOL scores in comparison to the placebo group. Although the deterioration in 6MWD in the active therapy group was less, -25.9 m vs -53.1 m respectively, this was not statistically significant. Whilst the average mPAP of 37 mmHg in the overall cohort suggests this population had severe PH, only 25/40 completed the study and characteristics of these patients were not reported. Other, smaller studies have reported more positive effects. Collard et al reported an increase in 6MWD by a mean 49 m after 3 months of sildenafil in 11 IPF patients with PH (353), whilst Hoeper et al demonstrated an increase in 6MWD and CO, and a decrease in PVR following therapy with Riociguat in 22 ILD patients with an average mPAP >30mmHg (although 4 had an alternate aetiology for PH) (354).

Therapy studies solely focussing on severe PH associated with lung disease are few but perhaps more encouraging. Valerio et al treated 16 COPD patients with an average mPAP 37 ± 5 mmHg at RHC with 18 months of Bosentan (355). 6MWD improved from 256 ±118 m to 321±122 m and mPAP fell (31±6 mmHg) whilst a trend towards deterioration in 6MWD occurred in the best standard care group. The ASPIRE (Assessing the Spectrum of Pulmonary Hypertension Identified at a Referral centre) registry reported no survival advantage in 43 COPD patients with severe PH treated with pulmonary vasodilators. However this group did demonstrate a fall in PVR of more than 20% in 4 of 7 patients with repeat haemodynamic data, but did not evaluate clinical response by commonly used outcome measures such as six minute walk distance or NTproBNP (356).

3.1.3 The right ventricle in chronic lung disease.

Post mortem study has demonstrated links between the degree of RV hypertrophy and hypoxaemia in COPD patients (357) and demonstrated that cardiac failure is leading cause of death in COPD patients during hospitalisation with acute exacerbations (358). Small cardiac MRI studies in COPD with normoxia or only mild hypoxaemia and the absence of PH (determined indirectly by preserved PA distensibility) have demonstrated increased RV mass, smaller RV volumes, and in one fifth, impaired RV function (defined as a RVEF <45%) (336). Marcus et al imaged the RV using cardiac MRI in 8 COPD patients with early PH suggested by a decreased pulmonary artery acceleration time, and also demonstrated increases in RV mass and SV but preserved RVEF (359). Correlations between increasing severity of COPD determined by FEV1 and increasing RVM or falling RVEF have been shown (360), with only severe COPD patients demonstrating impaired RV function and fall in SV. However, no PH screening or control for hypoxaemia was performed so it is difficult to attribute the changes in RV to severity of COPD alone. In a larger echocardiography study, Hilde et al demonstrated a reduction in 9 measures of RV systolic function, including RV fractional area change and myocardial performance index, in 72 COPD patients without PH at RHC and an average $Pa0_2$ 9.8KPa (361). In agreement with the former studies, an increase in RV wall thickness by 57% in comparison to controls was seen. Whilst RV wall thickness correlated with FEV1, this explained only 8% of the variance suggesting severity of airflow obstruction is a less significant driver of RV structural changes and other mechanisms such as systemic inflammation, increased afterload from hyperinflation, endothelial dysfunction or hypoxaemia have a greater detrimental impact. As discussed in section 1.2.3.2, it is known that pulmonary vascular remodelling occurs not only in advanced COPD, but also in patients with mild disease or even to some degree in smokers with normal lung function. RV adaptation and hypertrophy in the absence of significant resting hypoxaemia may be postulated to occur as a consequence of intermittent increase in PAP on exercise or during sleep that has been shown to occur in COPD patients (346, 362). Whilst the COPD patients in the study by Hilde et al are regarding as not having PH by the accepted diagnostic threshold (mPAP ≥25mmHg), mPAP was mildly increased with reduced PA compliance (mPAP 18±3mmHg in comparison to accepted normal 14.7 ±4mmHg (24)) indicating early changes in RV structure at subclinical levels of PH.

In populations of patients with end stage pulmonary disease undergoing assessment for lung transplantation, prevalence of RV dysfunction is higher, reported at 66% in one case series, with the prevalence higher still (94%) in those that also had pulmonary hypertension (205). In end stage IPF patients, echocardiographic indices of RV dysfunction have been shown to be independent predictors of mortality, whilst mPAP was not in a population with a PH prevalence of 29%, but moderate-severe RV dysfunction in only 11% (218). Biernacki reported largely preserved RV function (average RVEF 39% and normal CI) and pressure volume relationship in 100 hypoxaemic COPD patients with mPAP 26mmHg (range 10-60 mmHg, 72% with PH) in comparison to controls (363). On exercise, RVSP increased significantly, but no detriment in RV contractility occurred. RVEF correlated with PVR, but no relationship to $Pa0_2$ or FEV1, and surprisingly mPAP which may reflect use of less accurate radionucleotide ventriculography to determine RV function (363). Turnbull, using MRI derived RV free wall volume as surrogate for RVM, in COPD patients with average mPAP of 30mmHg demonstrated good correlation with mPAP and PVR (r=0.72 and 0.67 respectively) (364). CMR indices of RV structure or function may therefore have a potential role in detection of raised PAP in patients with chronic lung disease.

3.1.3.1 Biomarkers:

BNP or its precursor NTproBNP have been shown to predict survival in COPD patients both during acute exacerbations (365, 366) and in stable disease (367, 368), predict risk of hospitalisation or need for intensive care (369) and been postulated as a screening tool to identify those with co-existent PH (370). Levels of NTproBNP during exacerbations of COPD have shown to relate to both left and right ventricular dysfunction but not sPAP or severity of lung disease (371). Chang et al reported on 244 COPD patients with an average FEV1 of 35% of predicted hospitalised with an acute exacerbation, and demonstrated NTproBNP predicted 30 day but not 1 year mortality (365). Raised troponin was also associated with mortality, and elevation of both markers of cardiac dysfunction was associated with a 15 fold increased 30 day mortality. Levels of NTproBNP showed no relationship to $Pa0_2$ but were not compared to indices of either right or left ventricular function. Hosieth et al found that levels of troponin were a stronger predictor of long term mortality than NTproBNP in those hospitalised with a COPD exacerbation (366), although neither echocardiography nor screening for

pulmonary embolism (PE) was performed in the population to determine nature of elevation in cardiac markers.

BNP has also been shown to relate to mortality when measured in a stable outpatient population. In COPD patients, Inoue et al demonstrated that BNP levels were higher than control subjects, correlated with LVEF, sPAP and shorter time to exacerbation, and rose during the acute exacerbation (368). Leutche et al demonstrated a raised normalised BNP ratio predicted mortality in a large cohort of chronic lung disease patients, and made efforts to exclude those with either PE or raised PAWP (367). RHC was performed with severe PH present in over one quarter, however the study included patients with connective tissue disease and sarcoidosis with therefore a potential alternate aetiology for PH.

Biomarkers offer an attractive screening tool for detection of PH. The afore mentioned limitations of echocardiography in the lung disease population and invasive nature of RHC make this ethically unjustifiable as a screening tool when treatment option for PH associated with lung disease is not available. Prognostically, and also potentially for recruitment to studies, the prevalence and detection of PH in lung disease population is desirable. NTproBNP has been proven as a marker of RV dysfunction in PAH and as a PH screening tool in connective tissue disease (372). As discussed above, levels of NTproBNP have been shown to relate to ventricular function and sPAP in chronic lung disease, although not consistently depending on population studied and method of determination of sPAP. Andersen et al reported on the use of BNP to detect echocardiography derived pulmonary hypertension in 117 COPD patients, and reported a NPV 22% and PPV 100% using a surprisingly low cut-off level of BNP of <95pg/ml (370). However, only 14/117 had PH determined by echo, of which only 6 underwent confirmatory RHC (with 3/6 confirmed as having PH). The literature on utility of NTproBNP as a screening tool for precapillary PH in chronic lung disease, relationship to pure RV dysfunction and survival in PH due to lung disease rather than coexistent LV dysfunction is therefore lacking.

3.2 Aims.

As demonstrated by the studies above, the role of pulmonary vasodilator therapy in severe PH associated with lung disease is uncertain, clouded by small studies with less vigorous criteria for diagnosing PH and utilising mixed populations of patients both with and without PH or with co-existent pulmonary venous disease and with resultant mix of both positive and negative outcomes. We sought to

1. Explore diagnostic utility and accuracy of CMR for determining presence of PH in comparison to echocardiography and NTproBNP in chronic lung disease

2. Characterise and compare RV structure and function determined by CMR and relationship to prognosis in chronic lung disease patients without PH (mPAP <25mmHg), with mild-moderate (mPAP 25-34mmHg) and severe PH (mPAP ≥ 35mmHg).

3. Assess response to PH specific therapy in a large cohort of chronic lung disease patients with associated severe PH determined by change in 6MWD and NTproBNP and further explore impact of lung disease severity and phenotype on survival and therapeutic response.

3.3 Materials and methods

3.3.1 Patients in the study

We retrospectively studied 255 treatment naïve incident cases diagnosed between January 2000 and March 2014 at the Scottish Pulmonary Vascular Unit, Glasgow. Patients were referred for investigation of unexplained PH, or PH felt disproportionate to the degree of lung disease and included after conventional multidisciplinary evaluation as described in Methods section 2.1.1. Patients were excluded if there was incomplete RHC data, missing CT or lung function data, or an alternative aetiology for PH. Figure 3.1 describes the study population.

3.3.1.1 IPAH patients

81 IPAH patients who had no evidence of parenchymal disease of any severity on CT of thorax, and no other explanation for PH were included. PH was defined in the IPAH group as mPAP ≥25 mmHg with a PAWP ≤15 mmHg and a normal or impaired CO (defined as CI ≤4 l/min/m^2). 7 patients were excluded whom were smokers with airflow obstruction (defined as post bronchodilator FEV1 <80% with FEV1/FVC <0.7). The remaining 74 patients were included in the study as a "pure" IPAH cohort for comparison.

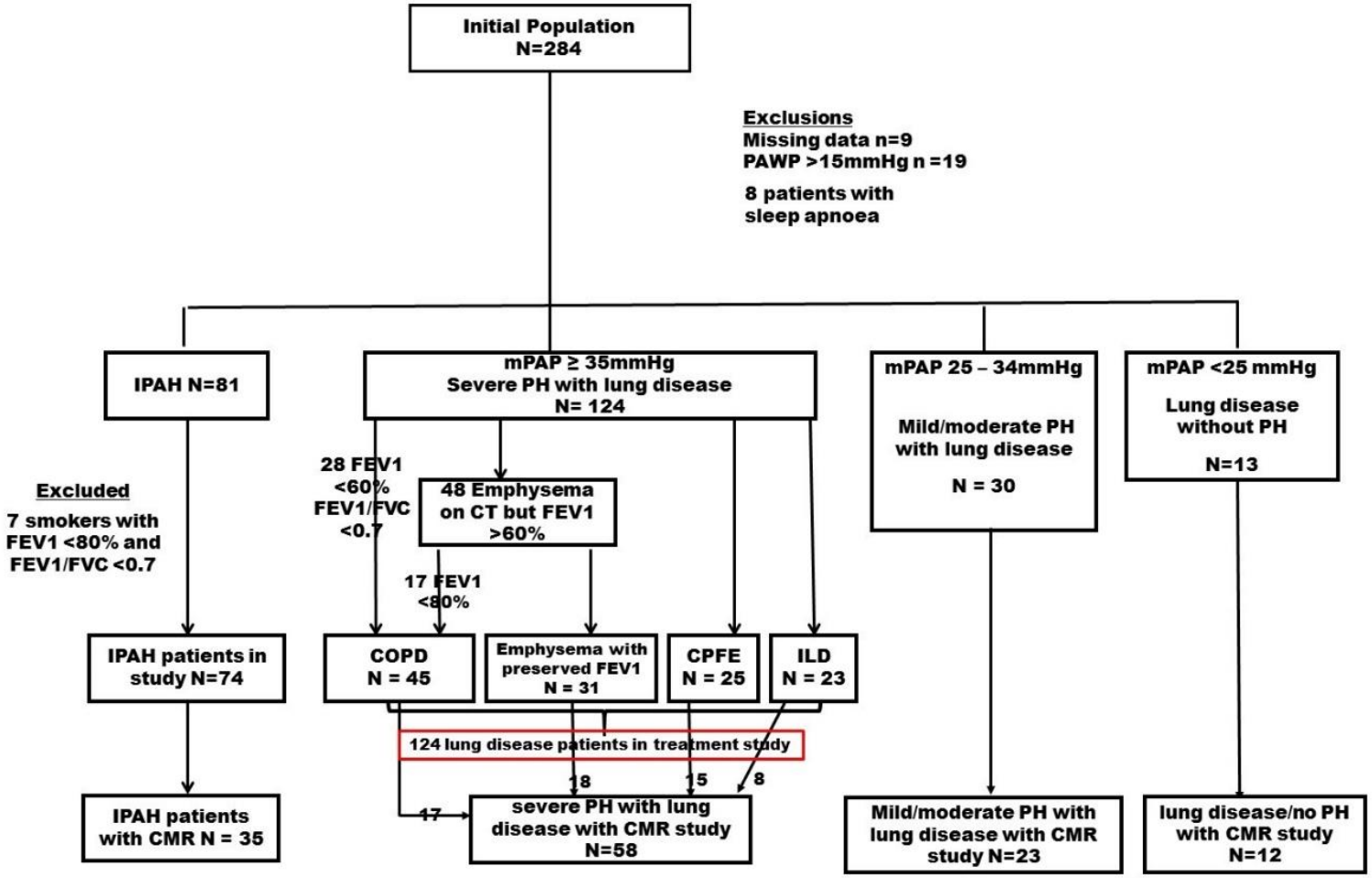

Figure 3.1 Study population

3.3.1.2 Severe PH in lung disease

There were 167 patients with pulmonary hypertension and associated lung disease. 124 patients met the criteria for severe PH, defined as a mPAP ≥35mmHg with a PAWP ≤15mmHg and normal or reduced CO, or a mPAP ≥30 mmHg with PAWP ≤15 mmHg and a CI <2 l/min/m^2 (n=3).

Patients were categorised by underlying lung disease into 1 of 4 phenotypes

(i) emphysema with preserved FEV1, defined as FEV1 >80% predicted with evidence of emphysema on CT thorax

(ii) combined pulmonary fibrosis and emphysema syndrome (CPFE), defined by coexistent predominantly apical emphysema and basal fibrosis on CT thorax with reduced DLCO.

(iii) Interstitial lung disease (ILD)

(iv) COPD, characterized by either post bronchodilator FEV1 <60% predicted, or emphysema on CT with FEV1 <80%, in conjunction with an FEV1/FVC ratio <0.7

In addition to the phenotypes described, the effect the severity of associated lung disease had on treatment outcome was evaluated. Patients were classified into one of two groups using criteria suggested at the Nice world PH symposium (253);

(i) severe PH/mild lung disease – defined as modest parenchymal abnormality on CT thorax, COPD with FEV1 ≥60% of predicted or ILD with FVC ≥70% of predicted

(ii) severe PH/severe lung disease - severe PH-CPFE, severe PH-COPD (defined by FEV1<60% of predicted), or severe PH-IPF (defined by FVC <70% of predicted).

3.3.1.3 PH "in proportion" to lung disease

Of the remaining patients with lung disease evaluated, 30 had mild-moderate PH "in proportion" to lung disease, defined as a mPAP 25-34 mmHg with the same PAWP and CO criteria as described above, and 13 had no PH defined as a mPAP <25 mmHg in accordance with guidelines.

3.3.2 Echocardiography

32 lung disease patients with mPAP <35 mmHg had both demonstrable tricuspid regurgitation to allow estimation of sPAP by echocardiogram and had undergone CMR. These were included for comparison with 53 severe PH/lung disease patients described in section 3.2.1.2 whom also had both echocardiography estimated sPAP and a CMR study to evaluate non invasive screening tools for detection of PH in lung disease. mPAP estimation by echo was derived from the formula mPAP = 0.61 sPAP + 2. Thresholds for detection of PH (i.e. mPAP ≥25 mmHg) and severe PH (i.e. mPAP ≥35mmHg) by echocardiogram derived sPAP were therefore 38 mmHg and 54 mmHg respectively. Unless otherwise stated, RAP was estimated at 5 mmHg. RV function was assessed by TAPSE (normal function defined by TAPSE >1.8cm) and RV dilatation by RVEDD (defined by >4.2cm).

3.3.3 Cardiac MRI

35 patients with IPAH and 93 with PH/lung disease underwent cardiac MRI. Of the later, 58 had severe PH/lung disease, 23 mild-moderate PH/lung disease and 12 lung disease patients without PH. Cardiac MRI image acquisition and data analysis was carried out as described in section 2.2. Inter-observer variability data has previously been published for our centre (373). CMR variables were indexed for BSA and adjusted for age.

3.3.4 Treatment and follow up

All patients with IPAH were treated with PH targeted therapy in accordance with guidelines (332). Patients with lung disease were treated with inhaled bronchodilators and LTOT in accordance with UK guidelines (374). Those with severe PH/lung disease received a minimum of 3 months compassionate use of PH targeted therapy. NYHA FC, 6MWD and NTproBNP were measured at diagnosis, and

reassessed at a time point greater than 3 months in those whom received PH therapy. As described in section 2.3 survival data was collected until last day of the study, 4th August 2014.

3.3.5 Statistical methods

Statistical analysis was carried out as described in methods section 2.3. In addition, ROC curves were derived to obtain thresholds for detection of both PH and severe PH in those with lung disease by level of NTproBNP and CMR indices of RVMI, RAC MPA and VMI. Agreement of RV parameters assessed by echocardiogram and CMR, and pulmonary artery pressure by echo and RHC was assessed by Pearson or Spearman correlation dependent on data distribution, and Bland-Altman analysis. Kaplan Meier survival curves were plotted by severity of pulmonary hypertension and by lung disease phenotype, and survival compared by logrank test.

3.4 Results

3.4.1 Population Characteristics

Patient characteristics are shown in tables 3-1 and 3-2 for those with lung disease and mild – moderate PH or no PH, and severe PH respectively. Whilst the 13 patients classified by current PH diagnostic guidelines as having "no PH" by mPAP <25 mmHg, the average mPAP in this group was mildly elevated in comparison to normal (14.7 mmHg ±4) at 21 mmHg (range 13-23). 6MWD was lower in those with mild-moderate PH compared to patients without PH (234±108 m vs 364±79 m p=0.001) indicating a greater degree of functional impairment associated with the development of PH.

There were 124 patients with severe PH/lung disease of which 84 died during follow up, and 74 IPAH patients of whom 25 died. 1 patient with severe PH/lung disease and 2 with IPAH underwent lung transplantation. Table 3-2 shows the patient characteristics of those with IPAH in comparison to severe PH with lung disease. IPAH patients were younger, more often female with less functional impairment and lower levels of NTproBNP despite similar haemodynamics.

In the severe PH/lung disease group, there were 31 patients with emphysema/preserved FEV1, 25 patients with CPFE, 23 patients with ILD and 45 with COPD phenotype. Of these 45 patients, 30 had emphysema, 4 respiratory bronchiolitis and 4 bronchiectasis on imaging. 6 had isolated spirometric abnormalities. Table 3-3 shows the characteristics of the lung phenotype groups. There were 88 patients meeting criteria suggested by Seeger et al. 30 patients had marked emphysema on CT but preserved FEV1 and were excluded as this group was not considered by this classification. 32 patients met criteria for severe PH/mild lung disease, and 58 patients with severe PH/severe lung disease; (22 CPFE, 26 COPD, 10 ILD).

In comparison to those with severe PH, those with mild to moderate PH in the setting of coexistent lung disease demonstrated preserved RV mass, volumes and function, were less hypoxaemic but had similar levels of functional impairment (mean 6MWD 234±108 m vs 206±105 m, p= 0.221).

3.4.1.1 Lung function

DLCO was worse in those with severe PH/lung disease in comparison to IPAH patients (24 (19-34) v 62 (39-76), p<0.0001) and both in those with lung disease with mild-moderate (30 (22-36) p=0.05) or no PH (45 (35-56) p=0.001). Pa02 was lower in those with severe PH/lung disease (7.4 ± 1.6 kPa) in comparison to IPAH (9.6 ± 2.0 kPa, p<0.0001) and lung disease without PH (10.0 ± 1.9 kPa, p<0.0001), but not lung disease mild-moderate PH (8.0 ± 1.7kPa, p=0.08).

In those with COPD, there was no relationship between FEV1 and mPAP or RVEF (r=0.04, P = 0.79 and r = 0.00, p = 1.0 respectively). FEV1:FVC ratio weakly correlated with mPAP (r = 0.29, p = 0.05) but not RVEF (r =-0.05, p = 0.79).

In those with ILD, there was no relationship between FVC and either mPAP or RVEF (r =-0.08, p = 0.67 and r = 0.19 p = 0.49 respectively), nor TLC with mPAP or RVEF (r = 0.08, p = 0.72 and r = 0.15, p = 0.60 respectively).

3.4.1.2 Functional Status

Patients with severe PH lung disease demonstrated greater degree of functional impairment than those with IPAH or lung disease without PH. NYHA FC was worse with 12% FC II, 71% FC III and 17% FC IV in comparison to 24%, 69% & 7% (p = 0.021) in IPAH and 46%, 54% & 0% in lung disease without PH (p = 0.005) respectively. There was a trend towards worsening function class in comparison to patients with mild-moderate PH with lung disease (21% FCII, 76% FCIII & 3% FCIV, p = 0.099).

6MWD was lower in severe PH/lung disease patients compared to IPAH patients (206±106m v 344±118m, p<0.0001) despite greater degree of PH in the latter (mPAP 46 v 54mmHg, p<0.0001). In a multivariate regression model with age, mPAP, CO and FEV1, RAP (r = -0.273 p = 0.004), compliance (SV/PP r = 0.282 p = 0.036) and DLCO (r = 0.281 p = 0.001) were independent determinants of 6MWD. Table 3-4 shows univariate regression analysis of determinants of 6MWD in lung disease patients. Table 3-5 shows the final multivariate regression model for 6MWD. In the subgroup with CMR variables, in a multivariate model with age, RAP, mPAP, CO & FEV1, neither RVEF nor LVEDVI were independent predictors of 6MWD (r = -0.07 p = 0.567 & r =.0.195 p = 0.06 respectively).

3.4.1.3 Right ventricular dysfunction in severe PH associated with lung disease

CMR data was available for 58 patients with severe PH/lung disease (17 COPD, 8 ILD, 15 CPFE, 18 emphysema) and 35 IPAH patients. Table 3-6 displays the characteristics of the two groups. There were no significant differences between right and left ventricular function. RVMI was lower in severe PH/lung disease group (50g/m2 versus 56g/m2 p=0.014). Lung disease patients were older (66 vs 48 years, p<0.0001) with a more significant smoking history (51/55 previous smokers vs 11/35).

In both IPAH and severe PH/lung disease patients, RVEF was reduced (32 ± 12% and 33 ± 13% respectively) with increased RV mass and volumes (RVEDVI 95 ± 28 ml/m2 and 91 ± 30 ml/m2 respectively).

Table 3-1 Characteristics of patients with mild - moderate pulmonary hypertension associated with lung disease

	All	mPAP 25-34mmHg	mPAP <25mmHg	p value
n	(43)	(30)	(13)	
Age years	68±10	69±10	66±9	0.395
Sex %	38♀62♂	37♀63♂	46♀54♂	
Smoking history %		86 (25)	100 (12)	
Pack Years	39±18	38±21	41±13	0.711
Aetiology % (n)				
COPD		40 (12)	23 (3)	
ILD		23 (7)	23 (3)	
CPFE		20 (6)	15 (2)	
Emphysema		17 (5)	39 (5)	
Baseline Haemodynamics				
mPAP mmHg	27 ± 5	29 ± 3	21 ± 3	<0.0001***
RAP mmHg	3 ±3	3±3	3±2	0.706
CI L/min/m^2	2.6 ± 0.6	2.6±0.5	2.6±0.6	0.909
PVR Wood units.	4.1 (2.9-5.4)	4.6 (3.8-6.0)	2.6 (2.3-3.0)	<0.0001***
PAWP mmHg	8±4	7±4	9±3	0.229
SV02 %	68 (65-75)	68 (65-75) (28)	71.8 (65.8-74.4) (11)	0.701
SV/PP mL/mmHg	2.28±0.9	1.9 ± 0.6 (28)	3.2 ±0.7	<0.0001***
Cardiac MRI		N=23	N=12	
RVEF %	50 ± 11	48 ± 10	54 ± 13	0.139
RVEDVI mL/m^2	63.0 (56.2-79.9)	62 (52-77)	68 (59-83)	0.260
RVMI g/m^2	32.9 (27.3-39.5)	35 (30-40)	29 (24-42)	0.172
LVEF %	66.2±8	65 ±14	68 ± 11	0.487
LVEDVI mL/m^2	54.5 (41.5-66.5)	49 (35-60)	67 (54-80)	0.006**
LVMI g/m^2	50.7 (44.6-58.0)	50 (43-57)	56 (50-61)	0.280
SVI mL/m^2	38 ± 9	37 ± 10	41 ± 9	0.244
RAC MPA %	30.4 (17-42)	23 (17-33) (23)	42 (34-51) (11)	0.006**
AoRAC %	18.9 (14-31) (35)	17 (11-31) (22)	22 (16-35)	0.729
Lung Function				
FEV1 %	79 (59-96)	72 (52-94)	91 (64-104)	0.212
FVC %	100±30	97 ± 32	109 ± 27	0.318
DLCO % (n)	33 (23-45) (39)	30 (22-36) (28)	45 (35-56) (11)	0.008**
$Pa0_2$ kPa (n)	8.6 ± 1.9 (31)	7.8±1.4 (20)	10.0±1.9 (11)	0.001**
Functional Class % (n)				
I/II	29 (12)	21 (6)	46 (6)	0.140
III	69 (29)	76 (22)	54 (7)	
IV	2 (1)	3 (1)	0 (0)	
6MWD (m) (n)	275 ± 116	234±108 (26)	364±79 (12)	0.001**
NTproBNP (pg/ml) (n)	209 (110 – 426)	218 (112– 412) (28)	200 (91 – 403) (12)	0.750

Table 3-2. Population characteristics of severe PH associated with lung disease patients in comparison to IPAH.

	IPAH (74)		Severe PH/ lung disease (124)		p value
Age years	49±18		67±10		<0.0001***
Sex %	72♀28♂		45♀55♂		<0.0001***
Smoking history % (n)	32 (22)		89 (107)		
Pack years	30±15		42±24		0.048*
Baseline Haemodynamics					
mPAP mmHg	54 (46-62)		46 (40-51)		<0.0001***
RAP mmHg (n)	8±6		8±5	(123)	0.935
CI L/min/m^2 (n)	2.0±0.5	(73)	2.0±0.5	(119)	0.557
PVR w.u.	12.5 (9.2-17.9)		10.6 (8.2-14.2)		0.011*
PAWP mmHg	7±4		8±3		0.047*
SV02 % (n)	63 (56-69)	(66)	61 (53-67)	(112)	0.185
SV/PP mL/mmHg	0.94 ± 0.5	(53)	0.98 ± 0.4	(110)	0.582
Initial PH therapy % (n)					
CCB	9.5 (7)		2 (3)		0.003**
PDE-5i	44.6 (33)		68 (84)		
ETRA	25.7 (19)		23 (28)		
Prostanoid	14.9 (11)		4 (5)		
Combination	5.4 (4)		3 (4)		
Lung Function					
FEV1 %	91 (83-97)		75 (58-93)		<0.0001***
FVC %	101 ± 13		96 ± 25		0.076
FEV1/FVC %	76 (70-79)		63 (55-71)		<0.0001***
TLC % (n)	93 ± 10	(68)	92 ± 18	(102)	0.602
DLCO % (n)	62 (39-76)	(71)	24 (19-34)	(104)	<0.0001***
$Pa0_2$ kPa (n)	9.6±2	(43)	7.4±1.6	(84)	<0.0001***
Functional Class % (n)					
I/II	24 (17)		12 (14)		0.021*
III	69 (49)		71 (85)		
IV	7 (5)		18 (21)		
6MWD m (n)	334±118	(62)	206±105	(102)	<0.0001***
NTproBNP pg/ml (n)	1128 (508 - 2890)	(46)	2273 (943 – 4506)	(94)	0.019*

Table 3-3. Population characteristics of severe PH associated with chronic lung disease according to lung disease phenotype

	Emphysema (31)	CPFE (25)	COPD (45)	ILD (23)	p value
Age years	70±10	68±7	63±11	69±10	0.015
Sex %	52♀48♂	36♀64 ♂	47♀53♂	46♀54♂	
Smoking history %	100	100	89	50	
Pack years	51±29	47±23	36±17	25±16	0.020*
LTOT usage %	87	91	60	73	
Baseline Haemodynamics					
mPAP mmHg	46±7	48±8	48±11	46±9	0.678
RAP mmHg	7±4	9±5	8±5	10±6 (22)	0.109
CI L/min/m^2 (n)	1.9±0.4	1.8±0.4 (24)	2.1±0.6 (44)	1.9±0.5 (20)	0.162
PVR w.u.	12.2±4	12.9±4	11.1±5	10.0±3	0.119
PAWP mmHg	8±3	8±3	9±3	9±3	0.357
SV02 % (n)	61±11 (29)	59±11 (24)	59±10 (39)	62±9 (20)	0.683
SV/PP ml/mmHg	0.9 ± 0.3	0.9 ± 0.4	1.1 ± 0.6 (37)	1.0 ± 0.3	0.037*
Initial PH therapy % (n)					
CCB	0	0	4.4 (2)	4 (1)	
PDE-5	71.0 (22)	60 (15)	66.7 (30)	74 (17)	
ETRA	19.4 (6)	24 (6)	24.4 (11)	22 (5)	
Prostanoid	6.5 (2)	4 (1)	4.4 (2)	0	
Combination	3.2 (1)	12 (3)	0	0	
Lung Function					
FEV1 %	99±17	81±22	55±16	79±20	<0.0001***
FVC %	117 (105-139)	101 (86-124)	84 (75-98)	74 (65-98)	<0.0001***
FEV1/FVC %	65±10	62±9	55±11	79±11	<0.0001***
TLC % (n)	102 ± 14 (27)	89 ± 15 (23)	95 ± 17 (35)	74 ± 16 (17)	<0.0001***
DLCO % (n)	26±9 (28)	21±7 (22)	31±14 (35)	28±11 (19)	0.017*
$Pa0_2$ kPa (n)	7.0±2.1 (22)	7.0±0.8 (15)	7.7±1.4 (32)	7.5±1.7 (15)	0.401
Function Class % (n)					
I/II	3 (1)	0	21 (9)	18 (4)	ns
III	81 (25)	79 (19)	65 (28)	59 (13)	
IV	16 (5)	21 (5)	14 (6)	23 (5)	
6MWD m (n)	224±99 (23)	174±78 (20)	215±110 (39)	199±121 (20)	0.409
NTproBNP pg/ml (n)	1447 (753–3881) (22)	2272 (1203-6384) (22)	2335 (650–4359) (32)	2703 (1259-4143) (18)	0.572

Table 3-4. Determinants of functional capacity (defined by 6MWD) in severe PH associated with lung disease

Variable	Correlation coefficient	95% CI	p value
Age	-0.154	-3.50 – 0.138	0.07
mPAP	**-0.175**	**-3.09 - -0.08**	**0.039**
RAP	**-0.323**	**-11.2 - -3.78**	**<0.0001**
PVR	**-0.284**	**-10.5 - -2.88**	**0.001**
CO	**0.377**	**21.61 – 52.0**	**<0.0001**
SV/PP	**0.428**	**36.6 – 81.0**	**<0.0001**
FEV1	**0.188**	**0.09 – 1.49**	**0.027**
DLCO	**0.425**	**2.10 – 4.67**	**<0.0001**
Pa02	**0.442**	**16.79 – 39.62**	**<0.0001**
RVEF	**0.241**	**0.20 – 3.23**	**0.027**
LVEF	0.199	-1.22 – 3.10	0.070
RVEDVI	0.016	-0.75 – 0.87	0.885
LVEDVI	**0.314**	**0.65 – 3.23**	**0.004**
SVI	**0.308**	**1.05 – 5.40**	**0.004**
RVMI	-0.096	-1.75 – 0.68	0.385
RAC MPA	**0.343**	**1.12 – 4.69**	**0.002**

Table 3-5. Multivariate regression model for 6MWD in lung disease patients

R = 0.629, adj r^2 = 0.395, p<0.0001 for the model.

Variable	Regression coefficient	95% CI	P value
Age	- 0.144	-3.55 – 0.40	0.118
mPAP	**0.261**	**0.07 – 4.75**	**0.043**
RAP	**-0.273**	**-11.65 - -2.26**	**0.004**
CO	0.179	-1.74 – 37.50	0.074
SV/PP	**0.282**	**2.59 – 74.90**	**0.036**
FEV1	0.154	-0.64 – 1.44	0.073
DLCO	**0.281**	**0.93 – 3.69**	**0.001**

Table 3-6. Characteristics of IPAH and severe PH/lung disease patients with CMR studies.

	IPAH	Severe PH/lung disease	p value
n	35	58	
Age (years)	48 ± 17	65 ± 11	<0.0001***
PVR (Wood Units)	14.5 (10 - 18)	10.5 (8 - 15)	0.012*
mPAP (mmHg)	57 ± 14	48 ± 9	<0.0001***
PAWP (mmHg)	8 ± 4	8 ± 4	0.604
SV/PP	0.89 ± 0.4 (31)	1.05 ± 0.5 (57)	0.105
RVEF (%)	32 ± 12	33 ± 13	0.644
LVEF (%)	66 (60 -71)	62 (54 -71)	0.470
RVMI (g/m^2)	56 (49-75)	50 (38 - 61)	0.014*
LVMI (g/m^2)	46 (41 -57)	48 (41 - 56)	0.916
RVEDVI (ml/m^2)	95 ± 28	91 ± 30	0.537
RVESVI (ml/m^2)	65 ± 26	62 ± 28	0.609
LVEDVI (ml/m^2)	40 (34 - 53)	44 (37 - 53)	0.414
SVI (ml/m^2)	25 ± 10	28 ± 8	0.182
RAC MPA (%)	21 (17 - 28) (28)	18 (16 – 22) (53)	0.096
RAC Ao (%)	24 (14 - 28) (22)	18 (14 - 24) (48)	0.241

3.4.2 Screening for pulmonary hypertension in lung disease

91 of the 167 lung disease patients had both CMR and echocardiography studies, 12 with no PH, 23 with mild-moderate and 56 with severe PH. It was not possible to estimate sPAP by echocardiogram in 10 of 164 patients. 3 patients had a CMR performed but had poor quality studies due to respiratory motion artefact and were excluded. Only 3 patients were classed as having severe PH phenotype by an mPAP 30 -34 (range 32-34mmHg) and CI <2 l/min/m^2 (1.5-1.9). None of these had a CMR study and were excluded from this analysis.

Tables 3-7 and 3-8 summarise the sensitivity and specificity for each screening tool for the detection of PH and severe PH respectively in patients with lung disease.

3.4.2.1 Echocardiography

Overall, echocardiography estimated sPAP was available for 154 patients with lung disease and 50 IPAH patients. Correlations between echocardiography estimated sPAP and invasively measured sPAP were similar in both, Pearson r = 0.53 p<0.0001 and r= 0.51 p=0.0002 respectively. These values are similar to those published in literature in patients with severe lung disease (r=0.69, Arcasoy 2003 (199)) Linear regression shown in figure 3.2.

In those with lung disease, for sPAP estimated by echocardiography versus invasive, mean difference was 0.84 mmHg with limits of agreement -36 and 38 mmHg. In IPAH patients, for sPAP by echo versus invasive, mean difference was -9 mmHg with limits of agreement -52 and 34 mmHg. Figure 3.3 shows the Bland-Altman plots of the difference between echo estimated sPAP and invasive sPAP against the mean of both values demonstrating poor accuracy of echocardiography estimated sPAP.

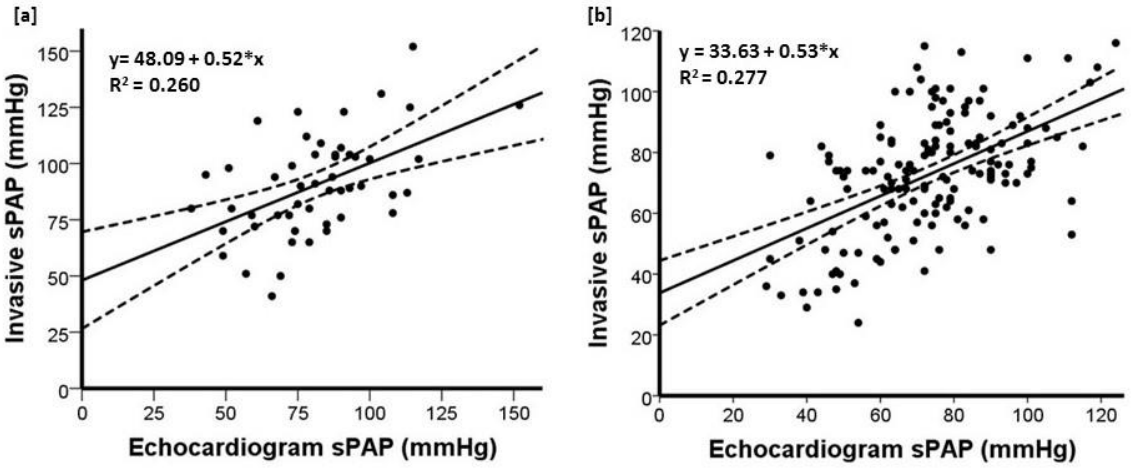

Figure 3.2 Correlation between echocardiogram estimated sPAP and invasive sPAP for [a] IPAH [b] lung disease patients.
Similar correlations were observed in both groups. $p<0.0001$, with poor R^2 values. Whilst statistically significant, degree of accuracy between echocardiography estimated and measured sPAP was poor, as shown in figure 3.4

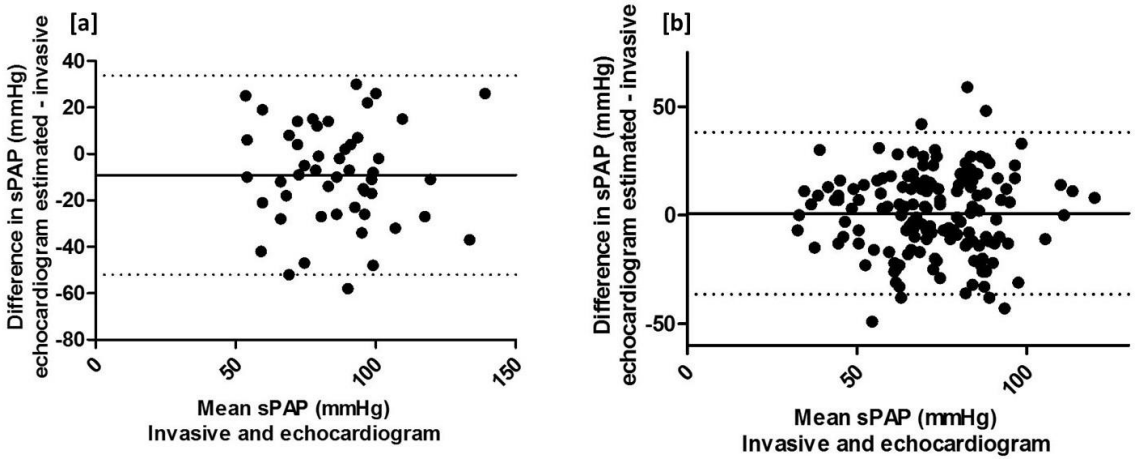

Figure 3.3 Bland Altman plots of the difference between echocardiogram estimated and invasive sPAP against mean of both values for [a] IPAH [b] lung disease patients.

Limits of agreement (dashed line) and mean difference (solid line) shown. Plots show large variation, up to 50mmHg between echo estimated and invasive measured sPAP in those with lung disease. This is in agreement with previous published study showing inaccuracy of echo in chronic lung disease were inaccuracies in 52% of echocardiograpy estimated sPAP has been shown (199).

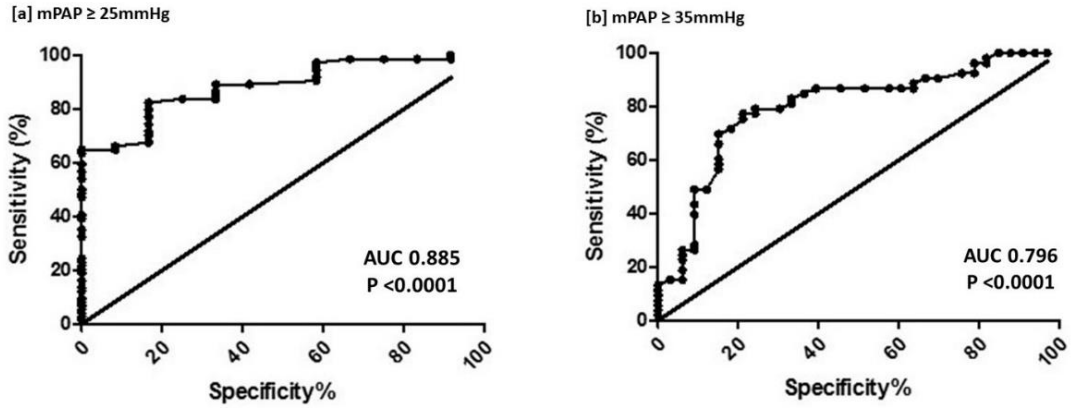

Figure 3.4 ROC curves of sensitivity and specificity of echocardiography estimated sPAP for [a] mPAP ≥ 25mmHg [b] ≥ 35mmHg

A level of sPAP of 38mm Hg was 97% sensitive & 41.7% specific for detection of PH, resulting in 7 out of 12 misclassified as having PH, and 1 out of 74 missed (91% (83%-96%) PPV and 83% (36%-100%) NPV). A level of sPAP of 54mmHg resulted in 15/33 false positives and 8/53 false negatives for detection of severe PH associated with lung disease (sensitivity 85% specificity 61%). ROC curves are shown in figure 3.4.

Right ventricular end diastolic diameter (RVEDD) was estimated in 8, 20 and 44 patients with no, mild – moderate and severe PH associated with lung disease respectively. RVEDD was increased in those with severe PH/lung disease only (4.6 ± 0.9, P= 0.006, ULN 4.2cm (49)) and correlated with RVEDVI measured by CMR, r= 0.572, p <0.0001. Figure 3.5 shows mean RVEDD by PH severity, and correlation with RVEDVI for the whole group. A RVEDD >3.2cm was 91% sensitive and 38% specific for detection of PH, LR 1.45, AUC 0.740 P=0.028, resulting in 5/8 false positives and 6/64 false negatives. RVEDD >3.5cm 89% sensitive 46% specific (AUC 0.787 P<0.0001) for detecting mPAP ≥ 35mmHg. 15/28 patients were misclassified as having severe PH and 5/44 cases were missed using this threshold.

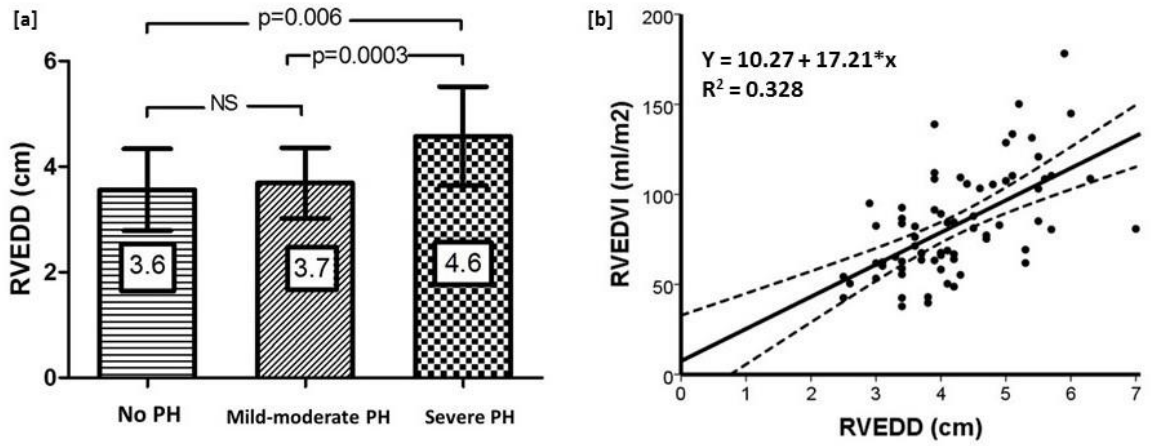

Figure 3.5 RV end diastolic diameter in patients with lung disease according to severity of pulmonary hypertension

[a] RVEDD was similar in patients with mild-moderate PH in comparison to those without PH but increased significantly in those with severe PH indicating RV dilatation in this group. [b]. RVEDD correlated well with RV end-diastolic volume index determined by gold standard cardiac MRI.

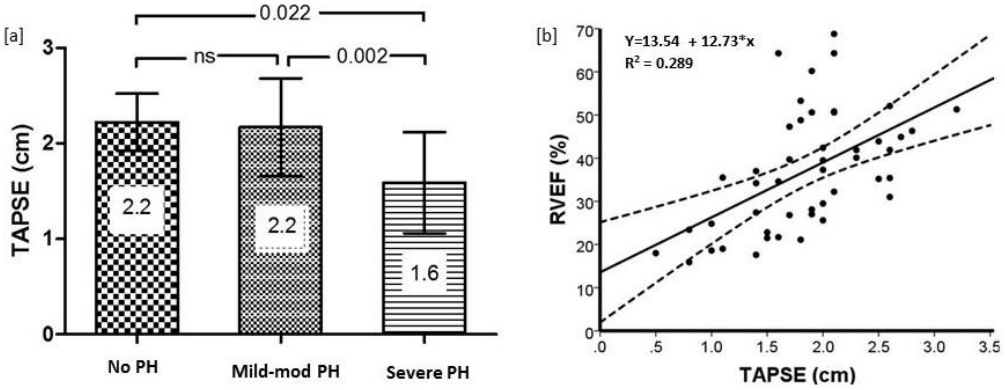

Figure 3.6 TAPSE in patients with lung disease with mild - moderate and severe PH in comparison to those without PH

TAPSE was preserved in those with mild-moderate PH but fell in those with severe PH/lung disease, mean value 1.6cm indicative of impaired RV function in this group. [b]. TAPSE showed good correlation with cardiac MRI measured RVEF ($p<0.0001$).

TAPSE was estimated in 4, 10 and 53 patients without PH, with mild-moderate and severe PH respectively. TAPSE was preserved in those with mild-moderate PH but reduced in those with severe PH (2.2 cm vs 1.6 cm, P=0.002, see figure 3.6a). Figure 3.6b shows the correlation between TAPSE and CMR derived RVEF (r= 0.548, p <0.0001).

3.4.2.2 NTproBNP

NTproBNP levels were available for 12, 24 and 46 patients with no, mild to moderate and severe PH respectively. Figure 3.7 shows the median NTproBNP by severity of PH. Levels of NTproBNP did not differ between those with mild-moderate and those without PH, 200 vs 218 pg/ml respectively, p= 0.47. NTproBNP was elevated in those with severe PH, 2258 pg/ml (416 - 4295) p<0.0001, and correlated with RV dilatation and inversely with RVEF (r = 0.484 & r = -0.678 respectively, both p<0.0001. see figure 3.8)

A level of NTproBNP of 106 pg/ml was 91% sensitive but only 33% specific (LR 1.37) for mPAP ≥25mmHg, resulting in 8/12 false positives and 6/67 false negatives. A level of NTproBNP >230 pg/ml was 91% sensitive 58% specific (LR 2.15) for detecting severe PH, missing 4/46 cases and misclassifying 14/33 (75% PPV 83% NPV). Receiver operator curves are shown in figure 3.9.

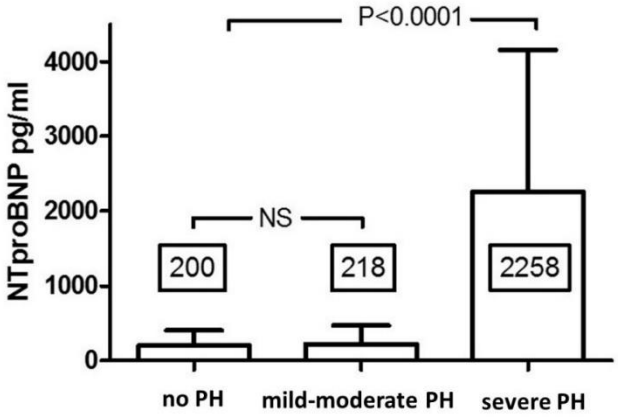

Figure 3.7 NTproBNP levels for patients with chronic lung disease without PH in comparison to those with mild-moderate and severe PH.

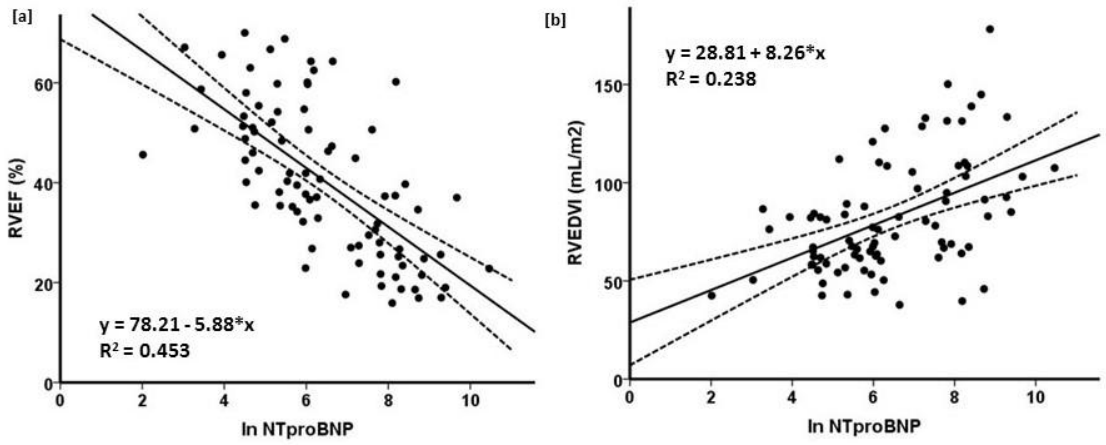

Figure 3.8 Correlation between NTproBNP and [a] RVEF [b] RVEDVI in patients with chronic lung disease.

Logarithmic transformation of NTproBNP shown due to data distribution. Increasing levels of NTproBNP showed good relationship to falling RVEF and increasing RVEDVI indicative of RV dysfunction. p<0.0001 for both.

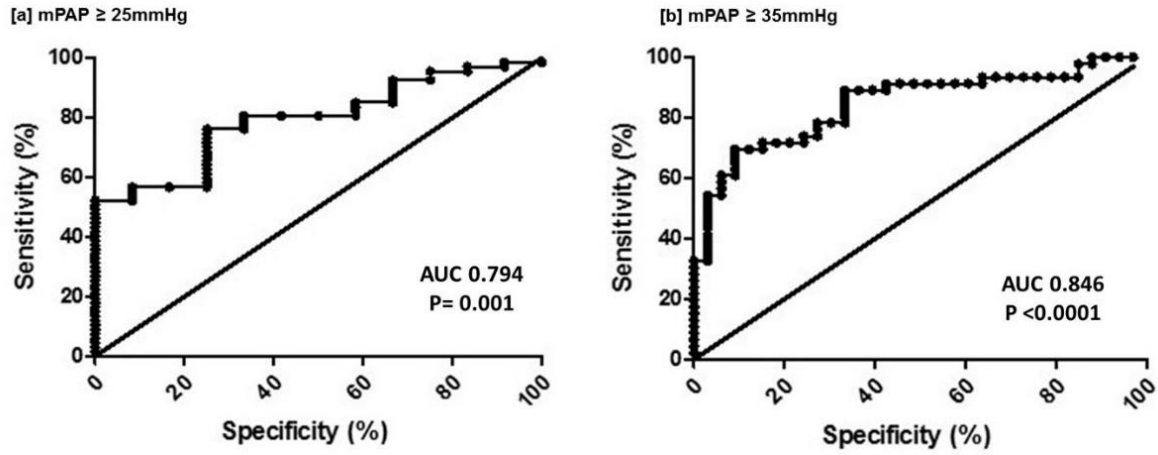

Figure 3.9 ROC curves for sensitivity and specificity of NTproBNP for detecting [a] mPAP ≥ 25mmHg [b] ≥ 35mmHg in patients with lung disease

3.4.2.3 Cardiac MRI

Lung disease patients with no PH or mild-moderate PH displayed preserved RV function (RVEF 54 ± 13 % and 48 ± 10 %, LLN 45%), with no RV dilatation (RVEDVI 62 ml/m^2 and 66 ml/m^2 respectively). In contrast, those with severe PH had impaired RVEF (34 ± 13 %) and increased RVEDVI (85 ml/m^2). Figure 3.10 shows the RVEF and RVEDVI for the groups. $Pa0_2$ and FEV1 correlated with RVEF (r=0.328 p= 0.006, r = 0.237 p = 0.024 respectively) but were not independent determinants of RVEF in a model with age and PVR (p = 0.063 and 0.227 respectively).

RVMI was increased in those with severe PH (50 g/m^2) in comparison to both mild-moderate (36 g/m^2 p = 0.003) and no PH patients (29g/m^2 p = 0.006). There was a trend towards an increase in RVMI between mild-moderate PH and no PH patients, but this did not meet statistical significance (p = 0.135). Figure 3.11 shows the median RVMI by severity of PH.

Receiver operator curves for RVMI are shown in figure 3.12. RVMI >26.45 g/m^2 was 89% sensitive and 42% specific for a mPAP ≥25mmHg (7/12 false positives, 8/73 false negatives. RVMI ≥32.8 g/m^2 was 87% sensitive and 57% specific for a mPAP ≥ 35mmHg (15/35 false positives, 7/53 false negatives).

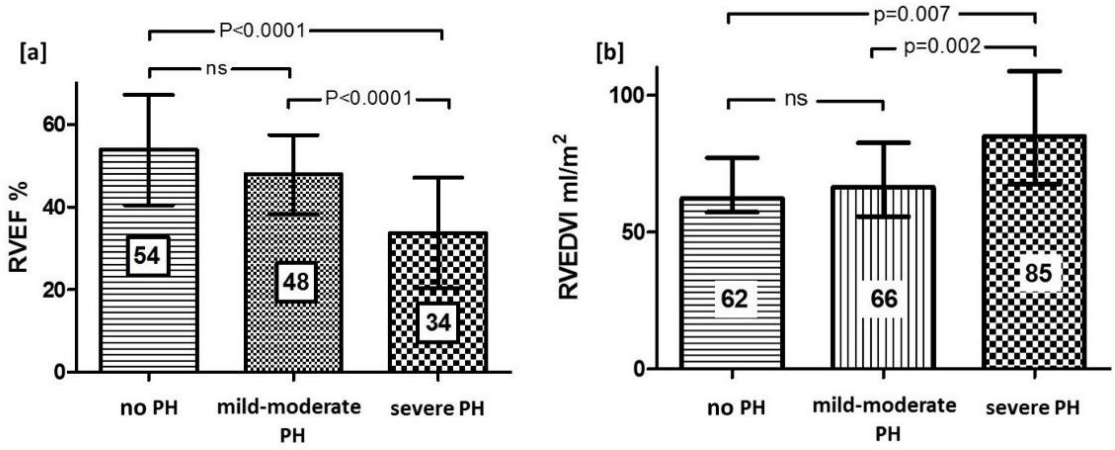

Figure 3.10 Right ventricular function and volume in lung disease patients by severity of pulmonary hypertension.
Patients with severe PH displayed reduced RV ejection fraction and RV dilatation in comparison to those with mild-moderate or without PH.

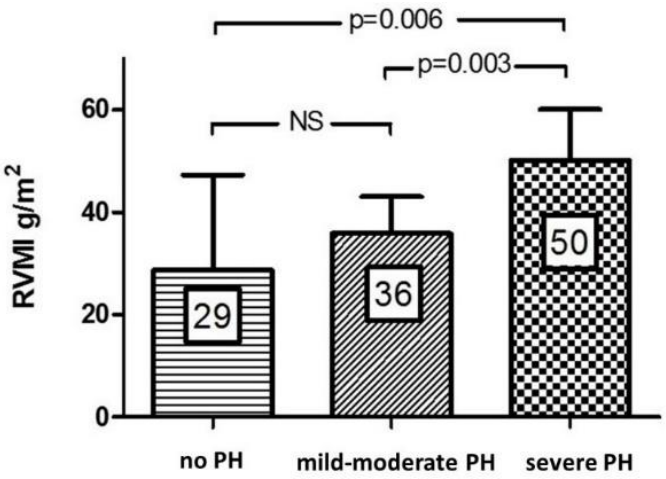

Figure 3.11 Right ventricular mass in patients with no, mild-moderate and severe PH in patients with associated lung disease

Patients with severe PH displayed increased RVM in comparison to those with mild-moderate and no PH. Patients with mild-moderate PH did not have statistically significant increase in RVM (p=0.135)

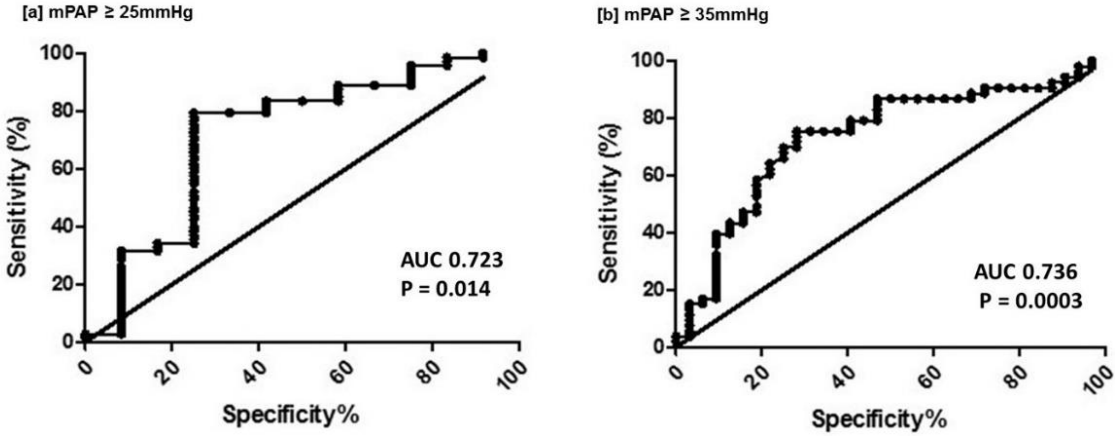

Figure 3.12. Receiver operator curves for sensitivity and specificity of RV mass to detect [a] mPAP ≥ 25mmHg and [b] mPAP ≥ 35mmHg.

Optimal thresholds of >26.5 g/m^2 and > 32.8g/m^2 respectively.

VMI (ventricular mass index, ratio of RVM:LVM) showed an increase from 0.53 (0.44 - 0.84) in those with no PH, to 0.76 (0.64 – 0.89) in patients with mild-moderate PH and to 1.01 (0.72 – 1.20) in patients with severe PH. Figure 3.13 shows the median VMI for each group.

A VMI of >0.525 was 97% sensitive and 50% specific for a mPAP ≥ 25mmHg (6/12 false positives 4/73 false negatives). A VMI >0.6 was 91% sensitive and 44% specific for a mPAP ≥35mmHg (18/32 false positives and 5/53 false negatives). Receiver operator curves are shown in figure 3.14.

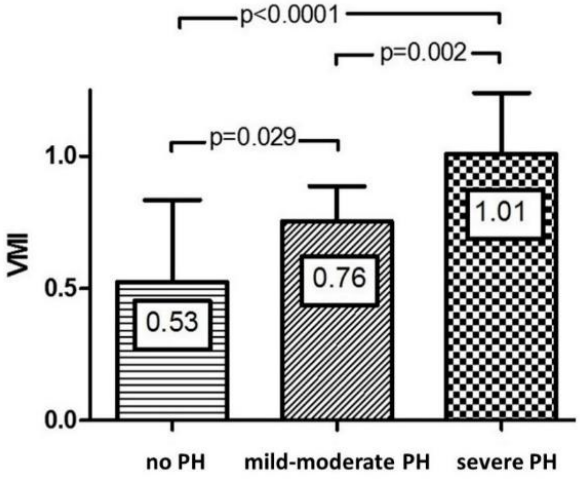

Figure 3.13. Ventricular mass index in patients with no, mild-moderate and severe PH and chronic lung disease.

VMI, the ratio of RV/LV mass, increased with increasing severity of pulmonary hypertension. Mean (SD) shown.

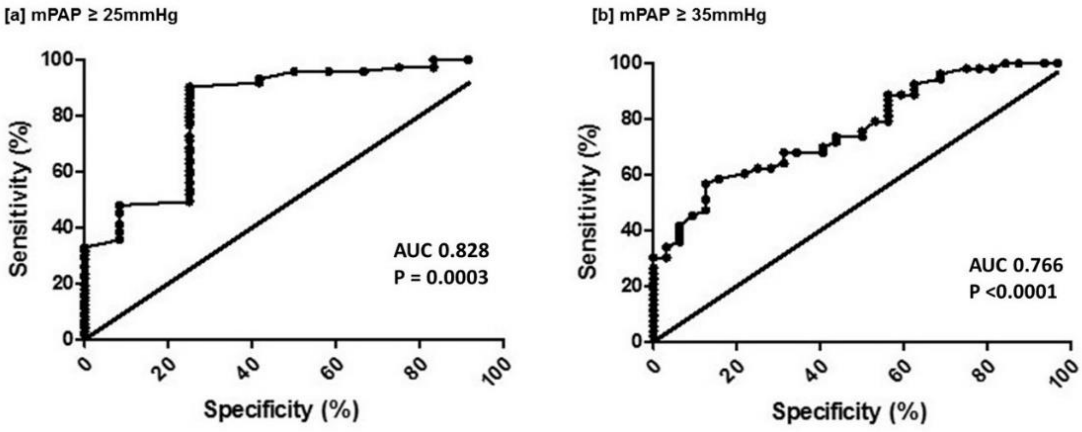

Figure 3.14 Receiver operator curves displaying sensitivity and specificity of ventricular mass index for detecting [a] mPAP ≥ 25mmHg and [b] mPAP ≥35mmHg.

Optimal thresholds of > 0.525 and > 0.60 respectively were identified.

3.4.2.4 Vascular stiffness

Vascular stiffness increased with PH of increasing severity. Compliance (SV/PP = 1/ vascular stiffness) fell from 3.2 ± 0.7 in those without PH, to 1.9 ± 0.7 in patients with mild-moderate PH and 0.98 ± 0.4 in patients with severe PH ($p<0.0001$ for both). RAC MPA fell from 42 (34-51) % to 23 (17-33) % and to 18 (16-22) respectively. Figure 3.15 shows measures of vascular compliance for each group. $Pa0_2$ but not FEV1 correlated with RAC MPA ($r = 0.265$ $p = 0.030$) and SV/PP ($r = 0.353$ $p<0.0001$). SV/PP correlated with RAC MPA for the whole cohort, $p<0.0001$ (see figure 3.16)

Receiver operator curves for RAC MPA for mPAP ≥25mmHg and ≥35mmHg are shown in figure 3.17. A RAC of <41.15% was 96% sensitive and 58% specific for a mPAP ≥ 25mmHg (5/12 false positives and 3/73 false negatives). A RAC of <32.5% was 94% sensitive and 47% specific for a mPAP ≥ 35mmHg (17/32 false positives and 3/53 false negatives).

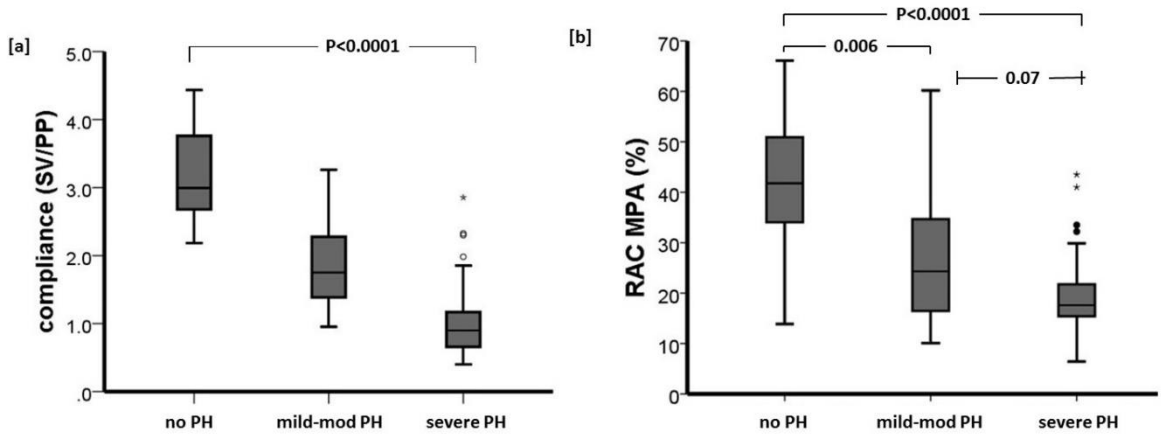

Figure 3.15 Invasive (SV/PP) and non-invasive (RAC MPA) determined pulmonary vascular compliance in patients with no, mild-moderate and severe PH associated with lung disease.

Falling vascular compliance (i.e. increasing stiffness) was demonstrated with increasing severity of PH by either method. Median (IQR) shown.

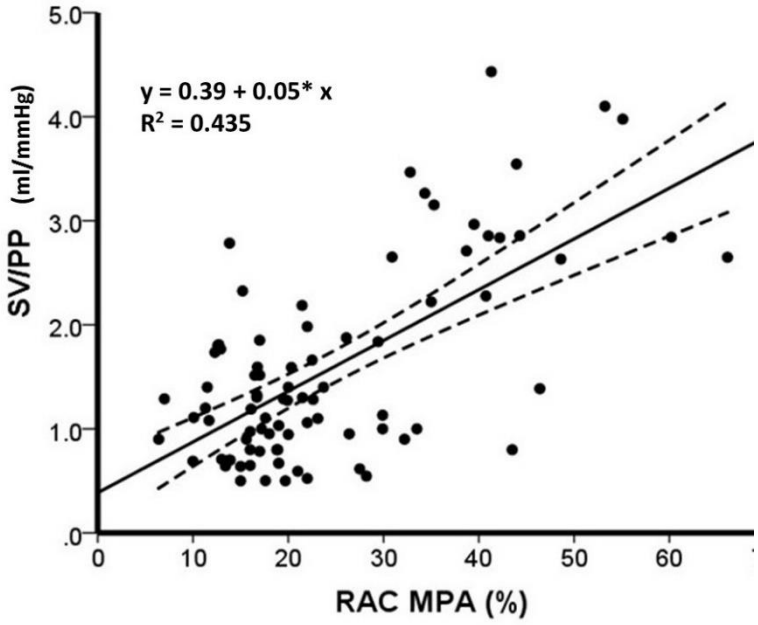

Figure 3.16 Correlation of invasive (SV/PP) and noninvasive (RAC MPA) estimates of pulmonary artery compliance for lung disease patients

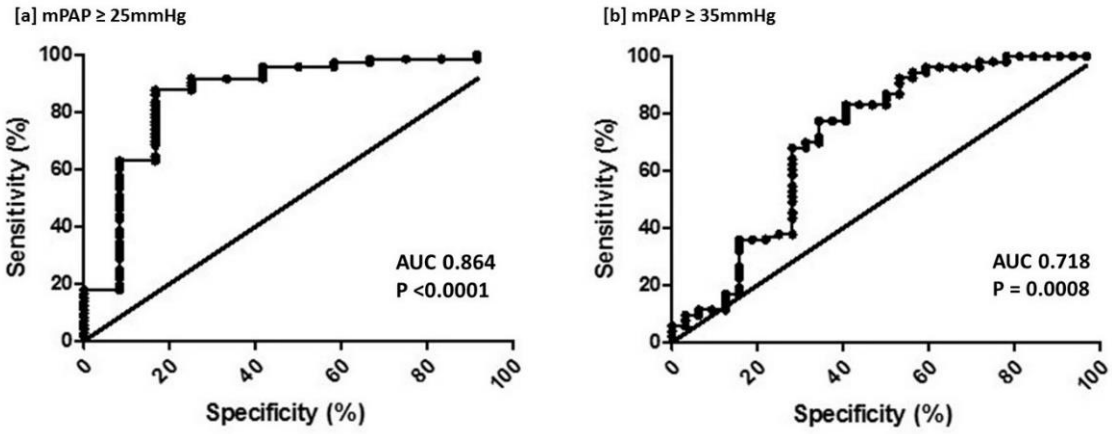

Figure 3.17 Receiver operator curves displaying sensitivity and specificity of RAC MPA for detecting [a] mPAP ≥ 25mmHg and [b] ≥ 35mmHg.

Optimal threshold of RAC MPA < 41.15 % and < 32.5% respectively were determined.

The combination of echocardiogram estimated sPAP and RAC MPA performed superiorly for the detection of a mPAP ≥25 mmHg (100% sensitivity, 83% specificity 98%PPV 100%NPV). Table 3-7 summarises the sensitivity, specificity, PPV and NPV for each screening method.

Table 3-7. Sensitivity and specificity of imaging and biomarker modalities for detection of PH in chronic lung disease patients

Variable threshold	Sensitivity (95% CI)	Specificity (95% CI)	PPV (95% CI)	NPV (95% CI)
Echo estimated sPAP >38mmHg	97 (91-99)	42 (15-72)	91 (83-96)	83 (36-100)
RVEDD >3.2cm	91 (81-97)	38 (9-76)	92 (82-97)	33 (8-50)
NTproBNP >106pg/ml	91 (82-97)	33 (10-65)	88 (78-95)	40 (12-74)
RVMI > 26.45g/m^2	89 (80-95)	42 (15-72)	90 (81-96)	39 (14-68)
VMI >0.525	97 (91-100)	50 (21-79)	92 (84-97)	75 (35-97)
RAC MPA <41.15%	96 (89-99)	58 (28-85)	93 (85-98)	70 (35-93)
Echo estimated sPAP + RAC	**100 (95-100)**	**83 (52-98)**	**98 (91-100)**	**100 (69-100)**
Echo estimated sPAP + VMI	100 (95-100)	67 (35-90)	95 (87-99)	100 (63-100)
Echo estimated sPAP + NTproBNP	100 (95-100)	50 (21-79)	93 (84-97)	100 (54-100)

Combination of imaging modalities, echocardiogram to estimate pressure and CMR to assess vascular stiffness (RAC MPA) optimal screening method for presence of pulmonary hypertension. And/or analysis used for combined modalities e.g. sPAP >38mmHg AND RAC <41%, or RAC <41% /unable to estimate sPAP.

The combination of echo estimated sPAP >54 mmHg and RVMI of > 32.8 g/m^2 had the highest accuracy for the detection of mPAP ≥ 35mmHg (98% sensitivity, 79% specificity 88% PPV and 96% NPV). Table 3-8 summarises performance characteristics for each screening method for detection of severe PH in lung disease patients.

Table 3-8 Sensitivity and specificity of imaging modalities and NTproBNP for detection of severe PH in chronic lung disease patients

Variable threshold	Sensitivity (95% CI)	Specificity (95% CI)	PPV (95% CI)	NPV (95% CI)
Echo estimated sPAP >54mmHg	85 (72-93)	61 (42-77)	78 (65-88)	71 (51-87)
RVEDD >3.5cm	89 (75-96)	46 (28-66)	72 (58-84)	72 (47-90)
NTproBNP >230pg/ml	91 (79-98)	58 (39-75)	75 (62-86)	83 (61-95)
RVMI > 32.8g/m^2	87 (76-95)	57 (39-74)	76 (64-86)	74 (54-89)
VMI >0.6	91 (79-97)	44 (26-62)	73 (60-83)	74 (49-91)
RAC MPA <32.5%	94 (84-99)	47 (29-65)	75 (63-85)	83 (59-96)
Echo estimated sPAP + RAC	98 (90-100)	73 (54-87)	85 (74-93)	96 (80-100)
Echo estimated sPAP + RVMI	**98 (90-100)**	**79 (61-91)**	**88 (77-95)**	**96 (81-100)**
Echo estimated sPAP + VMI	96 (87-100)	73 (54-87)	85 (73-93)	92 (75-99)
Echo estimated sPAP + NTproBNP	96 (87-100)	85 (68-95)	91 (80-97)	93 (78-99)

Combination of echocardiogram to assess pressure and CMR to measure RV mass optimal screening for severe PH in lung disease. And/or analysis used for combined modalities e.g. sPAP >54mmHg AND RVMI >32.8g/m^2, or RVMI >32.8 g/m^2 /unable to estimate sPAP

3.4.3 Survival and prognostic factors

Mean length of follow up for the entire population was 801 ± 722 days (range 17 – 3582 days). 22 (of 30) patients with mild-moderate PH and 3 (of 13) patients with lung disease but no PH died during the follow up period. Survival in those with mild-moderate PH in comparison to those with severe PH/lung disease, the latter of which were treated with pulmonary vasodilators was no different (1 and 3 year estimated survival 67.5% vs 76.6% and 32.1% vs 40.1% respectively, p=0.441). Both demonstrated poorer survival in comparison to those without PH (1 and 3 year estimated survival 92.3% and 80.8%, p= 0.006 & 0.023 with those with mild-moderate and severe PH respectively). KM survival curves according to PH severity are shown in figure 3.18.

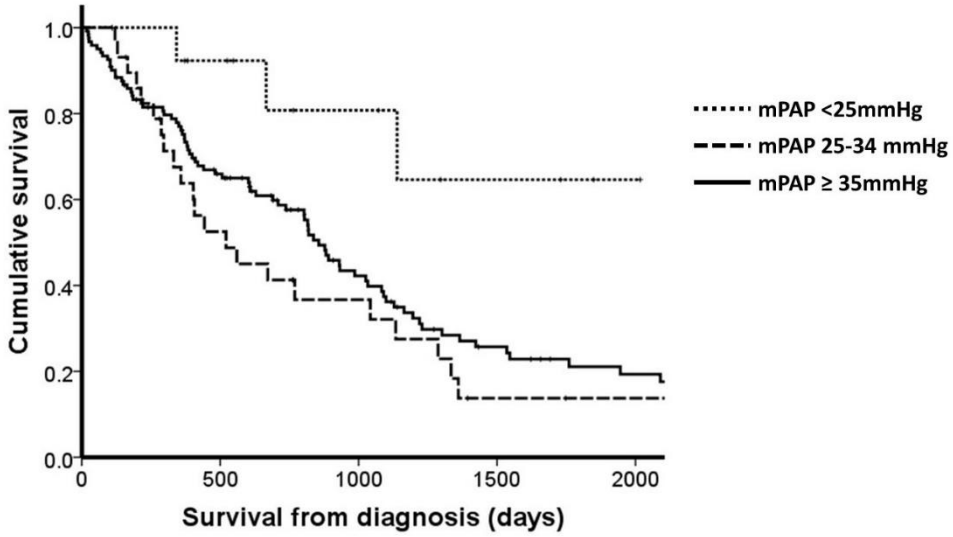

mPAP	Patients at risk				
<25mmHg	13	10	6	3	1
25-34mmHg	31	14	8	2	1
≥ 35mmHg	121	69	35	18	11

Figure 3.18. Kaplan Meier curves describing survival by severity of pulmonary hypertension in lung disease patients.

Survival was comparable in those with mild-moderate PH and severe PH who were treated with pulmonary vasodilators (logrank p = 0.441). Both groups displayed reduced survival in comparison to lung disease patients without PH (logrank p = 0.006 and p = 0.023 respectively).

All patients in severe PH group received pulmonary vasodilator therapy until date of death or censored due to loss of follow up (n=1).

Observed survival was worse in those with severe PH/lung disease, 1 & 3 year estimated survival rates compared to IPAH were 75% versus 90% and 40% versus 72% respectively (p <0.0001). However those with lung disease were significantly older, mean age 67 versus 49 years in IPAH (p <0.0001). When the older age of the population was considered on multivariate cox, the presence of lung disease remained associated with worse survival (HR 0.489 95%CI 0.299-0.798, p=0.004). Kaplan Meier curve describing the survival of severe PH/lung disease patients in comparison to IPAH patients is shown in figure 3.19.

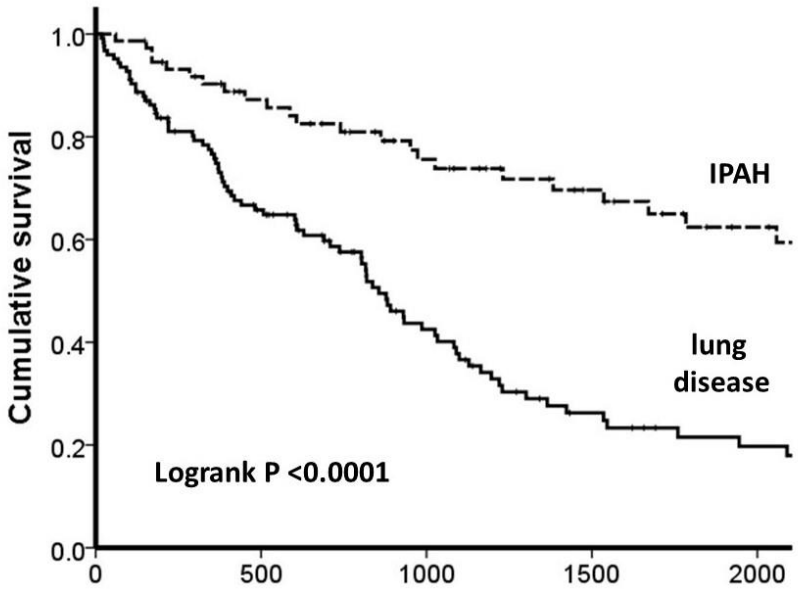

Patients at risk					
IPAH	74	56	42	31	22
Lung disease	124	70	36	18	11

Figure 3.19. Kaplan Meier survival plot comparing outcome of patients with severe PH and lung disease in comparison to IPAH patients.

Survival in those with emphysema was reduced in comparison to IPAH (1-year survival 74% and 3-year 32% p=0.002). CPFE patients had a comparable 1 year survival rate, although the overall survival at 3 years was significantly lower than IPAH (1-year survival 88%, 34% at 3 years, p=0.001). ILD patients had the poorest survival, 1-year survival 60%, 3-year 19%, worse than IPAH (p <0.0001) and COPD patients (p=0.014). Survival between other lung phenotypes did not differ. KM curve describing survival of the population according to lung disease phenotype is shown in figure 3.20.

There was no difference in survival observed between those with severe PH/mild lung disease and severe PH/severe lung disease (1 and 3 year estimated survival rates 87 % versus 76 % and 47 % v 44 % respectively, p = 0.411). KM survival curve according to lung disease severity is shown in Figure 3.21

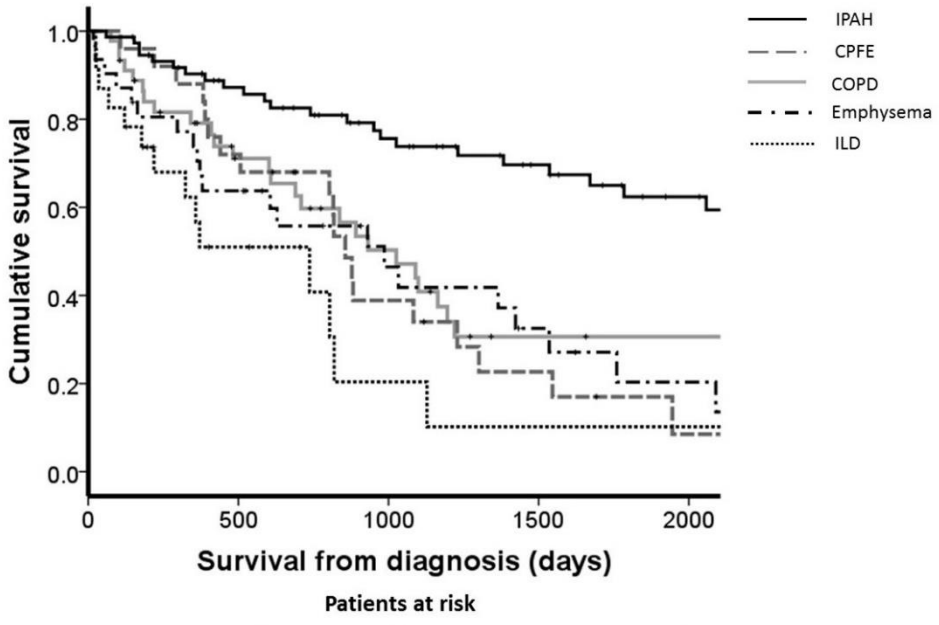

Patients at risk

CPFE	25	18	8	4	1
COPD	45	25	16	7	6
Emphysema	31	19	10	6	3
ILD	23	8	2	1	1

Figure 3.20. Survival according to lung disease phenotype associated with severe PH.

Survival between lung disease phenotypes did not differ, with the exception of poorer survival in those with ILD in comparison to COPD diagnoses (logrank p = 0.014).

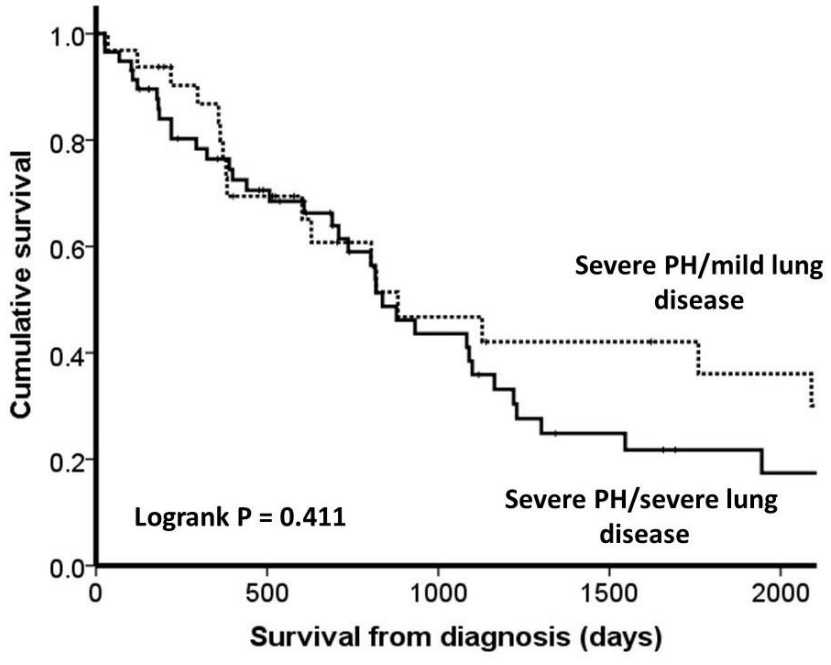

Patients at risk					
Mild lung disease	32	19	10	8	6
Severe lung disease	58	34	17	8	4

Figure 3.21. Kaplan Meier survival curve for patients with severe PH/severe lung disease in comparison to those with mild-moderate lung disease and severe PH.

No significant difference in survival was observed according to severity of associated lung disease (logrank p = 0.411)

In a multivariate model with age, male sex, higher mPAP and lower LVEDVI were independently associated with reduced survival in lung disease patients with mPAP <35mmHg (HR 1.153 95% CI 1.003-1.326, p=0.045 and HR 0.944 95% CI 0.907-0.984 p=0.006 respectively). Table 3-9 shows the univariate and multivariate survival analysis.

Table 3-10 displays prognostic relevance of mPAP and sPAP in comparison to indices of RV dysfunction measured by RHC, Echocardiography and CMR on univariate survival analysis for all 167 lung disease patients. Only 62 patients had all variables available for multivariate analysis. In a model with age, mPAP, and RAP, RVEF but not RVEDD on echo remained an independent prognostic factor (HR 0.965 95%CI 0.934-0.997, p=0.032).

Table 3-9. Prognostic variables in mild - moderate pulmonary hypertension associated with lung disease.

Variable	Univariate model		Multivariate model	
	HR (95%CI)	P value	HR (95%CI)	P value
Age	1.044 (0.997 - 1.092)	0.06	1.038 (0.989 - 1.090)	0.132
Sex (♂=0)	0.698 (0.308 - 1.583)	0.390	0.201 (0.069 - 0.583)	0.003
Echo sPAP	**1.061 (1.029 – 1.094)**	**<0.001**		
mPAP	**1.137 (1.033 - 1.252)**	**0.009**	**1.153 (1.003 - 1.326)**	**0.045**
RAP	0.846 (0.703 - 1.017)	0.075		
PVR	**1.288 (1.034 - 1.606)**	**0.024**		
SV/PP	**0.420 (0.228 – 0.777)**	**0.006**		
DLCO	**0.975 (0.954 - 0.997)**	**0.024**		
6MWD	0.997 (0.993 - 1.001)	0.162		
NTproBNP	1.421 (0.935 - 2.162)	0.100		
RVEF	0.964 (0.918 - 1.011)	0.131		
RVEDVI	0.998 (0.974 - 1.024)	0.901		
LVEF	0.973 (0.702 - 1.349)	0.871		
LVEDVI	**0.962 (0.930 - 0.994)**	**0.019**	**0.944 (0.907 - 0.984)**	**0.006**
RAC MPA	**0.964 (0.931 - 0.999)**	**0.046**		

Higher mPAP, male sex and lower LV end diastolic volume were independent predictors of survival on multivariate cox proportional regression analysis.

Table 3-10. Indices of RV function assessed by 4 modalities (RHC, Echocardiography, CMR and NTproBNP) as predictors of survival in all patients with chronic lung disease.

Variable	n	HR (95%CI)	p value
Right heart catheterisation			
mPAP	167	1.001 (0.987 - 1.015)	0.914
RAP	167	1.064 (1.026 – 1.104)	0.001**
CI	167	0.466 (0.313 – 0.694)	<0.001***
Echocardiography			
PASP	154	1.007 (0.998 – 1.016)	0.144
TAPSE	70	0.882 (0.457 – 1.702)	0.708
RVEDD	130	1.297 (1.031 – 1.631)	0.026*
Cardiac MRI			
RVEF	92	0.971 (0.952 – 0.990)	0.003**
RVESVI	92	1.013 (1.003 – 1.023)	0.009**
SVI	92	0.968 (0.940 – 0.996)	0.023*
NTproBNP	126	1.332 (1.139 – 1.559)	<0.001***

Univariate cox proportional regression analysis shown. Echocardiography derived parameters performed less well than other modalities in assessing prognosis related to RV dysfunction. The severity of PH, assessed by either echocardiography (PASP) or RHC (mPAP) did not relate to outcome in comparison.

3.4.3.1 Prognostic factors in severe PH associated with lung disease

A comparative analysis of severe PH/lung disease survivors at 3 years was carried out. Table 3-11 shows the characteristics of non survivors and survivors. Survivors were characterised by less RV dysfunction (lower RAP and NTproBNP, higher CI and RVEF) and lower vascular stiffness (greater SV/PP).

In a model with age, sex, PVR and NTproBNP, RAP and CI independently predicted survival in patients with severe PH/lung disease (HR 1.08195% CI 1.026 – 1.139, HR 0.350 95% CI 0.167 – 0.696 respectively, both p = 0.003). Table 3-12 shows the univariate and multivariate cox survival analysis for IPAH and severe PH/lung disease patients.

Univariate cox survival analysis for severe PH/lung disease patients according to phenotype is shown in table 3-13. Haemodynamics but not lung function related to outcome.

In patients with severe PH and ILD, lower CI and higher PAWP were associated with death (HR 0.098 95% CI 0.130 – 0.733 p=0.024 and HR 1.254 95% CI 1.006 – 1.562 p = 0.044 respectively).

In patients with severe PH and CPFE, increased RAP (HR 1.113 95% CI 1.029 – 1.204 p = 0.007), PVRI (HR 1.078 95% CI 1.005 – 1.157 p = 0.036) and NTproBNP (HR 1.857 95% CI 1.149 – 3.00 p = 0.011) and lower CI (HR 0.276 95% CI 0.083 – 0.912 p = 0.035) or SVO2 (HR 0.936 95% CI 0.898 – 0.977 p = 0.002) were associated with worse survival.

In patients with emphysema/preserved FEV1, lower 6MWD (HR 0.994 95% CI 0.990 – 0.998 p = 0.003), CI (HR 0.141 95% CI 0.039 – 0.512 p = 0.003) and SV/PP (HR 0.037 95% CI 0.005 – 0.235 p = 0.001) and increased RAP (HR 1.374 95% CI 1.182 – 1.597 p <0.0001) and PVRi (HR 1.138 95% CI 1.053 – 1.229 p = 0.001) were predictive of worse survival.

In those severe PH/lung disease patients whom had undergone CMR, in a multivariate model with age, sex, PVR and SVI, RVEF was an independent predictor of survival (HR 0.946 95% CI 0.907 – 0.986 p = 0.009). Table 3-14 shows the univariate and multivariate survival analysis.

Table 3-11. Characteristics of survivors and non-survivors at 3 years follow up with severe PH/lung disease.

	Survivors (32)	Non-survivors (65)	P value
Age years	64 ± 11	68 ± 9	0.028*
Sex %	52♀ 48♂	36♀ 64♂	ns
Haemodynamics			
mPAP mmHg	48 ± 12	47 ± 8	0.524
RAP mmHg	6 ± 4	10 ± 5	<0.0001***
CI L/min/m²	2.2 ± 0.5	1.7 ± 0.4	<0.0001***
PVR w.u.	10.6 ± 5	12.3 ± 4	0.084
PAWP mmHg	9 ± 3	8 ± 3	0.800
SV02 %	63 ± 10	58 ±10	0.010*
SV/PP	1.2 ± 0.5	0.9 ± 0.4	0.009**
Ventricular structure & function	n=18	n = 29	
RVEF %	40 ± 14	29 ± 12	0.003**
LVEF %	64 ± 16	59 ± 14	0.347
SVI L/min/m²	32 ± 10	25 ±7	0.010*
RVMI g/m²	53 ± 14	57 ± 20	0.446
RVEDVI ml/m²	77 ± 21	95 ± 32	0.036*
RVESVI ml/m²	48 ± 22	68 ± 28	0.010*
MPA RAC (%)	19.7 (17 - 22)	16.4 (15 - 20)	0.112
Lung Function			
FEV1 %	75 (59 - 102)	77 (60 - 90)	0.759
FVC %	101 (80-123)	98 (77 - 114)	0.402
TLC %	101 (94-108)	88 (80-103)	0.019*
DLCO %	25 (19-42)	24 (18-31)	0.360
$Pa0_2$ kPa (n)	7.6 ± 1.4 (23)	7.1 ± 1.6 (40)	0.198
Functional Class % (n)			
I/II	16.1 (5)	8.8 (5)	ns
III	74.2 (23)	63.2 (36)	
IV	9.7 (3)	28.0 (16)	
6MWD m (n)	226 ± 114 (30)	188 ± 93 (46)	0.117
NTproBNP pg/ml (n)	1051 (239 – 2741) (19)	2474 (1357 – 6883) (49)	0.002**
Δ NTproBNP pg/ml	0.0 (-609 - +325) (19)	-179 (-1378 - +637) (37)	0.809
Δ 6MWD m	27 (-29 - +80) (29)	31 (-32 - +73) (30)	0.958

Table 3-12. Univariate and multivariate cox proportional hazard analysis of prognostic factors in severe PH/lung disease in comparison to IPAH.

Variable	Univariate model				Multivariate model			
	IPAH		Severe PH/Lung disease		IPAH		Severe PH/Lung disease	
	HR(95%CI)	p-value	HR (95%CI)	p-value	HR (95%CI)	p-value	HR (95%CI)	p-value
Age	**1.047 (1.002-1.074)**	**0.001**	**1.033 (1.009-1.058)**	**0.007**	1.012 (0.981-1.043)	0.460	1.017 (0.992-1.042)	0.184
Sex	0.911 (0.383-2.165)	0.833	**0.630 (0.430-0.986)**	**0.043**	**0.339 (0.120-0.952)**	**0.040**	0.649 (0.402-1.048)	0.077
6MWD	**0.994 (0.990-0.998)**	**0.003**	0.998 (0.995-1.000)	0.056	**0.994 (0.998-0.999)**	**0.020**		
NTproBNP	1.066 (0.756 -1.503)	0.717	**1.445 (1.152-1.813)**	**0.001**			1.277 (0.990-1.139)	0.059
Haemodynamic Variables								
mPAP	1.005 (0.976 –1.034)	0.744	0.986 (0.965-1.008)	0.222				
RAP	1.006 (0.942-1.075)	0.855	**1.087 (1.044-1.133)**	**<0.0001**			**1.081 (1.026-1.139)**	**0.003**
PVR	1.009 (0.950-1.072)	0.767	1.030 (0.986-1.076)	0.185	1.036 (0.964-1.113)	0.335	0.930 (0.864-1.001)	0.052
PVRI	1.004 (0.970-1.039)	0.813	**1.039 (1.011-1.068)**	**0.006**				
CI	0.912 (0.436-1.905)	0.805	**0.324 (0.194-0.540)**	**<0.0001**			**0.350 (0.167-0.696)**	**0.003**
PAWP	0.964 (0.872-1.066)	0.477	1.000 (0.934-1.071)	0.998				
SV02	0.989 (0.948-1.032)	0.605	**0.974 (0.953-0.996)**	**0.021**				
SV/PP	0.537 (0.174-1.650)	0.278	**0.517 (0.288-0.929)**	**0.027**				
Lung Function								
DLCO	**0.954 (0.934-0.975)**	**<0.0001**	**0.977 (0.956-0.998)**	**0.030**	**0.966 (0.941-0.992)**	**0.011**		
Pa02	0.808 (0.597-1.094)	0.168	**0.798 (0.642-0.991)**	**0.041**				

CMR data is not included as only 58/124 patients had CMR data. The analysis of this subset can be seen in table 3-14

Table 3-13.Univariate cox proportional hazards analysis of prognostic factors according to lung disease phenotype associated with severe PH.

Variable	ILD		CPFE		Emphysema		COPD	
	HR(95%CI)	P value	HR(95%CI)	P value	HR(95%CI)	P value	HR(95%CI)	P value
Age	1.011 (0.964 – 1.061)	0.641	1.015 (0.950 – 1.086)	0.655	1.036 (0.985 - 1.089)	0.173	**1.051 (1.003-1.101)**	**0.037**
Sex ♂ = 0	0.900 (0.289 – 2.800)	0.856	1.149 (0.458 – 2.881)	0.767	1.022 (0.432 – 2.418)	0.961	**0.303 (0.126-0.730)**	**0.008**
6MWD	0.955 (0.989 - 1.00)	0.061	0.999 (0.991 – 1.008)	0.897	**0.994 (0.990-0.998)**	**0.003**	0.999 (0.996-1.003)	0.722
NTproBNP	1.424 (0.750 – 2.702)	0.280	**1.857 (1.149 - 3.000)**	**0.011**	1.514 (0.941 – 2.436)	0.088	1.385(0.898-2.137)	0.140
Haemodynamics								
mPAP	0.975 (0.916 – 1.038)	0.430	1.024 (0.973 – 1.078)	0.359	1.026 (0.975 – 1.079)	0.323	0.972 (0.939-1.006)	0.107
RAP	1.094 (0.997 - 1.200)	0.058	**1.113 (1.029 - 1.204)**	**0.007**	**1.374 (1.182 - 1.597)**	**<0.0001**	1.018 (0.941-1.101)	0.654
PVRi	1.063 (0.959 – 1.177)	0.245	**1.078 (1.005 - 1.157)**	**0.036**	**1.138 (1.053 - 1.229)**	**0.001**	1.004 (0.960-1.050)	0.853
CI	**0.098 (0.130 - 0.733)**	**0.024**	**0.276 (0.083 - 0.912)**	**0.035**	**0.141 (0.039 - 0.512)**	**0.003**	0.471 (0.213-1.039)	0.062
PAWP	**1.254 (1.006 - 1.562)**	**0.044**	1.018 (0.879 – 1.179)	0.815	0.909 (0.788 – 1.049)	0.192	0.927 (0.814-1.056)	0.255
SVO2	0.937 (0.873 - 1.005)	0.068	**0.936 (0.898 - 0.977)**	**0.002**	0.972 (0.929 – 1.017)	0.215	0.988 (0.949-1.028)	0.548
SV/PP	1.853 (0.126 – 26.859)	0.659	0.252 (0.061 - 1.048)	0.058	**0.037 (0.005 - 0.235)**	**0.001**	1.174 (0.553-2.493)	0.677
Lung Function								
FEV1			1.001 (0.982 – 1.021)	0.891	0.995 (0.971 – 1.012)	0.688	1.019 (0.989-1.051)	0.219
FVC	0.974 (0.938-1.012)	0.177						
DLCO	0.955(0.898-1.046)	0.146	1.022 (0.953 – 1.096)	0.539	0.951 (0.900 - 1.005)	0.077	0.976 (0.945-1.009)	0.152

CMR data is not included as only 58/124 patients had CMR data. The analysis of this subset can be seen in table 3-14

Table 3-14. Indices of right and left ventricular structure & function as prognostic factors in severe PH associated with chronic lung disease.

Variable	Univariate model		Multivariate model	
	HR (95%CI)	P value	HR (95%CI)	P value
RVEF	0.939(0.907-0.972)	<0.0001	0.946 (0.907-0.986)	0.009
RVEDVI	1.014(1.003-1.026)	0.017		
RVESVI	1.019(1.006-1.031)	0.003		
RVMI	1.030(1.009-1.051)	0.004		
LVEF	0.975(0.951-0.999)	0.040		
LVEDVI	0.993(0.972-1.015)	0.525		
LVMI	1.005(0.981-1.030)	0.682		
SVI	0.939(0.897-0.983)	0.007	0.943 (0.888-1.001)	0.053

In multivariate analysis with age, sex, PVRI and SVI, lower RVEF was an independent predictor of poorer prognosis.

3.4.4 Response to PH therapies

In those treated with pulmonary vasodilators due to a diagnosis of either IPAH or severe PH/lung disease, 29 patients (9 IPAH, 4 COPD, 5 CPFE, 2 ILD and 9 emphysema/preserved FEV1) were unable to perform a 6MWT at diagnosis. 18 patients died prior to their first follow up (4 IPAH, 4 emphysema/preserved FEV1, 1 CPFE, 6 ILD, 3 COPD). Of these, 9 were unable to carry out a 6MWT at diagnosis. Median time to follow up did not differ between IPAH and lung disease groups (111 (97-150) vs 111(96-148) days p=0.888). Exercise oxygen saturation data was available for 47 patients with severe PH/lung disease. No increase in desaturation on exercise following PH therapy was observed (-8% (-30 - -6) to -9 %(-15- -6) p=0.834).

Baseline and follow up 6MWD, NTproBNP and NYHA FC for all the groups are shown in table 3-15. Figures 3.22 and 3.23 show the median Δ6MWD and ΔNTproBNP following PH treatment for each group.

Table 3-15. Baseline and follow up 6MWD, NTproBNP and NYHA FC after a minimum of 3 months of therapy for severe PH/lung disease patients in comparison to IPAH.

Group	Baseline	Follow up	P value
IPAH			
6MWD (m) n=58	337±114	376±97	<0.0001***
NTproBNP n=42	1085 (449-2545)	788 (289-1655)	0.001**
NYHA FC n=63	17/41/4	30/29/3	0.055
Lung Disease (all)			
6MWD (m) n=80	224±102	243 ±102	0.032*
NTproBNP pg/ml n=82	2245 (850-4295)	1667 (614-3590)	0.008**
NYHA FC n=98	12/75/13	18/74/8	0.302
COPD			
6MWD (m) n=34	220±112	245±107	0.033*
NTproBNP pg/ml n=28	2501 (514-4213)	1938 (399-3817)	0.063
NYHA FC n=32	7/23/4	11/21/2	0.439
CPFE			
6MWD (m) n=16	191±70	230±94	0.103
NTproBNP pg/ml n=21	2258 (1153-5992)	2471 (461-3325)$^{+}$	0.015*
NYHA FC n=23	0/19/4	1/20/2	0.429
Emphysema			
6MWD (m) n=19	237±102	224±88	0.574
NTproBNP pg/ml n=19	1378 (440-3881)	1449 (663-3082)	0.365
NYHA FC n=27	1/23/3	1/24/2	0.895
ILD			
6MWD (m) n=11	261±100	287±119	0.180
NTproBNP pg/ml n=13	2474 (1085-5540)	1204 (750-3308)	0.011*
NYHA FC	4/10/2	5/9/2	0.921
Severe PH/mild lung disease (n=32)			
6MWD (m) n=22	255±109	259±118	0.788
NTproBNP pg/ml n=21	1852 (645-5594)	2073(599-3308)	0.110
NYHA FC	6/19/4	6/19/4	ns
Severe PH/severe lung disease (n=58)			
6MWD (m) n=36	191±85	224±100	0.009*
NTproBNP pg/ml n=44	3360 (1233-6831)	2536 (484-4309)	0.0009**
NYHA FC	2/36/8	7/36/3	0.08

Subgroup analysis according to phenotype of lung disease and severity of lung disease shown. Data displayed as mean ± SD or median (IQR) according to data distribution. Paired statistical analysis performed.

3.4.4.1 Six minute walk test

58 patients with IPAH and 80 patients with severe PH/lung disease had paired 6MWT observations for analysis. 6MWD improved in the IPAH cohort, from 337 ± 114 m at baseline to 376 ± 97 m ($p < 0.0001$) and in those with severe PH/lung disease from 224 ± 102 m to 243 ± 102m, $p = 0.032$). 6MWD improved by 31m after 3 months of PH targeted therapies in those with IPAH compared with 24m in those with severe PH/lung disease. Figure 3.22 shows the median Δ6MWD for IPAH and lung disease phenotype groups. There was no significant difference in Δ6MWD between the groups with the exception of fall in 6MWD in emphysema group (median -17m) in comparison to IPAH (+31m), $p = 0.033$.

Significant improvement in 6MWD according to lung disease phenotype was only seen in those with COPD, (220 + 112 m to 245 ± 107 m $p = 0.033$). 6MWD improved from 185 ± 85m to 216 ± 100m, $p=0.021$, in those with severe PH/severe lung disease in comparison to those with severe PH/mild lung disease where 6MWD was unchanged (255 ± 109 m to 259 ± 118 m).

6MWD increased in 49/80 severe PH/lung disease patients by average 59m (range 8 – 200m) and was unchanged or decreased in 31/80 patients, average -33m (range -195 to 0m). No baseline characteristic predicted likelihood of an improvement in 6MWD with therapy, with the exception of a lower baseline 6MWD (203m vs 257m, $p=0.018$). Table 3-16 displays the clinical characteristics of patients according to change in 6MWD.

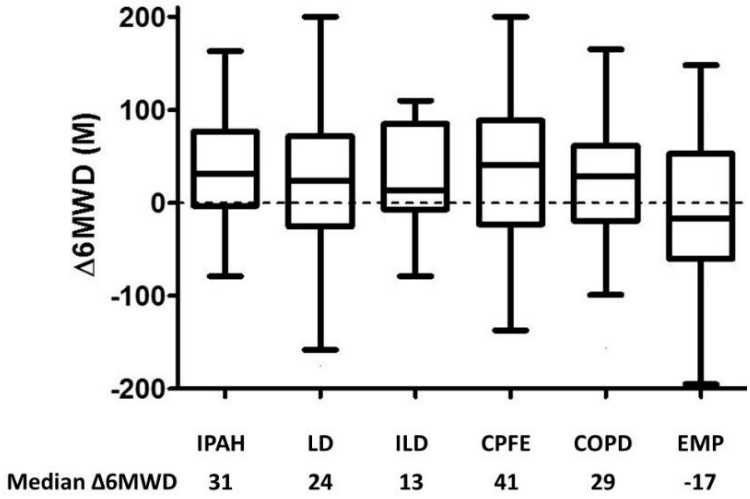

Figure 3.22 ∆6MWD with PH therapy in IPAH and severe PH/lung disease patients.

Median values shown. No significant difference across groups demonstrated, ANOVA p = 0.170, post hoc analysis, no difference in ∆6MWD between IPAH and lung disease patients (p = 0.236). only Emphysema group displayed fall in ∆6MWD in comparison to IPAH, p = 0.033. No significant difference between lung disease phenotypes demonstrated.

3.4.4.2 NTproBNP

42 IPAH patients and 78 patients with severe PH/lung disease had paired NTproBNP levels for analysis. NTproBNP fell following introduction of PH therapy in both groups, from 1085 (449 - 2545) pg/ml to 788 (289 - 1655) pg/ml ($p<0.0001$) in those with IPAH and from 2245 (850 – 4295) to 1667 (614 – 3590) pg/ml in those with severe PH/lung disease ($p = 0.008$). NTproBNP improved by an average -396 (-1133 - 97) pg/ml in IPAH and by -211 (-1311 - 205) pg/ml in severe PH/lung disease.

On subgroup analysis by lung disease phenotype, significant improvement in level of NTproBNP were seen in those with CPFE (median -596 pg/ml) and ILD (median -390 pg/ml) only. Figure 3.23 shows the median ΔNTproBNP following PH therapy for each phenotype. There was no significant difference in levels of ΔNTproBNP across groups ($p = 0.194$). Emphysema phenotype showed no improvement in NTproBNP (ΔNTproBNP +38pg/mL), significant difference in comparison to IPAH ($p=0.022$), ILD ($p=0.024$) and CPFE ($p=0.037$) where median ΔNTproBNP were -396, -412 and -596 pg/mL respectively.

NTproBNP levels fell in those classed as having severe PH/severe lung disease from 3360 (1233-6831) to 2536 (484 – 4309) pg/ml, $p = 0.0009$ but not those with severe PH/mild lung disease.

NTproBNP fell in 48/82 severe PH/lung disease patients, average -1034 (range -18101 to -4) pg/ml, and increased or remained static but elevated in 34/82, average 333 (range 0 to -17913) pg/ml. No baseline clinical characteristics predicted reduction in NTproBNP with PH therapy (data shown in table 3-16).

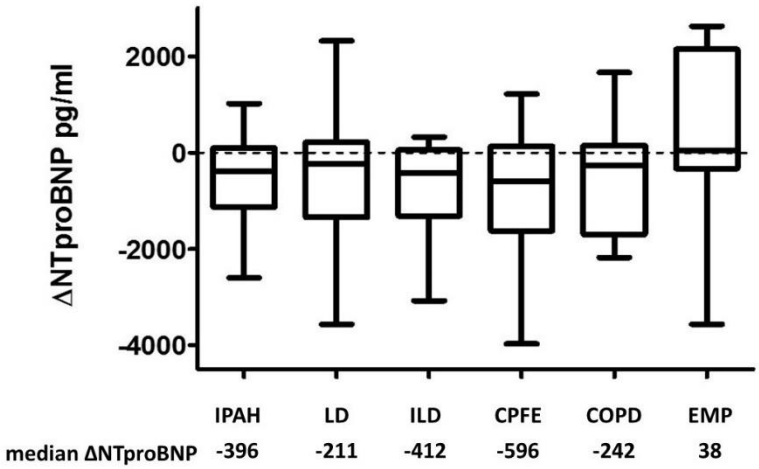

Figure 3.23 ∆NTproBNP with PH therapy for IPAH patients in comparison to severe PH/lung disease phenotypes

No significant difference was demonstrated across groups (Kruskall Wallace p=0.194). Similar levels of ∆NTproBNP observed between IPAH and lung disease patients (-211 and -396pg/mL respectively, p=0.526). On post hoc analysis, Emphysema phenotype demonstrated significant increase in NTproBNP (median +38pg/mL) in comparison to IPAH (p=0.022), CPFE (p=0.037), ILD (p=0.024) with trend in comparison to COPD (p=0.065). There was no difference between other phenotypes.

Table 3-16 Comparative analysis of baseline characteristics of severe PH/lung disease patients with improvement in 6MWD or NTproBNP after PH therapy against nonresponders.

Variable	6MWD			NTproBNP		
	increase	decrease	p-value	decrease	increase	p-value
n	49	31		48	34	
Age (years)	65 ± 11	65 ± 10	0.707	66 ± 12	68 ± 8	0.499
Phenotype % (n)						
Emphysema	16.3 (8)	35.5 (11)	0.239	16.7 (8)	32.4 (11)	0.200
COPD	50 (24)	32.3 (10)		33.3 (16)	38.2 (13)	
CPFE	20.4 (10)	19.3 (6)		29.2 (14)	20.6 (7)	
ILD	14.3 (7)	12.9 (4)		20.8 (10)	8.8 (3)	
mPAP (mmHg)	45 (39-54)	44 (42-51)	0.812	46 (41-51)	43 (39-50)	0.437
RAP (mmHg)	7 ± 4	8 ± 4	0.187	8 ± 5	8 ± 5	0.749
PVR (Wood Units)	10 (8-13)	10 (8-13)	0.924	11.3 (9 -15)	9.3 (8-16)	0.451
CI (l/min/m^2)	2.1 ± 0.5	2.1 ± 0.6	0.915	1.9 ± 0.5	2.0 ± 0.7	0.613
SV/PP	1.0 ± 0.4	1.0 ± 0.4	0.874	1.0 ± 0.5	1.0 ± 0.5	0.947
FEV1 (%)	69 (54-85)	80 (59-98)	0.168	74 (50 -95)	81 (66-93)	0.220
FEV1/FVC (%)	58 (49-67)	63 (56-69)	0.171	63 (56-71)	59 (53-68)	0.548
DLCO (%)	25 (21-36)	29 (21-37)	0.762	26 (18-36) (41)	24 (21-33) (32)	0.938
Pa02 (KPa)	7.6 ± 1.4	7.7 ± 1.9	0.841	7.6 ± 1.2	7.4 ± 2.2	0.659
6MWD (m)	203 ± 101	257 ± 94	0.018*	189 ± 86 (40)	231 ± 126 (30)	0.108
NTproBNP (pg/ml)	1715 (506-3967) (34)	1559 (485-2674) (24)	0.528	2867 (1213 – 6041)	1415 (361-2915)	0.011*
RVEF(%)	36 ± 14 (26)	33 ± 11 (20)	0.408	30 ± 12 (26)	36 ± 13 (14)	0.126
RVEDVI (ml/m^2)	86 ± 30	93 ± 25	0.397	89 ± 26	99 ± 36	0.288
SVI (ml/min/m^2)	29 ± 9	28 ± 9	0.863	26 ± 6	29 ± 9	0.163

No variable differed between responders and non responders, defined by improvement in 6MWD or NTproBNP. It was not therefore possible to identify those patients likely to benefit from PH specific therapy using baseline characteristics.

3.4.4.3 NYHA FC

Paired functional class status was available for 93 patients with severe PH/lung disease and 62 IPAH patients. After a minimum of 3 months of PH treatment, 77% (n=72) remained in FC III and 9% (n=8) in FC IV in those with severe PH/lung disease with no improvement in comparison to baseline (p=0.421). In IPAH, 47% (n=29) remained in FC III and 5% (n=3) in Fc IV at follow up. Although trend toward improvement was demonstrated this did not reach statistical significance (p=0.055). No improvement in FC was demonstrated on subgroup analysis by either lung disease phenotype or severity of the lung disease.

3.4.4.4 Right ventricular function

11 patients with PH associated with lung disease underwent CMR at diagnosis and after minimum 3 months of PH therapy. Patient demographics are shown in table 3-17. RVEF remained unchanged, 39 ± 15 % to 40 ± 15 % p=0.72. There was a trend towards improvement in LV filling, LVEDVI increased from 48 ± 12 to 53 ± 12 ml/m^2, p = 0.054. SV increased from 53 ± 17 ml to 62 ± 14 ml, p = 0.004. There was no relationship between change in SV and change in 6MWD (p = 0.39). Figure 3.24 displays the paired analysis.

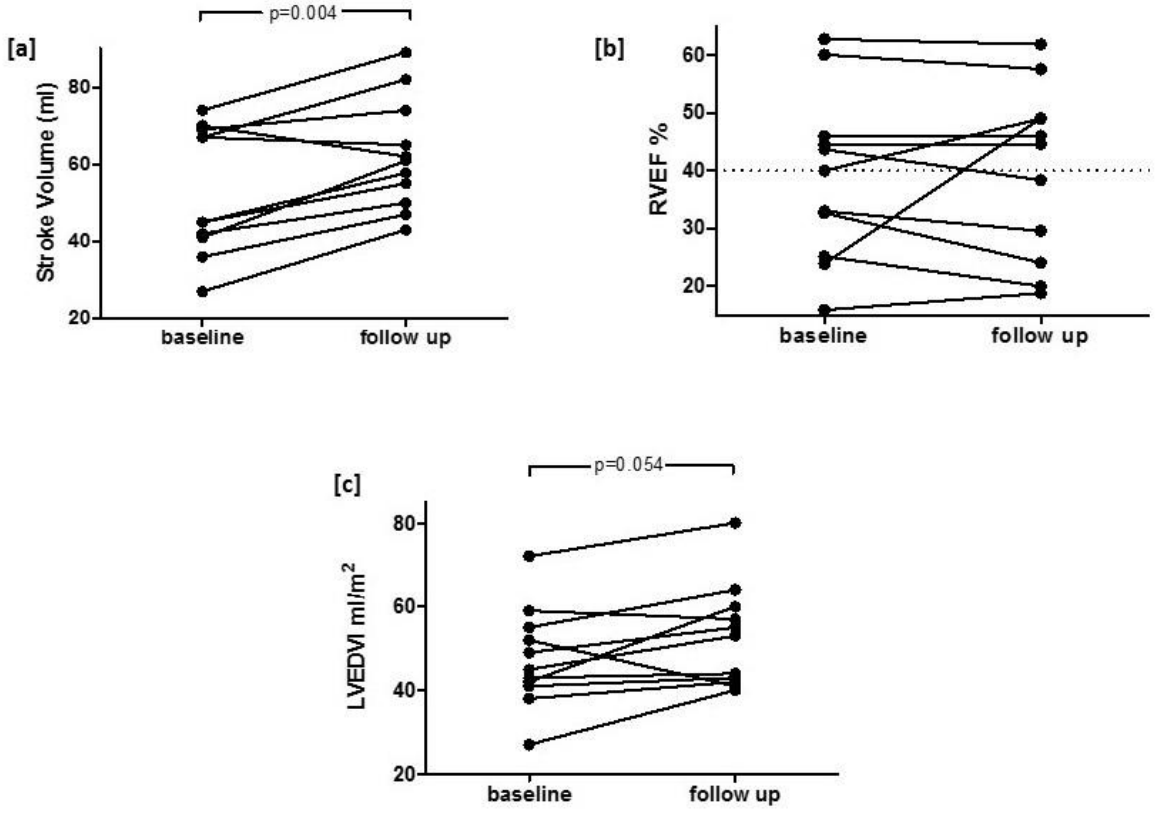

Figure 3.24 Change in stroke volume and RV function after PH therapy in patients with severe PH and lung disease.

Significant improvement in stroke volume [a] but not RV function (p=0.720) [b] and trend towards improved LV filling (LVEDVI [c]) demonstrated in paired analysis.

Table 3-17 Characteristics of severe PH/lung disease patients with follow up cardiac MRI after PH therapy.

Patient ID	Diagnosis	Age	Sex	mPAP mmHg	PVR w.u	CI l/min	FEV1 %	DLCO %	Therapy	ΔSV mL
1	COPD	35	M	73	24	1.3	58	61	ERA	16
2	COPD	61	M	35	5.9	2.9	35	25	ERA	-2
3	COPD	61	F	53	10.2	1.9	59	31	PDE5i	13
4	Emphysema	80	F	42	10.6	1.8	126	21	PDE5i	11
5	Emphysema	61	M	50	11	1.9	78	20	PDE5i	8
6	Emphysema	71	M	42	8.1	2.5	101	40	ERA	-7
7	CPFE	66	M	29	4.9	2.3	97	27	PDE5i	15
8	CPFE	54	M	65	19.5	1.8	30	15	PDE5i	20
9	CPFE	70	M	38	6.2	2.2	75	14	PDE5i	15
10	ILD	74	F	34	4.4	3.1	106	33	PDE5i	4
11	ILD	42	M	55	10.1	2.3	98	26	PDE5i	10

There was no difference in survival between severe PH/lung disease patients with an increase in 6MWD on PH therapy at follow up and those without (1 and 3 yr survival 87% V 77% and 42% v 46% respectively, p = 0.630). ROC analysis, shown in figure 3.26, determined an optimal threshold of 193m walked at follow up (youden index 0.45). Distance walked greater than this was not associated with improved survival (shown in figure 3.25, p = 0.08), but inability to perform a 6MWT despite therapy was significantly predictive of worse survival (p < 0.0001). KM curve for survival according to 6MWD at follow up is shown in figure 3.25.

Δ6MWD did not predict survival in those with lung disease on either univariate (p = 0.820) or multivariate analysis in a model with age, sex and mPAP (p = 0.427).

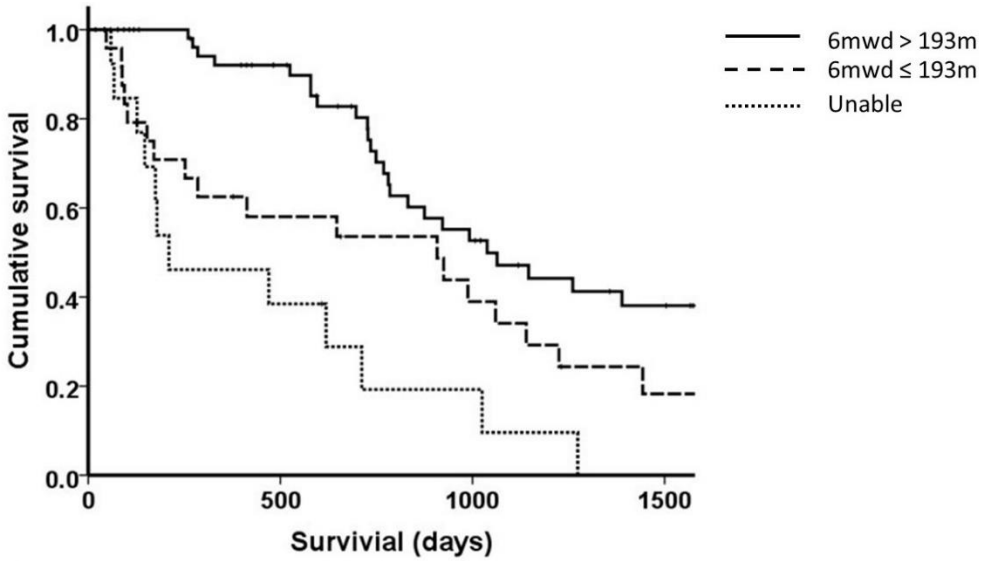

6MWD	Patients at risk			
≤ 193m	25	13	8	3
>193m	59	41	21	12
Unable	13	5	2	0

Figure 3.25. Kaplan Meier survival curves described survival in severe PH/lung disease according to 6MWD at follow up in comparison to those unable to perform 6MWT

Patients unable to perform a 6MWT had reduced survival in comparison to both those 6MWD ≤193m and >193m, logrank p = <0.0001 for both), but similar survival observed in walkers (p = 0.08).

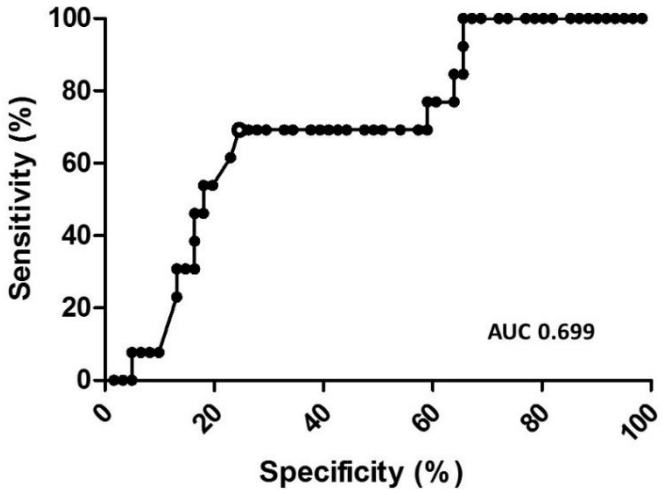

Figure 3.26 Receiver operator curve for sensitivity and specificity of 6MWD whilst undergoing PH therapy to determine risk of death at 1 year.

Optimal threshold < 193m walked determined by Youden analysis.

Survival did not differ in severe PH/lung disease patients whose NTproBNP fell (by any amount) with PH therapy compared to those who did not (1 yr survival 76 % v 67 % and 3 yr 38 % v 25 % respectively p = 0.430).

In a model with age, sex, PVR and RAP, ΔNTproBNP independently predicted survival in those with severe PH/ lung disease (HR 1.479 95%CI 1.045-2.093, p=0.027).

Receiver operator curve for survival at 1 year (shown in figure 3.28) identified an optimal threshold of <1222 pg/ml whilst on therapy (youden index 0.53). NTproBNP > 1222 pg/ml 91% sensitive and 62% specific for risk of death.

A level of NTproBNP < 1222 pg/ml was associated with improved survival (1 and 3 year survival 95 % versus 54 % and 52 % versus 21% respectively, p < 0.0001). Figure 3.27 shows KM survival curves.

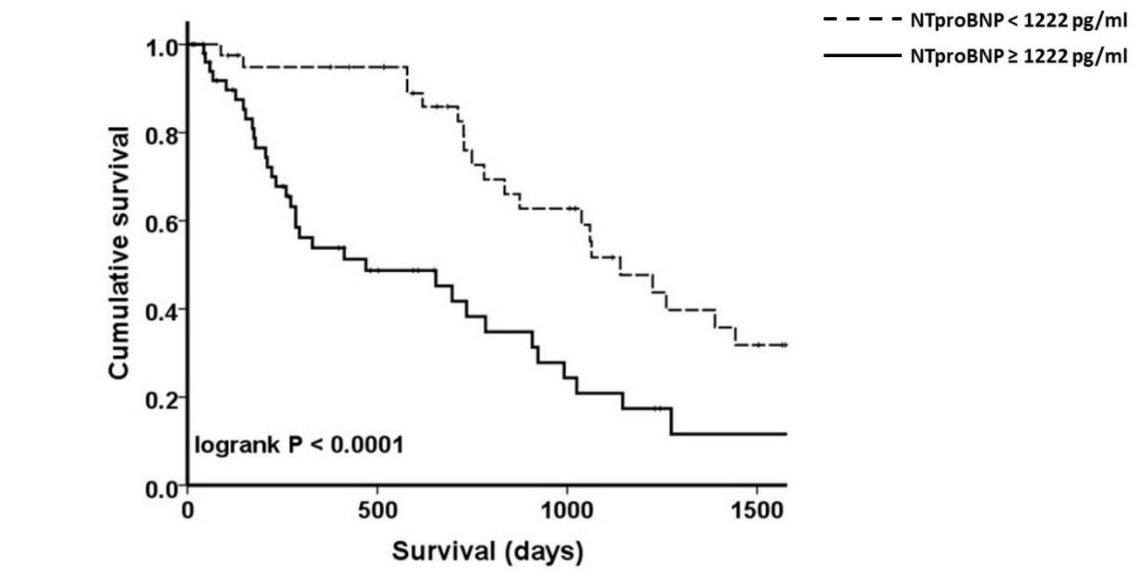

NTproBNP	Patients at risk			
< 1222 pg/ml	43	34	19	8
≥ 1222 pg/ml	51	18	7	2

Figure 3.27. Kaplan Meier survival curves describing outcome in severe PH/lung disease according to level of NTproBNP at follow up.

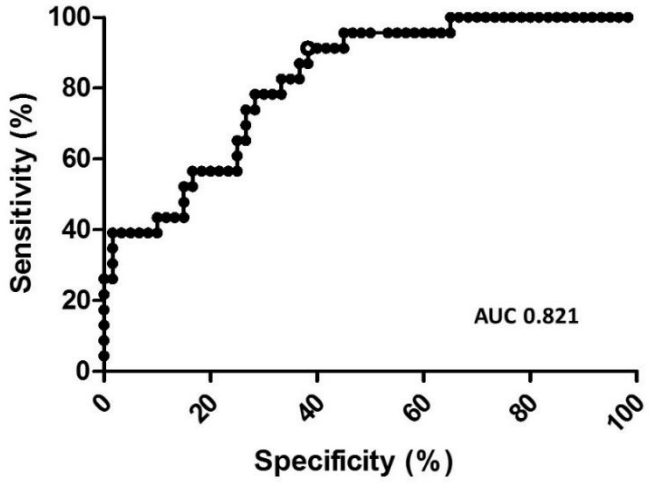

Figure 3.28. Receiver operator curve to identify optimal threshold level of NTproBNP at follow up for increased risk of death at 1 year.

Threshold value of >1222 pg/mL determined by Youden analysis.

3.5 Discussion

The clinical characteristics described in this chapter demonstrate that mild to moderate pulmonary hypertension in chronic lung disease is characterised by early increases in vascular stiffness with adaptive RVH but preserved RV function in agreement with previous small studies (359). The development of elevation in pulmonary artery pressure is associated with worse survival, and deterioration in functional status defined by a drop in 6MWD. Consequently, survival in mild to moderate PH associated with lung disease is predicted by mPAP and pulmonary artery compliance (SV/PP). Severe PH associated with lung disease however, shares many characteristics with IPAH, with evidence of right ventricular failure. In the latter, it is indices of RV function, such as RAP, CI or RVEF rather than pulmonary artery pressure that relates to survival. This has implications for screening for PH in these populations. As described in results section 3.4.2, non invasive screening for PH is best approached by a combination of echo and index of vascular stiffness (such as relative area change of the main pulmonary artery by CMR) and severe PH by combination of echo and parameters of RV dysfunction, such as RV mass or NTproBNP.

3.5.1 Characteristics and right ventricular dysfunction

Severe PH in lung disease patients described in this chapter demonstrated severe hypoxaemia, grossly impaired DLCO, relatively mild impairment in lung function and more severe functional impairment measured by NYHA FC and 6MWD than IPAH patients despite similar haemodynamics. Similar characteristics have previously been reported in patients with COPD and severe PH (208, 356) and in small case series of smokers with emphysema but preserved lung volumes (375). The severity of lung function impairment (FEV1 in COPD or FVC in ILD) did not correlate with mPAP nor have prognostic value in our study. FEV1 did correlate with RVEF, and $Pa0_2$ with vascular compliance and RVEF, and inversely with mPAP. Correlations between $Pa0_2$ or lung function impairment and PAP have been described variably in the literature (204, 206, 334). In one study, $Pa0_2$ explained only 25% of the variance in PAP suggesting impairment of gas exchange is not the main determinant in development of PH in chronic lung disease (376). Scharf et al showed no relationship between right ventricular EF or volumes with measures of airflow obstruction (204) and minimally with $Pa0_2$ (r^2=0.041). In IPF, poor or no

correlation between severity of PH and lung function impairment or CT fibrosis score have also been described (219, 377). The limited dispersion of FEV1 and $Pa0_2$ values and use of LTOT in our cohort could have affected correlation. However, previous studies suggest only a weak or even no relationship between impaired lung function and PAP or RV function. It has been postulated that loss of >80% of normal lung function is required to cause a rise in PAP >25mmHg. The severe PH seen in or cohort therefore is unlikely to be predominantly driven by lung function impairment and alternate explanations for progressive vascular remodelling and characteristic similarities with IPAH.

3.5.1.1 Imaging right ventricular function in chronic lung disease

Good correlation occurred between echocardiography and CMR imaging of right ventricle dilatation, (RVEDD with RVEDVI) and to a lesser extent TAPSE with RVEF, in chronic lung disease patients. The latter is not surprising, as TAPSE only assesses longitudinal shortening and ventricular ejection, particularly in PH, has significant impairment from transverse contraction and TR. The strong relationship between RV dysfunction and survival in this chapter demonstrates importance of employing imaging modalities to assess RV function when monitoring these patients.

3.5.1.2 Vascular stiffness

Good correlation between cardiac MRI index of vascular stiffness (RAC MPA) and invasive SV/PP was seen. Both measures were found to have prognostic significance and additionally RAC was shown to reliably detect the presence of PH. Cardiac MRI therefore cannot only be applied to assess RV function in chronic lung disease, but also vascular stiffness in a single sitting.

3.5.1.3 Functional status

mPAP, RAP, SV/PP and DLCO independently predicted distance walked on 6MWT in all lung disease patients. This suggests that in addition to predicting survival, haemodynamics are a better predictor of functional status. This is in agreement with previous literature in severe PH/lung disease demonstrating more severe exertional dyspnoea than COPD patients with more marked airflow obstruction but lower PAP (208), and exhausted circulatory but residual breathing reserve at end

exercise (378). mPAP has also been shown to independently predict 6MWD in large cohort COPD patients some of whom had PH (207).

3.5.1.4 NTproBNP

Levels of NTproBNP were comparable in chronic lung disease patients without PH and those with mild-moderate PH, but were markedly elevated in the severe PH group. Good correlations with CMR determined RV dilatation and dysfunction (RVEDVI and RVEF respectively) in chronic lung disease patients without left ventricular dysfunction were demonstrated. Previous studies have shown levels of NTproBNP (or BNP) to be elevated in chronic lung disease and relate to left ventricular function, or left of right ventricular function during acute exacerbations (368, 371).

NTproBNP was higher in severe PH/lung disease patients than IPAH patients despite similar haemodynamics. Furthermore, RVMI was higher in those with IPAH. This could suggest a greater degree of right ventricular dysfunction and impaired adaptation to afterload in lung disease patients. There was no significant difference in renal function to account for the higher NTproBNP (MDRD eGFR 63 (51-82) vs 71 (53-82) ml/min/1.73m2 p=0.340). Lung disease patients were significantly older (67 vs 49 years) and NTproBNP has been shown to increase with age, +36% in men and +15% in females per 8.4 years in one study (379). PVR was higher (and therefore RV afterload) in the IPAH patients whom underwent MRI, and therefore we would expect a greater degree of RV adaptation. Additionally, RVMI has been shown to fall with age, a 5% reduction per decade of age has been shown (101). Differences in the demographics of the populations may therefore account for the apparent difference in NTproBNP and RVMI.

3.5.2 Imaging the right ventricle to detect PH in chronic lung disease

Echocardiography estimated sPAP has been shown previously to have low sensitivity, specificity and predictive values in patients with chronic lung disease, with success rates of 24-77% in estimating PAP in the literature (199, 380-383). When estimation of sPAP is possible, in COPD and pulmonary fibrosis, positive predictive values of 32% and 68% and negative predictive vales 93% and 67% respectively have been reported in the literature (199, 384). In our hands,

echocardiography estimated sPAP had a 91% PPV and 83% NPV for PH, and correlations between echocardiography sPAP and sPAP at right heart catheterisation were similar in both IPAH and chronic lung disease patients. It is however worth noting that the population described by this chapter is subject to selection bias, as all patients were assessed at a tertiary pulmonary hypertension centre due to a suspicion of pulmonary hypertension which largely would be as a result of echocardiography raised sPAP. There were therefore fewer patients with normal pulmonary artery pressures, and fewer still in whom sPAP could not be estimated. For severe PH, we found 78% PPV and 71% NPV with echocardiography estimated sPAP, reflecting poorer accuracy at higher levels of PH. This can be explained by greater degree of functional tricuspid regurgitation as right ventricular dilatation and dysfunction develops in severe PH. Regardless of the severity of PH, the non invasive detection of either PH or severe PH in chronic lung disease patients was improved by the addition of a second imaging method, RAC MPA in mild PH, and RVM or addition of biomarker NTproBNP, in severe PH. Additionally, cardiac MRI could be used to detect PH in those chronic lung disease patients where echocardiography is unable to estimate sPAP as RAC MPA and ventricular mass index (VMI) had comparable PPV. In severe PH, NTproBNP >230 pg/ml or RAC MPA <32.5 % could be useful detection tools as they performed superiorly to echocardiography in this population.

3.5.3 Survival and prognostic variables

The development of pulmonary hypertension in patients with chronic lung disease was associated with significant impairment in prognosis. Interestingly, survival in those with mild-moderate PH and those with severe PH treated with pulmonary vasodilator therapy did not differ. Chaouat et al previously demonstrated worse survival in COPD patients with severe PH (208), which could suggest that pulmonary vasodilator therapy improved outcome in those with severe PH. Without a control arm it is impossible to conclude this, but suggests need for such study to be performed. Survival in patients with severe PH/lung disease in comparison to IPAH was reduced, despite age adjustment with ILD patients displayed poorer survival in comparison to other lung phenotypes.

Our results show that pulmonary haemodynamics and right ventricular dysfunction are stronger predictors of survival than indices of lung function in chronic lung

disease. This is in agreement with previous studies of COPD patients receiving LTOT which reported no influence of FEV1 or $Pa0_2$ on survival (210, 385, 386). A PAP above 25 mmHg in LTOT treated chronic lung disease patients was associated with lower survival at 5 years, 33 % vs 66 % $p<0.0001$ (210) and prognostic significance of a raised mPAP in COPD both with and without LTOT has been recurrently reported (335, 376, 385) with threshold values of 30 mmHg or 40 mmHg to define those at significantly increased risk (208, 387). In IPF, even a marginally elevated mPAP above 17 mmHg associated with reduced survival (213) and mPAP shown to be an independent predictor of survival (214). In the entire cohort of chronic lung disease patients included in this chapter, RV dysfunction whether assessed by invasive haemodynamics (RAP, CI), echocardiography (RVEDD), cardiac MRI (RVEF, RVESVI and SVI) or NTproBNP all related to prognosis. In patients with mild-moderate PH, mPAP was an independent predictor of survival in agreement with the studies above. In those with severe PH raised right atrial pressure and reduced cardiac index and ejection fraction were associated with poorer outcome, which is similar to studies of prognostic variables in pulmonary arterial hypertension.

Reduced LVEF as a prognostic variable in severe PH with lung disease occurred without clinical left ventricular dysfunction and normal PAWP. Evidence of subclinical LV dysfunction on echocardiogram has been reported in COPD (388) alongside increased risk of cardiovascular abnormalities including increased arterial stiffness, (316, 389, 390) ischaemic heart disease and heart failure. LV dysfunction has been shown to relate to fat free mass and IL-6 linking to the catabolic-inflammatory COPD phenotype, and increased arterial stiffness (388). 51/55 patients whom underwent CMR were smokers with an average 40 pack year history. Smoking has been shown to have acute effects on aortic pulse wave velocity (a measure of vascular stiffness) (391) and LV function (392).

The ASPIRE registry reported similar 1 year but worse 3 year survival rates of 70% and 33% compared to 79% and 47% in our cohort (ILD patients excluded for comparison) respectively. 43 of 59 patients received PH therapy, were of similar age to our cohort however had a greater degree of pulmonary function impairment and included patients with elevated PAWP indicating left ventricular dysfunction. In addition severe PH was defined by an mPAP ≥40mmHg. ASPIRE reported SV02, age, FC IV and DLCO as independent predictors of survival however included

patients with mild and moderate PH in the survival analysis (356). Cottin et al reported a 1 year survival rate of 60% in patients with PH and CPFE syndrome, of whom 24/40 (60%) received PH therapy (227). Patients with mild to moderate PH (mPAP 24-56 mmHg) were also included, higher PVR, lower CI and DLCO were shown to predicted worse survival. Direct comparison with this cohort is therefore not possible, but both studies agree haemodynamics are more important determinants of prognosis.

3.5.4 Response to PH therapy

There is no evidence in the literature to support the use of pulmonary vasodilators in severe PH with lung disease. As discussed in section 3.1.3 previous studies have been of small sample size, did not always include RHC derived mPAP, and included patients with mild or even no PH with resultant contradictory conclusions (340, 342). Concern of inducing worse hypoxaemia has been raised by previous vasodilator studies in COPD patients demonstrating a fall in $Pa0_2$ due to increased VQ mismatch (343). We did not demonstrate a deterioration in oxygen desaturation on 6MWT, although this should be interpreted with caution given the retrospective analysis of this data.

Functional capacity defined by 6MWD (but not NYHA FC) improved, but to a lesser extent than IPAH patients despite similar haemodynamic characteristics at baseline. We did not demonstrate a survival benefit in those with an improved 6MWD on treatment. This should be interpreted with caution as it possible that chronic lung disease patients are more ventilatory limited so an alternate endpoint should be considered to determine efficacy. It is also possible that treatment led to a stabilisation of the clinical condition as 6MWD did not fall at follow up which previous smaller studies in PH associated with lung disease have suggested (355). A prospective trial with an untreated control arm could investigate this possibility further.

Improvement in NTproBNP, a marker of RV dysfunction is encouraging. Previous studies have not used this biomarker as outcome measure in PH associated with lung disease. NTproBNP correlated with RVEF and RVEDVI so we can speculate that disease targeted therapy may lead to improved outcome in those with improved RV function. Furthermore, in the small subgroup with follow up CMR study,

improvement in stroke volume (an indices of RV function) was demonstrated. Interestingly in a small study of COPD patients with mild or no associated PH no change in SV was seen after sildenafil administration (340), possibly suggesting severe PH associated with lung disease does respond differently to PH therapy. In IPAH, NTproBNP has been shown to correlate with RV function (297) and changes in serial NTproBNP with treatment have been shown to predict survival (301). As discussed in section 3.1.4.1 NTproBNP has been shown to predict outcome following acute exacerbations of airways disease, (365, 366, 393) identify those with concurrent LV dysfunction (393, 394) and as a screening tool for PH in COPD (370) and we have shown that RV function predicts survival in the patients described in this chapter. ΔNTproBNP but not Δ6MWD predicted survival, and a level of NTproBNP below 1222pg/ml whilst on PH therapy was associated with improved survival. This could suggest NTproBNP may be a better outcome measure than 6MWD in therapeutic trials involving patients with PH associated with lung disease where exercise capacity will be ventilatory limited in addition to cardiovascular limitation. The negative correlation observed here between FEV1 and 6MWD in those with COPD could support this ventilatory limitation (378).

The patients described in this chapter represent the largest treated population of severe PH in lung disease and further explores the impact of lung disease phenotype and severity on response to vasodilator therapy. The Emphysema/preserved FEV1 phenotype responded poorly to PH therapy, with non significant fall in 6MWD and increase in NTproBNP. Suggested mechanisms leading to the development of PH include vascular ablation, excessive hypoxic pulmonary vasoconstriction, pulmonary artery remodelling and endothelial dysfunction from inflammation and exposure to cigarette smoke (235). One hypothesis may be that the emphysema phenotype demonstrated poorer response to therapy because the pathophysiology may relate more to vascular loss than potentially treatment responsive vascular dysfunction.

Surprisingly using the classification suggested by Seeger et al at the 5th world PH symposium demonstrated no difference in survival between severe PH/mild lung disease and severe PH/severe lung disease groups. In addition, those with severe-PH/severe lung disease demonstrated improvements in both 6MWD and NTproBNP with therapy whereas those who was classified as having co-existent mild lung disease did not. Characteristics of patients improving either 6MWD or NTproBNP

did not differ. The severity of lung disease in severe PH therefore cannot reliably be used to determine therapeutic response to pulmonary vasodilators.

Pulmonary haemodynamic data of COPD patients exhibiting PH in the literature demonstrates moderate elevations in PVR, but RV preload pressures and CO are usually in the normal range. In contrast, large increase in PVR and haemodynamic signs of RV dysfunction are commonly reported in PAH patients (142, 208, 335, 395). The severe PH/lung disease patients described in this chapter however, share more characteristics with the latter, and improvement in 6MWD and NTproBNP with PAH therapies is perhaps therefore not unexpected. Current guidelines have suggested differentiating severe PH/lung disease on basis of pressure at RHC (mPAP ≥35mmHg) or degree of associated lung disease, but the RV characteristics described in this chapter could suggest it may be better to define this by the presence of RV dysfunction rather than a level of pressure.

3.5.5 Limitations

This study has several limitations. This was a single centre retrospective observational study which allowed for variation in therapy used for each cohort, and the numbers of patients in each lung disease phenotype were small. There was also no control arm with severe PH and lung disease whom did not receive therapy to contrast outcomes. It is possibility that changes in outcome measures with treatment may represent regression towards the mean as the only predictor of improvement in either NTproBNP or 6MWD was a poorer baseline value (see table 3-16). CT evidence of lung disease was based on the multidisciplinary report as it was not possible to score the severity of emphysema on CT due to the long recruitment period scans were performed at multiple sites with varying acquisition protocols. Finally, the lung disease cohort was recruited at a PH tertiary referral centre and therefore few patients with normal PA pressure were included.

3.5.6 Clinical implications

During the 14 year study period, more patients with coexistent lung disease than “pure” IPAH were seen. This could possibly be explained by the large proportion of smokers (68%) and older age of the study population (mean age 60). The demographics of incident IPAH cases has shown a trend towards increasing age at

diagnosis, and increasing presence of comorbid diseases in PH registries (147). In the REVEAL registry up to 17% of PAH diagnoses had coexistent COPD (252). This highlights the importance of assessing impact of coexistent lung disease on PH therapy in efforts to develop management strategies for “real life” patients, many of which are excluded in drug trials.

Clinical guidelines recommend consideration of right heart catheterisation in chronic lung disease patients for PH diagnosis with disproportionate functional limitation to ventilatory impairment, need for accurate prognostic assessment or lung transplantation and when severe PH is suspected by noninvasive measures and consideration is being made for recruitment into clinical trial of PH therapies (253). The non-invasive screening methods described in this chapter potentially could improve identification and recruitment of such patients.

3.5.7 Conclusions

The studies described in this chapter demonstrate the importance of imaging right ventricular function in patients with pulmonary hypertension and chronic lung disease to determine prognosis, as a potential screening tool and to assess treatment effect in future therapeutic trials of pulmonary vasodilators. Mild to moderate PH in lung disease is characterised by increases in vascular stiffness but preserved RV function, whereas severe PH associated with lung disease shares many of the phenotypic characteristics of significant RV dysfunction associated with pulmonary arterial hypertension. NTproBNP reflects RV dysfunction in severe PH lung disease patients, can be used to as a screening tool for severe PH, predict survival and change in NTproBNP after PH therapy also predicts survival. This may reflect improvement in RV function, and be a useful marker of therapy response in future studies.

In comparison to IPAH patients, patients with severe PH associated with lung disease have poorer survival which is not abolished by adjusting for age. PH therapy lead to improvements in 6MWD and NTproBNP. Survival and response to therapy may vary according to lung phenotype. Further studies with an untreated control group may establish if PH therapy has a role in delaying the progression of the pulmonary hypertension and improving survival.

Chapter 4 - Right Ventricular (RV) – arterial coupling in pulmonary hypertension

4.1 Introduction

It has been consistently demonstrated that right ventricular function is a major determinant of functional state, exercise capacity and survival in patients with pulmonary arterial hypertension (260). As discussed in chapter 1, imaging of RV function and structure either by CMR or echocardiogram to determine metrics such as ejection fraction or SV (41), invasive measures of RV function RAP or CI and biomarkers which reflect RV dysfunction such as NTproBNP have all been demonstrated in the literature to predict prognosis in PAH. We have also shown in chapter 3 that RV function is additionally a major determinant of outcome in patients with severe PH and lung disease. However, uncertainty persists about the optimal method to evaluate RV function and what variables might be most clinically relevant in these patients (396).

The gold standard measure of RV systolic functional adaptation to increased loading conditions is end-systolic elastance (E_{es}), (or end-systolic pressure (ESP) divided by end-systolic volume (ESV)), corrected for arterial elastance (E_a), (or stroke volume (SV) divided by ESP). The E_{es}/E_a ratio defines RV-arterial coupling, or the matching of contractility to afterload. E_{es} is a measure of RV contractility and unlike other measures of RV function is load independent. E_{es} is chamber volume dependent and in animal studies shown to relate to myocardial mass (397)

E_{max} is the maximal ventricular elastance described by the maximal ratio of ventricular pressure to volume during the cardiac cycle (130) and is regarded as the gold standard measure of contractility (396). In the LV (characterised by a square PV loop) E_{max} coincides with ESP and therefore equals ESP/ESV. E_{es} is measured at the upper left corner of a square PV loop and therefore E_{es} approximates E_{max} (398) . In the normal RV where pulmonary vascular impedence is low, the PV loop is triangular in shape, and E_{max} occurs before the end of ejection or end systole. E_{max} is determined by family of PV loops at decreasing venous return. RV-arterial coupling can be determined as a measure of volumes provided ESV is measured at Emax and not end ejection. The appearance of the PV loop in PAH or the systemic RV resembles the normal LV however (399) and

therefore contractility can be approximated by ESP/ESV. Increasing discrepancy between E_{es} and E_{max} may therefore occur at lower levels of RV afterload.

E_a is a measure of the total afterload faced by the RV and incorporates resistance, compliance and impedance of the pulmonary circulation. The optimal balance between RV work and oxygen consumption occurs at an E_{es}/E_a ratio of 1.5-2 (123, 260).

4.1.1 Methods of evaluating RV-arterial coupling

The reference method for the determination of E_{es} requires instantaneous and simultaneous measurements of RV pressure and volume and generation of a family of pressure-volume loops at decreasing venous return (123), as shown in figure 4.1. Experimentally this is achieved by IVC occlusion, which is associated with unacceptable risks for widespread clinical application, and is not practical at the bedside.

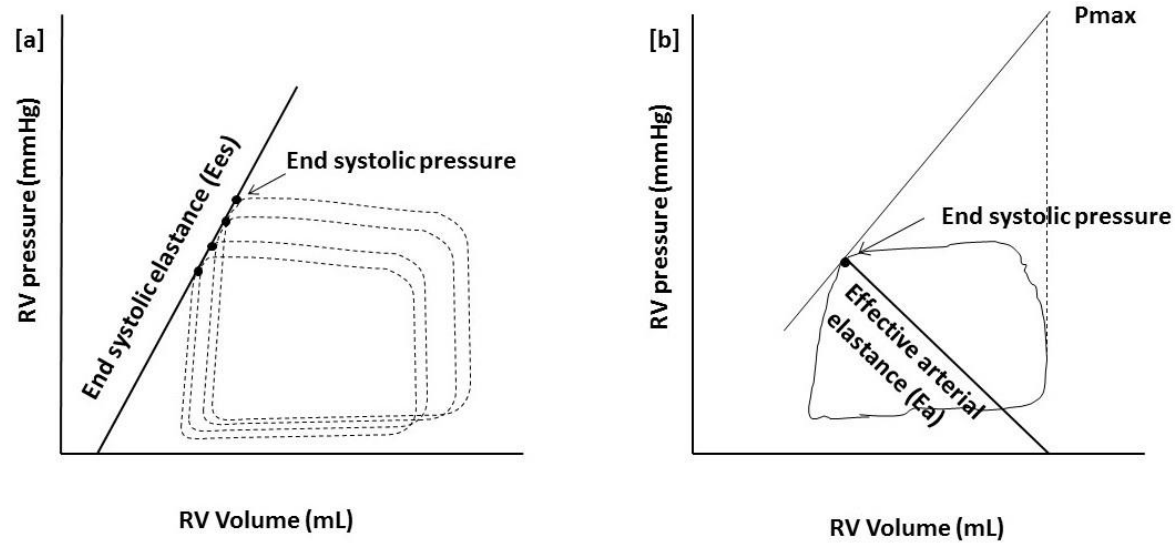

Figure 4.1 RV pressure-volume loops.

[a] shows PV loops at decreasing levels of venous return (usually created by IVC occlusion). Ees is then determined from ESP as shown. [b]. Ea determined as slope connecting ESP with EDV.

However E_{es} can also be estimated from a single P-V loop, often referred to as the single beat method (125). This method relies on the calculation of a maximum RV pressure (P_{max}) from the extrapolation of early and late systolic portions of a RV pressure curve and the continuous recording of RV pressure and relative change in volume to define ESP and ESV. From P_{max}, E_{es} and E_a are easily calculated as shown in figure 4.2. Excellent correlation between P_{max} estimated by this method and values measured directly by clamping the main pulmonary artery in animals models has been demonstrated (125).

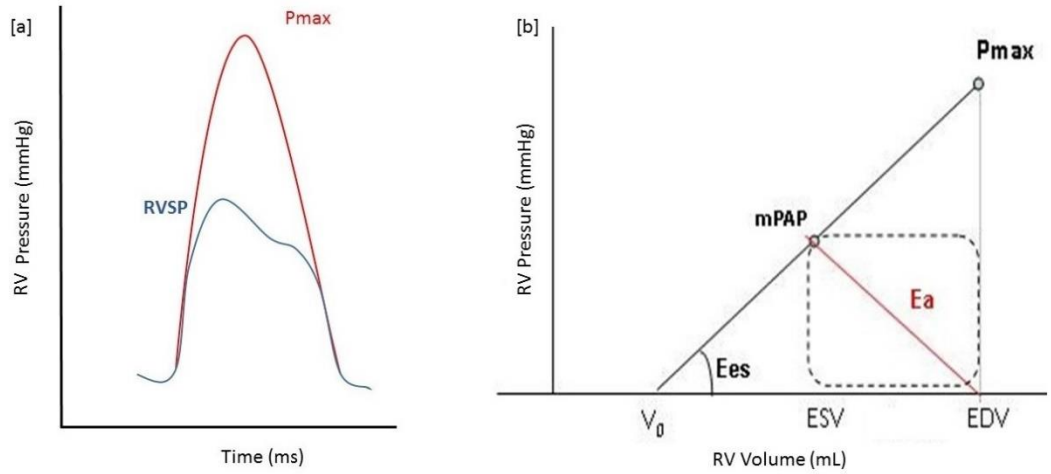

Figure 4.2 Single beat method.

[a]. Pmax is generated by sine wave extrapolation of RV pressure time curve and plotted on RV pressure volume plot as shown in [b] at RV end diastolic volume (EDV) with mPAP at end systolic volume (ESV). End systolic elastance (Ees) calculated as slope of pressure/volume relationship, V0 as the x axis intercept of this relationship and effective arterial elastance (Ea) as mPAP/(EDV-ESV) as shown.

As discussed in chapter 1, the estimation of RV-arterial coupling by an E_{es}/E_a ratio can further be simplified for pressure and expressed as SV/ESV (400), i.e. the *volume* method. Alternatively the ratio can be simplified for volumes and expressed as P_{max} divided by mean pulmonary artery pressure (mPAP), taken as a surrogate for ESP, minus 1 (132), i.e. the *pressure* method. A RV pressure curve is easily obtained during a right heart catheterisation. RV volumes are ideally determined by cardiac magnetic resonance imaging (CMR) which has been shown to have good inter and intra-observer reproducibility in PAH (64). As shown in figure 4.3, the volume method (which assumes RV volume is negligible at zero pressure, V_0=0) results in lower values for RV-arterial coupling.

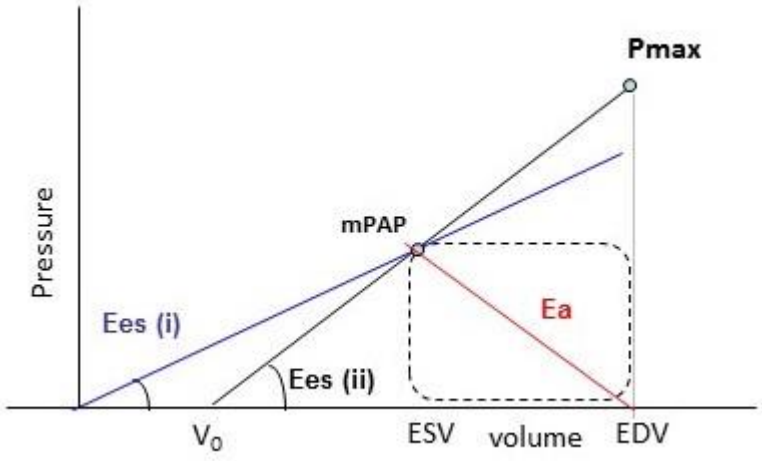

Figure 4.3 Comparison of pressure and volume methods to estimate RV-arterial coupling.

Method (i) volume method where $V_0 = 0$. Ees equates to mPAP/ESV and RV coupling estimated by ratio of SV/ESV. Method (ii) pressure method. Ees equates to (Pmax-mPAP)/(EDV-ESV) and RV coupling by Pmax/mPAP-1. As shown, method (i) results in lower values for Ees than method (ii).

4.1.2 Estimates of RV-arterial coupling in experimental and clinical pulmonary hypertension

RV-arterial coupling has been investigated in various animal models of acute and chronic pulmonary hypertension both with and without evidence of RV failure. In acute hypoxia induced models of PH where an acute rise in E_a was demonstrated, preserved RV coupling occurred by adaptive increase in RV contractility (125, 401-403). Preserved RV-arterial coupling has also been reported in acute PH models induced by microembolism or PA banding (401), and initially during endotoxic shock induced increased PVR, although in the latter deterioration was then observed due to unsustained adaptive increase in contractility (404). In a rat monocrotaline induced PH model, a decrease in RV-arterial coupling occurred due to failure of increase in contractility to match the increased afterload (405). Monocrotaline is known to have systemic toxic effects and causes inflammatory type pulmonary vascular disease (406). Correlation between some markers of inflammation and apoptosis with RV-arterial coupling in both acute and chronic models of RV failure have been reported (407-409).

In experimental models of chronic PH, initial preservation of RV arterial coupling was demonstrated at 3 months in a chronic aortopulmonary shunting model (410) with subsequent uncoupling at 6 months in association with the development of

RV systolic failure (408). In a tachycardiomyopathy model with mild PH induced by chronic overpacing, RV arterial uncoupling was also observed due to absence of an increase in contractility (411). These experimental studies suggest at least initial preservation of RV systolic functional adaptation to an increase in afterload in PH, with uncoupling in context of inflammation (i.e. endotoxin or monocrotaline), chronic sustained elevation of afterload or in left heart failure.

Several small studies have reported values of E_{es}, E_a and RV-arterial coupling estimated by varying methods in patients with PH. Using MRI compatible conductance catheters Kuehne et al derived P-V loops from instantaneous pressure and volume measurements during MRI acquisition in 6 PAH subjects in comparison to 6 controls (412). PAH subjects demonstrated significantly higher E_a and E_{es} in comparison to controls. RV-arterial coupling was 1.9 ± 0.4 in controls in comparison to 1.1 ± 0.3 in PAH patients.

Tedford et al reported impaired RV contractility using PV loop analysis in 7 patients with PAH secondary to systemic sclerosis (SScPAH) in comparison to 5 IPAH patients (413). Despite similar net afterload (E_a) SScPAH exhibited almost 70% lower E_{es} (normalised for RV volume) and lower E_{es}/E_a ratio (1.0±0.5 vs 2.1±1.0 mmHg/mL) suggesting differential ability of the RV to adapt to afterload in SScPAH in comparison to IPAH. However, other indices of RV function, RVEF, CI and RAP or indices of diastolic function did not differ between the groups. Additionally, IPAH patients were on chronic PH medications, such as PDE-5i or epoprostenol in comparison to only 1/7 SScPAH patients, which may alter RV contractility and potentially lead to preservation of RV-arterial coupling demonstrated in the IPAH group.

Trip et al reported a simplified measurement of RV contractility utilising P_{max} generated by the single beat method from a RV pressure curve obtained at standard RHC, and ventricular volumes measured by CMR in 28 IPAH patients (132). mPAP was used as a surrogate for ESP. Contractility was then estimated by either mPAP/ESV (assuming $V_0 = 0$) or (P_{max} - mPAP)/(EDV/ESV). V_0 was also estimated by the linear extrapolation of the pressure-volume relationship. mPAP/ESV was lower by approximately half the value of (P_{max} - mPAP)/SV (0.61 vs 1.34 mmHg/mL respectively) with increased difference at higher values of E_{es}. V_0 ranged from -8 to 171mL which correlated with increasing RV volumes. They concluded that V_0 is

not negligible in PAH patients, and as V_0 is dependent on RV dilatation, E_{es} may be more preload dependent than previously regarded. However, the methods implemented to estimate V_0 relied on a number of surrogate pressures and volumes (such as mPAP for ESP) and extrapolation from a linear fit of the PV relationship which has been shown in the literature to be curvilinear (414).

Sanz demonstrated an initial increase in RV contractility (using the simplified ratio of mPAP/RVESV) with increasing severity of PH in a large cohort of subjects with PH of varied aetiologies (400). With more severe disease, this increase however plateaued with a trend towards even a decrease in the most severe group (defined by PVRI >14.4 Wood units). RV-arterial coupling (as determined by either simplified equations or non-invasive metric SV/ESV) therefore whilst relatively maintained in early disease declined with more severe PH. This suggests that the ratio of SV/ESV may provide prognostic and functional relevance in patients with PH.

Cardiac CMR studies have shown that decreased SV and RVEF are predictive of poor outcome (41), and that a deterioration in RVEF during therapy predicts a poor survival irrespective of improvements in PVR (288). However, EF is preload-dependent while E_{es}/E_a is theoretically not. Therefore, estimates of RV arterial coupling should be superior to other measures of RV function in determining outcome. Accordingly, a recent study on a limited number of patients referred for investigation of PH of all aetiologies (27/41 with PAH diagnoses), many of whom did not receive PH specific therapy, showed RV arterial coupling estimated by SV/ESV to be an independent predictor of outcome while RVEF was not (415). RV volumes were determined by the inferior gated CT imaging rather than CMR in the majority (44/50 patients) which may have influenced this observation.

Overall, these studies suggest increased RV contractility (E_{es}) in response to increased PVR, with or without preservation of RV-arterial coupling. Additionally, the aetiology of the increase in afterload may be important, with potentially earlier RV failure and uncoupling in the presence of systemic disease and inflammation, such as systemic sclerosis. The extent of RV-arterial uncoupling in PH associated with hypoxic lung disease is unknown. Smoking and hypoxia related inflammation are known to have roles in both pulmonary and systemic vascular stiffness, and LV dysfunction has been linked to catabolic COPD phenotype and IL6

(389, 390, 392). Patient characteristics described in chapter 3 suggest possibility of greater RV dysfunction (higher NTproBNP) and impaired adaptation (lower RVM) in comparison to IPAH patients, although this may relate to demographics of the populations. RV-arterial coupling could potentially examine more closely differences in RV adaptation to afterload in PH/lung disease.

4.2 Aims

As demonstrated by these studies, whilst it is clear that RV functional adaptation is the major determinant of outcome in PAH the optimal method for evaluation is uncertain. Gold standard measures of RV-arterial coupling may potentially be superior to more commonly measured indices of RV function, but are cumbersome to perform and invasive, and therefore unlikely to be acceptable for routine monitoring of patients. Additionally there is suggestion from small clinical and experimental models that RV functional adaptation may differ between PH aetiologies. The aims of this chapter are to:

1. Investigate the prognostic utility of RV-arterial coupling determined by both the volume and pressure methods, compared to more usual determinations of RV function, CMR RVEF, NTproBNP, and right heart catheterisation-derived RAP and SV in a large cohort of patients with PAH.

2. Explore the potential deterioration in RV-arterial coupling in patients with chronic lung disease and PH in comparison to IPAH and connective tissue disease PAH.

4.3 Materials and methods

4.3.1 Patient recruitment

140 treatment naïve incident PAH cases diagnosed between January 2004 and April 2014 whom had undergone cardiac MRI at diagnosis were identified. 81 patients with Group 3 PH secondary to lung disease described in chapter 3 with baseline CMR were included for comparison. Patients with lung disease were classified by severity of PH as described in section 3.3.1. Patients underwent multidisciplinary investigation as described in methods section 2.1.1. CMR image acquisition and data analysis was carried out as described in section 2.2. All patients underwent cardiac MRI and RV pressure measurement within 72 hours. All PAH patients were treated with pulmonary vasodilators in accordance with guidelines. Patients were excluded if the RV pressure trace was not available for analysis.

4.3.2 Right ventricular pressure trace analysis

Right ventricular pressure traces were available for 61/140 PAH patients and 32/81 with PH secondary to lung disease. 22 control patients without pulmonary hypertension (defined as a mPAP <25mmHg) who had right heart catheterisation and CMR to investigate breathlessness were included to provide reference values for RV-arterial coupling by the two methods. Of these, 8 had lung disease. Analogue traces were manually redigitised using GetData Graph Digitizer 2.26. An example is shown in Figure 4.4.

In those patients for whom an RV pressure trace was available for analysis, E_{es} was calculated using the single beat method (125). P_{max}, the maximum theoretical pressure the ventricle could generate if isovolumetric contraction occurred, was calculated using a manual sine-wave extrapolation of the early systolic and diastolic portions of the RV pressure curve. P_{max} derivation was carried out by Dr R. Vanderpool at Department of Biomedical Engineering, University of Pittsburgh and Dr A. Bellofiore University of San Jose State.

ESP was approximated by mPAP (132). E_{es} was calculated as the slope of end-systolic pressure volume line,

$E_{es} = (P_{max} – mPAP) / (RVEDV – RVESV)$.

Arterial elastance (E_a) was estimated by mPAP/(RVEDV – RVESV).

RV-arterial coupling (E_{es}/E_a) was simplified for volumes as P_{max}/mPAP – 1 (hereafter referred to as the pressure method, E_{es}/E_a-P), or simplified for pressures as SV/ESV (hereafter referred to as the volume method, SV/ESV) (400).

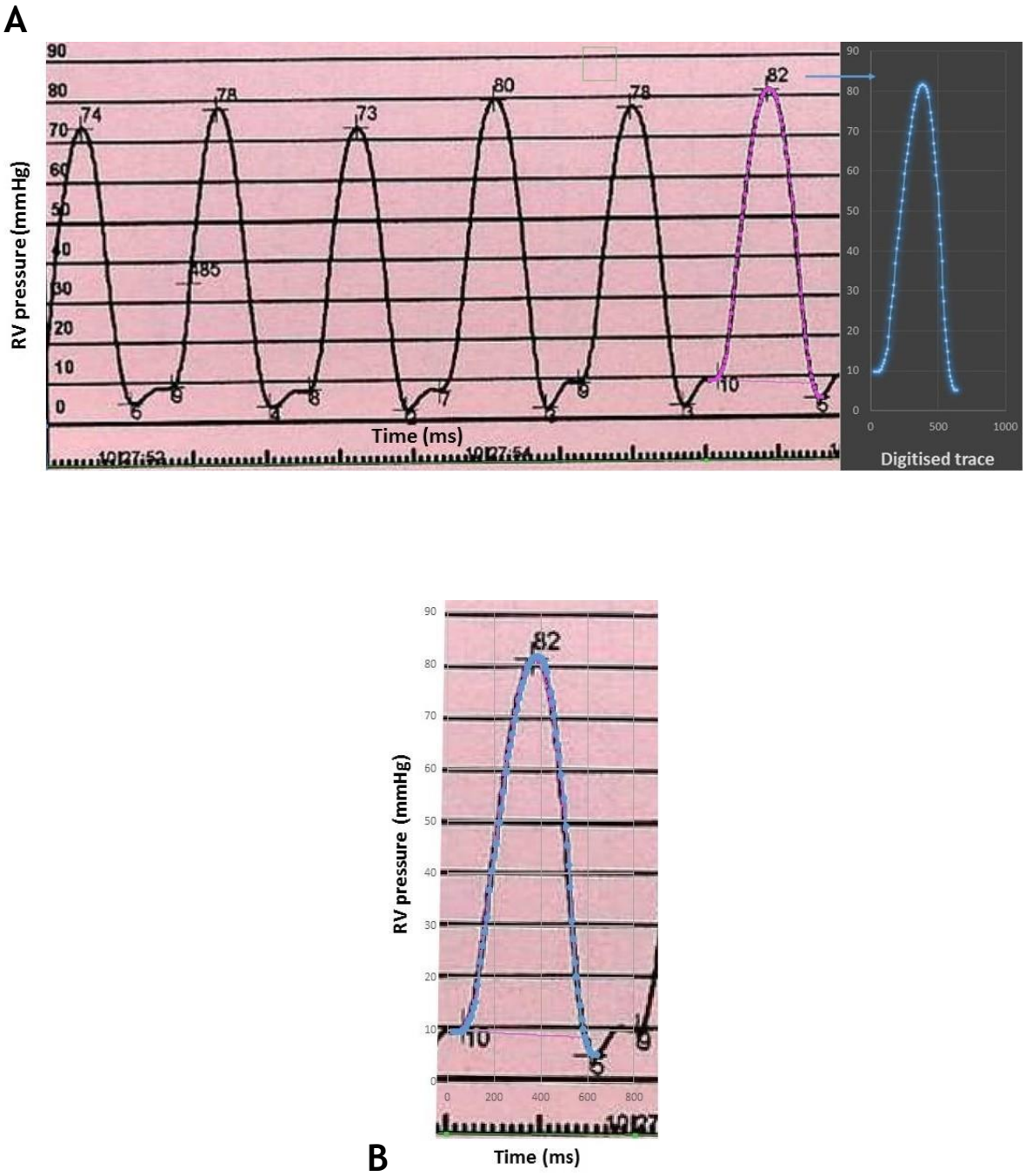

Figure 4.4 Example of digitised RV pressure trace analysis.

A Manual tracing of RV pressure time plot obtained at right heart catheterisation with data points exported to excel. Re-constructed digitised trace is shown in blue.

B. Overlay of original RV pressure/time trace with digitised trace (again shown in blue)

On preliminary analysis of 3 beats from a single patient, significant beat to beat variation in calculated values for P_{max}, E_{es} and E_{es}/E_a-P was observed. An example is shown in Figure 4.5.

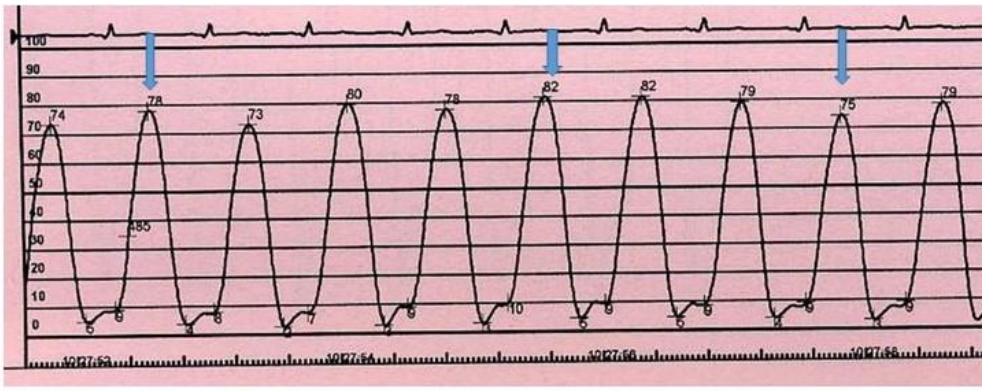

	Beat 1	Beat 2	Beat 3
Ees/Ea	1.03	1.75	1.13
PMAX	95.4	129.3	100.9
Ees	1.87	3.18	2.05

Figure 4.5 Beat to beat variation in calculated Pmax.

3 RV pressure time curves for a single patient acquired at right heart catheterisation are indicated by blue arrows with the corresponding calculated values for Pmax, Ees and RV-arterial coupling Ees/Ea.

An average RV pressure trace was therefore generated for each patient across a respiratory cycle, typically 4-6 beats. Figure 4.6 shows the correlation between the RV systolic pressure from the average trace, and the average RVSP determined by RHC demonstrating good agreement (Pearson r =0.991, $p<0.001$). The average RV pressure trace was used to determine P_{max} for each patient as described above.

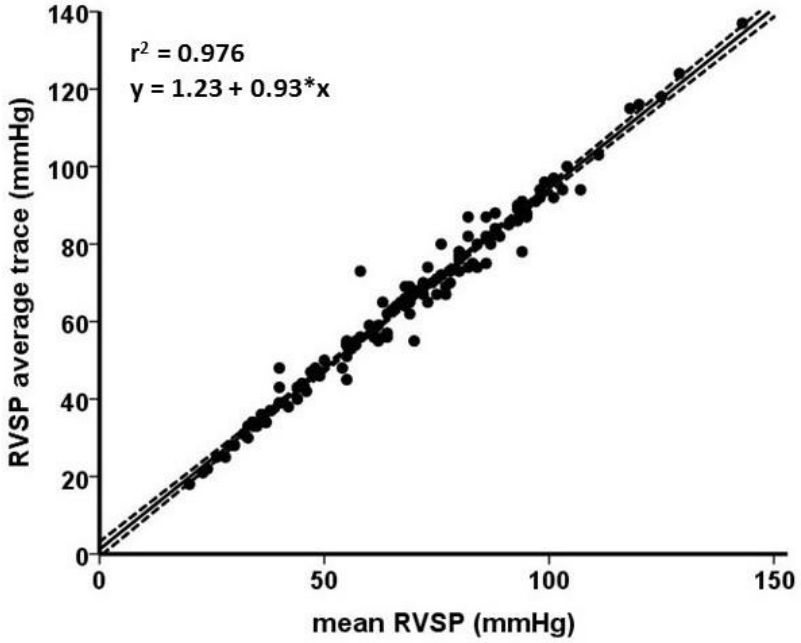

Figure 4.6 Correlation of calculated RVSP from average trace generation with invasively measured RVSP.

4.3.3 Statistical methods

Statistical analysis was carried out as described in section 2.3. Survival was from date of diagnostic right heart catheter and endpoint was date of either death, lung transplantation or censoring. Patients were censored if they were lost to follow up or alive at last day of study (4th August 2014). Only patients who received pulmonary vasodilator therapy (92/125) were included in survival analysis.

4.4 Results

4.4.1 Patient Characteristics

Patient haemodynamics, RV indices of structure and function and measures of RV arterial coupling are summarised in table 4-1. In comparison to normal subjects, PAH patients showed reduced RVEF, SVI and pulmonary arterial compliance (measured as either SV/PP or RAC MPA), and increased RV volumes (RVEDVI and RVESVI) and mass.

4.4.2 Estimates of RV-arterial coupling

4.4.2.1 Effective Arterial Elastance (Ea)

E_a correlated with increasing levels of pulmonary vascular resistance (r^2 = 0.616, p<0.001) and inversely with pulmonary artery compliance measured invasively (SV/PP, r^2 = 0.538, p <0.001) and non invasively by cardiac MRI (RAC MPA, r^2 = 0.252, p <0.001). Correlations are shown in Figures 4.7 – 4.9.

E_a was increased in PAH patients in comparison to normal subjects, 0.88 (0.63-1.31) versus 0.23 (0.14 – 0.28) mmHg/mL, p <0.001.

Table 4-1. Clinical characteristics, haemodynamics, right ventricular dimensions and function in PAH patients in comparison to normal subjects and patients with PH secondary to chronic lung disease.

	No PH	Group 1 PAH	p value	HLDPH
n	14	61		42
Aetiology % (n)		CTDPAH 26 IPAH 30 POPH 4 CHDAPH 1		
Age (years)	54 ± 15	52 ± 16	0.637	65 ± 12
Sex (%female)	71	74		40
mPAP (mmHg)	17 ± 4	49 ± 14	<0.001	44 ± 12
PVR (Wood Units)	1.8 (1.1 – 2.3)	11.9 (7.5 – 15.5)	<0.001	8.9 (5.9 -14.0)
CI (L/min/m^2)	3.3 ± 0.8	2.2 ± 0.7	<0.001	2.2 ± 0.6
SV/PP (mL/mmHg)	3.23 (3.0 – 5.7)	0.93 (0.65 – 1.20)	<0.001	1.09 (0.76-1.42)
RVEF (%)	62 ± 12	34 ± 13	<0.001	37 ± 16
RVEDVI (mL/m^2)	77 ± 27	93 ± 26	0.043	88 ± 35
RVMI (g/m^2)	34 ± 11	53 ± 18	<0.001	50 ± 18
SVI (mL/m^2)	45 (42 – 54)	28 (21-33)	<0.001	30 (24-35)
RAC MPA (%)	45 (36 – 59)	21 (12 – 27)	<0.001	19 (14-22)
Ees mmHg/mL	0.31 (0.21 – 0.47)	1.19 (0.81 – 2.26)	<0.001	0.89 (0.57 – 1.22)
Ees (EDV adj)	0.46 (0.30 – 0.58)	1.79 (1.20 – 2.52)	<0.001	1.53 (0.80 – 1.97)
Ea mmHg/mL	0.23 (0.14 – 0.28)	0.88 (0.63 – 1.31)	<0.001	0.82 (0.68 – 1.09)
Ees/Ea-P	1.81 (1.33 – 2.23)	1.33 (0.88 – 1.73)	0.019	1.07 (0.69 – 1.35)
SV/ESV	1.65 (1.17 – 1.79)	0.53 (0.30 – 0.84)	<0.001	0.53 (0.30 – 0.88)

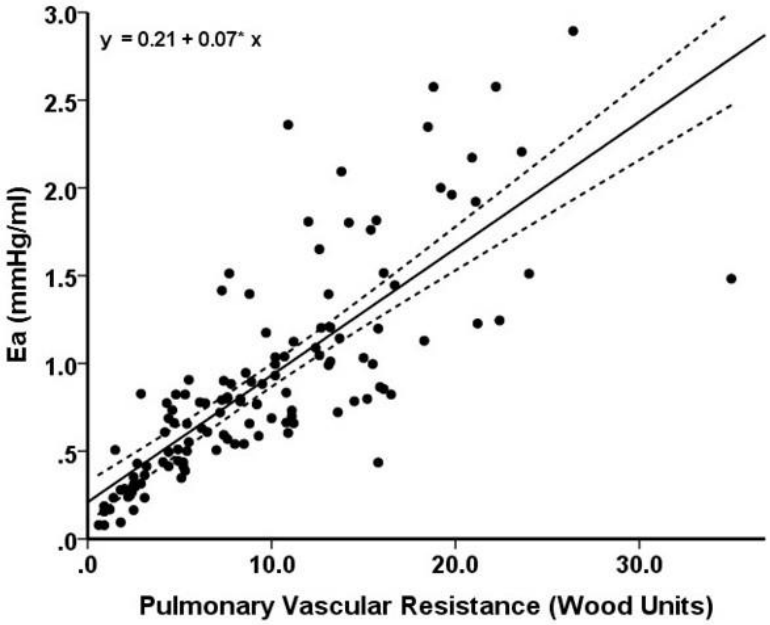

Figure 4.7 Correlation of Effective arterial elastance (Ea) with pulmonary vascular resistance.

E_a positively correlated with increasing PVR, $R^2 = 0.616$, $p<0.001$

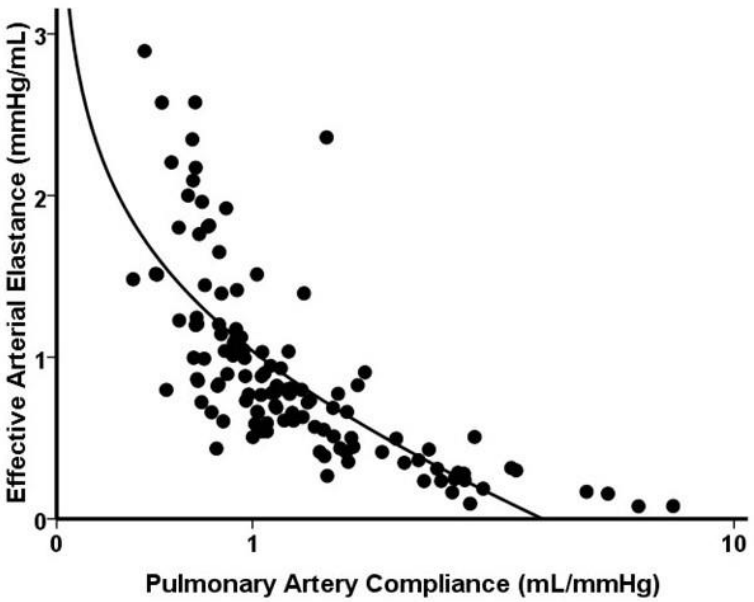

Figure 4.8 Correlation of Effective arterial elastance (Ea) with pulmonary artery compliance (SV/PP).

E_a fell with increasing PA compliance, logarithmic regression $r^2 = 0.538$, $p<0.001$. $y = 1.038 + -0.682* \log(x)$.

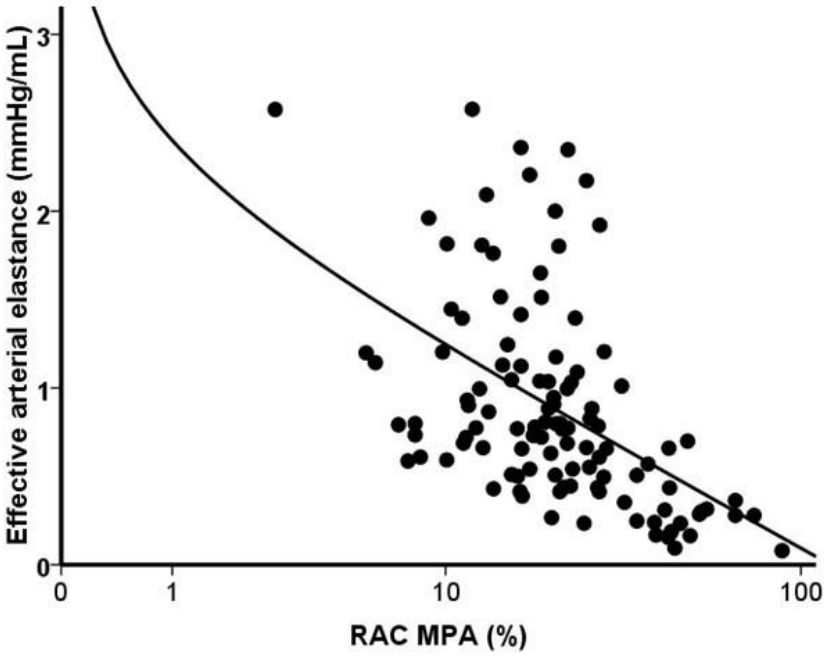

Figure 4.9 Correlation of effective arterial elastance (Ea) with pulmonary artery compliance estimated MPA RAC.

Ea also fell with increasing PA compliance assessed by CMR MPA RAC, $r^2 = 0.252$, $p<0.001$. $y = 2.399 + -0.501 * \log(x)$.

4.4.2.2 RV Contractility (Ees)

E_{es} correlated with increasing levels of afterload, measured as either PVR (r^2 = 0.259 p <0.001) or E_a (r^2 = 0.354, p <0.001). Correlations are shown in figures 4.10 and 4.11 respectively.

E_{es} was increased in PAH patients in comparison to normal subjects, 1.19 (0.81 – 2.26) versus 0.31 (0.21 – 0.47) mmHg/mL p <0.001.

After adjustment for PVR, neither age nor sex were determinants of E_{es} using linear regression analysis. In comparison to IPAH subjects, a diagnosis of HLD (despite correction for PVR) was associated with lower E_{es}. Table 4-2 shows the regression analysis.

Table 4-2 Determinants of RV contractility (Ees).

Variable	Regression Coefficient	P value
age	0.018	0.827
Male Sex	-0.063	0.421
PH aetiology (IPAH control variable)		
CTDPH	-0.117	0.214
HLDPH	-0.216	0.029*
POPH	-0.152	0.057
Normal subjects	-0.356	0.002**

Linear regression of Ees with PVR

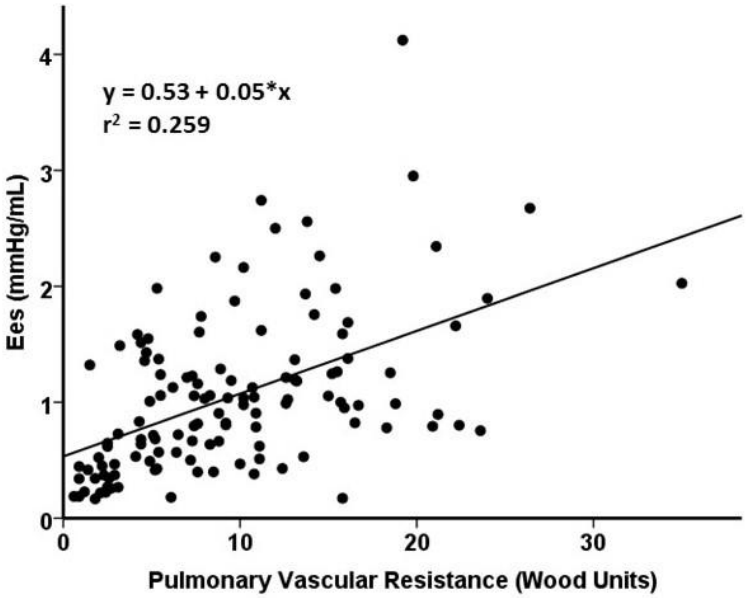

Figure 4.10 Correlation of RV contractility (Ees) with pulmonary vascular resistance.

E_{es} increased in response to increasing levels of PVR, r^2=0.259, p<0.0001

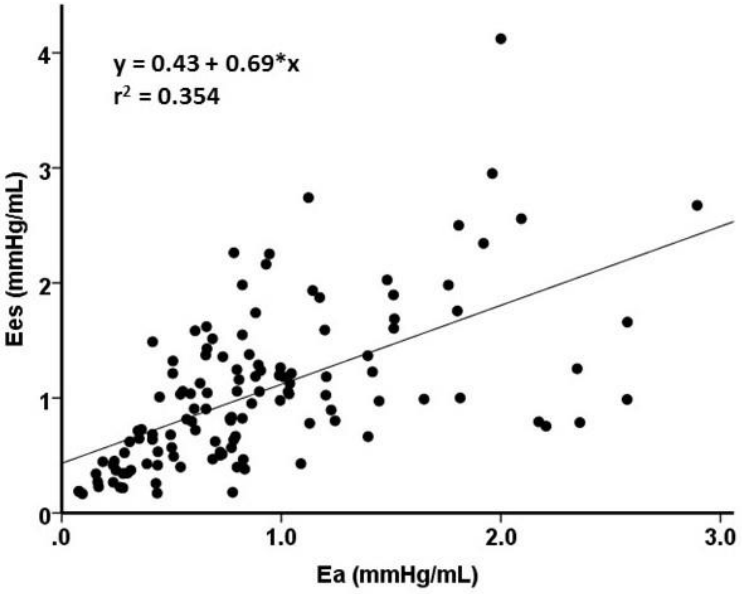

Figure 4.11 Correlation of RV contractility (Ees) with afterload (Ea)

E_{es} increased with increasing E_a, r^2=0.354, p<0.0001

4.4.2.3 Pressure (Ees/Ea-P) and volume (SV/ESV) estimates of RV-arterial Coupling

Both pressure (E_{es}/E_a-P) and volume (SV/ESV) estimates of RV-arterial coupling fell with increasing severity of pulmonary hypertension.

E_{es}/E_a-P was lower in PAH patients compared with normal subjects, 1.33 (0.88 – 1.73) versus 1.81 (1.33 – 2.23), p = 0.019 and inversely correlated with mPAP (Pearson r = -0.338, p <0.001) and PVR (Pearson r -0.381, p <0.001).

SV/ESV was lower in PAH patients, 0.53 (0.30-0.84) in comparison to controls, 1.65 (1.17 – 1.79), p <0.001. SV/ESV fell with increasing levels of mPAP (spearman r = -0.588 p <0.001) and PVR (spearman r = -0.715, p <0.001).

E_{es}/E_a-P correlated with other measures of RV function, RVEF (Pearson r = 0.403, p <0.001) and negatively with RAP (r = -0.352, p <0.001) and NTproBNP (Spearman r = -0.248, p <0.001). SV/ESV more closely related to RAP (Spearman r = -0.449, p <0.001) and NTproBNP (Spearman r = -0.723, p <0.001).

Both E_{es}/E_a-P and SV/ESV were moderate predictors of 6MWD in the whole cohort, r = 0.257 p = 0.002 and r = 0.272 p = 0.001 respectively, after adjustment for age. RVEF and SV were both superior predictors of 6MWD r = 0.288 p = 0.001 and r = 0.453 p <0.001 respectively.

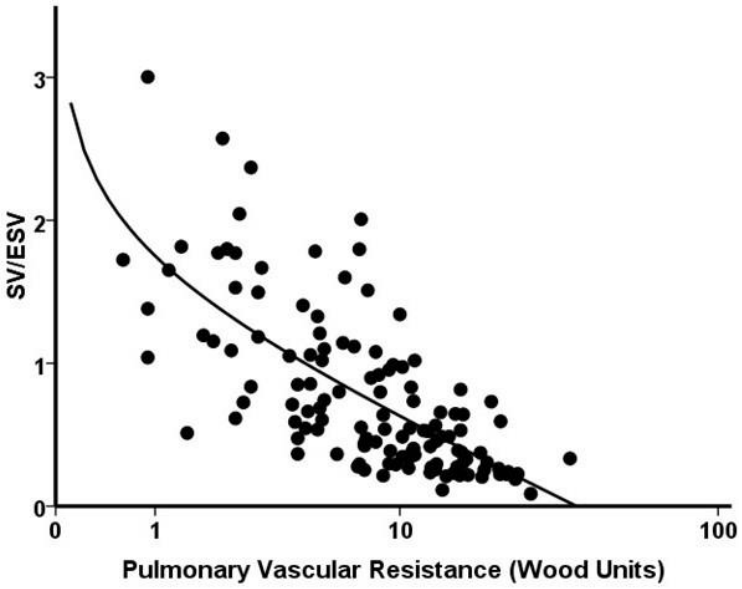

Figure 4.12 Regression of SV/ESV with pulmonary vascular resistance.

SV/ESV fell with increasing severity of PH (determined by PVR), logarithmic regression shown, r^2 = 0.484 p<0.001, y = 1.751 + -0.486* log(x)

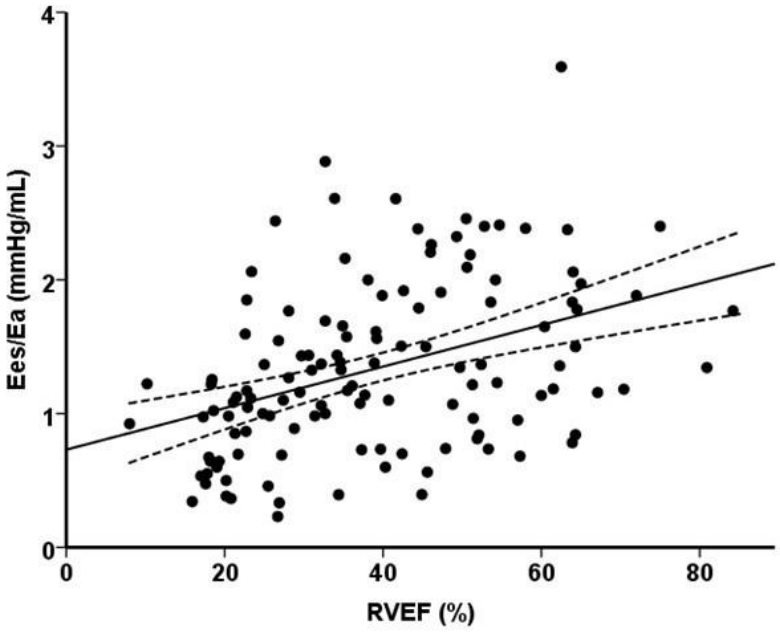

Figure 4.13 Correlation of Ees/Ea-P with RV ejection fraction.

r^2 = 0.162, p <0.001. y = 0.73 + 0.02*x

4.4.2.4 RV-arterial coupling in pulmonary arterial hypertension

Population characteristics of CTDPH and IPAH patients are shown in table 4-3. Between IPAH and CTDPH patients, there was no difference in E_{es}/E_a-P, (1.25 ± 0.7 vs 1.30 ± 0.5 p = 0.759) or SV/ESV (0.48 (0.29 -0.80) vs 0.50 (0.29 – 0.87) p=0.637). 14 of the 26 CTDPH patients had systemic sclerosis associated PAH (SSc-PAH). E_{es}/E_a-P and SV/ESV in comparison to IPAH patients was similar, 1.39 ± 0.5 (p = 0.52) and 0.60 (0.30 – 0.89) (p = 0.44) respectively.

4.4.2.5 RV-arterial coupling in pulmonary hypertension associated with chronic lung disease

Table 4-4 summarises population characteristics and indices of RV function and coupling according to severity of associated pulmonary hypertension in patients with lung disease. As discussed in chapter 3, lung disease patients were older and more often male in comparison to PAH patients. E_{es} was lower in HLDPH patients (0.89 mmHg/mL) in comparison to both all PAH subjects (1.19 mmHg/mL, p=0.017) and IPAH (1.23 mmHg/mL p = 0.001) despite similar levels of afterload, E_a 0.82 vs 0.88 mmHg/mL p = 0.442 and 0.98 mmHg/mL p = 0.09 respectively. As a result, E_{es}/E_a-P was lower in HLDPH patients in comparison to IPAH subjects (1.07 mmHg/mL vs 1.37 mmHg/mL p = 0.02) and trend towards lower values in comparison to PAH patients (1.33 mmHg/mL p = 0.058). Imaging measures of RV function SV/ESV and RVEF did not differ between groups, SV/ESV of 0.53 for all groups, p = 0.773 and p = 0.954 respectively, and RVEF 37% vs 34% p = 0.436 with PAH and 35%, p = 0.727 with IPAH subjects.

Figure 4.14 displays RV contractility (E_{es}) according to severity of PH associated with chronic lung disease. E_{es} was increased in those with PH in comparison to controls with lung disease without PH, 0.94 versus 0.41 mmHg/mL, p = 0.021. No further increase E_{es} was demonstrated in those with severe PH, 0.89 mmHg/mL p = 0.791. E_a increased in parallel to increasing severity of PH, 0.31 vs 0.66 vs 0.95 mmHg/mL in those with no, mild-moderate and severe PH respectively. As a result, significant decrease in RV-arterial coupling was seen in those with severe PH only, whether determined by the pressure or volume method, E_{es}/E_a-P 1.52 mmHg/mL versus 1.26 mmHg/mL, p = 0.700 and 1.01 mmHg/mL, p = 0.008 in no, mild-moderate and severe PH (shown in Figure 4.15). SV/ESV (shown in Figure 4.16) did not significantly decline between those with no PH and mild/moderate

PH, 1.28 versus 0.84 p = 0.280, but significant uncoupling occurred in the severe PH group, 0.37 p = 0.002 and p = 0.001 in comparison to those with no or mild/moderate PH respectively.

Table 4-3 Characteristics of Idiopathic PAH patients in comparison to Connective tissue disease associated PAH and Systemic Sclerosis associated PAH.

	IPAH	CTDPH	p-value	SSc-PAH	p-value
n	30	26		14	
Age years	49 ± 18	55 ± 14	0.148	61 ± 11	0.024*
Sex %female	70	85		93	
mPAP mmHg	56 ± 16	43 ± 8	0.001**	41 ± 7	0.002**
PVR Wood Units	12.5 (9.3 – 19.1)	9.1 (5.4 – 13.1	0.011*	9.5 (5.4 – 13.1)	0.021*
CI L/min/m^2	2.1 ± 0.5	2.4 ± 0.7	0.106	2.3 ± 0.5	0.338
SV/PP mL/mmHg	0.91 (0.65 – 1.11)	0.96 (0.68 – 1.40)	0.293	0.95 (0.75 – 1.35)	0.392
RVEF %	35 ± 12	34 ± 14	0.810	34 ± 13	0.896
RVEDVI mL/m^2	92 ± 28	93 ± 28	0.870	87 ± 30	0.575
RVMI g/m^2	54 ± 18	51 ± 18	0.516	52 ± 20	0.714
SVI mL/m^2	27 (22 – 31)	30 (19 - 35)	0.532	27 (22 – 31)	0.801
Ees mmHg/mL	1.23 (0.98 – 2.06)	1.04 (0.71 – 1.59)	0.068	1.13 (0.86 – 1.61)	0.226
Ees (EDV adj)	2.04 (1.43 – 2.91)	1.69 (1.03 – 2.23)		1.67 (1.17 – 2.31)	
Ea mmHg/mL	0.98 (0.79 – 1.56)	0.79 (0.57 – 1.25)	0.119	0.70 (0.60 – 1.66)	0.082
Ees/Ea-P	1.37 (0.72 – 2.01)	1.21 (0.94 – 1.63)	0.532	1.29 (0.98 – 1.79)	0.980
SV/ESV	0.53 (0.34 – 0.82)	0.50 (0.29 – 0.87)	0.948	0.60 (0.30 – 0.89)	0.762
NTproBNP pg/mL	886 (448 – 1197)	2989 (595 – 4206)	0.029*	2756 (608 – 4262)	0.039*

Table 4-4 Haemodynamic, pulmonary and RV function characteristics of chronic lung disease patients with no, mild-moderate and severe pulmonary hypertension

	mPAP <25mmHg	mPAP 25-34mmHg	mPAP ≥35mmHg
n	8	12	30
Aetiology % (n)			
COPD	(6)	(4)	(19)
CPFE	-	(2)	(10)
ILD	(2)	(6)	(1)
Age years	64 ± 9	70 ± 10	63 ± 12
Sex (% female)	50	50	37
mPAP mmHg	20 ± 3	30 ± 3	49 ± 9
PVR Wood Units	2.7 (2.4-3.1)	5.0 (3.5-6.9)	10.8 (7.7-15.6)
CI L/min/m^2	2.5 ± 0.4	2.6 ± 0.4	2.0 ± 0.5
RAP mmHg	4 ± 1	3 ± 4	9 ± 4
SV/PP mL/mmHg	2.97 (2.63 – 3.88)	1.59 (1.15 -1.77)	0.87 (0.68 – 1.28)
FEV1 %	82 ± 32	77 ± 30	73 ± 20
FEV1:FVC	64 ± 23	68 ± 19	58 ± 12
TLCO %	43 (29-65)	33 (26-36)	24 (19-36)
$Pa0_2$ kPa	9 (7.9-11.8) (7)	7.3 (6.9-9.8) (7)	7.3 (6.8-8.5) (23)
RVEF %	52 ± 16	49 ± 14	31 ± 13
RVEDVI mL/m^2	71 ± 20	65 ± 23	97 ± 34
SVI mL/m^2	38 ± 7	35 ± 10	29 ± 8
Ees mmHg/mL	0.41 (0.35-0.63)	0.94 (0.49-1.47)	0.89 (0.64-1.17)
Ea mmHg/mL	0.31 (0.26 – 0.40)	0.66 (0.44 – 0.81)	0.95 (0.77 – 1.46)
Ees/Ea	1.52 (1.16 – 2.00)	1.26 (1.08 – 2.14)	1.01 (0.67 -1.18)
SV/ESV	1.28 (0.64 – 1.98)	0.84 (0.59 – 1.40)	0.37 (0.27 – 0.69)

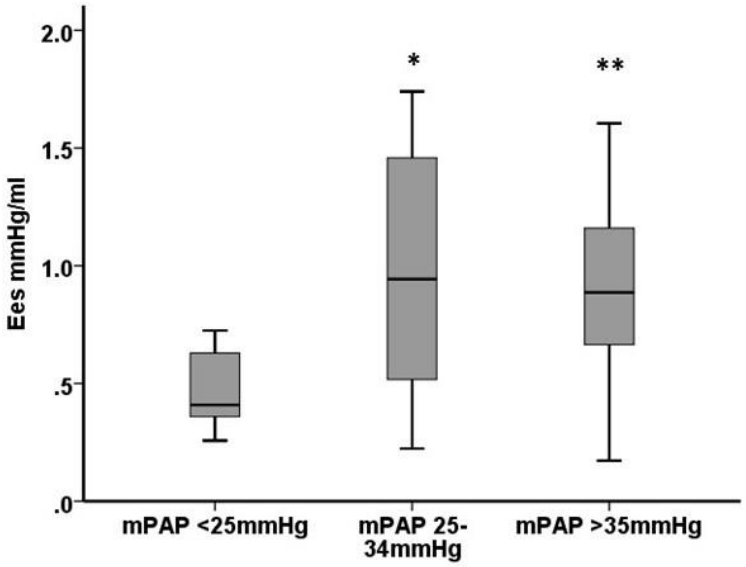

Figure 4.14 RV contractility in chronic lung disease patients with no, mild/moderate and severe PH.

Median values 0.41, 0.94 and 0.89 in no, mild/moderate and severe PH groups. * p = 0.021 **p = 0.002 in comparison to no PH group. p = 0.791 between those with mild/moderate and severe PH.

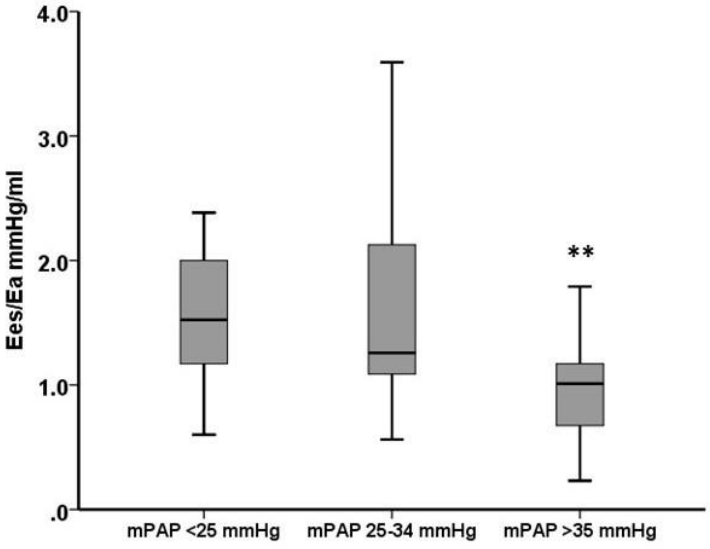

Figure 4.15 Ees/Ea-P in chronic lung disease patients with no, mild/moderate and severe PH

Median values 1.52, 1.26 and 1.01 mmHg/mL for no, mild/moderate and severe PH respectively. ** p = 0.008 in comparison to both no PH and mild/moderate PH groups. p = 0.700 between no PH and mild/moderate PH groups.

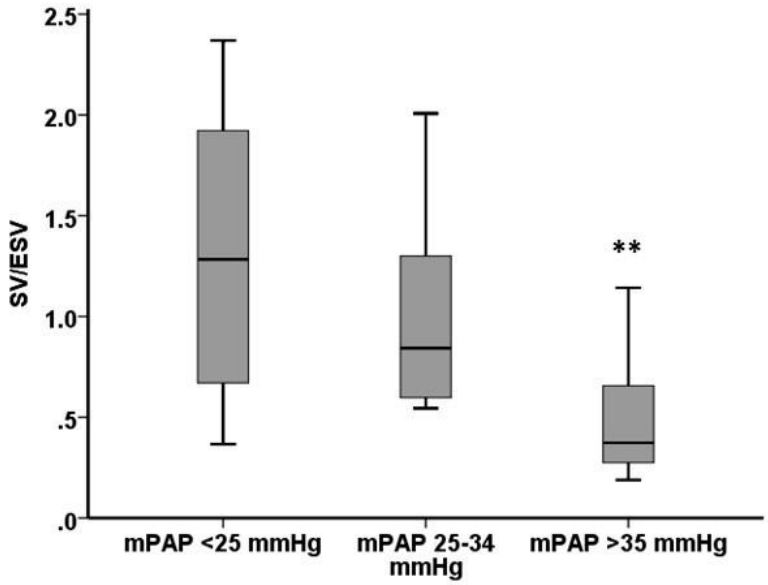

Figure 4.16 SV/ESV for chronic lung disease patients with no, mild/moderate and severe PH.

Median values 1.28, 0.84 and 0.37 respectively. ** p = 0.002 in comparison to no PH and p = 0.001 mild/moderate PH respectively. p = 0.280 between no PH and mild/moderate PH groups.

4.4.3 RV-arterial coupling and prognosis

41 deaths occurred during the follow up period in the 92 patients who received pulmonary vasodilator therapy and were included in this analysis. Higher E_a, RAP, RVESVI and NTproBNP, and lower RVEF, SVI, SV/PP and SV/ESV predicted survival on bivariate cox proportional hazards regression with age. In a multivariate model with age and PVR, RAP and SV/ESV (but not E_{es}/E_a-P) independently predicted outcome (HR 0.329 95%CI 0.165 – 0.656, p = 0.002). In the same multivariate model, RVEF independently predicted survival (HR 0.958 95% CI 0.929-0.988 p=0.006). Table 4-4 shows the bivariate and multivariate cox analysis.

Youden analysis identified optimal threshold level of 0.463 for SV/ESV and 31.6% for RVEF. Figure 4.17 displays the Kaplan Meier survival curves according to these threshold values. SV/ESV >0.463 was associated with improved outcome,1 and 3 year survival 91% vs 80%, and 66% versus 38% respectively, p = 0.011. RVEF >31.6% predicted improved survival, 1 and 3 year survival 91% versus 80%, and 65% versus 37% respectively, p = 0.011.

Table 4-5 Bivariate and multivariate cox proportional hazards regression for baseline predictors of survival in patients treated for PAH.

Variable	Bivariate model*		Multivariate model**	
	HR (95% CI)	p-value	HR (95% CI)	p-value
mPAP	1.007 (0.979 – 1.035)	0.626		
PVR	1.043 (0.981 – 1.108)	0.179	0.938 (0.861 – 1.022)	0.142
RAP	1.084 (1.019 – 1.153)	0.011*	1.088 (1.013 – 1.168)	0.020*
CI	0.600 (0.326 – 1.105)	0.101		
SV/PP	0.379 (0.150 – 0.954)	0.039*		
Ees	1.178 (0.795 – 1.745)	0.414		
Ea	2.456 (1.299 – 4.908)	0.011*		
Ees/Ea-P	0.592 (0.316 – 1.107)	0.101		
SV/ESV	0.399 (0.228 – 0.700)	0.001**	0.329 (0.165 – 0.656)	0.002**
RVEF	0.957 (0.931 – 0.984)	0.002**	#	
RVESVI	1.016 (1.005 – 1.028)	0.007**		
SVI	0.939 (0.900 – 0.980)	0.004**		
NTproBNP	1.491 (1.147 – 1.939)	0.003**		

*bivariate model with age ** multivariate model with age & PVR # RVEF 0.958 (0.929 – 0.988) p=0.006 in multivariate model with age, PVR & RAP

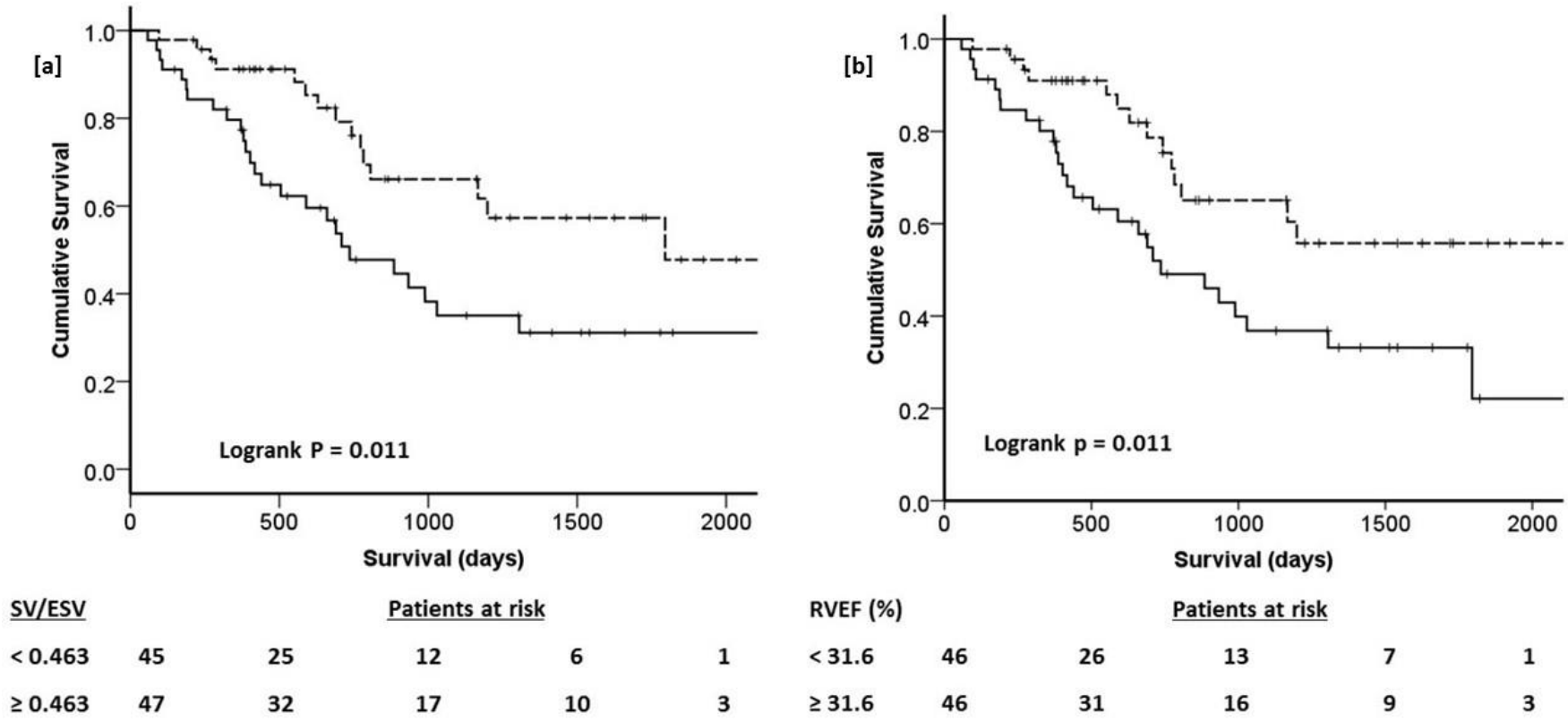

SV/ESV	Patients at risk				
< 0.463	45	25	12	6	1
≥ 0.463	47	32	17	10	3

RVEF (%)	Patients at risk				
< 31.6	46	26	13	7	1
≥ 31.6	46	31	16	9	3

Figure 4.17 Kaplan Meier survival curves dichotomised according to [a] SV/ESV >0.463 and [b] RVEF >31.6%.

4.4.4 Correlation between pressure and volume methods of measuring RV-arterial coupling

E_{es}/E_a-P correlated with SV/ESV ($r = 0.441$, $p < 0.001$), shown in figure 4.18. Bland Altman analysis of the two methods bias 0.556, SD 0.683 with limits of agreement -0.784-1.9 is shown in figure 4.19.

V_0 estimated by the volume intercept of the pressure-volume regression line correlated with RV EDV and ESV ($r = 0.607$ and $r = 0.804$ respectively, both $p<0.001$). Correlations are shown in Figures 4.20 and 4.21. Estimated values of V_0 ranged from -129ml to 285ml.

Figures 4.22 and 4.23 show the difference between pressure and volume methods E_{es}/E_a-P – SV/ESV at increasing levels of mPAP and RV dilatation (RVESV).

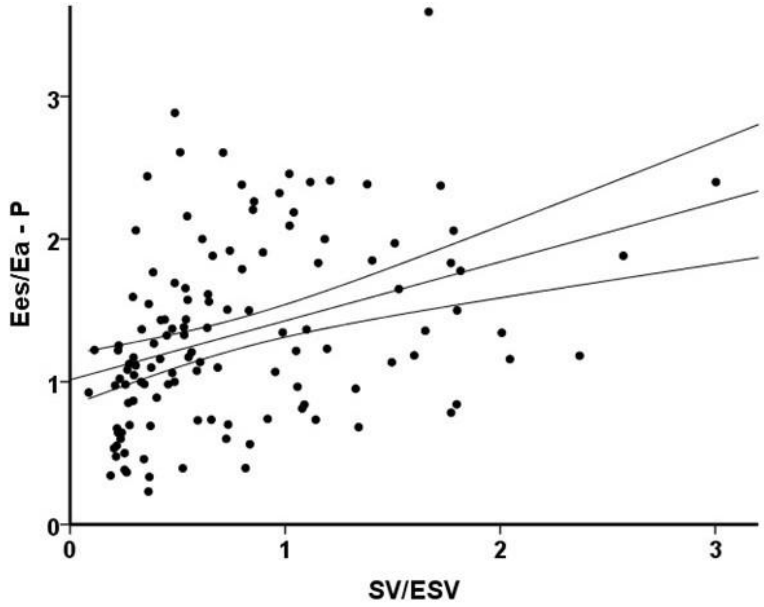

Figure 4.18 Correlation between pressure (Ees/Ea-P) and volume (SV/ESV) estimates of RV-arterial coupling.

Linear regression $r^2 = 0.135$, $y = 1.01 + 0.41*x$. $p<0.001$

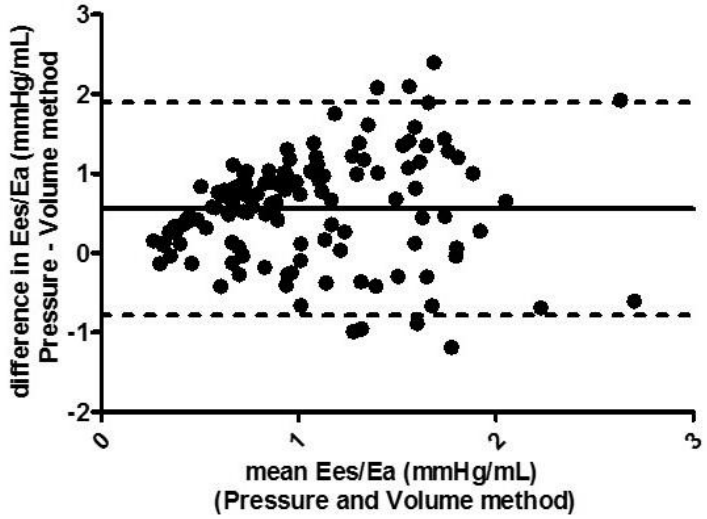

Figure 4.19 Bland-Altman analysis of difference in Ees/Ea-P - SV/ESV against mean of both values

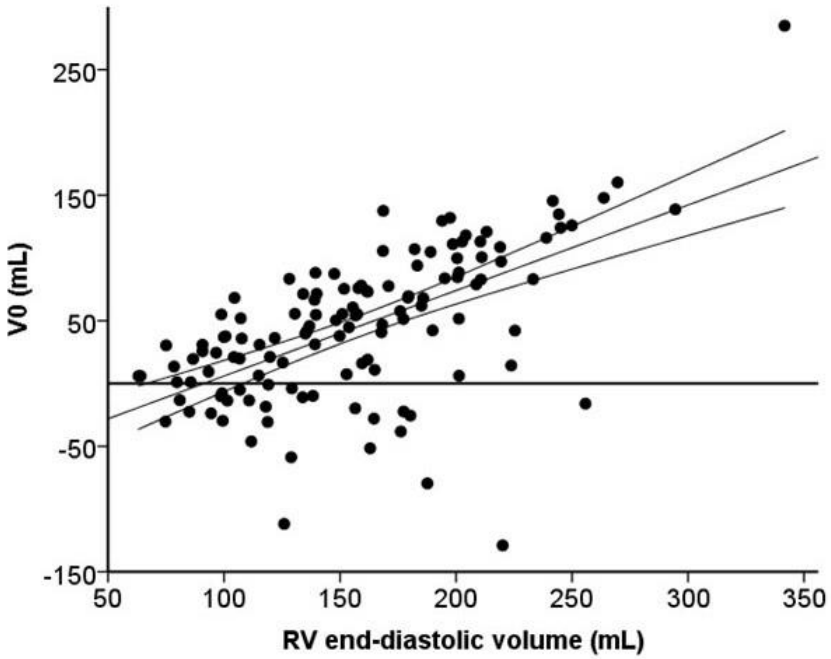

Figure 4.20 Correlation of V0 with RV end diastolic volume.

r^2= 0.365 p<0.001. y = -62.1 + 0.68*x. p<0.001

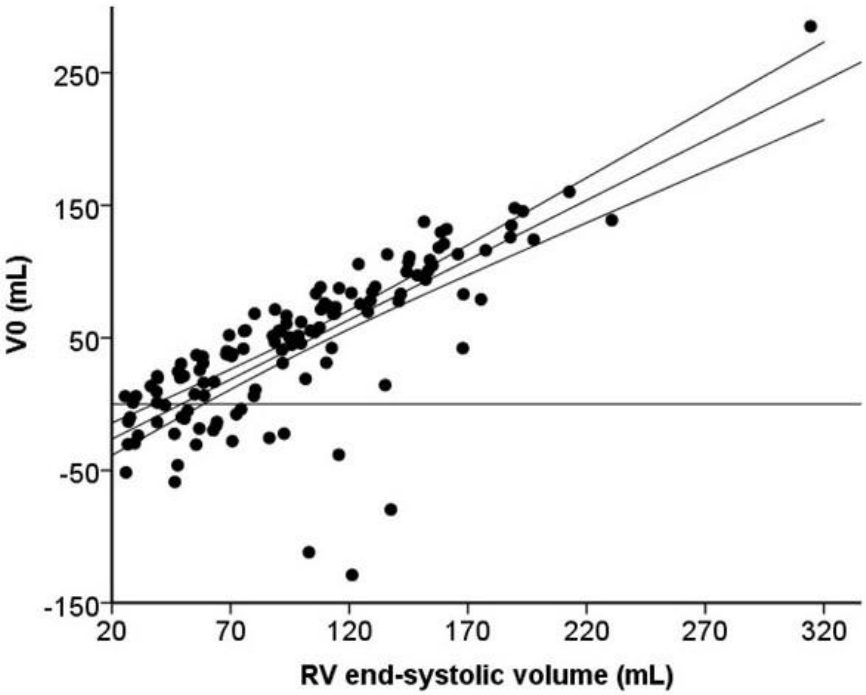

Figure 4.21 Correlation of V0 with RV end-systolic volume.

r^2 = 0.606, p<0.001. y = -44.4 + 0.9*x. p<0.001

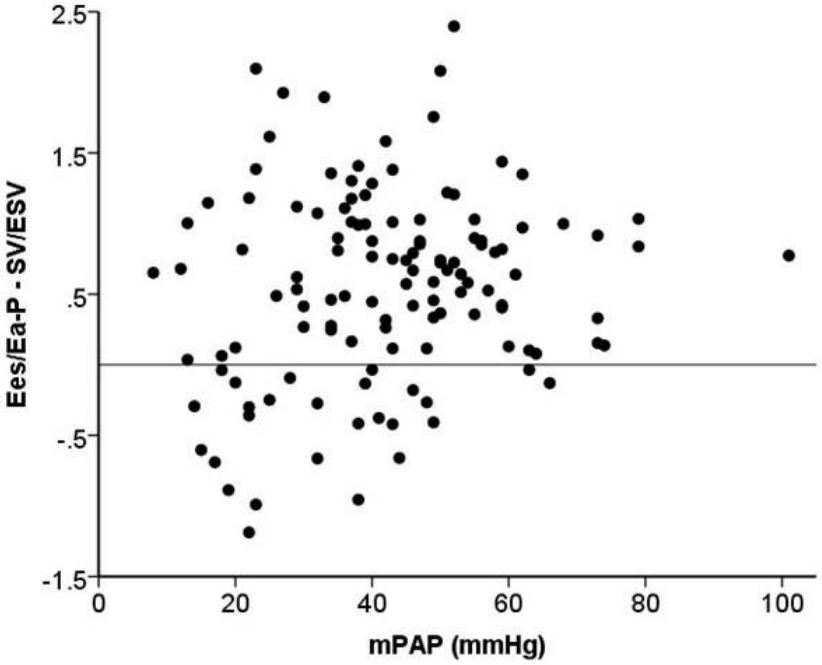

Figure 4.22 Difference in pressure and volume estimates of Ees/Ea with increasing levels of mPAP.

Greater discrepancy between values seen at lower levels of mPAP.

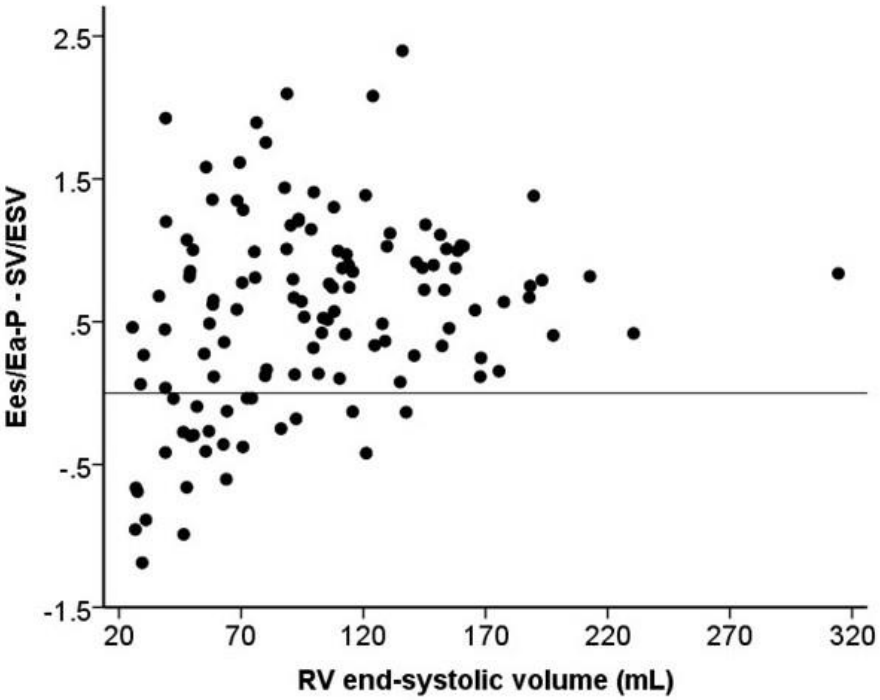

Figure 4.23 Difference in pressure and volume estimates of Ees/Ea with increasing RV dilatation.

Greater discrepancy between values seen at lower RV volume (RVESV)

4.5 Discussion

The results described in this chapter show that effective arterial elastance (E_a) estimated by mPAP determined at RHC and CMR imaging to determine RV volumes reflects commonly quoted measures of RV afterload PVR or SV/PP. In agreement with previous studies, ventricular contractility (E_{es}) when estimated by the single beat method increased in response to this increased afterload in PAH subjects. RV-arterial coupling when estimated by the pressure method, E_{es}/E_a-P was lower in PAH subjects but a greater difference when estimated by the volume method, SV/ESV was observed. We found comparable estimates of E_{es}/E_a-P in normal subjects, 1.8 mmHg/mL in our study in comparison to 1.9 mmHg/mL in the study by Kuehne at al, where gold standard pressure-volume loop analysis was employed (412), suggesting validity of the single beat method employed in this chapter.

RV-arterial coupling estimated by either E_{es}/E_a-P or SV/ESV related to functional status (determined by 6MWD), although this relationship was poorer than other measures of RV function such as SV or RVEF. E_{es}/E_a-P related to other indices of RV function determined by imaging (RVEF), RHC (RAP) or by biomarker NTproBNP, but this relationship was stronger with SV/ESV.

4.5.1 Influence of PH aetiology on RV adaptation to afterload.

Tedford et al have previously reported depressed RV contractility in PAH associated with systemic sclerosis in comparison to IPAH (413). In this study, E_{es}/E_a-P were similar in both, and the presence of associated connective tissue disease was not a determinant of E_{es}. E_{es}/E_a-P was 1.37 mmHg/mL which is similar to recent published data in IPAH patients (412, 416). One potential explanation for the differences reported by Tedford et al may be that a higher value of 2.1 mmHg/mL for IPAH patients was a result of PH therapies such as epoprostenol in this cohort, and the value of 1.0 mmHg/mL in the Ssc-PAH patients more representative of treatment naïve population described in this study regardless of aetiology.

Disproportionate elevation of NTproBNP was observed similar to previous studies and potentially still supports evidence for intrinsic myocardial dysfunction in CTDPH (417, 418).

In patients with PH secondary to chronic lung disease, RV-arterial coupling was preserved in early disease (mPAP 25-34mmHg) but uncoupling was demonstrated in severe PH characterised by an increase in RV volumes, and no further increase in RV contractility. This suggests similarities to IPAH patients where previous studies have reported initial preservation of RV-arterial coupling in patients with no increase in RV volumes (413). In agreement with the results presented in chapter 3, severe PH associated with chronic lung disease is characterised by not only RV dysfunction determined by falling RVEF and increasing RV volumes but also by impaired RV contractile response to the increased afterload, with resulting inefficient RV-arterial coupling whether determined by either pressure or volume method. Potentially, intrinsic myocardial dysfunction due to smoking related microvascular disease or inflammation which has been linked to LV dysfunction in COPD patients could explain impaired contractile response and be a future direction for study.

4.5.2 RV-arterial coupling and relationship to outcome

The results show that CMR imaging of RV volumes allows for the prediction of outcome in PAH by RV function defined either as EF or SV/ESV. Right heart catheterisation derived estimates of RV function such as RAP also independently predicted survival, but not CI nor measures of afterload such as PVR or SV/PP. Furthermore, there was no added value of combining invasive measurements of pressure with non-invasive measurements of volumes to assess the prognostic value of RV-arterial coupling.

In agreement with the previous study by Vanderpool et al (415) E_{es}/E_a estimated by the volume method but not the pressure method predicted outcome. The pressure method applied to estimate E_{es}/E_a-P relies on a P_{max} calculation based on the analysis of a RV pressure curve to estimate maximum pressure of an isovolumic beat at EDV (125), and mPAP assumed equal to ESP (132) as described in section 4.1.1 While the pressure method generated E_{es}/E_a values that are quantitatively in the range of values reported by more robust methods (413, 419), the number of assumptions in the method may result in insufficient precision and explain the failure to predict outcome. The volume method rests on the indirect assumptions that E_{es} is a volume independent straight line crossing the origin, which is not correct (396). However, measurements of ESV and EDV by CMR have a high level

of accuracy and precision (64, 357), so that the information content of SV/ESV to estimate E_{es}/E_a is preserved and predicts outcome.

Mathematically the volume method of estimating RV-arterial coupling, SV/ESV is similar to RVEF, where RVEF is the ratio of SV/EDV, so the advantage of SV/ESV over the traditionally used RVEF to assess RV adaptation to afterload could arguably be unclear. Whilst mathematically linked, they exhibit a non-linear relationship. This suggests a possible reason why SV/ESV could be more predictive because it widens the physiological range of values thereby increasing resolution of SV/ESV in patients with relatively normal RVEF (values of RVEF range 0.14-0.58 in comparison to 0.18-1.5 for SV/ESV).(420)

Right heart catheterisation is mandatory for the diagnosis of PH. However, the procedure allows for only an indirect description of RV function, with RAP to estimate EDV, or preload, SV/PP or PVR to estimate afterload, and SV to reflect contractility. In spite of these limitations, RAP, cardiac output and PVR have been reported to predict outcome in PAH (144, 269, 286, 287). However, this was in studies considering exclusively these invasive measurements. In the work presented here which combined right heart catheterisation and CMR measurements, only RAP and imaging of RV function (either RVEF or SV/ESV) independently predicted outcome. This result agrees with the notion that imaging provides a more accurate and relevant definition of RV function than a standard right heart catheterisation, without the added benefit of measures of afterload such as PVR or SV/PP. Furthermore, repeated invasive RHC to monitor an individual throughout the course of disease is likely less acceptable to the patient when the option of noninvasive imaging of RV function is equally or even superior modality in relation to prognosis. This is in agreement with previous study where improvement in PVR at RHC did not lead to improved outcome if RVEF continued to deteriorate (288).

4.5.3 Limitations

The correlation between pressure and volume estimates (E_{es}/E_a-P and SV/ESV) whilst highly significant displayed wide confidence intervals and limits of agreement on Bland Altman analysis (-0.78 to 1.9). This effect appeared more significant at greater values and at smaller values of RV ESV. V_0 estimated by the

regression of the pressure-volume relationship (and therefore reliant on only two data points, including mPAP at RVESV (as shown in Figure 4.2b) unsurprisingly correlated with ESV in agreement with Trip et al (132), however would therefore not account for the greater disagreement between coupling estimates at lower values of RVESV. As discussed above, estimates of V_0 by this method are likely inherently less accurate due to application of a linear regression of a slightly curvilinear relationship. The limitations of agreement therefore relates to impaired precision as a result of the several assumptions made in the derivation of each method as discussed in section 4.5.2.

This was a single centre retrospective observational study. The invasive RV trace analysis required manual digitisation from analogue traces for analysis. The RHC and CMR (and therefore pressure and volumes) were not performed simultaneously. There were however no changes in therapy between measurements. The single beat method employed requires several inherent assumptions, such as the use of a sine wave to approximate the waveform of isovolumetric contraction (421), but despite this P_{max} generated from single beat method has shown excellent correlation with P_{max} derived from multi-beat PV-loop analysis at varying levels of venous return (125), which is regarded as the gold standard for measuring RV-arterial coupling and ideally should have been included for comparison. These studies however would have required alteration of venous return through techniques such as inferior vena cava balloon occlusion with potential for complications and were felt unacceptable risk to the patient.

4.5.4 Clinical Implications

The results described by this chapter indicate that invasive measures of RV function (such as RAP or CI) or pressure estimates of RV arterial coupling do not add prognostic advantage over imaging of RV volumes to determine function and coupling, when assessed at baseline. Imaging is more acceptable than right heart catheterisation to the patient particularly for serial monitoring. The results presented herein reinforce previous work that outcomes in PAH should focus on RV function, rather than metrics of afterload.

4.6 Conclusions

In this chapter we have shown that RV-arterial coupling is inefficient in patients with PAH, relates to functional status and other metrics of RV function, and predicts outcome when determined by the volume but not the pressure method. Patients with PH related to hypoxic lung disease demonstrate impaired RV contractile response to increasing afterload in comparison to PAH subjects. RV function to predict outcome in PAH is best evaluated by imaging derived SV/ESV or EF. In this study, there was no added value of invasive simplified pressure-derived estimates of RV-arterial coupling. In the following chapter the effect of PAH therapy on the simplified volume estimate of RV-arterial coupling will be explored.

Chapter 5 - Non invasive monitoring of the RV-pulmonary circulation unit in patients treated for pulmonary hypertension

5.1 Introduction

The results discussed in chapters 3 and 4 show that RV function at diagnosis is a strong prognostic factor in both PAH and severe PH associated with chronic lung disease. In this chapter, I propose to examine the effect of PH therapy on RV function assessed by both SV/ESV in comparison to other indices such as RV ejection fraction and stroke volume, and the prognostic value of this change in comparison to other commonly implemented outcome measures such as NTproBNP and 6MWD.

As discussed in section 1.3.1, the ability of the right ventricle to adapt to the increased afterload that occurs in patients with pulmonary arterial hypertension has been recognised in recent years as the major determinant of functional status, exercise capacity and prognosis. Whether determined invasively with measures of right atrial pressure or cardiac index at RHC (142, 269), or by use of imaging modalities such as echocardiogram (422) or cardiac MRI (41), RV dysfunction both at diagnosis and during PAH therapy is associated with poorer outcome. Importantly, progressive RV dysfunction despite improvement in PVR with therapy has been demonstrated by cardiac MRI and associated with poorer outcome (288), highlighting the need for monitoring RV function in these patients.

5.1.1 Effect of pulmonary vasodilator therapy on RV volumes and mass

As discussed in section 1.3.4, several small pharmacological therapeutic studies have demonstrated no improvement in RV volumes or mass (302, 326, 327), with the exception of some studies showing a reduction in RV mass with sildenafil, but not Bosentan suggesting possibility of a drug class effect (324, 325, 329). Larger single or multicentre studies with mixed drug therapies have demonstrated improvement in RV EDVI and LVEDVI (41, 288, 373). Reverse remodelling after lung transplantation (321) or pulmonary endarterectomy (323) has however been demonstrated suggesting ability of the RV to recover if significant improvements in afterload are made. Increasing RVEDVI and falling LVEDVI but not change in RVM during PAH therapy have been demonstrated to predict worse survival (41).

5.1.2 Vascular stiffness

As discussed in section 1.3.2 reduced vascular compliance (i.e. increased stiffness) assessed either invasively by SV/PP (285) or non-invasively by RAC MPA (314) measured at diagnosis in PAH is associated with poorer survival. In Chapter 4 RAC MPA was shown to inversely correlate with E_a (Figure 4.9, $r^2 = 0.252$, $p < 0.001$), a measure of total RV afterload. Invasive studies have demonstrated a reduction in PVR with PAH therapy, but the effect of therapy on vascular stiffness as assessed by RAC MPA is unknown, and if this is a useful marker of therapeutic response.

5.1.3 RV function during PH therapy

Small therapeutic studies have reported consistently on improved SV with PDE-5i, and Epoprostenol therapy (302, 324), with mixed outcomes in RV ejection fraction, with either no effect (326, 327) or improvement with dual therapy in one study (329). Larger single or multicentre studies have demonstrated improvement in both measures of RV function after PAH therapy (41, 288, 373). Furthermore, any further deterioration in RV function assessed by these indices during therapy has been clearly linked to worse prognosis despite improvements in afterload (288).

As discussed in chapter 4, RV-arterial coupling, and in particular SV/ESV may be a preferable parameter for monitoring RV function during PH therapy as it is less pre-load dependent then RV ejection fraction (SV/EDV). Systemic vasodilatory effects of pulmonary vasodilators may increase venous return and therefore increase EDV, which decreases EF if SV is unaltered. Alternatively, an increase in CO (from either increase in heart rate or preload) may decrease PVR (mPAP – PAWP /CO) without any change in functional state of the pulmonary circulation. SV/ESV as a measure of RV arterial coupling may clarify cofounding effect of preload on longitudinal change in RV systolic function in patients undergoing PAH therapy.

Various experimental animal models have examined the pharmacological effects of both inotropic agents and pulmonary vasodilators on RV-arterial coupling. Dobutamine has been shown to increase RV-arterial coupling by inotropy (increase in contractility, E_{es}) both with (423) and without a decrease in afterload (125,

424). Norepinephrine improves RV-arterial coupling through an exclusively inotropic effect (423), whilst levosimendan has been shown to improved coupling through combined increase in contractility and reduction in afterload in a pulmonary banding model of RV failure (424, 425). Epoprostenol has been shown to improve RV-arterial coupling by exclusive pulmonary vasodilatory (i.e. reduction in E_a) in both overcirculation induced PH (426) and pulmonary artery banding models of RV failure (427). Sildenafil administration improved RV-arterial coupling due solely to pulmonary vasodilatory effects in acute hypoxic model of PH (428), but additionally through positive inotropic effects in a PA banding chronic PH model (429). Bosentan administration in a chronic overcirculatory PH model did not demonstrate any improvement in contractility (410). These experimental studies suggest overall predominantly vasodilatory rather than inotropy related effects, with again the suggestion that PDE-5i may have some direct myocardial effects. To date no clinical studies have examined effect of PH therapy on RV-arterial coupling in PAH.

5.1.4 6MWD and NTproBNP, surrogate markers of RV dysfunction.

Cardiac MRI is regarded as the gold standard modality for interrogating RV structure and function due to the complex shape and contractile pattern of the RV being better suited to a 3D imaging modality. Cardiac MRI is not however available in all centres, and not tolerated by some patients due to claustrophobia or breathlessness, whilst 3D echocardiography is still largely limited to the research field.

As discussed in section 1.2.5.3, exercise testing in the form of either a walking test or cardiopulmonary exercise test in addition to assessing the patient's functional capacity has been used as a surrogate measure of RV function due to the relationships demonstrated with peak VO2, cardiac output, and stroke volume (290). The 6MWT is commonly employed as it is easy to perform. Absolute distance walked has been shown to predict survival both at diagnosis and whilst undergoing therapy (286, 290). However, change in 6MWD does not consistently predict survival benefit (430), its utility in less affected individuals is confounded by a ceiling effect (295) and distance walked is influenced by a number of confounders including patient motivation and comorbidity.

As discussed in section 1.2.5.4, the biomarker brain natriuretic peptide (BNP) is secreted by ventricular cardiomyocytes in response to increased stretch as a result of cardiac wall stress. The BNP precursor is split into a biologically active peptide and the more stable N terminal fragment (NTproBNP) (296). Both have been shown to reflect RV dysfunction and predict prognosis in PAH (301, 431). Biomarkers have the advantages of being independent of interpretation or operator skill, non-invasive and quick to perform in an outpatient clinic.

Figure 5.1 shows CMR measured RVEF, RVEDVI, 6MWD and NTproBNP for a patient with PAH undergoing pulmonary vasodilator therapy from point of diagnosis. As can be seen, whilst 6MWD continues to improve almost to a level considered as a treatment goal by current guidelines, this masks continued poor RV ejection fraction and increasing RV volume which may have been suspected by the persistently raised NTproBNP.

5.2 Aims

The results described in chapter 4 show that SV/ESV at diagnosis confers no prognostic advantage over RVEF, but both are strong predictors of outcome. As discussed earlier in this chapter, 6MWD, whilst a commonly employed outcome measure in clinical studies, has a number of limitations as a method of monitoring during PH therapy, but NTproBNP could potentially be a stronger prognostic variable due to a closer relationship to RV function. The aims of this chapter are:

1. To examine the effect of PAH therapy on RV-arterial coupling assessed by the volume method SV/ESV.

2. To assess the prognostic relevance of change in SV/ESV in comparison to other metrics of RV function, RVEF, SV and volumes, MPA RAC (as a noninvasive marker of RV afterload), 6MWD and NTproBNP.

3. To compare relationship of change in NTproBNP (ΔNTproBNP) with change in RV function in comparison to change in 6MWD (Δ6MWD) during time course of the patient's therapy.

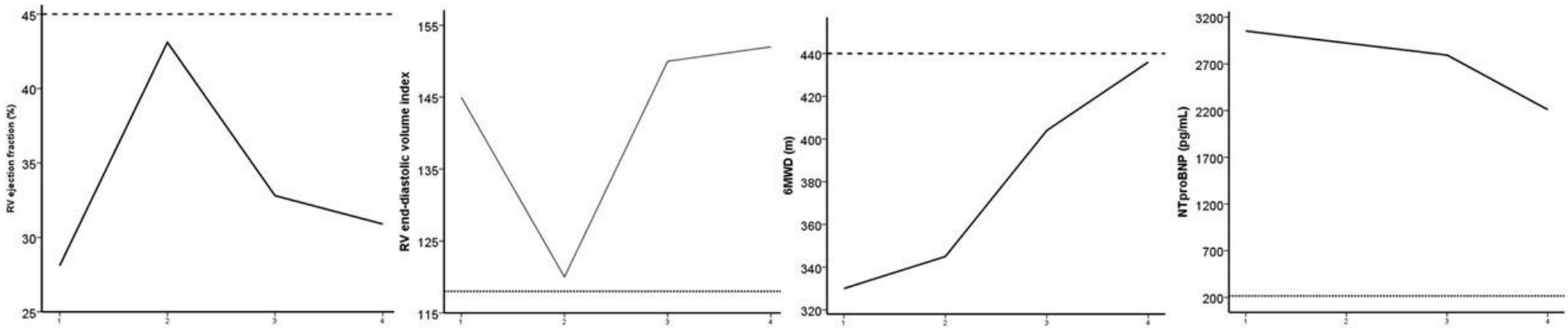

Figure 5.1. Patient example of serial RV function and volumes in comparison to 6MWD and NTproBNP data from time of diagnosis.

Time points represent 1. Diagnosis. 2. After 4 weeks of drug therapy. 3. At 3 months 4. At 1 year. Reference lines ----- lower limit of normal. ••••• upper limit of normal (85).

Panel A demonstrates RV ejection fraction remains below normal range and B RV volume remains increased, with minimal improvement during therapy. Panel C however shows that 6MWD continues to increase, reference line of 440m represents ESC guideline for treatment target as a low risk patient (estimated 1 year mortality <5%) (432) and as a means of monitoring may provide false reassurance of treatment efficacy in this patient. Panel D demonstrates NTproBNP levels remain high (in agreement with suboptimal RV indices). Reference line 215 pg/mL represents ULN in females (379) (guideline target 300 ng/L).

5.3 Materials and methods

5.3.1 Patient recruitment

52 PAH patients who had a CMR study performed at diagnosis and at least one follow up study after a minimum of 3 months of PH therapy were identified from the cohort of 140 incident PAH cases described in chapter 4. Patients underwent multidisciplinary investigation as described in section 2.1.1. Cardiac MRI acquisition and data analysis were carried out as described in section 2.2. 6MWD and/or NTproBNP performed within 1 month of CMR was included for comparison. Several patients had undergone multiple CMR studies during PH therapy, (between 2 and 5 CMR studies) with a total of 126 ΔRV values included in the analysis. All patients were treated with pulmonary vasodilators in accordance with guidelines.

5.3.2 Statistical methods

Statistical analysis was carried out as described in section 2.3. Survival was from date of second CMR study used to calculate ΔRV value, and endpoint was date of either death, lung transplantation or censoring. Patients were censored if they were lost to follow up or alive at last day of study (1st December 2015). Kaplan-Meier survival curves were calculated, grouping subjects according to increase or decrease in SV/ESV, 6MWD or NTproBNP during PH therapy, with comparison of groups using logrank test.

Correlations were performed to examine relationship between absolute and change in 6MWD or NTproBNP with RV volumes, function (SV/ESV and RVEF) and SV using Pearson or Spearman r and linear or nonlinear regression dependent on data distribution.

5.4 Results

The 52 PAH patients in this study, 33 IPAH, 16 CTDPH and 3 POPH, displayed impaired RV function at diagnosis, RVEF 36%, SVI 28 mL/m^2 and raised NTproBNP. The average time to first follow up study was 5.7 months. Table 5-1 shows the population characteristics.

Table 5-1. Population Characteristics

Age (years)	53 ± 16
% Female	64
Aetiology % (n)	
IPAH	63 (33)
CTDPH	31 (16)
POPH	6 (3)
mPAP (mmHg)	47 ± 14
RAP (mmHg)	6 ± 4
PVR (Wood Units)	10.0 (5.9 – 15.7)
CI (mL/m^2)	2.2 ± 1.7
RVEF (%)	36 ± 16
SV/ESV	0.462 (0.295 – 0.837)
RVEDVI (mL/m^2)	88 ± 29
RVESVI (mL/m^2)	59 ± 30
SVI (mL/m^2)	28 ± 11
6MWD (m)	312 ± 90
NTproBNP (pg/mL)	852 (272 – 2657)

Mean ±SD or median (IQR) shown depending on data distribution.

5.4.1 Correlations of NTproBNP and 6MWD with RV function

At diagnosis, NTproBNP correlated with RAP ($r = 0.568$, $p < 0.0001$), PVR ($r = 0.669$, $p < 0.001$) and RVMI ($r = 0.693$, $p < 0.0001$) whilst 6MWD did not ($r = -0.130$, $p = 0.374$, $r = 0.079$, $p = 0.588$ and $r = 0.175$, $p = 0.230$ respectively). There was no significant relationship between NTproBNP levels and 6MWD ($r = 0.106$, $p = 0.494$).

6MWD did not correlate with RVEF ($r = 0.052$) or SV/ESV ($r = -0.077$), but weakly correlated with SVI ($r = 0.296$, $p < 0.0001$) and increasing RV volumes, RVEDVI $r = 0.281$, $p = 0.003$ and RVESVI $r = 0.193$, $p = 0.041$). Figures 5.2 – 5.5 display the correlations.

NTproBNP strongly correlated with RV volumes, $r = 0.504$ with RVEDVI and $r = 0.655$ with RVESVI, and inversely with RV function, $r = -0.665$ with SV/ESV, $r = -0.727$ with RVEF and $r = -0.406$ with SVI, all $p < 0.001$. Figures 5.6 to 5.9 describe the correlations.

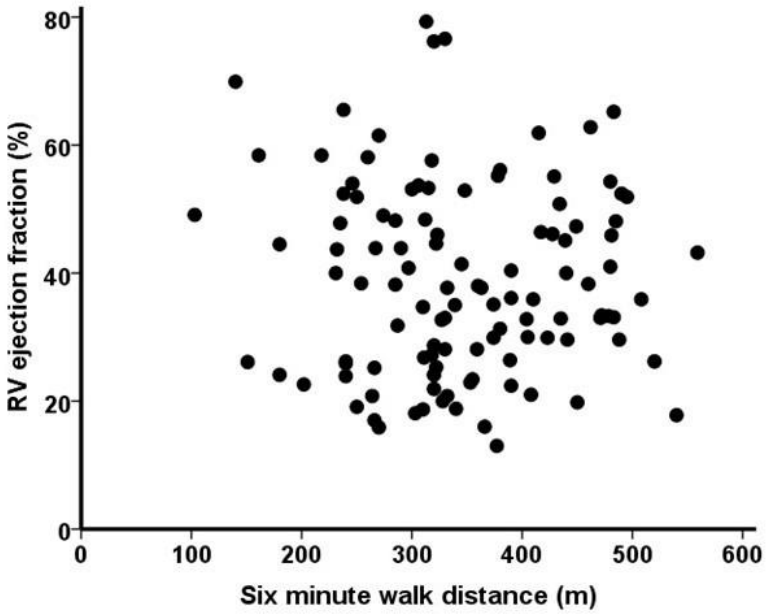

Figure 5.2. Correlation of six minute walk distance with RV ejection fraction.

No significant relationship was demonstrated, $r^2 = 0.003$, $p = 0.585$.

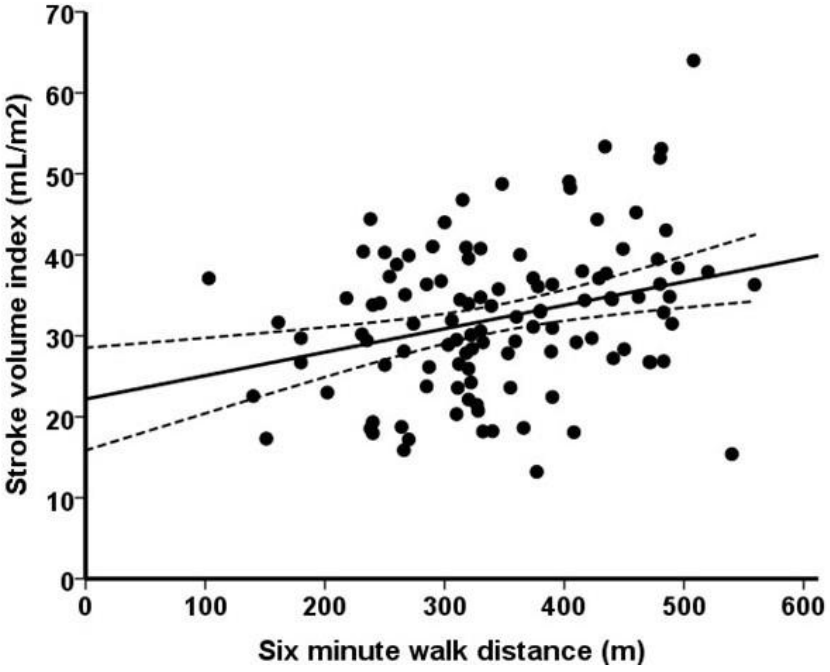

Figure 5.3. Correlation of six minute walk distance with stroke volume.

Weak correlation was demonstrated (Pearson r = 0.296), $y = 22.19 + 0.03x$, $r^2 = 0.088$, $p = 0.002$.

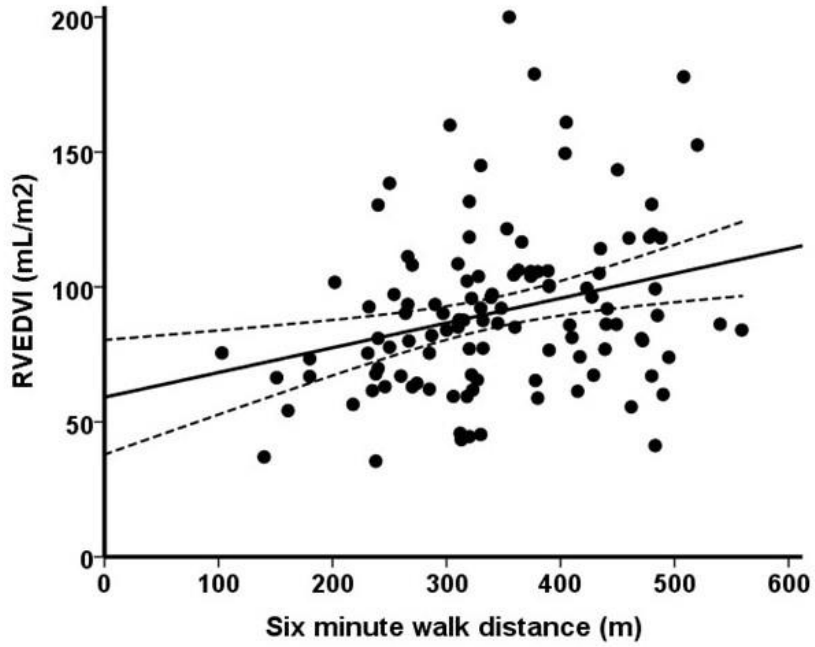

Figure 5.4. Correlation of RV end-diastolic volume with six minute walk distance.

Weak positive correlation was demonstrated, y = 0.09x + 59.15, r^2=0.079, p=0.003

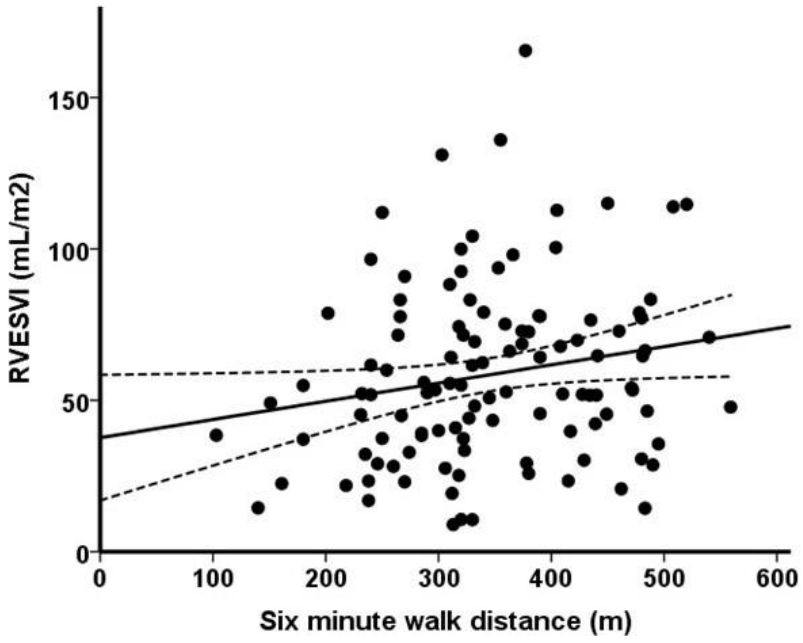

Figure 5.5 Correlation of RV end-systolic volume with 6MWD.

Weak positive correlation was seen, y = 0.06x + 37.66. r^2= 0.037, p = 0.041

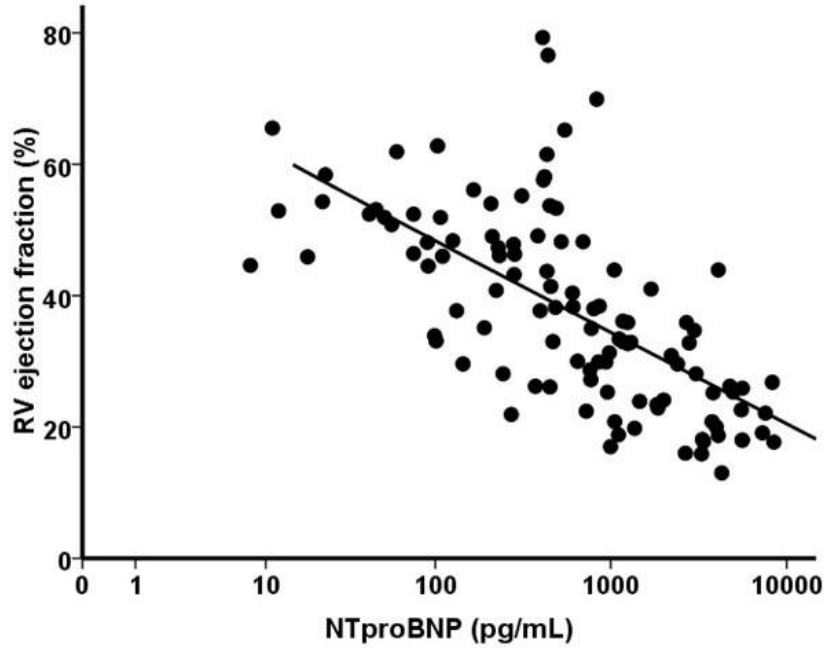

Figure 5.6 Inverse correlation of RV ejection fraction with NTproBNP.

Logarithmic regression shown, y = 76.19 + -6.05*log(x). r^2 = 0.433, p<0.0001.

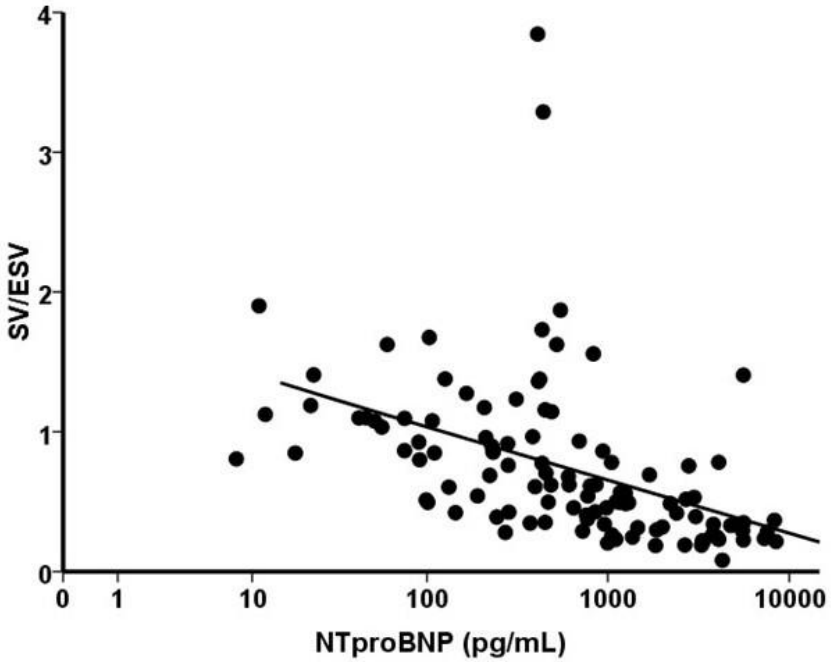

Figure 5.7 Inverse correlation of SV/ESV with NTproBNP.

Logarithmic regression shown, y = 1.79 + -0.16*log(x). r^2= 0.209, p<0.0001.

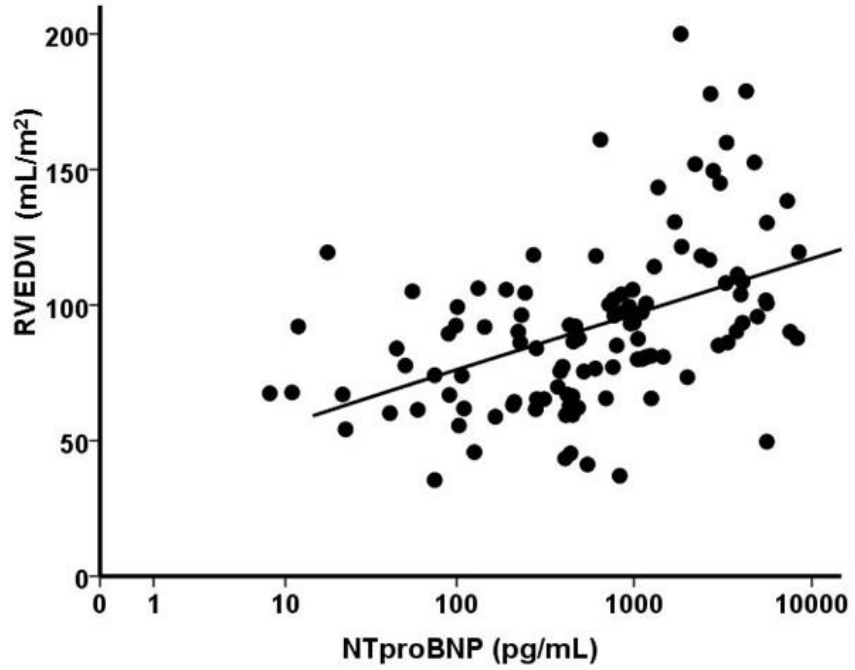

Figure 5.8 Correlation of RV end-diastolic volume with NTproBNP.

Y = 35.2 + 8.9*log(x). r^2= 0.208 , p<0.0001

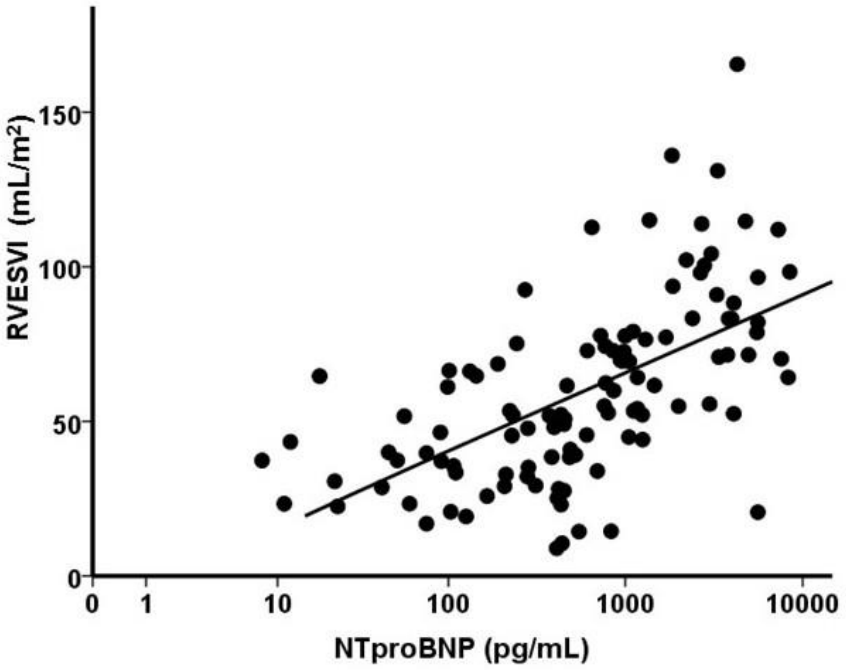

Figure 5.9 Correlation of RV end-systolic volume with NTproBNP.

y = -10.1 + 10.97*log(x), r^2= 0.350, p<0.0001.

5.4.2 Change in RV function with therapy

48/52 patients had CMR performed at diagnosis, and at less than 1 year of follow up. RVEF increased from 35±16 to 39±15, p = 0.008 and SV/ESV from 0.461 (0.295 – 0.837) to 0.616 (0.341 – 1.066) p = 0.036. There was no improvement in RV volumes observed, but SVI increased from 27 ± 9 to 31 ± 10, p = 0.004. Figure 5.8 – 5.12 display the paired analysis.

35/48 patients had NTproBNP data at both diagnosis and to coincide with first follow up CMR, and 42/48 had 6MWD performed. Significant improvement in 6MWD but not NTproBNP was demonstrated. Figure 5.13 displays the analysis.

23 patients had serial CMR measurements at diagnosis, after 3–8 months and 12-18 months of therapy. A sustained improvement in both SV/ESV and RVEF was demonstrated (shown in figures 5.14 – 5.15), SV/ESV increased from 0.390 (0.317-0.714) at diagnosis to 0.622 (0.421 – 1.099) at 3-8 months (p = 0.028) and sustained (but no further significant increase) at 12-18 months, 0.848 (0.489 – 1.157) p = 0.354. Friedman test p = 0.006. RV volumes did not improve, RVESVI 63 ± 23 to 57 ± 27 and 59 ± 32 mL/m^2 (ANOVA 0.242), RVEDVI 92 ± 29 to 91 ± 28 and 97 ± 34 (ANOVA 0.206) at 3-8 and 12-18 months respectively.

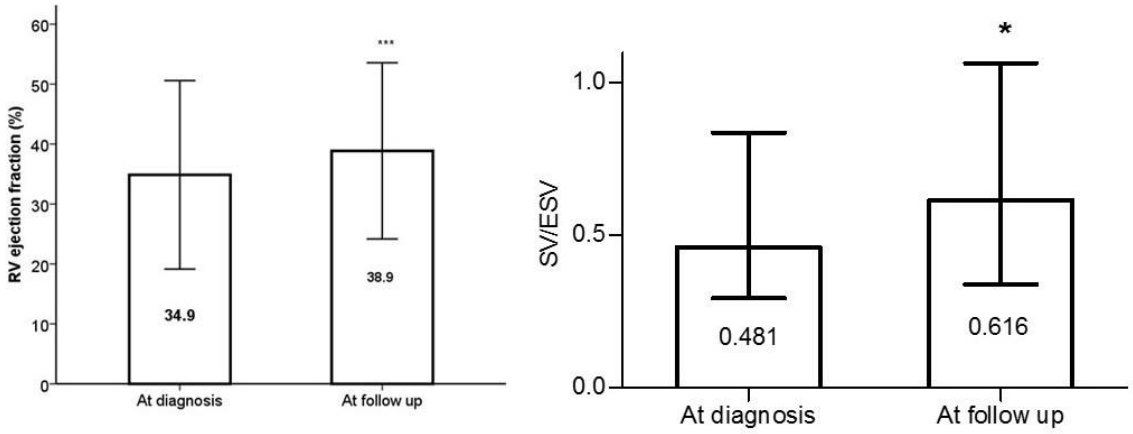

Figure 5.10 Improvement in indices of RV systolic function following PH therapy.

RVEF increased from 34.9 ± 16 to 38.9 ± 15 5, p = 0.008 (mean ± SD shown) and SV/ESV from 0.481 (0.295 – 0.837) to 0.616 (0.341 – 1.066), p = 0.036 (median (IQR) shown). Paired statistical analysis performed.

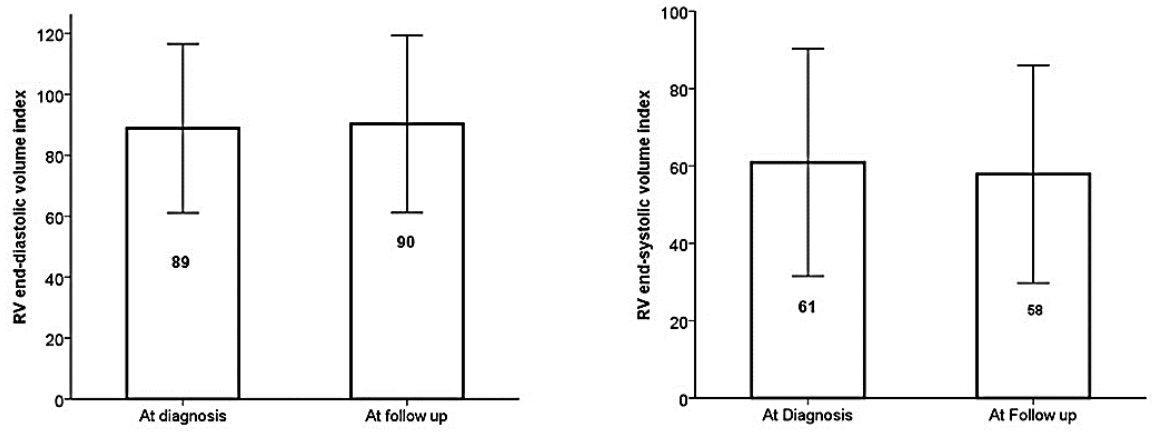

Figure 5.11. RV volumes at diagnosis and after PH therapy.

No improvement in either RVEDVI (89 ± 28 to 90 ± 29 mL/m^2, p=0.555) or RVESVI (61 ± 29 to 58 ± 28 mL/m^2, p=0.233) was observed. Mean and SD shown. Paired statistical analysis performed.

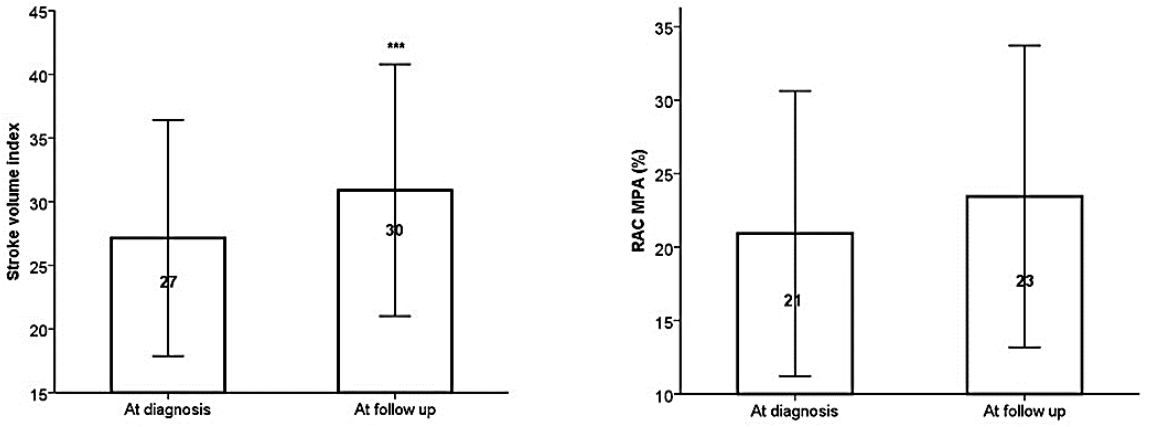

Figure 5.12. Change in stroke volume and vascular stiffness with PH therapy.

SVI improved from 27 ± 9 to 31 ± 10 mL/m^2, p=0.004 but no improvement in RAC MPA was observed (21 ± 10 to 23 ± 10%, p=0.174). mean ± SD shown. Paired statistical analysis performed.

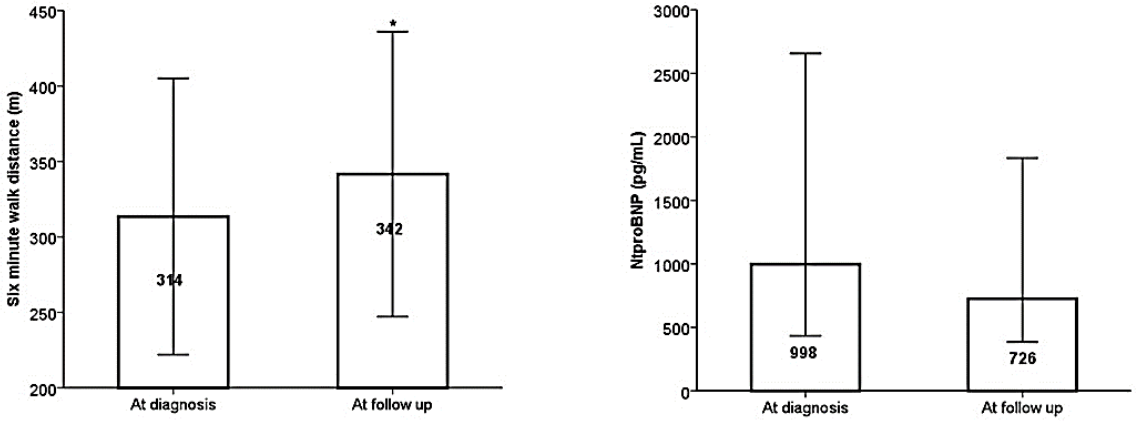

Figure 5.13. Change in six minute walk distance and NTproBNP following PH therapy.

6MWD increased from 314 to 342 m (p=0.016, n=42) but NTproBNP did not, 998 to 726 pg/mL, (p=0.534, n=35). Mean ± SD or median (IQR) shown dependent on data distribution, paired statistical analysis performed.

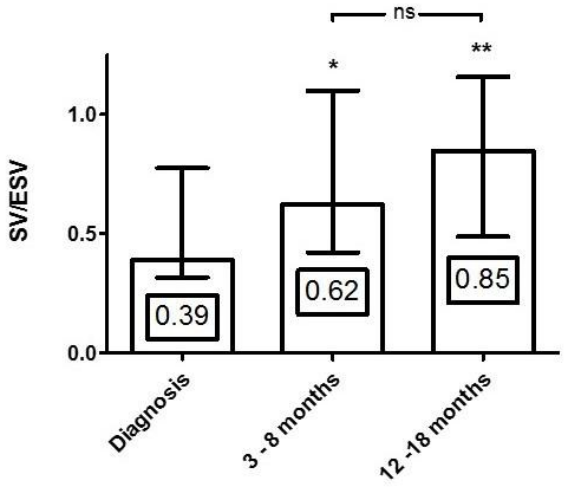

Figure 5.14 Serial SV/ESV in patients undergoing PH therapy.

Significant and sustained improvement in SV/ESV demonstrated (Friedman test p = 0.006 across series). Median (IQR) shown, n = 23. * p = 0.028 ** p = 0.005. no significant increase between 3-8 and 12-18 months, p = 0.354.

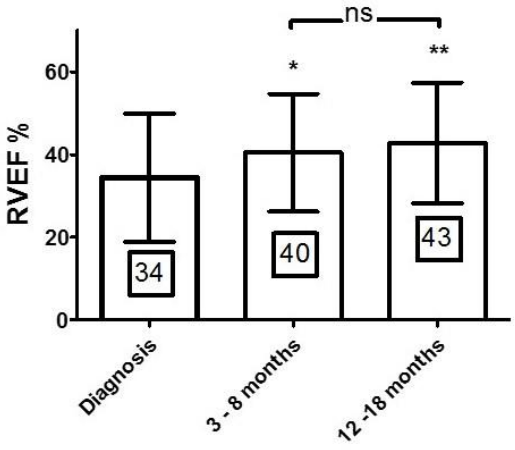

Figure 5.15 Serial RV ejection fraction in patients undergoing PH therapy.

RVEF improved at 3-8 months of therapy and was sustained at 12-18 months (ANOVA p = 0.002), mean ± SD shown. * p = 0.02 ** p = 0.001, both in comparison to baseline. No significant further improvement between 3-8 months and 12-18 months (p = 0.254).

26/48 patients received PDE-5i therapy and 18/48 ETRAs (in the remaining patients, 1 received Prostanoid therapy, 1 patient a CCB and 2 patients combination therapy with both ETRA & PDE5i). Both groups had similar baseline characteristics, shown in table 5-2, although more CTD patients received ETRA therapy. Those receiving PDE-5i showed greater improvement in RV function assessed by either RVEF (36 ± 16 to 41 ± 15 %, p = 0.03) or SV/ESV (0.486 (0.307 – 0.850) to 0.710 (0.414-1.111) p = 0.049), whilst those receiving ETRAs greater improvement in SVI (27 ±11 mL/m^2 to 33 ± 11 mL/m^2, p = 0.014) and 6MWD (271 ± 65 to 319 ± 85 m, p = 0.011), shown in table 5-3. There was no change in RVMI with PDE-5i (49 ± 17 to 49 ± 15 g/m^2, p = 0.805) or ETRA therapy (58 ± 28 to 53 ± 19 g/m^2, p = 0.177).

Examining those with pure IPAH only (excluding patients with co-existent lung disease as a factor), similar differential effects on RV function and SV were still present (data shown in table 5-4).

Table 5-2. Characteristics of patients receiving Phosphodiesterase 5 inhibitors in comparison to those receiving endothelin receptor antagonists.

	Patients receiving PDE-5i (n=26)	Patients receiving ETRA (n=18)	p value
Age (years)	55 ± 17	52 ± 16	0.607
Sex (% F)	62	72	
Aetiology			
IPAH	73 (19)	50 (9)	
CTDPAH	19 (5)	50 (9)	
POPH	8 (2)		
mPAP (mmHg)	45 ± 12	50 ± 15	0.285
PVR (Wood Units)	10.0 (5.5 – 14.2)	9.5 (5.9 – 17.8)	0.583
CI (mL/m^2)	2.2 ± 0.6	2.2 ± 0.6	0.908

Table 5-3. Change in right ventricular function according to class of drug therapy.

	At diagnosis	During therapy	p value
RVEF			
ETRA	34 ± 17	38 ± 14	0.098
PDE5i	36 ± 16	41 ± 15	0.031*
SV/ESV			
ETRA	0.447 (0.275-0.979)	0.620 (0.338-0.923)	0.396
PDE5i	0.486 (0.307-0.850)	0.710 (0.414-1.111)	0.049*
SVI			
ETRA	27 ± 11	33 ± 11	0.014*
PDE5i	28 ± 9	30 ± 10	0.146
RVEDVI			
ETRA	91 ± 30	89 ± 30	0.352
PDE5i	85 ± 25	86 ± 23	0.722
6MWD			
ETRA (14)	271 ± 65	319 ± 85	0.011*
PDE5i (24)	325 ± 80	347 ± 94	0.154
NTproBNP			
ETRA (11)	2989 (434-4278)	1107 (456-4954)	0.722
PDE5i (22)	998 (238-2059)	490 (87-1784)	0.106

Mean ± SD or median (IQR) shown and paired t test or wilcoxon matched pairs analysis depending on data distribution. 26 patients treated with PDE5i and 18 with ETRA therapy. Reduced number of patients receiving ETRA and PDE5i indicated (n) due to missing data for 6MWD and NTproBNP only.

Table 5-4. Change in RV function in IPAH patients receiving either Phosphodiesterase 5 inhibitors or endothelin receptor antagonists.

	At diagnosis	During therapy	p value
RVEF			
ETRA	30 ± 17	33 ± 12	0.245
PDE5i	32 ± 12	38 ± 14	0.022*
SV/ESV			
ETRA	0.317 (0.193-0.844)	0.512 (0.286-0.657)	0.678
PDE5i	0.390 (0.284-0.781)	0.566 (0.403-0.965)	0.031*
SVI			
ETRA	24 ± 13	34 ± 11	0.029*
PDE5i	25 ± 7	27 ± 10	0.367

Mean ± SD or median (IQR) shown. Paired data analysis performed. 15 IPAH patients received PDE5i and 9 ETRA, no missing data.

5.4.3 Relationship between change in RV function with change in NTproBNP and 6MWD.

105 Δ6MWD, 88 ΔNTproBNP and 126 ΔRV values were derived from serial measurements from 52 PAH patients described in table 5-1. Table 5-5 displays the population median and range.

Δ6MWD correlated with ΔSVI (r = 0.441, p <0.001), ΔRVEF (r = 0.344, p <0.001) and ΔSV/ESV (r = 0.272, p = 0.005) and negatively with ΔRVESVI (r = -0.235, p = 0.016) but not RVEDVI (r = -0.04, p = 0.632). Figures 5.16 – 5.20 display the correlations.

ΔNTproBNP strongly correlated with ΔRVEDVI (r = 0.372) and ΔRVESVI (r = 0.555) and negatively with ΔRVEF (r = - 0.569), ΔSV/ESV (r = -0.469) and ΔSVI (r = -0.545), all p <0.001. Figures 5.21 – 5.26 display the correlations with change in NTproBNP and log transformation of NTproBNP.

Δ6MWD did not correlate with ΔNTproBNP, Pearson r = - 0.202, p = 0.08.

Table 5-5 Population range and median change in RV indices, 6MWD and NTproBNP.

	n	median	range
ΔRVEF (%)	126	3.8	-24.8 – 47.2
ΔSV/ESV		0.105	-1.18 – 1.65
ΔSVI (mL/m^2)		5.2	-16 – 40
ΔRVEDVI (mL/m^2)		-0.31	-59 – 66
ΔRVESVI (mL/m^2)		-3.9	-68 – 60
Δ6MWD (m)	105	24	-137 – 224
ΔNTproBNP (pg/mL)	88	-83	-5041 – 3193
Relative change in NTproBNP (%)		-27	-99 - 412

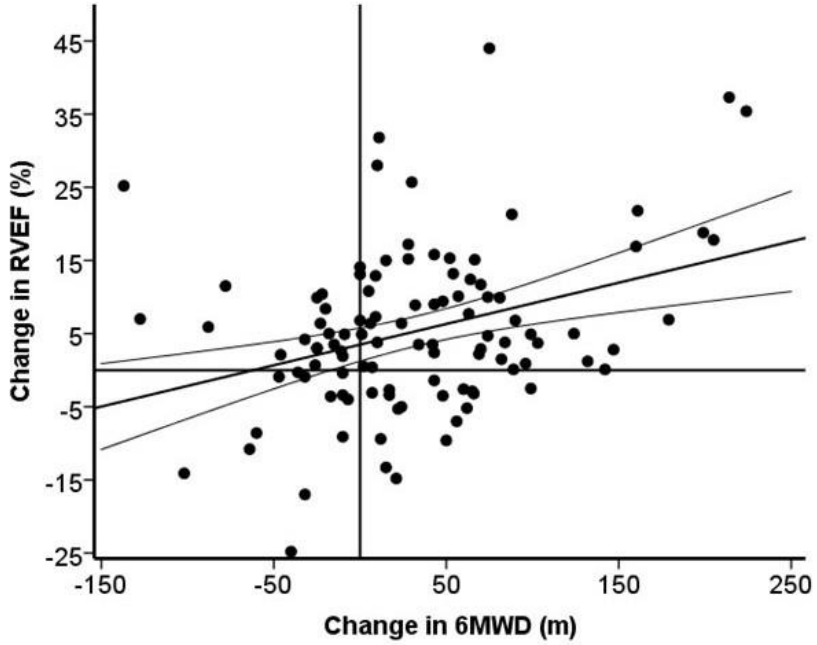

Figure 5.16. Correlation of change in 6MWD with change in RV ejection fraction.

Positive correlation between ΔRVEF and Δ6MWD, y = 3.5 + 0.06x, r^2= 0.118, p <0.001

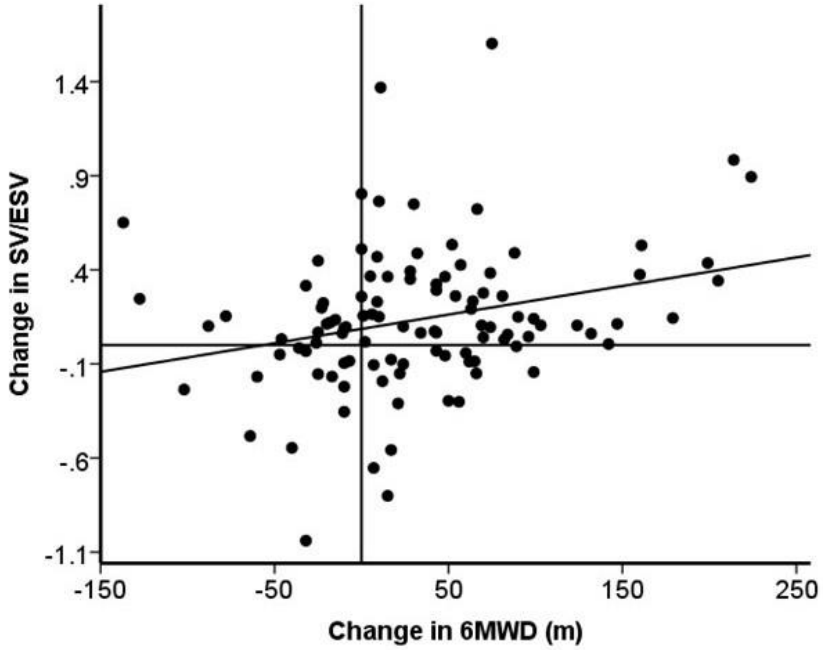

Figure 5.17 Correlation of change in SV/ESV with change in 6MWD.

Improvement in SV/ESV weakly correlated with 6MWD improvement, y = 0.09 + 1.52E-3x, r^2 = 0.074, p = 0.005

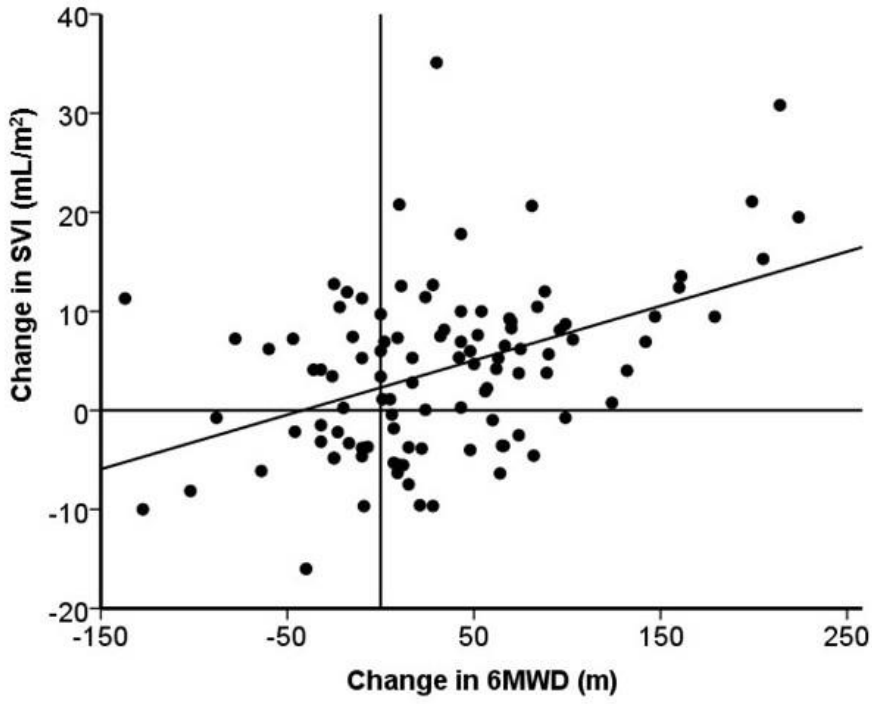

Figure 5.18 Correlation of change in stroke volume with change in 6MWD.

An increase in SVI was associated with increase in 6MWD, $y = 2.31 + 0.05x$, $r^2 = 0.195$, $p < 0.0001$

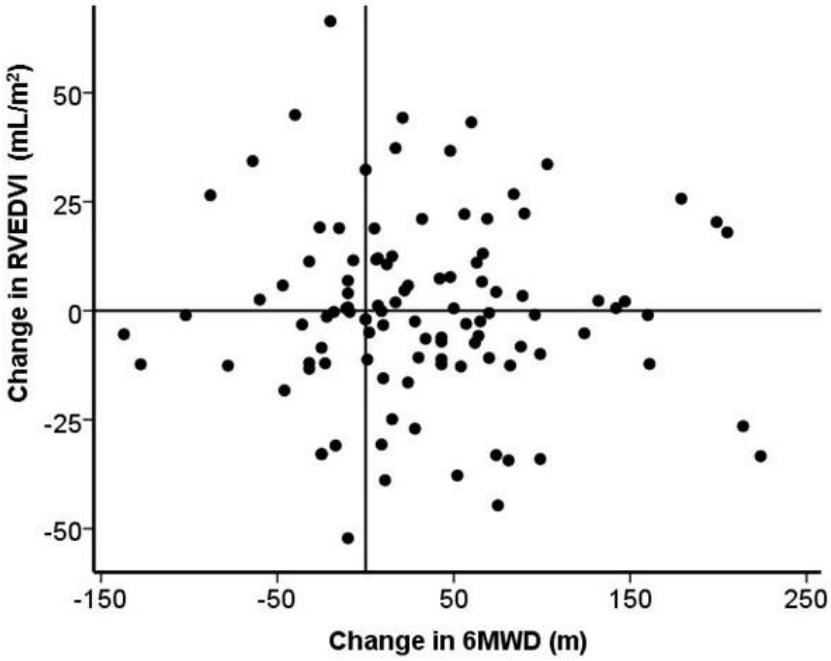

Figure 5.19 Change in 6MWD in comparison to change in RV end-diastolic volume.

No significant correlation was observed, r = -0.04, p = 0.682.

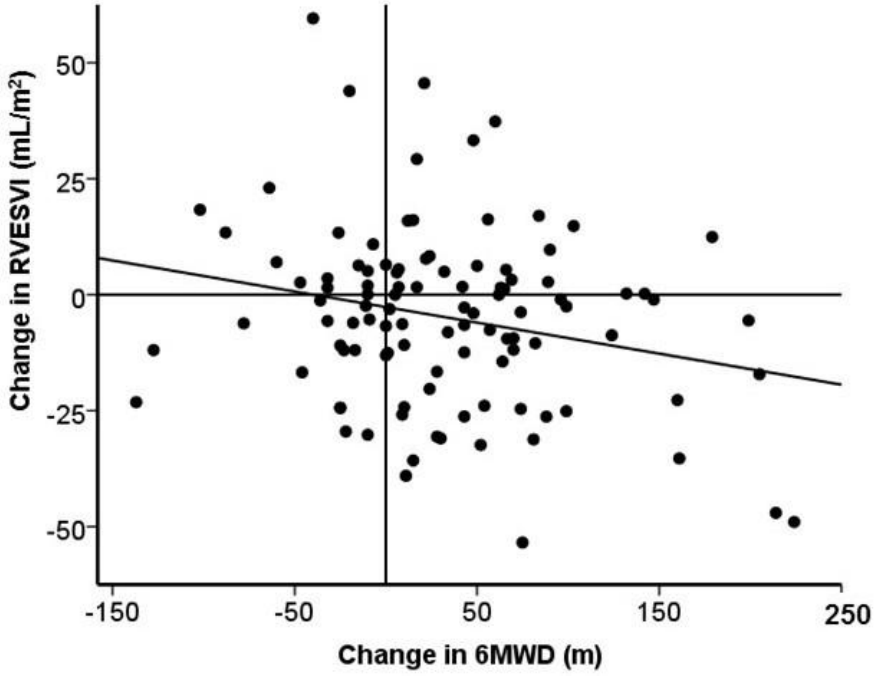

Figure 5.20 Correlation of change in RV end-systolic volume with change in 6MWD.

Weak relationship only seen, $y = -2.67 + -0.07x$, $r^2 = 0.06$, $p = 0.016$

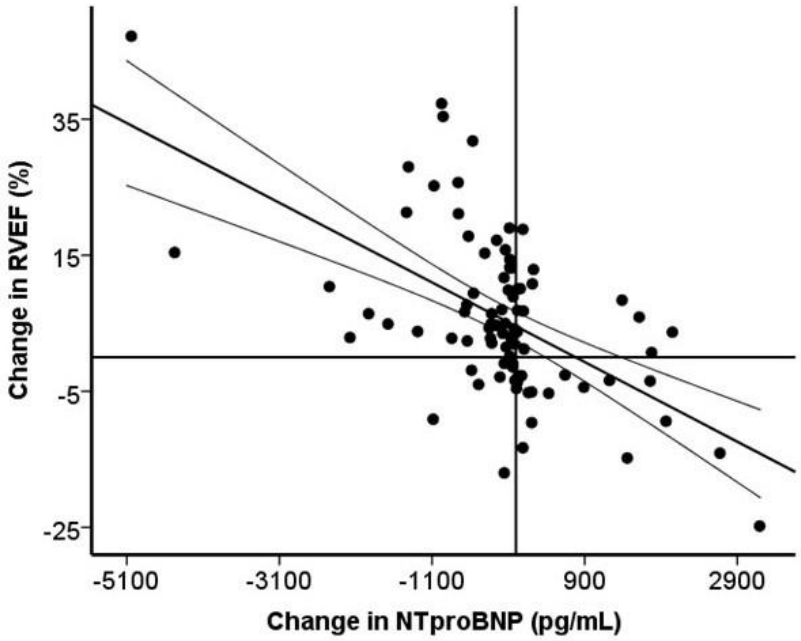

Figure 5.21 Correlation of change in RV ejection fraction with change in NTproBNP.

Falling RVEF strongly associated with increased NTproBNP, $y = 4.57 + -5.85E^{-3}x$, $r^2 = 0.324$, $p<0.0001$

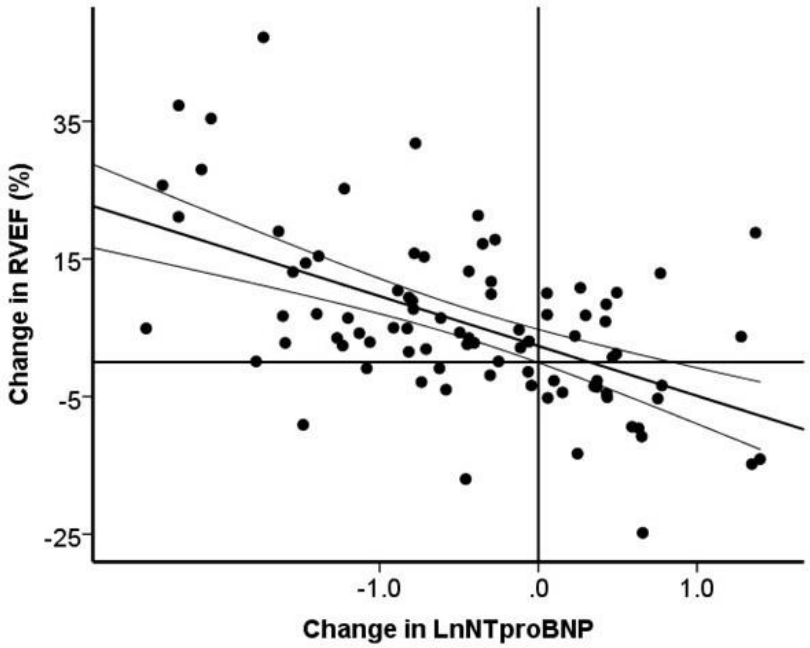

Figure 5.22 Correlation of change in RV ejection fraction with change in log transformation of NTproBNP.
$y = 2.35 + -5.42x$, $r^2 = 0.299$, $p<0.0001$.

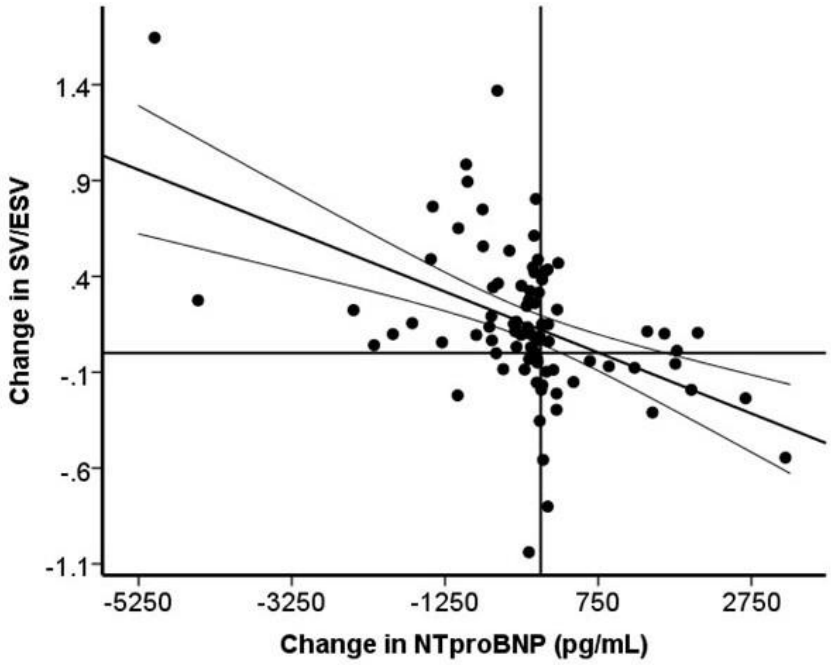

Figure 5.23 Correlation of change in SV/ESV with change in NTproBNP.

Fall in SV/ESV strongly associated with increase in NTproBNP, $y = 0.12 + -1.59E^{-4}x$, $r^2 = 0.220$, $p<0.0001$

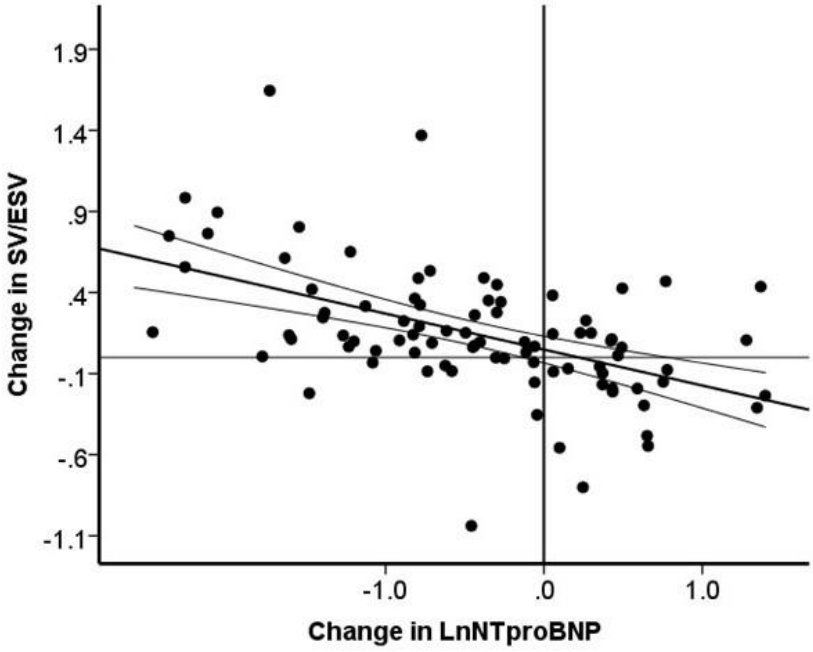

Figure 5.24 Correlation of change in SV/ESV with change in log transformation of NTproBNP

$y = 0.05 + -0.16x$, $r^2 = 0.255$, $p<0.0001$

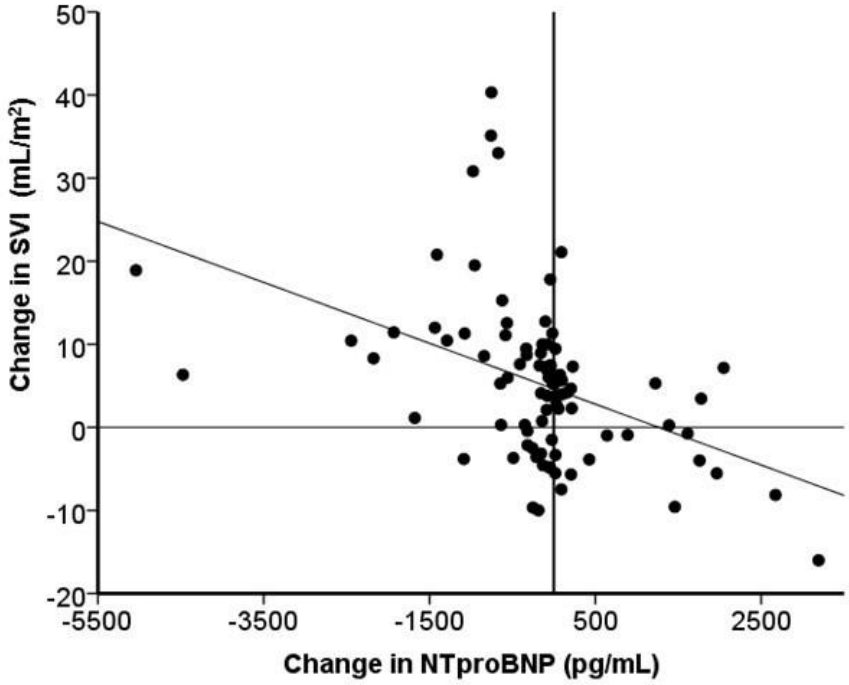

Figure 5.25 Correlation of change in stroke volume with change in NTproBNP.

$y = 4.62 + -3.66E^{-3}x$, $r^2 = 0.189$, $p < 0.0001$.

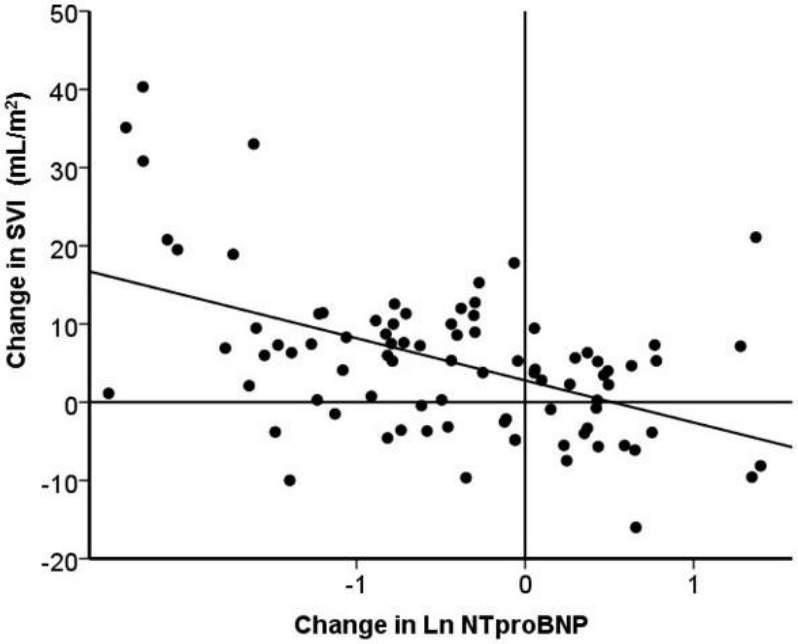

Figure 5.26 Correlation of change in stroke volume with change in log transformation of NTproBNP.

$y = 62.59 + -4.36x$, $r^2 = 0.248$, $p<0.0001$

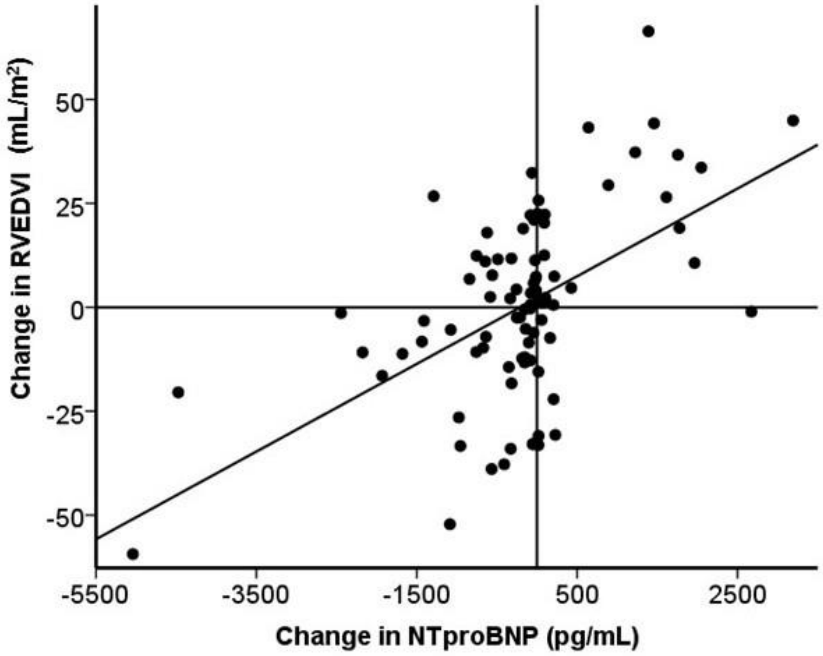

Figure 5.27 Correlation of change in RVEDVI with change in NTproBNP.

Increasing RV end diastolic volume associated with increase in NTproBNP, $y = 2.21 + 0.01x$, $r^2 = 0.297$, $p < 0.0001$

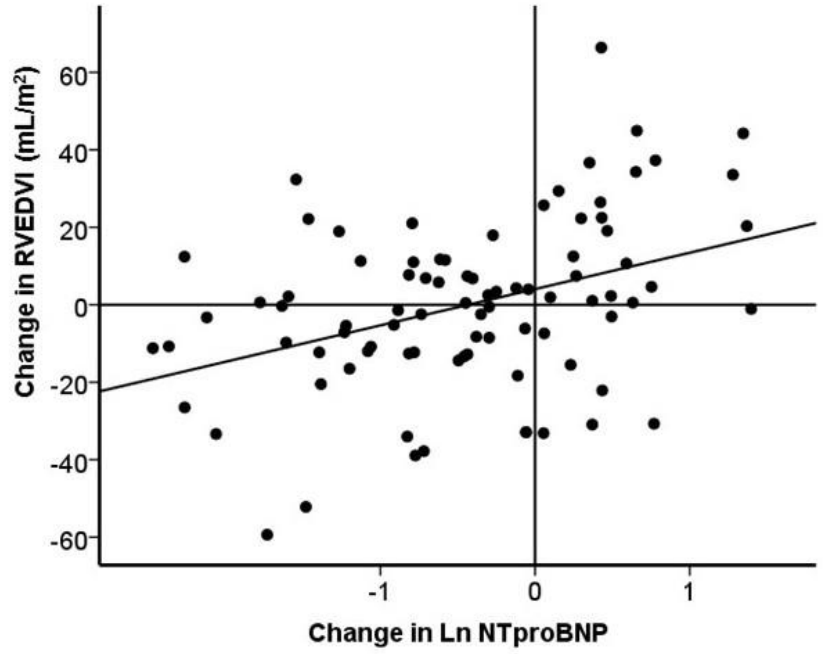

Figure 5.28 Correlation of change in RV end-diastolic volume with change in log transformation of NTproBNP.

$y = 3.57 + 6.18x$, $r^2 = 0.149$, $p<0.0001$

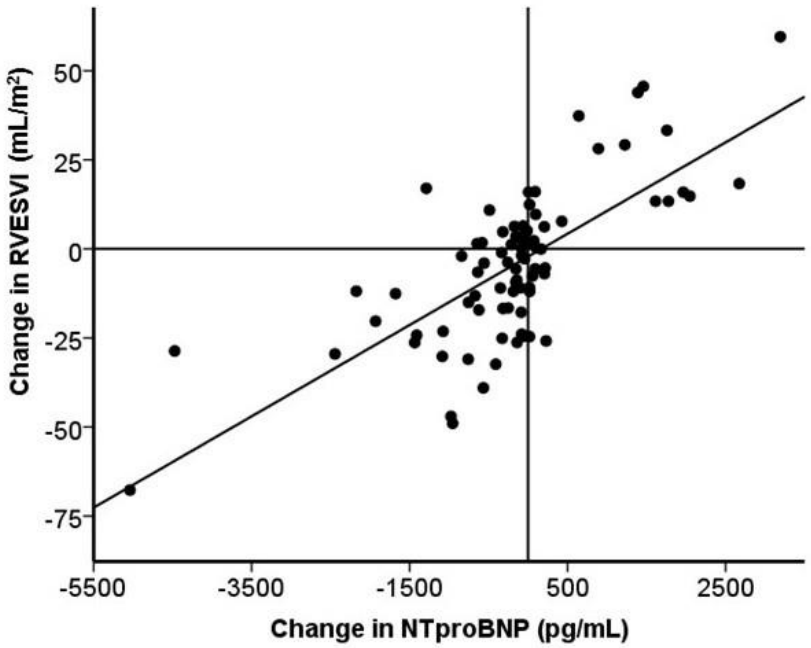

Figure 5.29 Correlation of change in RV end-systolic volume with change in NTproBNP.

Increasing RV end diastolic volume associated with increase in NTproBNP, $y = -2.14 + 0.01x$, $r^2 = 0.512$, $p<0.0001$

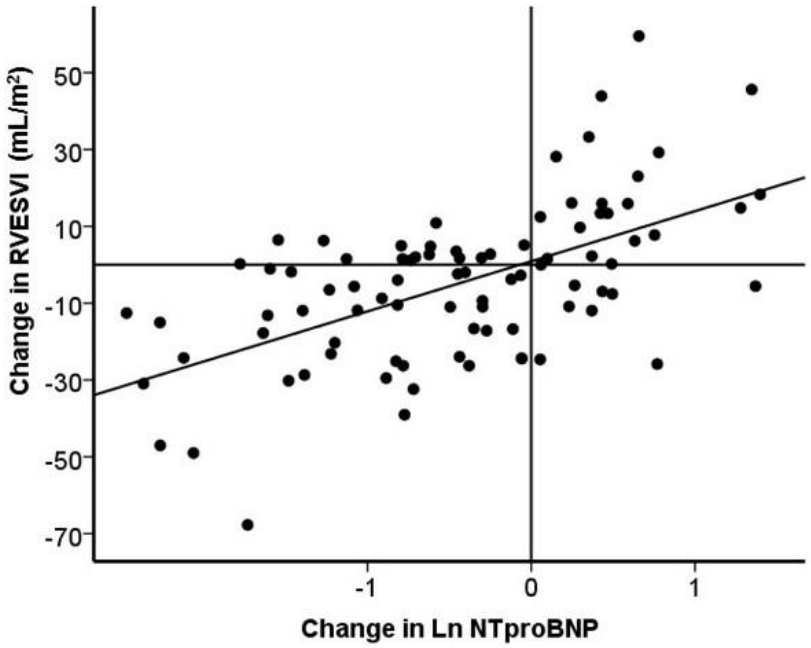

Figure 5.30 Correlation of change in RV end-systolic volume with change in log transformation of NTproBNP.

$y = 0.51 + 9.06x$, $r^2 = 0.337$, $p<0.0001$

5.4.4 Prognostic significance of change in RV function during PH therapy.

26 deaths (50%) and 1 lung transplantation occurred during the mean follow up period of 2626 days. A comparative analysis of survivors and non survivors after 5 years of follow up is shown in table 5-6. Survivors demonstrated greater improvement in 6MWD, NTproBNP and RVESVI.

There were 7 deaths (50%) in the cohort of 14 patients with a fall in 6MWD at follow up in comparison to 16/32 (50%) in those with a stable or increased 6MWD, mean estimated survival 1909 versus 2495 days respectively, logrank p = 0.176. Figure 5.31 displays the KM survival curve.

Patients with a decrease in NTproBNP showed a significantly improved outcome over those with an increase in levels, mean survival 2788 vs 1451 days, logrank p <0.001. 14/15 (93%) versus only 5/22 (23%) died during the follow up period. Figure 5.32 displays the KM survival curve.

Table 5-6 Comparative analysis of survivors and non survivors at 5 years according to change in RV indices, 6MWD and NTproBNP.

	Alive (n=29)	Deceased (n=17)	p value
ΔRVEF	5 (-3 – 9)	-3 (-9 – 9)	0.241
ΔSV/ESV	0.096 (-0.08 – 0.321)	-0.069 (-0.156 – 0.146)	0.328
ΔSVI	5 ± 9	2 ± 7	0.266
ΔRVEDVI	-0.5 ± 17	10 ± 21	0.062
ΔRVESVI	-5 ± 16	8 ± 20	0.026*
Δ6MWD	50 ± 61	-5 ± 72	0.015*
ΔNTproBNP	-130 (-615 – 51)	163 (-43 – 1458)	0.013*
Relative change in NTproBNP	-41 (-74 – 15)	21 (-26 – 66)	0.022*

Survivors displayed reduction in NTproBNP (expressed as either absolute or %change) and RV end-systolic volume and increase in 6MWD in comparison to non-survivors.

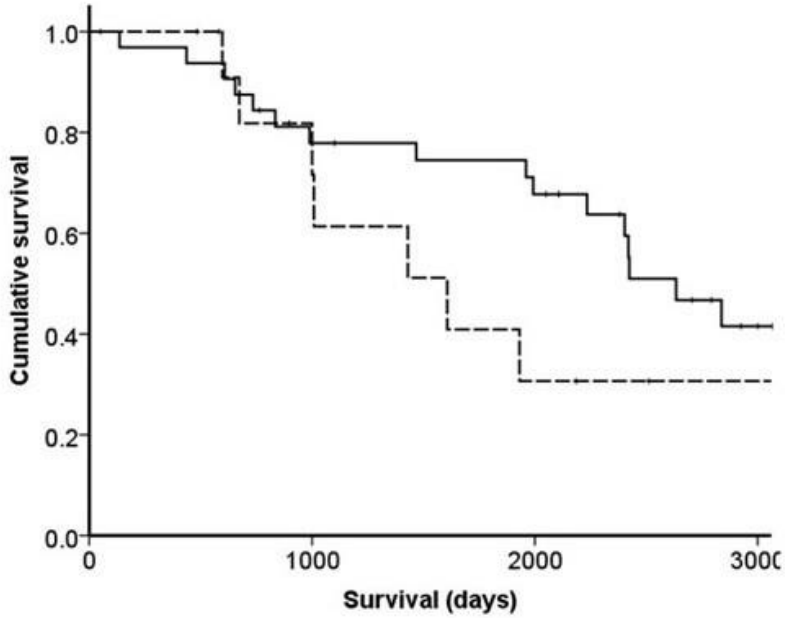

Patients at risk

Increase 6MWD	**32**	**24**	**20**	**7**
Decrease 6MWD	**14**	**8**	**3**	**1**

Figure 5.31 Kaplan Meier survival curve according to change in 6MWD after instigation of PH therapy.

No significant difference in outcome observed between those with stable/increase in 6MWD (n = 32, solid line) and those with decrease in 6MWD (n = 14, dashed line), logrank p = 0.176.

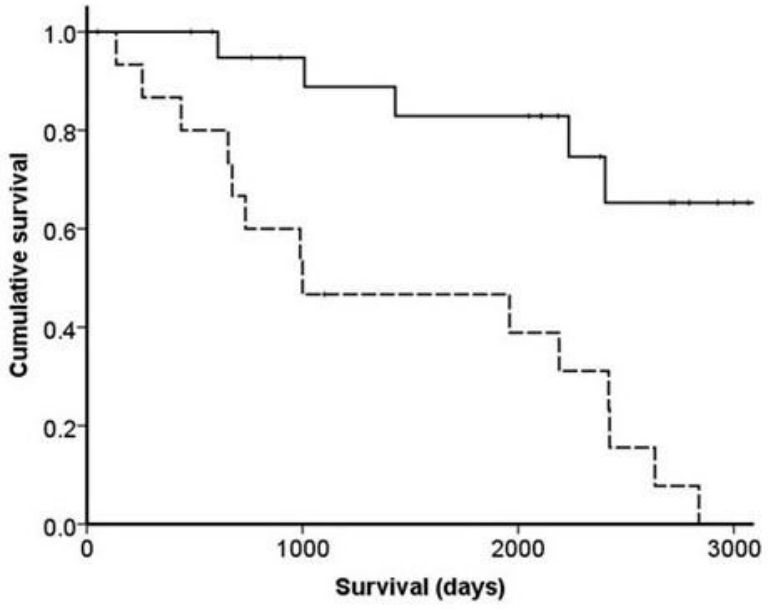

Patients at risk				
Decrease NTproBNP	22	16	14	3
Increase NTproBNP	15	8	5	0

Figure 5.32 Kaplan Meier survival curve according to change in NTproBNP after initiation of PH therapy.

Patients with reduction in NTproBNP levels (n = 22, solid line) showed improved survival in comparison to those with increasing levels (n = 15, dashed line), logrank p<0.0001.

15/18 (83%) patients with decrease in SV/ESV died in comparison to 12/34 (35%) with a stable or increased SV/ESV after initiation of PH therapy. Mean survival estimates 1594 versus 2704 days, p = 0.002. Figure 5.33 displays the KM survival curve. All patients with change in RV function according to SV/ESV displayed same increase or decrease in function according to RVEF (i.e. KM survival curve identical) defined by a ≥3% change (433).

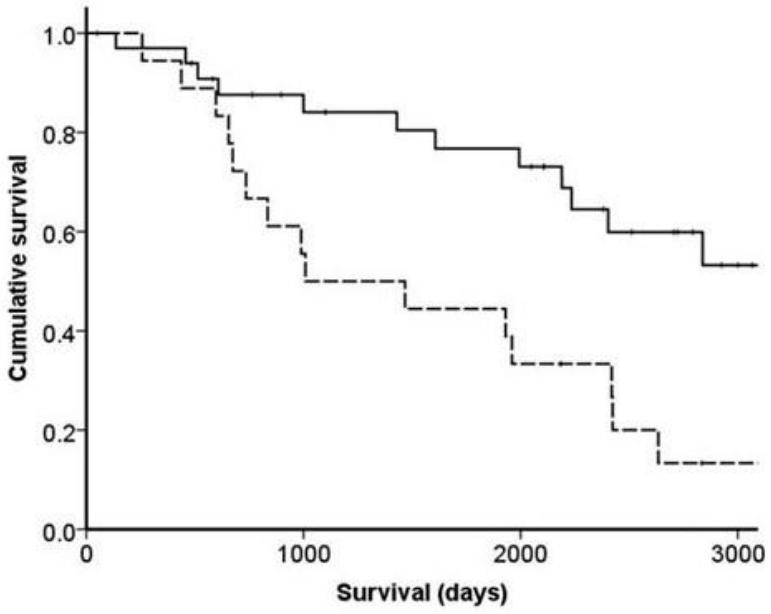

Patients at risk				
Increase/stable SV/ESV	34	25	20	7
Decrease SV/ESV	18	10	6	1

Figure 5.33. Kaplan Meier survival curve according to change in SV/ESV with PH therapy.

Decreased survival was demonstrated in those patients with a fall in SV/ESV (n = 18, dashed line) in comparison to those with a stable or increased in SV/ESV (n = 34, solid line). Logrank p = 0.002.

Increasing NTproBNP, RV volumes and decreasing SV/ESV, SVI, RVEF and 6MWD were associated with poorer outcome on univariate cox proportional hazards regression. Table 5-7 displays the hazard ratios for the analysis. On multivariate survival analysis with age and mPAP at diagnosis, ΔNTproBNP (HR 1.622 95%CI 1.066-2.468, p=0.024) and ΔRVESVI (HR 1.030 95%CI 1.010 – 1.050, p=0.003) but not Δ6MWD (HR 0.995 95% CI 0.990-1.001, p=0.129) remained independent predictors of outcome.

Table 5-7. Change in 6MWD, NTproBNP and indices of RV function to predict outcome.

	Univariate model		Multivariate model *	
	HR (95%CI)	p value	HR (95%CI)	p value
ΔRVEF	0.949 (0.920 – 0.979)	0.001		
ΔSV/ESV	0.316 (0.166 – 0.604)	<0.001		
ΔSVI	0.959 (0.925 – 0.994)	0.023		
ΔRVEDVI	1.020 (1.006 – 1.034)	0.004		
ΔRVESVI	1.032 (1.016 – 1.047)	<0.001	1.030 (1.01 – 1.05)	0.003
Δ6MWD	0.994 (0.989 – 0.999)	0.016	0.995 (0.990 – 1.001)	0.129
ΔNTproBNP	2.125 (1.452 – 3.111)	<0.001	1.622 (1.066 – 2.468)	0.024

Univariate and multivariate (with age and mPAP at diagnosis) cox proportional hazards regression. Increasing ΔRVESVI and ΔNTproBNP predictive of poorer survival..

5.4.5 Change in vascular stiffness (RAC MPA) as an outcome measure

At diagnosis, PVR negatively correlated with RAC MPA, r = -0.350, p = 0.013 (n = 50) suggesting RAC was reasonable measure of RV afterload in this population. 108 ΔRAC values were calculated from 47/50 patients with serial measurements. Median ΔRAC -0.20% (range -23 to +42 %). ΔRAC did not correlate with Δ6MWD (n = 90, r = 0.173, p = 0.104) nor change in RV function, ΔRVEF (r = 0.169, p = 0.081), ΔSV/ESV (r = 0.174, p = 0.072).

ΔRAC did not predict survival on univariate cox proportional hazards regression, HR 0.992 95%CI 0.971 – 1.013, p = 0.444. There was no associated improvement in survival in those whom improved RAC (n = 21) in comparison to those with further decrease in RAC (n = 26) after PH therapy, logrank p = 0.917. Figure 5.34 displays the Kaplan Meier survival curves.

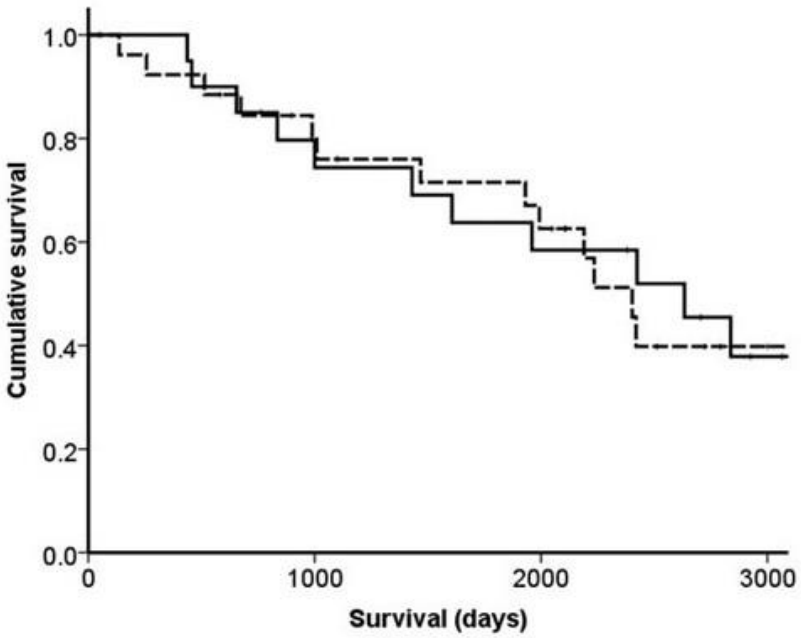

Patients at risk				
Increase RAC	21	14	11	4
Decrease RAC	26	19	14	3

Figure 5.34. Kaplan Meier survival plot according to those with improved RAC MPA in comparison to those with further fall during PH therapy.

No significant difference in survival was observed in those with improved (increase) in RAC (n=21, solid line) versus further decrease (n=26, dashed line), 1 year and 3 year survival 100 versus 92 % and 74 versus 76% respectively, logrank p = 0.917.

5.5 Discussion

The results described by this chapter show improvement in RV-arterial coupling determined by the volume method SV/ESV with PAH therapy, and poorer survival in those patients with a further fall during therapy. In agreement with previous studies, improvement in RVEF and SV but not RV volumes or mass was also seen. These results confirm previous studies that parameters of RV dysfunction obtained at diagnosis and monitoring of those same variables (i.e. NTproBNP, RV ejection fraction and volumes) have prognostic significance in the evaluation of patients with PAH undergoing drug therapies. Additionally, changes in NTproBNP were shown to more closely parallel changes in RV volumes and systolic function than 6MWD in patients undergoing PH therapy and independently predict survival.

5.5.1 Determining change in RV function and afterload with CMR

PAH specific therapies in current clinical use target one of three pathways involved in vascular remodelling and vasoreactivity of the pulmonary vasculature resulting in a reduction in PVR. As already discussed, progressive RV dysfunction however may occur despite this decrease in PVR. In early PAH, with largely preserved RV function and cardiac output, this reduction in PVR results in a fall in mPAP (as PVR equals mPAP-PAWP/CO) and therefore RV power output (CO x mPAP). In severe PH where RV dysfunction and failure has already ensued, therapeutic fall in PVR will translate to improvement in CO rather than fall in mPAP and therefore no change in RV work and little/no beneficial impact on the RV. Recent meta-analysis looking at pump function across clinical trials demonstrated that PAH specific therapies whilst reducing PVR and leading to reduction in mPAP and increase in SV are not associated with increase in contractility suggesting these therapies have predominantly vasodilatory and little or no cardiac specific effects (331). The results here show increase in SVI with therapy, but no improvement in RAC MPA with PH therapy, and no relationship to outcome in those with increased RAC (i.e. improved vascular stiffness). Due to the inverse hyperbolic relationship between compliance and PAP, by the time mPAP rises to diagnostic threshold compliance has reached plateau. This may explain a lack of effect seen with PH therapy in RAC, and the lack of significance of ΔRAC as a prognostic variable. Perhaps the utility of assessing RAC MPA lies in screening at risk populations for early pulmonary vascular disease where large falls in RAC

(or SV/PP) with minimal rise in PVR or mPAP as shown in chapter 3 for lung disease patients with PH. Further fall in either SV/ESV or RVEF however was associated with worse survival, but there was no prognostic advantage of SV/ESV over RVEF. This again suggests in agreement previous studies that outcome measures to assess improvements in RV function rather than afterload with PAH therapy are of more prognostic significance. In the situation where CMR is not readily available for this purpose, the closer relationship to NTproBNP suggests this is a more suitable measure for the clinic than 6MWD, which showed some relationship to SV, but poor (or contradictory relationship as 6MWD positively correlated with increased RVEDVI) relation to RVEF.

Whilst RVEF at baseline was a strong predictor of outcome as shown in chapter 4 and further fall during therapy was associated with poorer survival, ΔRVESVI but not ΔRVEF was an independent predictor of outcome. This may reflect the small change in RVEF observed (median 4%), although range showed considerable variation around this. RV ejection fraction is both a composite measure and preload dependent measure of RV systolic function, and perhaps use of ΔRVEF lacks sensitivity whilst increasing ΔRVESVI suggests declining contractility and is less preload affected. ΔSV/ESV which is proposed as less preload dependent did not perform superiorly in this study however.

5.5.2 Significance of change in NTproBNP during PAH therapy

Levels of NTproBNP (and BNP) have been shown to inversely correlate with RVEF and cardiac output, and correlate with mPAP, RAP, RVM and total pulmonary vascular resistance in PAH (297, 298). Changes in levels have been shown to parallel haemodynamics and functional status of PAH patients during treatment, and relative change in NTproBNP reflect relative change in CMR indices of RV structure and systolic function. High NTproBNP levels or in particular increasing levels during follow up have been shown to be independent predictors of mortality (299-301). The results described here add to the growing evidence in the literature that biomarkers such as NTproBNP are strong prognostic variables in PAH and reflect RV function, with increasing levels indicative of increasing RV volumes and reduction in systolic function. Additionally, in agreement with the recent study by Nickel et al (283), the results here show that ΔNTproBNP is an independent predictor of outcome in patients undergoing PH therapy, and potentially a superior

outcome measure than Δ6MWD. Increasing ΔRVESVI was also an independent predictor of outcome. However serial NTproBNP measurements have the added benefit of being readily obtained and monitored in a clinical outpatient setting unlike cardiac MRI indices of RV function.

5.5.3 Significance of change in 6MWD during PAH therapy

6MWD is known to correlate with peak oxygen pulse (which in turn correlates to SV and therefore indirectly RV function), CO and total pulmonary resistance, and to fall in proportion to worsening FC in PAH (290). Data in the literature is limited on the relationship between change in RV function and change in 6MWD during therapy. In patients with pulmonary hypertension of varying aetiology, 6MWD has been shown to correlate with SVI but not to RV ejection fraction or volume (434). Improved RV stroke volume with Epoprostenol therapy has been shown to relate to improved 6MWD in one small study, with the most significant increase in SV occurring in the first 4 months (302). In a small clinical study of Bosentan treated PAH patients, 6MWD improved more in those with an increase in RVEF in comparison to those with a stable or decreased RVEF (+98 vs -37 m, p = 0.01) (326). Other clinical studies have not however correlated functional improvement with improvement in haemodynamic parameters. 6MWD has several important limitations as an outcome measure. As discussed in section 1.2.5.3 6MWD is influenced by a number of confounders including patient motivation, age, weight and comorbidity. A recent study looking at utility of exercise variables including 6MWT to predict outcome in IPAH versus associated PAH found whilst distance walked was of significance in those with IPAH this was not the case in patients with PAH associated with other aetiology such as connective tissue disease where one would expect limitations related to other factors such as degree of musculoskeletal disease (292). Additionally, a ceiling effect may occur whereby in those with greater baseline walk distance treatments that improve haemodynamics and symptoms may not translate into further additional significant increment in distance walked (295). All of these studies provide explanations for the poorer or even lack of correlation described here between absolute or Δ6MWD with absolute or ΔRVEF and ΔSVI.

At diagnosis, lower 6MWD, between 250 – 332 m, have been shown to predict poor survival in IPAH patients (286, 290, 435). Improvement in absolute 6MWD above

380m after 3 months of PH therapy has been shown to confer improved survival, but prognostic significance of a change in 6MWD has not been consistently demonstrated (430, 436). A pooled analysis of 10 placebo controlled drug trials in PAH found that Δ6MWD accounted for only 22.1% of the treatment effect (291), with a calculated minimum of 41.8m corresponding to a significant reduction in clinical events. These studies however are confounded by select population for trial entry including a threshold minimum distance walked. The patients described in this chapter reflect treatment in a real life clinical setting, but in agreement with previous meta-analyses did not find Δ6MWD to independently predict outcome.

5.5.4 Differential effects of PDE-5i and ETRA therapy on RV function

The results described here suggest the possibility of greater improvement in RV function (assessed by either RVEF or SV/ESV) with PDE-5i than ETRAs. This would be in agreement with pre-clinical studies in animal models which have raised the possibility of direct myocardial effects with improvement in contractility with PDE-5i but not ETRAs (429). The conclusions that can be drawn from this study however are limited due to the retrospective nature of the study, so whilst characteristics of groups were similar this effect would be better examine in case matched prospective manner. More patients received PDE-5i than ETRAs which could bias the statistical analysis. Differential effects of class of PAH therapy on RV function would be important to evaluate further, as it would provide evidence for need of patient tailored therapy, such as combination therapy or PDE-5i in those with RV dysfunction at diagnosis.

5.5.5 Limitations

This was a single centre retrospective observational study. 6MWD and NTproBNP levels included for the study were obtained within 1 month of MRI measurements. Data on renal function was not collected and therefore unable to examine the potential influence of fluctuations in renal function on NTproBNP levels. Despite these limitations, correlations between 6MWD and NTproBNP with RV indices were comparable to previous work (431, 434).

5.6 Conclusion

Both SV/ESV and RVEF are improved by PAH therapies. Further fall in SV/ESV during PAH therapy is associated with poorer survival, but this measure of RV function offers no additional prognostic value over RVEF in this study. Both absolute and ΔNTproBNP more closely reflect changing RV function and volume than 6MWD in patients undergoing PH therapies. ΔNTproBNP but not Δ6MWD is an independent predictor of outcome and is an attractive readily accessible method for monitoring RV function in a clinic setting.

Chapter 6 - General Discussion and Conclusions.

6.1 Background

Whilst the initial insult in PAH involves progressive vasculopathy of the pulmonary circulation, survival is determined by RV adaptation to the increased afterload that occurs, with patients ultimately dying of RV failure. Factors that influence this adaptation are complex, and include not only the severity of pulmonary vascular disease but rate of onset of PH, underlying disease aetiology, genetics, inflammation, neurohormonal activation, coronary perfusion and myocardial metabolism. RV afterload is a complex interplay of resistance, compliance and wave reflection and whilst commonly quoted measures of PVR are employed clinically, this assesses only part of this afterload, perhaps described better by effective arterial elastance (E_a). We know from the literature that reduction in afterload (defined by PVR) is not indicative of improved outcome in the face of continued RV dysfunction, and indeed further fall in RVEF despite improved PVR is associated with poorer survival.

Given the importance of the right ventricle in PAH, preservation and improvement of RV function should be an important goal of PH therapy, but to date there is little data on the effect of these treatments on RV function and contractility, and whether one therapy has benefits over another in the setting of RV dysfunction. Simple, reproducible noninvasive measures of RV function may help establish the optimal therapeutic approach to RV dysfunction and improve management of PAH patients. At present it is unclear what the optimal method of assessing RV function is, with hemodynamic studies demonstrating the predictive value of RAP and CI (142, 269), echocardiography studies indicating the value of TAPSE and pericardial effusion (272, 437), CMR studies highlighting predictive value of RVEF, RV volumes and SV (41), and finally the biomarker NTproBNP (299, 300) or 6MWD have been linked to RV function and prognosis. Additionally recent research interest has focused on RV-arterial coupling, a measure of RV contractility in the context of the pulmonary vascular load which ideally requires instantaneous pressure and volume measurement determined invasively at increasing levels of preload, which therefore has limited clinical application at the bedside. From physiological

principles this measure has advantages over other commonly quoted measures of RV function and may be a superior metric to monitor RV function in patients undergoing therapy. CMR can be used to estimate RV-arterial coupling by the ratio of SV to RV ESV, which is a more attractive modality for clinical use.

Whilst the prognostic significance of RV dysfunction in PAH is well established in the literature, less study has focussed on the importance of RV dysfunction in PH associated with lung disease, and the utility of imaging the RV with CMR or monitoring indirect markers of RV dysfunction such as NTproBNP may be of use in a disease where development of PH is associated with significant morbidity and mortality, and treatment options other than transplantation or supplementary oxygen provision, non-existent.

6.1.1 Limitations of current methods employed to assess RV function and treatment response in PAH

Right heart catheterisation is essential for the diagnosis of PAH, but invasive in nature and a small but real risk of complications limits its use as a regular follow up tool to monitor the patient during treatment. Over 20 different echocardiography parameters of RV structure and function have been identified, with several linked to prognosis in PAH (438). As discussed in section 1.1.2 however, the complex structure and contractile pattern of the RV is less well suited to accurate measurement using 2D methodology, and particularly in PAH after onset of RV dilatation and dysfunction, systolic function is less representative by TAPSE due to presence of increasing TR and importance of transverse shortening in RV ejection. In addition, the technique is operator dependent, lacks standardised models for determination of volume or ejection fraction and may be difficult to interpret in clinical situations such as lung disease or obesity. Despite this, echo is readily available, inexpensive and safe and therefore likely to remain an important modality for both detecting PH, and assessing the RV. The development and validation of new methods including research field of 3D echo may address some of these limitations in the future.

As discussed in section 1.2.5.3 6MWT is commonly employed in the clinic and as endpoint in clinical drug trials to assess both functional status but also indirectly RV function due to its relationship with V02max and CO. 6MWD is known to relate

to survival (290), but change in 6MWD does not consistently relate to outcome. Furthermore, relationship to RV EF has not been demonstrated and distance walked is also influenced by a number of factors such as patient co-morbidity or effort.

The biomarker NTproBNP, as discussed in section 1.2.5.4, is known to correlate with RV volumes and falling RVEF, and change in levels reflects change in RV structure during therapy (297). Additionally, high levels are associated with poorer prognosis (300). Levels are affected by LV dysfunction, renal clearance and age, and it is uncertain what constitutes a validated threshold for increased risk from current literature. It is however easy to monitor in an outpatient setting.

6.1.2 Potential advantages of cardiac MRI as a clinical outcome measure

The advantages of CMR in assessing RV structure and function were described in detail in section 1.3. It is regarded in the literature as the gold standard method for assessing the RV due to high inter and intra observer reproducibility, and 3D modality is better suited to complex morphology of the RV. RV dilatation, low SV and RVEF have all been shown to predict poor outcome in PAH, with further decline during therapy particularly associated with poorer survival (41, 288).

Furthermore, this modality offers the opportunity to study the RV-pulmonary circulation as a unit, with flow measurements in the great vessels also available. RV-arterial coupling represents matching of RV adaptation to the increased afterload that occurs in PAH. As discussed in detail in section 1.1.4.3 it is possible to assess this using CMR as SV/ESV ratio. This method of assessing RV function, particularly during the monitoring of patients undergoing PAH therapy, should be superior based on physiological reasoning to the commonly employed RVEF as it is less preload dependent.

CMR imaging is expensive and not readily available in all PH centres. The advantages described above, and the non-invasive nature make this an attractive modality to employ in monitoring of patients and is likely more acceptable to the patient.

6.2 Imaging right ventricular dysfunction in pulmonary hypertension

The aims of this thesis were to identify the optimal non-invasive method of monitoring RV dysfunction in PAH where treatment is clearly established, and contrast this to PH in chronic lung disease where the right ventricular characteristics, particularly with regard to severe or "disproportionate" PH has not been previously well studied with CMR.

In chapter 3 CMR imaging demonstrated that in PH associated with lung disease RV function is preserved, however in severe PH/lung disease (defined as mPAP ≥ 35mmHg) RV dysfunction is prevalent and shows similar characteristics to IPAH patients. This RV dysfunction strongly relates to prognosis, and a reduction in NTproBNP and improvement in 6MWD was seen with PAH targeted therapy. Previous trials of PAH therapy in group 3 disease has not focussed on treating severe PH phenotype, which may explain lack of treatment response reported previously in the literature (340, 342, 343). Additionally, CMR indices of PA stiffness or RVM performed well as screening tools to detect PH associated with lung disease where echocardiography to estimate sPAP may be difficult due to poor acoustic windows that often result in hyperinflated lung disease patients.

In chapter 4 we saw that RV-arterial coupling assessed by either the pressure (E_{es}/E_a-P) or volume (SV/ESV) method was reduced in PH in comparison to normal subjects. Those with severe PH associated with lung disease potentially had disproportionately worse RV adaptation in comparison to PAH subjects (assessed by E_{es}/E_a-P in this chapter, and by higher NTproBNP, lower RV mass in chapter 3) which may be a potential explanation (in addition to the lung disease) for the significantly worse survival in this group. There was no advantage of SV/ESV over RVEF in predicting survival (although arguably the p-value was stronger for SV/ESV) suggesting despite physiological reasoning that SV/ESV is a superior metric of RV function, that either can be employed to determine outcome. Invasive measurements of E_{es}/E_a-P or RAP/CI had no prognostic advantage over CMR imaging of RV function.

In Chapter 5 we saw improvement in RV-arterial coupling (assessed by SV/ESV) with PH therapy, and in agreement with previous studies improvement in other

indices of RV function, RVEF and SV. Deterioration in either measure of RV systolic function SV/ESV or RVEF during therapy was associated with worse outcome, with nether variable having prognostic advantage. NTproBNP closely related to change in RV function, whilst 6MWD did not, and change in NTproBNP but not 6MWD related to outcome, which was also seen in chapter 3 in patients with severe PH/lung disease.

These studies suggest that CMR imaging of RV function, or use of NTproBNP in the clinic, in either PAH or severe PH/lung disease patients has the strongest prognostic benefit in monitoring patients undergoing therapy. Invasive haemodynamics or estimates of RV-arterial coupling had no additional prognostic advantage. 6MWD, whilst a good measure of functional limitation, performed inferiorly as an outcome measure in both pulmonary arterial disease, but also in a treated population with severe PH and chronic lung disease, and poorly related to RV function. This has implications in terms of endpoints for clinical trials where RV imaging is not commonly employed as an outcome measure of treatment efficacy, and in the clinic where NTproBNP can be readily employed to monitor RV response to therapy.

6.3 Future directions.

In the past the right heart was largely ignored by researchers or clinicians in cardiopulmonary fields. In 2006, the National Heart, lung and Blood Institute identified RV physiology as a priority in cardiovascular research (439). It is now increasingly evident the fundamental role the right heart plays in cardiopulmonary performance in not only pulmonary hypertension, but in normal subjects and those with left heart or intrinsic right heart disease. Future treatment advances in pulmonary hypertension will not only depend on development of drugs to target the molecular pathways involved in pulmonary vascular remodelling, but for the reasons drawn together in this thesis, recognise that the RV is an important therapeutic target in its own right.

In chapter 3 we saw that RV performance is of equal significance in severe pulmonary hypertension related to lung disease as it is in IPAH, and is a potential focus for research in therapies for this poorly studied disease. Significant increase in SV was demonstrated in this small cohort, which has not been shown in previous

studies of haemodynamic response to pulmonary vasodilators in chronic lung disease with mild-moderate PH (340, 349) and may explain why an increase in 6MWD was seen in this study and not consistently in previous studies of mixed (or even no) severity of associated PH. Future study on the role of pulmonary vasodilators in severe PH/lung disease could focus on improvement in RV performance as an outcome, rather than 6MWD which will also be hampered by ventilatory limitation, and whether if such an improvement is demonstrated this translates to improved survival. Additionally, the results in both chapter 3 and 4 suggest impaired RV adaptation to increased afterload in severe PH/chronic lung disease in comparison to PAH which would be better addressed in a case matched prospective study.

The work described in chapter 5 may support differential effects of PH therapies ETRAs and PDE-5i on RV function. This avenue is of interest in light of recent study AMBITION where up front combination therapy at diagnosis was associated with improved outcome (440). Focussing future research on pharmacological effects of these therapies on RV function may lead to better understanding of therapy regimes for those with RV dysfunction. Pre and post therapy studies combining RHC and CMR to determine E_{es} by the single beat method may address differential effects on RV contractility between drug classes.

This work clearly shows that RV function is strongly linked to outcome in both PAH and lung disease PH, and that improvement in 6MWD, the most commonly employed outcome measure in current PAH therapy clinical trials, does not necessarily translate in to improved survival nor reflect RV function. Future clinical trials of pulmonary vasodilator therapy should also include RV specific functional outcomes, and either SV/ESV or RV ejection fraction determined by CMR is an attractive non-invasive endpoint.

6.4 Conclusions.

This thesis demonstrates the strong prognostic significance of RV function assessed by CMR imaging by either RV-arterial coupling (SV/ESV) or ejection fraction in both PAH and severe PH complicating chronic lung disease. Equal focus on RV function in addition to pulmonary vascular disease is therefore critical in determining clinical response and development of therapeutic avenues.

List of References

1. Naeije R. Physiology of the pulmonary circulation and the right heart. Curr Hypertens Rep. 2013 Dec;15(6):623-31.
2. Cope DK, Grimbert F, Downey JM, Taylor AE. Pulmonary capillary pressure: a review. Crit Care Med. 1992 Jul;20(7):1043-56.
3. Greyson CR. The right ventricle and pulmonary circulation: basic concepts. Rev Esp Cardiol. 2010 Jan;63(1):81-95.
4. Krenz GS, Dawson CA. Flow and pressure distributions in vascular networks consisting of distensible vessels. Am J Physiol Heart Circ Physiol. 2003 Jun;284(6):H2192-203.
5. Reeves JT, Linehan JH, Stenmark KR. Distensibility of the normal human lung circulation during exercise. Am J Physiol Lung Cell Mol Physiol. 2005 Mar;288(3):L419-25.
6. Argiento P, Vanderpool RR, Mule M, Russo MG, D'Alto M, Bossone E, et al. Exercise stress echocardiography of the pulmonary circulation: limits of normal and sex differences. Chest. 2012 Nov;142(5):1158-65.
7. Naeije R, Vanderpool R, Dhakal BP, Saggar R, Vachiery JL, Lewis GD. Exercise-induced pulmonary hypertension: physiological basis and methodological concerns. Am J Respir Crit Care Med. 2013 Mar 15;187(6):576-83.
8. Saouti N, Westerhof N, Postmus PE, Vonk-Noordegraaf A. The arterial load in pulmonary hypertension. Eur Respir Rev. 2010 Sep;19(117):197-203.
9. Sniderman AD, Fitchett DH. Vasodilators and pulmonary arterial hypertension: the paradox of therapeutic success and clinical failure. Int J Cardiol. 1988 Aug;20(2):173-81.
10. Milnor WR, Conti CR, Lewis KB, O'Rourke MF. Pulmonary arterial pulse wave velocity and impedance in man. Circ Res. 1969 Dec;25(6):637-49.
11. Syyed R, Reeves JT, Welsh D, Raeside D, Johnson MK, Peacock AJ. The relationship between the components of pulmonary artery pressure remains constant under all conditions in both health and disease. Chest. 2008 Mar;133(3):633-9.
12. Chemla D, Castelain V, Humbert M, Hebert JL, Simonneau G, Lecarpentier Y, et al. New formula for predicting mean pulmonary artery pressure using systolic pulmonary artery pressure. Chest. 2004 Oct;126(4):1313-7.

13. Yock PG, Popp RL. Noninvasive estimation of right ventricular systolic pressure by Doppler ultrasound in patients with tricuspid regurgitation. Circulation. 1984 Oct;70(4):657-62.

14. Lankhaar JW, Westerhof N, Faes TJ, Gan CT, Marques KM, Boonstra A, et al. Pulmonary vascular resistance and compliance stay inversely related during treatment of pulmonary hypertension. Eur Heart J. 2008 Jul;29(13):1688-95.

15. Lankhaar JW, Westerhof N, Faes TJ, Marques KM, Marcus JT, Postmus PE, et al. Quantification of right ventricular afterload in patients with and without pulmonary hypertension. Am J Physiol Heart Circ Physiol. 2006 Oct;291(4):H1731-7.

16. MacKenzie Ross RV, Toshner MR, Soon E, Naeije R, Pepke-Zaba J. Decreased time constant of the pulmonary circulation in chronic thromboembolic pulmonary hypertension. Am J Physiol Heart Circ Physiol. 2013 Jul 15;305(2):H259-64.

17. Pagnamenta A, Vanderpool R, Brimioulle S, Naeije R. Proximal pulmonary arterial obstruction decreases the time constant of the pulmonary circulation and increases right ventricular afterload. J Appl Physiol (1985). 2013 Jun;114(11):1586-92.

18. Naeije R, Melot C, Mols P, Hallemans R. Effects of vasodilators on hypoxic pulmonary vasoconstriction in normal man. Chest. 1982 Oct;82(4):404-10.

19. Melot C, Naeije R, Hallemans R, Lejeune P, Mols P. Hypoxic pulmonary vasoconstriction and pulmonary gas exchange in normal man. Respir Physiol. 1987 Apr;68(1):11-27.

20. Maggiorini M, Melot C, Pierre S, Pfeiffer F, Greve I, Sartori C, et al. High-altitude pulmonary edema is initially caused by an increase in capillary pressure. Circulation. 2001 Apr 24;103(16):2078-83.

21. Naeije R. Pulmonary vascular function. In: Peacock AJ NRRL, editor. Pulmonary Circulation. 3rd ed: Hodder Arnold; 2011.

22. Granath A, Jonsson B, Strandell T. Circulation in Healthy Old Men, Studied by Right Heart Catheterization at Rest and during Exercise in Supine and Sitting Position. Acta Med Scand. 1964 Oct;176:425-46.

23. Granath A, Strandell T. Relationships between Cardiac Output, Stroke Volume and Intracardiac Pressures at Rest and during Exercise in Supine Position and Some Anthropometric Data in Healthy Old Men. Acta Med Scand. 1964 Oct;176:447-66.

24. Kovacs G, Berghold A, Scheidl S, Olschewski H. Pulmonary arterial pressure during rest and exercise in healthy subjects: a systematic review. Eur Respir J. 2009 Oct;34(4):888-94.

25. West JB, Dollery CT, Naimark A. Distribution of Blood Flow in Isolated Lung; Relation to Vascular and Alveolar Pressures. J Appl Physiol. 1964 Jul;19:713-24.

26. von Euler US LG. Observations on the pulmonary arterial blood pressure in the cat. Acta Physiol Scand. 1946;12:301-20.

27. Weir EK, Archer SL. The mechanism of acute hypoxic pulmonary vasoconstriction: the tale of two channels. FASEB J. 1995 Feb;9(2):183-9.

28. Hillier SC, Graham JA, Hanger CC, Godbey PS, Glenny RW, Wagner WW, Jr. Hypoxic vasoconstriction in pulmonary arterioles and venules. J Appl Physiol (1985). 1997 Apr;82(4):1084-90.

29. Olschewski O. Hypoxic pulmonary vasoconstriction and hypertension. In: Peacock AJ NRRL, editor. Pulmonary Circulation. Third ed: Hodder Arnold; 2011. p. 46-58.

30. Sommer N, Dietrich A, Schermuly RT, Ghofrani HA, Gudermann T, Schulz R, et al. Regulation of hypoxic pulmonary vasoconstriction: basic mechanisms. Eur Respir J. 2008 Dec;32(6):1639-51.

31. Downing SE, Lee JC. Nervous control of the pulmonary circulation. Annu Rev Physiol. 1980;42:199-210.

32. West JB. Ibn al-Nafis, the pulmonary circulation, and the Islamic Golden Age. J Appl Physiol (1985). 2008 Dec;105(6):1877-80.

33. Young RA. The Pulmonary Circulation-Before and After Harvey: Part I. Br Med J. 1940 Jan 6;1(4122):1-5.

34. Haddad F, Hunt SA, Rosenthal DN, Murphy DJ. Right ventricular function in cardiovascular disease, part I: Anatomy, physiology, aging, and functional assessment of the right ventricle. Circulation. 2008 Mar 18;117(11):1436-48.

35. Trip P WN, Vonk Noordegraaf A. Function of the right ventricle. In: Gaine SP NRPA, editor. The Right Heart: Springer; 2014.

36. Starr I JW, Meade RH. The absence of conspicuous increments of venous pressure after severe damage to the RV of the dog, with discussion of the relation between clinical congestive heart failure and heart diseases. Am heart J. 1943;26:291-301.

37. Kagan A. Dynamic responses of the right ventricle following extensive damage by cauterization. Circulation. 1952 Jun;5(6):816-23.

38. Puga FJ MD. Exclusion of the right ventricle from the circulation: haemodynamic observations. Surgery. 1973;73:607-13.

39. Rose JC CJS, Hufnagel CA, Massullo EA. The effects of exclusion of the right ventricle from the circulation in dogs. J clin Invest. 1955;34:1625-31.

40. Goldstein JA, Vlahakes GJ, Verrier ED, Schiller NB, Tyberg JV, Ports TA, et al. The role of right ventricular systolic dysfunction and elevated intrapericardial pressure in the genesis of low output in experimental right ventricular infarction. Circulation. 1982 Mar;65(3):513-22.

41. van Wolferen SA, Marcus JT, Boonstra A, Marques KMJ, Bronzwaer JGF, Spreeuwenberg MD, et al. Prognostic value of right ventricular mass, volume, and function in idiopathic pulmonary arterial hypertension. European Heart Journal. 2007;28(10):1250-7.

42. La Gerche A, Gewillig M. What Limits Cardiac Performance during Exercise in Normal Subjects and in Healthy Fontan Patients? Int J Pediatr. 2010;2010.

43. Zehender M, Kasper W, Kauder E, Schonthaler M, Geibel A, Olschewski M, et al. Right ventricular infarction as an independent predictor of prognosis after acute inferior myocardial infarction. N Engl J Med. 1993 Apr 8;328(14):981-8.

44. Dell'Italia LJ. Anatomy and physiology of the right ventricle. Cardiol Clin. 2012 May;30(2):167-87.

45. Geva T, Powell AJ, Crawford EC, Chung T, Colan SD. Evaluation of regional differences in right ventricular systolic function by acoustic quantification echocardiography and cine magnetic resonance imaging. Circulation. 1998 Jul 28;98(4):339-45.

46. Meier GD, Bove AA, Santamore WP, Lynch PR. Contractile function in canine right ventricle. Am J Physiol. 1980 Dec;239(6):H794-804.

47. Lorenz CH, Walker ES, Morgan VL, Klein SS, Graham TP, Jr. Normal human right and left ventricular mass, systolic function, and gender differences by cine magnetic resonance imaging. J Cardiovasc Magn Reson. 1999;1(1):7-21.

48. Jain D, Zaret BL. Assessment of right ventricular function. Role of nuclear imaging techniques. Cardiol Clin. 1992 Feb;10(1):23-39.

49. Rudski LG, Lai WW, Afilalo J, Hua L, Handschumacher MD, Chandrasekaran K, et al. Guidelines for the echocardiographic assessment of the right heart in adults: a report from the American Society of Echocardiography endorsed by the European Association of Echocardiography, a registered branch of the European

Society of Cardiology, and the Canadian Society of Echocardiography. J Am Soc Echocardiogr. 2010 Jul;23(7):685-713; quiz 86-8.

50. Lowensohn HS, Khouri EM, Gregg DE, Pyle RL, Patterson RE. Phasic right coronary artery blood flow in conscious dogs with normal and elevated right ventricular pressures. Circ Res. 1976 Dec;39(6):760-6.

51. Weber KT, Janicki JS, Shroff S, Fishman AP. Contractile mechanics and interaction of the right and left ventricles. Am J Cardiol. 1981 Mar;47(3):686-95.

52. Marcus JT, Gan CT, Zwanenburg JJ, Boonstra A, Allaart CP, Gotte MJ, et al. Interventricular mechanical asynchrony in pulmonary arterial hypertension: left-to-right delay in peak shortening is related to right ventricular overload and left ventricular underfilling. J Am Coll Cardiol. 2008 Feb 19;51(7):750-7.

53. Haddad F, Doyle R, Murphy DJ, Hunt SA. Right ventricular function in cardiovascular disease, part II: pathophysiology, clinical importance, and management of right ventricular failure. Circulation. 2008 Apr 1;117(13):1717-31.

54. Molloy WD, Lee KY, Girling L, Schick U, Prewitt RM. Treatment of shock in a canine model of pulmonary embolism. Am Rev Respir Dis. 1984 Nov;130(5):870-4.

55. Farman GP, Gore D, Allen E, Schoenfelt K, Irving TC, de Tombe PP. Myosin head orientation: a structural determinant for the Frank-Starling relationship. Am J Physiol Heart Circ Physiol. 2011 Jun;300(6):H2155-60.

56. Cingolani HE, Perez NG, Cingolani OH, Ennis IL. The Anrep effect: 100 years later. Am J Physiol Heart Circ Physiol. 2013 Jan 15;304(2):H175-82.

57. Katz J, Whang J, Boxt LM, Barst RJ. Estimation of right ventricular mass in normal subjects and in patients with primary pulmonary hypertension by nuclear magnetic resonance imaging. J Am Coll Cardiol. 1993 May;21(6):1475-81.

58. Boxt LM, Katz J, Kolb T, Czegledy FP, Barst RJ. Direct quantitation of right and left ventricular volumes with nuclear magnetic resonance imaging in patients with primary pulmonary hypertension. J Am Coll Cardiol. 1992 Jun;19(7):1508-15.

59. Doherty NE, 3rd, Fujita N, Caputo GR, Higgins CB. Measurement of right ventricular mass in normal and dilated cardiomyopathic ventricles using cine magnetic resonance imaging. Am J Cardiol. 1992 May 1;69(14):1223-8.

60. Pattynama PM, Willems LN, Smit AH, van der Wall EE, de Roos A. Early diagnosis of cor pulmonale with MR imaging of the right ventricle. Radiology. 1992 Feb;182(2):375-9.

61. Bottini PB, Carr AA, Prisant LM, Flickinger FW, Allison JD, Gottdiener JS. Magnetic resonance imaging compared to echocardiography to assess left ventricular mass in the hypertensive patient. Am J Hypertens. 1995 Mar;8(3):221-8.

62. McLure LER, Peacock AJ. Cardiac magnetic resonance imaging for the assessment of the heart and pulmonary circulation in pulmonary hypertension. European Respiratory Journal. 2009;33(6):1454-66.

63. Grothues F, Smith GC, Moon JC, Bellenger NG, Collins P, Klein HU, et al. Comparison of interstudy reproducibility of cardiovascular magnetic resonance with two-dimensional echocardiography in normal subjects and in patients with heart failure or left ventricular hypertrophy. Am J Cardiol. 2002 Jul 1;90(1):29-34.

64. Grothues F, Moon JC, Bellenger NG, Smith GS, Klein HU, Pennell DJ. Interstudy reproducibility of right ventricular volumes, function, and mass with cardiovascular magnetic resonance. Am Heart J. 2004 Feb;147(2):218-23.

65. Vonk-Noordegraaf A, van Wolferen SA, Marcus JT, Boonstra A, Postmus PE, Peeters JWL, et al. Noninvasive assessment and monitoring of the pulmonary circulation. European Respiratory Journal. 2005;25(4):758-66.

66. Pennell DJ, Sechtem UP, Higgins CB, Manning WJ, Pohost GM, Rademakers FE, et al. Clinical indications for cardiovascular magnetic resonance (CMR): Consensus Panel report. J Cardiovasc Magn Reson. 2004;6(4):727-65.

67. Muthurangu V, Lurz P, Critchely JD, Deanfield JE, Taylor AM, Hansen MS. Real-time assessment of right and left ventricular volumes and function in patients with congenital heart disease by using high spatiotemporal resolution radial k-t SENSE. Radiology. 2008 Sep;248(3):782-91.

68. Zhang H, Wahle A, Johnson RK, Scholz TD, Sonka M. 4-D cardiac MR image analysis: left and right ventricular morphology and function. IEEE Trans Med Imaging. 2010 Feb;29(2):350-64.

69. Ridgway JP. Cardiovascular magnetic resonance physics for clinicians: part I. J Cardiovasc Magn Reson. 2010 Nov 30;12:71.

70. Zur Y, Wood ML, Neuringer LJ. Spoiling of transverse magnetization in steady-state sequences. Magn Reson Med. 1991 Oct;21(2):251-63.

71. Frahm J, Haase A, Matthaei D. Rapid NMR imaging of dynamic processes using the FLASH technique. Magn Reson Med. 1986 Apr;3(2):321-7.

72. Scheffler K, Lehnhardt S. Principles and applications of balanced SSFP techniques. Eur Radiol. 2003 Nov;13(11):2409-18.

73. Simonetti OP, Finn JP, White RD, Laub G, Henry DA. "Black blood" T2-weighted inversion-recovery MR imaging of the heart. Radiology. 1996 Apr;199(1):49-57.

74. Sakuma H, Fujita N, Foo TK, Caputo GR, Nelson SJ, Hartiala J, et al. Evaluation of left ventricular volume and mass with breath-hold cine MR imaging. Radiology. 1993 Aug;188(2):377-80.

75. Barkhausen J, Ruehm SG, Goyen M, Buck T, Laub G, Debatin JF. MR evaluation of ventricular function: true fast imaging with steady-state precession versus fast low-angle shot cine MR imaging: feasibility study. Radiology. 2001 Apr;219(1):264-9.

76. Reeder SB, Faranesh AZ. Ultrafast pulse sequence techniques for cardiac magnetic resonance imaging. Top Magn Reson Imaging. 2000 Dec;11(6):312-30.

77. Lanzer P, Barta C, Botvinick EH, Wiesendanger HU, Modin G, Higgins CB. ECG-synchronized cardiac MR imaging: method and evaluation. Radiology. 1985 Jun;155(3):681-6.

78. Lenz GW, Haacke EM, White RD. Retrospective cardiac gating: a review of technical aspects and future directions. Magn Reson Imaging. 1989 Sep-Oct;7(5):445-55.

79. Lee VS, Resnick D, Bundy JM, Simonetti OP, Lee P, Weinreb JC. Cardiac function: MR evaluation in one breath hold with real-time true fast imaging with steady-state precession. Radiology. 2002 Mar;222(3):835-42.

80. Plein S, Smith WH, Ridgway JP, Kassner A, Beacock DJ, Bloomer TN, et al. Qualitative and quantitative analysis of regional left ventricular wall dynamics using real-time magnetic resonance imaging: comparison with conventional breath-hold gradient echo acquisition in volunteers and patients. J Magn Reson Imaging. 2001 Jul;14(1):23-30.

81. Winter MM, Bernink FJ, Groenink M, Bouma BJ, van Dijk AP, Helbing WA, et al. Evaluating the systemic right ventricle by CMR: the importance of consistent and reproducible delineation of the cavity. J Cardiovasc Magn Reson. 2008;10:40.

82. Lotz J, Meier C, Leppert A, Galanski M. Cardiovascular flow measurement with phase-contrast MR imaging: basic facts and implementation. Radiographics. 2002 May-Jun;22(3):651-71.

83. Gatehouse PD, Keegan J, Crowe LA, Masood S, Mohiaddin RH, Kreitner KF, et al. Applications of phase-contrast flow and velocity imaging in cardiovascular MRI. Eur Radiol. 2005 Oct;15(10):2172-84.

84. Biglands JD, Radjenovic A, Ridgway JP. Cardiovascular magnetic resonance physics for clinicians: Part II. J Cardiovasc Magn Reson. 2012 Sep 20;14:66.

85. Herzog B GJ, Plein S. Cardiovascular Magnetic Resonance pocket guide.: European Society of Cardiology; 2013.

86. Nayler GL, Firmin DN, Longmore DB. Blood flow imaging by cine magnetic resonance. J Comput Assist Tomogr. 1986 Sep-Oct;10(5):715-22.

87. Beerbaum P, Korperich H, Barth P, Esdorn H, Gieseke J, Meyer H. Noninvasive quantification of left-to-right shunt in pediatric patients: phase-contrast cine magnetic resonance imaging compared with invasive oximetry. Circulation. 2001 May 22;103(20):2476-82.

88. van der Graaf AW, Bhagirath P, Ghoerbien S, Gotte MJ. Cardiac magnetic resonance imaging: artefacts for clinicians. Neth Heart J. 2014 Dec;22(12):542-9.

89. Salton CJ, Chuang ML, O'Donnell CJ, Kupka MJ, Larson MG, Kissinger KV, et al. Gender differences and normal left ventricular anatomy in an adult population free of hypertension. A cardiovascular magnetic resonance study of the Framingham Heart Study Offspring cohort. J Am Coll Cardiol. 2002 Mar 20;39(6):1055-60.

90. Natori S, Lai S, Finn JP, Gomes AS, Hundley WG, Jerosch-Herold M, et al. Cardiovascular function in multi-ethnic study of atherosclerosis: normal values by age, sex, and ethnicity. AJR Am J Roentgenol. 2006 Jun;186(6 Suppl 2):S357-65.

91. Cheng S, Fernandes VR, Bluemke DA, McClelland RL, Kronmal RA, Lima JA. Age-related left ventricular remodeling and associated risk for cardiovascular outcomes: the Multi-Ethnic Study of Atherosclerosis. Circ Cardiovasc Imaging. 2009 May;2(3):191-8.

92. Slotwiner DJ, Devereux RB, Schwartz JE, Pickering TG, de Simone G, Ganau A, et al. Relation of age to left ventricular function in clinically normal adults. Am J Cardiol. 1998 Sep 1;82(5):621-6.

93. Hangartner JR, Marley NJ, Whitehead A, Thomas AC, Davies MJ. The assessment of cardiac hypertrophy at autopsy. Histopathology. 1985 Dec;9(12):1295-306.

94. Kitzman DW, Scholz DG, Hagen PT, Ilstrup DM, Edwards WD. Age-related changes in normal human hearts during the first 10 decades of life. Part II

(Maturity): A quantitative anatomic study of 765 specimens from subjects 20 to 99 years old. Mayo Clin Proc. 1988 Feb;63(2):137-46.

95. Olivetti G, Giordano G, Corradi D, Melissari M, Lagrasta C, Gambert SR, et al. Gender differences and aging: effects on the human heart. J Am Coll Cardiol. 1995 Oct;26(4):1068-79.

96. Sandstede J, Lipke C, Beer M, Hofmann S, Pabst T, Kenn W, et al. Age- and gender-specific differences in left and right ventricular cardiac function and mass determined by cine magnetic resonance imaging. Eur Radiol. 2000;10(3):438-42.

97. Danias PG, Tritos NA, Stuber M, Kissinger KV, Salton CJ, Manning WJ. Cardiac structure and function in the obese: a cardiovascular magnetic resonance imaging study. J Cardiovasc Magn Reson. 2003 Jul;5(3):431-8.

98. Bild DE, Bluemke DA, Burke GL, Detrano R, Diez Roux AV, Folsom AR, et al. Multi-ethnic study of atherosclerosis: objectives and design. Am J Epidemiol. 2002 Nov 1;156(9):871-81.

99. Dewey FE, Rosenthal D, Murphy DJ, Jr., Froelicher VF, Ashley EA. Does size matter? Clinical applications of scaling cardiac size and function for body size. Circulation. 2008 Apr 29;117(17):2279-87.

100. de Simone G, Kizer JR, Chinali M, Roman MJ, Bella JN, Best LG, et al. Normalization for body size and population-attributable risk of left ventricular hypertrophy: the Strong Heart Study. Am J Hypertens. 2005 Feb;18(2 Pt 1):191-6.

101. Kawut SM, Lima JA, Barr RG, Chahal H, Jain A, Tandri H, et al. Sex and race differences in right ventricular structure and function: the multi-ethnic study of atherosclerosis-right ventricle study. Circulation. 2011 Jun 7;123(22):2542-51.

102. Hudsmith LE, Petersen SE, Francis JM, Robson MD, Neubauer S. Normal human left and right ventricular and left atrial dimensions using steady state free precession magnetic resonance imaging. J Cardiovasc Magn Reson. 2005;7(5):775-82.

103. Fiechter M, Fuchs TA, Gebhard C, Stehli J, Klaeser B, Stahli BE, et al. Age-related normal structural and functional ventricular values in cardiac function assessed by magnetic resonance. BMC Med Imaging. 2013;13:6.

104. Maceira AM, Prasad SK, Khan M, Pennell DJ. Reference right ventricular systolic and diastolic function normalized to age, gender and body surface area from steady-state free precession cardiovascular magnetic resonance. Eur Heart J. 2006 Dec;27(23):2879-88.

105. Tandri H, Daya SK, Nasir K, Bomma C, Lima JA, Calkins H, et al. Normal reference values for the adult right ventricle by magnetic resonance imaging. Am J Cardiol. 2006 Dec 15;98(12):1660-4.

106. Rominger MB, Bachmann GF, Pabst W, Rau WS. Right ventricular volumes and ejection fraction with fast cine MR imaging in breath-hold technique: applicability, normal values from 52 volunteers, and evaluation of 325 adult cardiac patients. J Magn Reson Imaging. 1999 Dec;10(6):908-18.

107. Skavdahl M, Steenbergen C, Clark J, Myers P, Demianenko T, Mao L, et al. Estrogen receptor-beta mediates male-female differences in the development of pressure overload hypertrophy. Am J Physiol Heart Circ Physiol. 2005 Feb;288(2):H469-76.

108. Mendelsohn ME, Karas RH. The protective effects of estrogen on the cardiovascular system. N Engl J Med. 1999 Jun 10;340(23):1801-11.

109. Ventetuolo CE, Ouyang P, Bluemke DA, Tandri H, Barr RG, Bagiella E, et al. Sex hormones are associated with right ventricular structure and function: The MESA-right ventricle study. Am J Respir Crit Care Med. 2011 Mar 1;183(5):659-67.

110. Pluim BM, Zwinderman AH, van der Laarse A, van der Wall EE. The athlete's heart. A meta-analysis of cardiac structure and function. Circulation. 2000 Jan 25;101(3):336-44.

111. Scharhag J, Schneider G, Urhausen A, Rochette V, Kramann B, Kindermann W. Athlete's heart: right and left ventricular mass and function in male endurance athletes and untrained individuals determined by magnetic resonance imaging. J Am Coll Cardiol. 2002 Nov 20;40(10):1856-63.

112. Perseghin G, De Cobelli F, Esposito A, Lattuada G, Terruzzi I, La Torre A, et al. Effect of the sporting discipline on the right and left ventricular morphology and function of elite male track runners: a magnetic resonance imaging and phosphorus 31 spectroscopy study. Am Heart J. 2007 Nov;154(5):937-42.

113. Erol MK, Karakelleoglu S. Assessment of right heart function in the athlete's heart. Heart Vessels. 2002 Jul;16(5):175-80.

114. Aaron CP, Tandri H, Barr RG, Johnson WC, Bagiella E, Chahal H, et al. Physical activity and right ventricular structure and function. The MESA-Right Ventricle Study. Am J Respir Crit Care Med. 2011 Feb 1;183(3):396-404.

115. Kasper EK, Hruban RH, Baughman KL. Cardiomyopathy of obesity: a clinicopathologic evaluation of 43 obese patients with heart failure. Am J Cardiol. 1992 Oct 1;70(9):921-4.

116. McGavock JM, Victor RG, Unger RH, Szczepaniak LS. Adiposity of the heart, revisited. Ann Intern Med. 2006 Apr 4;144(7):517-24.

117. Chahal H, McClelland RL, Tandri H, Jain A, Turkbey EB, Hundley WG, et al. Obesity and right ventricular structure and function: the MESA-Right Ventricle Study. Chest. 2012 Feb;141(2):388-95.

118. Sanner BM, Konermann M, Sturm A, Muller HJ, Zidek W. Right ventricular dysfunction in patients with obstructive sleep apnoea syndrome. Eur Respir J. 1997 Sep;10(9):2079-83.

119. Messerli FH, Sundgaard-Riise K, Reisin E, Dreslinski G, Dunn FG, Frohlich E. Disparate cardiovascular effects of obesity and arterial hypertension. Am J Med. 1983 May;74(5):808-12.

120. Lieb W, Sullivan LM, Aragam J, Harris TB, Roubenoff R, Benjamin EJ, et al. Relation of serum leptin with cardiac mass and left atrial dimension in individuals >70 years of age. Am J Cardiol. 2009 Aug 15;104(4):602-5.

121. Tansey DK, Aly Z, Sheppard MN. Fat in the right ventricle of the normal heart. Histopathology. 2005 Jan;46(1):98-104.

122. Naeije R, Brimioulle S, Dewachter L. Biomechanics of the right ventricle in health and disease (2013 Grover Conference series). Pulm Circ. 2014 Sep;4(3):395-406.

123. Maughan WL, Shoukas AA, Sagawa K, Weisfeldt ML. Instantaneous pressure-volume relationship of the canine right ventricle. Circ Res. 1979 Mar;44(3):309-15.

124. Sunagawa K, Yamada A, Senda Y, Kikuchi Y, Nakamura M, Shibahara T, et al. Estimation of the hydromotive source pressure from ejecting beats of the left ventricle. IEEE Trans Biomed Eng. 1980 Jun;27(6):299-305.

125. Brimioulle S, Wauthy P, Ewalenko P, Rondelet Bt, Vermeulen F, Kerbaul F, et al. Single-beat estimation of right ventricular end-systolic pressure-volume relationship. American Journal of Physiology - Heart and Circulatory Physiology. 2003 May 1, 2003;284(5):H1625-H30.

126. Tedford RJ. Determinants of right ventricular afterload (2013 Grover Conference series). Pulm Circ. 2014 Jun;4(2):211-9.

127. Vonk-Noordegraaf A, Westerhof N. Describing right ventricular function. Eur Respir J. 2013 Jun;41(6):1419-23.

128. Chesler NC, Roldan A, Vanderpool RR, Naeije R. How to measure pulmonary vascular and right ventricular function. Conf Proc IEEE Eng Med Biol Soc. 2009;2009:177-80.

129. Kelly RP, Ting CT, Yang TM, Liu CP, Maughan WL, Chang MS, et al. Effective arterial elastance as index of arterial vascular load in humans. Circulation. 1992 Aug;86(2):513-21.

130. Sagawa K ML, Suga H, Sunagawa K. Cardiac contraction and the pressure-volume relationship: New York Oxford University Press; 1988.

131. Naeije R, Manes A. The right ventricle in pulmonary arterial hypertension. Eur Respir Rev. 2014 Dec;23(134):476-87.

132. Trip P, Kind T, van de Veerdonk MC, Marcus JT, de Man FS, Westerhof N, et al. Accurate assessment of load-independent right ventricular systolic function in patients with pulmonary hypertension. J Heart Lung Transplant. 2013 Jan;32(1):50-5.

133. Romberg E. Uber die Sklerose der Lungenarterien. Dtsch Arch Klin Med. 1891;48:197.

134. Dresdale DT, Schultz M, Michtom RJ. Primary pulmonary hypertension. I. Clinical and hemodynamic study. Am J Med. 1951 Dec;11(6):686-705.

135. Hatano S ST. Primary pulmonary hypertension. Report on a WHO-meeting. Geneva: WHO1975.

136. Simonneau G, Galie N, Rubin LJ, Langleben D, Seeger W, Domenighetti G, et al. Clinical classification of pulmonary hypertension. J Am Coll Cardiol. 2004 Jun 16;43(12 Suppl S):5S-12S.

137. Simonneau G, Robbins IM, Beghetti M, Channick RN, Delcroix M, Denton CP, et al. Updated clinical classification of pulmonary hypertension. J Am Coll Cardiol. 2009 Jun 30;54(1 Suppl):S43-54.

138. Simonneau G, Gatzoulis MA, Adatia I, Celermajer D, Denton C, Ghofrani A, et al. Updated clinical classification of pulmonary hypertension. J Am Coll Cardiol. 2013 Dec 24;62(25 Suppl):D34-41.

139. Humbert M, Sitbon O, Chaouat A, Bertocchi M, Habib G, Gressin V, et al. Pulmonary arterial hypertension in France - Results from a national registry. Am J Respir Crit Care Med. 2006;173(9):1023-30.

140. Fourth Annual report. National audit of pulmonary hypertension for the UK, Channel Islands, Gibraltor & Isle of Man. Audit period April 2012 - March 2013.2014.

141. Peacock AJ, Murphy NF, McMurray JJV, Caballero L, Stewart S. An epidemiological study of pulmonary arterial hypertension. European Respiratory Journal. 2007;30(1):104-9.

142. Dalonzo GE, Barst RJ, Ayres SM, Bergofsky EH, Brundage BH, Detre KM, et al. Survival in patients with pulmonary hypertension - results from a national prospective registry. Annals of Internal Medicine. 1991 Sep;115(5):343-9.

143. Rich S, Dantzker DR, Ayres SM, Bergofsky EH, Brundage BH, Detre KM, et al. Primary pulmonary hypertension. A national prospective study. Ann Intern Med. 1987 Aug;107(2):216-23.

144. Benza RL, Miller DP, Gomberg-Maitland M, Frantz RP, Foreman AJ, Coffey CS, et al. Predicting survival in pulmonary arterial hypertension: insights from the Registry to Evaluate Early and Long-Term Pulmonary Arterial Hypertension Disease Management (REVEAL). Circulation. 2010 Jul 13;122(2):164-72.

145. Benza RL, Miller DP, Barst RJ, Badesch DB, Frost AE, McGoon MD. An evaluation of long-term survival from time of diagnosis in pulmonary arterial hypertension from the REVEAL Registry. Chest. 2012 Aug;142(2):448-56.

146. Condliffe R, Kiely DG, Peacock AJ, Corris PA, Gibbs JS, Vrapi F, et al. Connective tissue disease-associated pulmonary arterial hypertension in the modern treatment era. Am J Respir Crit Care Med. 2009 Jan 15;179(2):151-7.

147. Ling Y, Johnson MK, Kiely DG, Condliffe R, Elliot CA, Gibbs JS, et al. Changing demographics, epidemiology, and survival of incident pulmonary arterial hypertension: results from the pulmonary hypertension registry of the United Kingdom and Ireland. Am J Respir Crit Care Med. 2012 Oct 15;186(8):790-6.

148. Archer SL, Weir EK, Wilkins MR. Basic science of pulmonary arterial hypertension for clinicians: new concepts and experimental therapies. Circulation. 2010 May 11;121(18):2045-66.

149. Guignabert C, Tu L, Le Hiress M, Ricard N, Sattler C, Seferian A, et al. Pathogenesis of pulmonary arterial hypertension: lessons from cancer. Eur Respir Rev. 2013 Dec;22(130):543-51.

150. Tuder RM, Abman SH, Braun T, Capron F, Stevens T, Thistlethwaite PA, et al. Development and pathology of pulmonary hypertension. J Am Coll Cardiol. 2009 Jun 30;54(1 Suppl):S3-9.

151. Dorfmuller P, Perros F, Balabanian K, Humbert M. Inflammation in pulmonary arterial hypertension. Eur Respir J. 2003 Aug;22(2):358-63.

152. Hassoun PM, Mouthon L, Barbera JA, Eddahibi S, Flores SC, Grimminger F, et al. Inflammation, growth factors, and pulmonary vascular remodeling. J Am Coll Cardiol. 2009 Jun 30;54(1 Suppl):S10-9.

153. Tuder RM, Chacon M, Alger L, Wang J, Taraseviciene-Stewart L, Kasahara Y, et al. Expression of angiogenesis-related molecules in plexiform lesions in severe pulmonary hypertension: evidence for a process of disordered angiogenesis. J Pathol. 2001 Oct;195(3):367-74.

154. Toshner M, Voswinckel R, Southwood M, Al-Lamki R, Howard LS, Marchesan D, et al. Evidence of dysfunction of endothelial progenitors in pulmonary arterial hypertension. Am J Respir Crit Care Med. 2009 Oct 15;180(8):780-7.

155. Yuan JX, Aldinger AM, Juhaszova M, Wang J, Conte JV, Jr., Gaine SP, et al. Dysfunctional voltage-gated K+ channels in pulmonary artery smooth muscle cells of patients with primary pulmonary hypertension. Circulation. 1998 Oct 6;98(14):1400-6.

156. Pugh ME, Robbins IM, Rice TW, West J, Newman JH, Hemnes AR. Unrecognized glucose intolerance is common in pulmonary arterial hypertension. J Heart Lung Transplant. 2011 Aug;30(8):904-11.

157. Tofovic SP. Estrogens and development of pulmonary hypertension: interaction of estradiol metabolism and pulmonary vascular disease. J Cardiovasc Pharmacol. 2010 Dec;56(6):696-708.

158. Morrell NW, Adnot S, Archer SL, Dupuis J, Jones PL, MacLean MR, et al. Cellular and molecular basis of pulmonary arterial hypertension. J Am Coll Cardiol. 2009 Jun 30;54(1 Suppl):S20-31.

159. Wilkins MR. Pulmonary hypertension: the science behind the disease spectrum. Eur Respir Rev. 2012 Mar 1;21(123):19-26.

160. Giaid A, Saleh D. Reduced expression of endothelial nitric oxide synthase in the lungs of patients with pulmonary hypertension. N Engl J Med. 1995 Jul 27;333(4):214-21.

161. Bowers R, Cool C, Murphy RC, Tuder RM, Hopken MW, Flores SC, et al. Oxidative stress in severe pulmonary hypertension. Am J Respir Crit Care Med. 2004 Mar 15;169(6):764-9.

162. Zakrzewicz D, Eickelberg O. From arginine methylation to ADMA: a novel mechanism with therapeutic potential in chronic lung diseases. BMC Pulm Med. 2009;9:5.

163. Nagendran J, Archer SL, Soliman D, Gurtu V, Moudgil R, Haromy A, et al. Phosphodiesterase type 5 is highly expressed in the hypertrophied human right ventricle, and acute inhibition of phosphodiesterase type 5 improves contractility. Circulation. 2007 Jul 17;116(3):238-48.

164. Giaid A, Yanagisawa M, Langleben D, Michel RP, Levy R, Shennib H, et al. Expression of endothelin-1 in the lungs of patients with pulmonary hypertension. N Engl J Med. 1993 Jun 17;328(24):1732-9.

165. Bauer M, Wilkens H, Langer F, Schneider SO, Lausberg H, Schafers HJ. Selective upregulation of endothelin B receptor gene expression in severe pulmonary hypertension. Circulation. 2002 Mar 5;105(9):1034-6.

166. Herve P, Launay JM, Scrobohaci ML, Brenot F, Simonneau G, Petitpretz P, et al. Increased plasma serotonin in primary pulmonary hypertension. Am J Med. 1995 Sep;99(3):249-54.

167. Eddahibi S, Guignabert C, Barlier-Mur AM, Dewachter L, Fadel E, Dartevelle P, et al. Cross talk between endothelial and smooth muscle cells in pulmonary hypertension: critical role for serotonin-induced smooth muscle hyperplasia. Circulation. 2006 Apr 18;113(15):1857-64.

168. Deng Z, Morse JH, Slager SL, Cuervo N, Moore KJ, Venetos G, et al. Familial primary pulmonary hypertension (gene PPH1) is caused by mutations in the bone morphogenetic protein receptor-II gene. Am J Hum Genet. 2000 Sep;67(3):737-44.

169. Lane KB, Machado RD, Pauciulo MW, Thomson JR, Phillips JA, 3rd, Loyd JE, et al. Heterozygous germline mutations in BMPR2, encoding a TGF-beta receptor, cause familial primary pulmonary hypertension. Nat Genet. 2000 Sep;26(1):81-4.

170. Machado RD, Aldred MA, James V, Harrison RE, Patel B, Schwalbe EC, et al. Mutations of the TGF-beta type II receptor BMPR2 in pulmonary arterial hypertension. Hum Mutat. 2006 Feb;27(2):121-32.

171. Newman JH, Trembath RC, Morse JA, Grunig E, Loyd JE, Adnot S, et al. Genetic basis of pulmonary arterial hypertension: current understanding and future directions. J Am Coll Cardiol. 2004 Jun 16;43(12 Suppl S):33S-9S.

172. Trembath RC, Thomson JR, Machado RD, Morgan NV, Atkinson C, Winship I, et al. Clinical and molecular genetic features of pulmonary hypertension in patients with hereditary hemorrhagic telangiectasia. N Engl J Med. 2001 Aug 2;345(5):325-34.

173. Chaouat A, Coulet F, Favre C, Simonneau G, Weitzenblum E, Soubrier F, et al. Endoglin germline mutation in a patient with hereditary haemorrhagic

telangiectasia and dexfenfluramine associated pulmonary arterial hypertension. Thorax. 2004 May;59(5):446-8.

174. Shintani M, Yagi H, Nakayama T, Saji T, Matsuoka R. A new nonsense mutation of SMAD8 associated with pulmonary arterial hypertension. J Med Genet. 2009 May;46(5):331-7.

175. Austin ED, Ma L, LeDuc C, Berman Rosenzweig E, Borczuk A, Phillips JA, 3rd, et al. Whole exome sequencing to identify a novel gene (caveolin-1) associated with human pulmonary arterial hypertension. Circ Cardiovasc Genet. 2012 Jun;5(3):336-43.

176. Ma L, Roman-Campos D, Austin ED, Eyries M, Sampson KS, Soubrier F, et al. A novel channelopathy in pulmonary arterial hypertension. N Engl J Med. 2013 Jul 25;369(4):351-61.

177. Girerd B, Montani D, Coulet F, Sztrymf B, Yaici A, Jais X, et al. Clinical outcomes of pulmonary arterial hypertension in patients carrying an ACVRL1 (ALK1) mutation. Am J Respir Crit Care Med. 2010 Apr 15;181(8):851-61.

178. Elliott CG, Glissmeyer EW, Havlena GT, Carlquist J, McKinney JT, Rich S, et al. Relationship of BMPR2 mutations to vasoreactivity in pulmonary arterial hypertension. Circulation. 2006 May 30;113(21):2509-15.

179. Borgeson DD, Seward JB, Miller FA, Jr., Oh JK, Tajik AJ. Frequency of Doppler measurable pulmonary artery pressures. J Am Soc Echocardiogr. 1996 Nov-Dec;9(6):832-7.

180. Berger M, Haimowitz A, Van Tosh A, Berdoff RL, Goldberg E. Quantitative assessment of pulmonary hypertension in patients with tricuspid regurgitation using continuous wave Doppler ultrasound. J Am Coll Cardiol. 1985 Aug;6(2):359-65.

181. Valerio CJ, Schreiber BE, Handler CE, Denton CP, Coghlan JG. Borderline mean pulmonary artery pressure in patients with systemic sclerosis: transpulmonary gradient predicts risk of developing pulmonary hypertension. Arthritis Rheum. 2013 Apr;65(4):1074-84.

182. Galie N, Manes A, Negro L, Palazzini M, Bacchi-Reggiani ML, Branzi A. A meta-analysis of randomized controlled trials in pulmonary arterial hypertension. Eur Heart J. 2009 Feb;30(4):394-403.

183. Dupuis J, Hoeper MM. Endothelin receptor antagonists in pulmonary arterial hypertension. Eur Respir J. 2008 Feb;31(2):407-15.

184. Wilkins MR, Wharton J, Grimminger F, Ghofrani HA. Phosphodiesterase inhibitors for the treatment of pulmonary hypertension. Eur Respir J. 2008 Jul;32(1):198-209.

185. Galie N, Ghofrani AH. New horizons in pulmonary arterial hypertension therapies. Eur Respir Rev. 2013 Dec;22(130):503-14.

186. Bai Y, Sun L, Hu S, Wei Y. Combination therapy in pulmonary arterial hypertension: a meta-analysis. Cardiology. 2011;120(3):157-65.

187. Galie N, Corris PA, Frost A, Girgis RE, Granton J, Jing ZC, et al. Updated treatment algorithm of pulmonary arterial hypertension. J Am Coll Cardiol. 2013 Dec 24;62(25 Suppl):D60-72.

188. Rubin LJ, Badesch DB, Barst RJ, Galie N, Black CM, Keogh A, et al. Bosentan therapy for pulmonary arterial hypertension. N Engl J Med. 2002 Mar 21;346(12):896-903.

189. Galie N, Olschewski H, Oudiz RJ, Torres F, Frost A, Ghofrani HA, et al. Ambrisentan for the treatment of pulmonary arterial hypertension: results of the ambrisentan in pulmonary arterial hypertension, randomized, double-blind, placebo-controlled, multicenter, efficacy (ARIES) study 1 and 2. Circulation. 2008 Jun 10;117(23):3010-9.

190. Pulido T, Adzerikho I, Channick RN, Delcroix M, Galie N, Ghofrani HA, et al. Macitentan and morbidity and mortality in pulmonary arterial hypertension. N Engl J Med. 2013 Aug 29;369(9):809-18.

191. Galie N, Ghofrani HA, Torbicki A, Barst RJ, Rubin LJ, Badesch D, et al. Sildenafil citrate therapy for pulmonary arterial hypertension. N Engl J Med. 2005 Nov 17;353(20):2148-57.

192. Galie N, Brundage BH, Ghofrani HA, Oudiz RJ, Simonneau G, Safdar Z, et al. Tadalafil therapy for pulmonary arterial hypertension. Circulation. 2009 Jun 9;119(22):2894-903.

193. Ghofrani HA, Galie N, Grimminger F, Grunig E, Humbert M, Jing ZC, et al. Riociguat for the treatment of pulmonary arterial hypertension. N Engl J Med. 2013 Jul 25;369(4):330-40.

194. Rubin LJ, Galie N, Grimminger F, Grunig E, Humbert M, Jing ZC, et al. Riociguat for the treatment of pulmonary arterial hypertension: a long-term extension study (PATENT-2). Eur Respir J. 2015 Jan 22.

195. Barst RJ, Rubin LJ, Long WA, McGoon MD, Rich S, Badesch DB, et al. A comparison of continuous intravenous epoprostenol (prostacyclin) with

conventional therapy for primary pulmonary hypertension. New England Journal of Medicine. 1996;334(5):296-301.

196. Rubin LJ, Mendoza J, Hood M, McGoon M, Barst R, Williams WB, et al. Treatment of primary pulmonary hypertension with continuous intravenous prostacyclin (epoprostenol). Results of a randomized trial. Ann Intern Med. 1990 Apr 1;112(7):485-91.

197. Olschewski H, Simonneau G, Galie N, Higenbottam T, Naeije R, Rubin LJ, et al. Inhaled iloprost for severe pulmonary hypertension. N Engl J Med. 2002 Aug 1;347(5):322-9.

198. Simonneau G, Torbicki A, Hoeper MM, Delcroix M, Karlocai K, Galie N, et al. Selexipag: an oral, selective prostacyclin receptor agonist for the treatment of pulmonary arterial hypertension. Eur Respir J. 2012 Oct;40(4):874-80.

199. Arcasoy SM, Christie JD, Ferrari VA, Sutton MS, Zisman DA, Blumenthal NP, et al. Echocardiographic assessment of pulmonary hypertension in patients with advanced lung disease. Am J Respir Crit Care Med. 2003 Mar 1;167(5):735-40.

200. Wrobel JP, Thompson BR, Williams TJ. Mechanisms of pulmonary hypertension in chronic obstructive pulmonary disease: a pathophysiologic review. J Heart Lung Transplant. 2012 Jun;31(6):557-64.

201. Kessler R, Faller M, Fourgaut G, Mennecier B, Weitzenblum E. Predictive factors of hospitalization for acute exacerbation in a series of 64 patients with chronic obstructive pulmonary disease. Am J Respir Crit Care Med. 1999 Jan;159(1):158-64.

202. Abraham AS, Cole RB, Green ID, Hedworth-Whitty RB, Clarke SW, Bishop JM. Factors contributing to the reversible pulmonary hypertension of patients with acute respiratory failure studies by serial observations during recovery. Circ Res. 1969 Jan;24(1):51-60.

203. Weitzenblum E, Sautegeau A, Ehrhart M, Mammosser M, Hirth C, Roegel E. Long-term course of pulmonary arterial pressure in chronic obstructive pulmonary disease. Am Rev Respir Dis. 1984 Dec;130(6):993-8.

204. Scharf SM, Iqbal M, Keller C, Criner G, Lee S, Fessler HE. Hemodynamic characterization of patients with severe emphysema. Am J Respir Crit Care Med. 2002 Aug 1;166(3):314-22.

205. Vizza CD, Lynch JP, Ochoa LL, Richardson G, Trulock EP. Right and left ventricular dysfunction in patients with severe pulmonary disease. Chest. 1998 Mar;113(3):576-83.

206. Thabut G, Dauriat G, Stern JB, Logeart D, Levy A, Marrash-Chahla R, et al. Pulmonary hemodynamics in advanced COPD candidates for lung volume reduction surgery or lung transplantation. Chest. 2005 May;127(5):1531-6.

207. Cuttica MJ, Kalhan R, Shlobin OA, Ahmad S, Gladwin M, Machado RF, et al. Categorization and impact of pulmonary hypertension in patients with advanced COPD. Respir Med. 2010 Dec;104(12):1877-82.

208. Chaouat A, Bugnet AS, Kadaoui N, Schott R, Enache I, Ducolone A, et al. Severe pulmonary hypertension and chronic obstructive pulmonary disease. Am J Respir Crit Care Med. 2005 Jul 15;172(2):189-94.

209. Andersen KH, Iversen M, Kjaergaard J, Mortensen J, Nielsen-Kudsk JE, Bendstrup E, et al. Prevalence, predictors, and survival in pulmonary hypertension related to end-stage chronic obstructive pulmonary disease. J Heart Lung Transplant. 2012 Apr;31(4):373-80.

210. Oswald-Mammosser M, Weitzenblum E, Quoix E, Moser G, Chaouat A, Charpentier C, et al. Prognostic factors in COPD patients receiving long-term oxygen therapy. Importance of pulmonary artery pressure. Chest. 1995 May;107(5):1193-8.

211. King TE, Jr., Schwarz MI, Brown K, Tooze JA, Colby TV, Waldron JA, Jr., et al. Idiopathic pulmonary fibrosis: relationship between histopathologic features and mortality. Am J Respir Crit Care Med. 2001 Sep 15;164(6):1025-32.

212. Nathan SD, Shlobin OA, Weir N, Ahmad S, Kaldjob JM, Battle E, et al. Long-term course and prognosis of idiopathic pulmonary fibrosis in the new millennium. Chest. 2011 Jul;140(1):221-9.

213. Hamada K, Nagai S, Tanaka S, Handa T, Shigematsu M, Nagao T, et al. Significance of pulmonary arterial pressure and diffusion capacity of the lung as prognosticator in patients with idiopathic pulmonary fibrosis. Chest. 2007 Mar;131(3):650-6.

214. Kimura M, Taniguchi H, Kondoh Y, Kimura T, Kataoka K, Nishiyama O, et al. Pulmonary hypertension as a prognostic indicator at the initial evaluation in idiopathic pulmonary fibrosis. Respiration. 2013;85(6):456-63.

215. Behr J, Ryu JH. Pulmonary hypertension in interstitial lung disease. Eur Respir J. 2008 Jun;31(6):1357-67.

216. Minai OA, Santacruz JF, Alster JM, Budev MM, McCarthy K. Impact of pulmonary hemodynamics on 6-min walk test in idiopathic pulmonary fibrosis. Respir Med. 2012 Nov;106(11):1613-21.

217. Nathan SD, Shlobin OA, Ahmad S, Koch J, Barnett SD, Ad N, et al. Serial development of pulmonary hypertension in patients with idiopathic pulmonary fibrosis. Respiration. 2008;76(3):288-94.

218. Rivera-Lebron BN, Forfia PR, Kreider M, Lee J, Holmes JH, Kawut SM. Echocardiographic and Hemodynamic Predictors of Mortality in Idiopathic Pulmonary Fibrosis. Chest. 2013 Feb 28.

219. Shorr AF, Wainright JL, Cors CS, Lettieri CJ, Nathan SD. Pulmonary hypertension in patients with pulmonary fibrosis awaiting lung transplant. Eur Respir J. 2007 Oct;30(4):715-21.

220. Lettieri CJ, Nathan SD, Barnett SD, Ahmad S, Shorr AF. Prevalence and outcomes of pulmonary arterial hypertension in advanced idiopathic pulmonary fibrosis. Chest. 2006 Mar;129(3):746-52.

221. Zisman DA, Karlamangla AS, Ross DJ, Keane MP, Belperio JA, Saggar R, et al. High-resolution chest CT findings do not predict the presence of pulmonary hypertension in advanced idiopathic pulmonary fibrosis. Chest. 2007 Sep;132(3):773-9.

222. Boutou AK, Pitsiou GG, Trigonis I, Papakosta D, Kontou PK, Chavouzis N, et al. Exercise capacity in idiopathic pulmonary fibrosis: the effect of pulmonary hypertension. Respirology. 2011 Apr;16(3):451-8.

223. Patel NM, Lederer DJ, Borczuk AC, Kawut SM. Pulmonary hypertension in idiopathic pulmonary fibrosis. Chest. 2007 Sep;132(3):998-1006.

224. Cottin V, Cordier JF. The syndrome of combined pulmonary fibrosis and emphysema. Chest. 2009 Jul;136(1):1-2.

225. Cottin V. The impact of emphysema in pulmonary fibrosis. Eur Respir Rev. 2013 Jun 1;22(128):153-7.

226. Cottin V, Nunes H, Brillet PY, Delaval P, Devouassoux G, Tillie-Leblond I, et al. Combined pulmonary fibrosis and emphysema: a distinct underrecognised entity. Eur Respir J. 2005 Oct;26(4):586-93.

227. Cottin V, Le Pavec J, Prevot G, Mal H, Humbert M, Simonneau G, et al. Pulmonary hypertension in patients with combined pulmonary fibrosis and emphysema syndrome. Eur Respir J. 2010 Jan;35(1):105-11.

228. Mejia M, Carrillo G, Rojas-Serrano J, Estrada A, Suarez T, Alonso D, et al. Idiopathic pulmonary fibrosis and emphysema: decreased survival associated with severe pulmonary arterial hypertension. Chest. 2009 Jul;136(1):10-5.

229. Wilkinson M, Langhorne CA, Heath D, Barer GR, Howard P. A pathophysiological study of 10 cases of hypoxic cor pulmonale. Q J Med. 1988 Jan;66(249):65-85.

230. Magee F, Wright JL, Wiggs BR, Pare PD, Hogg JC. Pulmonary vascular structure and function in chronic obstructive pulmonary disease. Thorax. 1988 Mar;43(3):183-9.

231. Jacobson G, Turner AF, Balchum OJ, Jung R. Vascular changes in pulmonary emphysema. The radiologic evaluation by selective and peripheral pulmonary wedge angiography. Am J Roentgenol Radium Ther Nucl Med. 1967 Jun;100(2):374-96.

232. Scarrow GD. The pulmonary angiogram in chronic bronchitis and emphysema. Proc R Soc Med. 1965 Sep;58(9):684-7.

233. Wright JL, Lawson L, Pare PD, Hooper RO, Peretz DI, Nelems JM, et al. The structure and function of the pulmonary vasculature in mild chronic obstructive pulmonary disease. The effect of oxygen and exercise. Am Rev Respir Dis. 1983 Oct;128(4):702-7.

234. Santos S, Peinado VI, Ramirez J, Melgosa T, Roca J, Rodriguez-Roisin R, et al. Characterization of pulmonary vascular remodelling in smokers and patients with mild COPD. Eur Respir J. 2002 Apr;19(4):632-8.

235. Barbera JA. Mechanisms of development of chronic obstructive pulmonary disease-associated pulmonary hypertension. Pulm Circ. 2013 Jan;3(1):160-4.

236. Barbera JA, Peinado VI, Santos S, Ramirez J, Roca J, Rodriguez-Roisin R. Reduced expression of endothelial nitric oxide synthase in pulmonary arteries of smokers. Am J Respir Crit Care Med. 2001 Aug 15;164(4):709-13.

237. Santos S, Peinado VI, Ramirez J, Morales-Blanhir J, Bastos R, Roca J, et al. Enhanced expression of vascular endothelial growth factor in pulmonary arteries of smokers and patients with moderate chronic obstructive pulmonary disease. Am J Respir Crit Care Med. 2003 May 1;167(9):1250-6.

238. Peinado VI, Barbera JA, Abate P, Ramirez J, Roca J, Santos S, et al. Inflammatory reaction in pulmonary muscular arteries of patients with mild chronic obstructive pulmonary disease. Am J Respir Crit Care Med. 1999 May;159(5 Pt 1):1605-11.

239. Ferrer E, Peinado VI, Diez M, Carrasco JL, Musri MM, Martinez A, et al. Effects of cigarette smoke on endothelial function of pulmonary arteries in the guinea pig. Respir Res. 2009;10:76.

240. Ferrer E, Peinado VI, Castaneda J, Prieto-Lloret J, Olea E, Gonzalez-Martin MC, et al. Effects of cigarette smoke and hypoxia on pulmonary circulation in the guinea pig. Eur Respir J. 2011 Sep;38(3):617-27.

241. Joppa P, Petrasova D, Stancak B, Tkacova R. Systemic inflammation in patients with COPD and pulmonary hypertension. Chest. 2006 Aug;130(2):326-33.

242. Eddahibi S, Chaouat A, Tu L, Chouaid C, Weitzenblum E, Housset B, et al. Interleukin-6 gene polymorphism confers susceptibility to pulmonary hypertension in chronic obstructive pulmonary disease. Proc Am Thorac Soc. 2006 Aug;3(6):475-6.

243. Chaouat A, Naeije R, Weitzenblum E. Pulmonary hypertension in COPD. Eur Respir J. 2008 Nov;32(5):1371-85.

244. Renzoni EA, Walsh DA, Salmon M, Wells AU, Sestini P, Nicholson AG, et al. Interstitial vascularity in fibrosing alveolitis. Am J Respir Crit Care Med. 2003 Feb 1;167(3):438-43.

245. Colombat M, Mal H, Groussard O, Capron F, Thabut G, Jebrak G, et al. Pulmonary vascular lesions in end-stage idiopathic pulmonary fibrosis: Histopathologic study on lung explant specimens and correlations with pulmonary hemodynamics. Hum Pathol. 2007 Jan;38(1):60-5.

246. Nathan SD, Noble PW, Tuder RM. Idiopathic pulmonary fibrosis and pulmonary hypertension: connecting the dots. Am J Respir Crit Care Med. 2007 May 1;175(9):875-80.

247. Charbeneau RP, Peters-Golden M. Eicosanoids: mediators and therapeutic targets in fibrotic lung disease. Clin Sci (Lond). 2005 Jun;108(6):479-91.

248. Giaid A, Michel RP, Stewart DJ, Sheppard M, Corrin B, Hamid Q. Expression of endothelin-1 in lungs of patients with cryptogenic fibrosing alveolitis. Lancet. 1993 Jun 19;341(8860):1550-4.

249. Saleh D, Furukawa K, Tsao MS, Maghazachi A, Corrin B, Yanagisawa M, et al. Elevated expression of endothelin-1 and endothelin-converting enzyme-1 in idiopathic pulmonary fibrosis: possible involvement of proinflammatory cytokines. Am J Respir Cell Mol Biol. 1997 Feb;16(2):187-93.

250. Trakada G, Spiropoulos K. Arterial endothelin-1 in interstitial lung disease patients with pulmonary hypertension. Monaldi Arch Chest Dis. 2001 Oct;56(5):379-83.

251. Eddahibi S, Chaouat A, Morrell N, Fadel E, Fuhrman C, Bugnet AS, et al. Polymorphism of the serotonin transporter gene and pulmonary hypertension in chronic obstructive pulmonary disease. Circulation. 2003 Oct 14;108(15):1839-44.
252. Poms AD, Turner M, Farber HW, Meltzer LA, McGoon MD. Comorbid conditions and outcomes in patients with pulmonary arterial hypertension: a REVEAL registry analysis. Chest. 2013 Jul;144(1):169-76.
253. Seeger W, Adir Y, Barbera JA, Champion H, Coghlan JG, Cottin V, et al. Pulmonary hypertension in chronic lung diseases. J Am Coll Cardiol. 2013 Dec 24;62(25 Suppl):D109-16.
254. Fishman A, Martinez F, Naunheim K, Piantadosi S, Wise R, Ries A, et al. A randomized trial comparing lung-volume-reduction surgery with medical therapy for severe emphysema. N Engl J Med. 2003 May 22;348(21):2059-73.
255. Long term domiciliary oxygen therapy in chronic hypoxic cor pulmonale complicating chronic bronchitis and emphysema. Report of the Medical Research Council Working Party. Lancet. 1981 Mar 28;1(8222):681-6.
256. Continuous or nocturnal oxygen therapy in hypoxemic chronic obstructive lung disease: a clinical trial. Nocturnal Oxygen Therapy Trial Group. Ann Intern Med. 1980 Sep;93(3):391-8.
257. Weitzenblum E, Sautegeau A, Ehrhart M, Mammosser M, Pelletier A. Long-term oxygen therapy can reverse the progression of pulmonary hypertension in patients with chronic obstructive pulmonary disease. Am Rev Respir Dis. 1985 Apr;131(4):493-8.
258. Zielinski J, Tobiasz M, Hawrylkiewicz I, Sliwinski P, Palasiewicz G. Effects of long-term oxygen therapy on pulmonary hemodynamics in COPD patients: a 6-year prospective study. Chest. 1998 Jan;113(1):65-70.
259. Minai OA, Chaouat A, Adnot S. Pulmonary hypertension in copd: Epidemiology, significance, and management: pulmonary vascular disease: the global perspective. CHEST Journal. 2010;137(6_suppl):39S-51S.
260. Vonk-Noordegraaf A, Haddad F, Chin KM, Forfia PR, Kawut SM, Lumens J, et al. Right heart adaptation to pulmonary arterial hypertension: physiology and pathobiology. J Am Coll Cardiol. 2013 Dec 24;62(25 Suppl):D22-33.
261. Vonk-Noordegraaf A, Marcus JT, Gan CT, Boonstra A, Postmus PE. Interventricular mechanical asynchrony due to right ventricular pressure overload in pulmonary hypertension plays an important role in impaired left ventricular filling. Chest. 2005 Dec;128(6 Suppl):628S-30S.

262. Bogaard HJ, Abe K, Vonk Noordegraaf A, Voelkel NF. The right ventricle under pressure: cellular and molecular mechanisms of right-heart failure in pulmonary hypertension. Chest. 2009 Mar;135(3):794-804.

263. Bogaard HJ, Natarajan R, Henderson SC, Long CS, Kraskauskas D, Smithson L, et al. Chronic pulmonary artery pressure elevation is insufficient to explain right heart failure. Circulation. 2009 Nov 17;120(20):1951-60.

264. Velez-Roa S, Ciarka A, Najem B, Vachiery JL, Naeije R, van de Borne P. Increased sympathetic nerve activity in pulmonary artery hypertension. Circulation. 2004 Sep 7;110(10):1308-12.

265. McCann GP, Gan CT, Beek AM, Niessen HW, Vonk Noordegraaf A, van Rossum AC. Extent of MRI delayed enhancement of myocardial mass is related to right ventricular dysfunction in pulmonary artery hypertension. AJR Am J Roentgenol. 2007 Feb;188(2):349-55.

266. Sanz J, Dellegrottaglie S, Kariisa M, Sulica R, Poon M, O'Donnell TP, et al. Prevalence and correlates of septal delayed contrast enhancement in patients with pulmonary hypertension. Am J Cardiol. 2007 Aug 15;100(4):731-5.

267. Kramer MR, Valantine HA, Marshall SE, Starnes VA, Theodore J. Recovery of the right ventricle after single-lung transplantation in pulmonary hypertension. Am J Cardiol. 1994 Mar 1;73(7):494-500.

268. Kasimir MT, Seebacher G, Jaksch P, Winkler G, Schmid K, Marta GM, et al. Reverse cardiac remodelling in patients with primary pulmonary hypertension after isolated lung transplantation. Eur J Cardiothorac Surg. 2004 Oct;26(4):776-81.

269. Humbert M, Sitbon O, Chaouat A, Bertocchi M, Habib G, Gressin V, et al. Survival in Patients With Idiopathic, Familial, and Anorexigen-Associated Pulmonary Arterial Hypertension in the Modern Management Era. Circulation. 2010;122(2):156-63.

270. Raymond RJ, Hinderliter AL, Willis PW, Ralph D, Caldwell EJ, Williams W, et al. Echocardiographic predictors of adverse outcomes in primary pulmonary hypertension. J Am Coll Cardiol. 2002 Apr 3;39(7):1214-9.

271. Tei C, Dujardin KS, Hodge DO, Bailey KR, McGoon MD, Tajik AJ, et al. Doppler echocardiographic index for assessment of global right ventricular function. J Am Soc Echocardiogr. 1996 Nov-Dec;9(6):838-47.

272. Forfia PR, Fisher MR, Mathai SC, Housten-Harris T, Hemnes AR, Borlaug BA, et al. Tricuspid annular displacement predicts survival in pulmonary hypertension. Am J Respir Crit Care Med. 2006 Nov 1;174(9):1034-41.

273. Badano LP, Ginghina C, Easaw J, Muraru D, Grillo MT, Lancellotti P, et al. Right ventricle in pulmonary arterial hypertension: haemodynamics, structural changes, imaging, and proposal of a study protocol aimed to assess remodelling and treatment effects. Eur J Echocardiogr. 2010 Jan;11(1):27-37.

274. Hinderliter AL, Willis PWt, Long W, Clarke WR, Ralph D, Caldwell EJ, et al. Frequency and prognostic significance of pericardial effusion in primary pulmonary hypertension. PPH Study Group. Primary pulmonary hypertension. Am J Cardiol. 1999 Aug 15;84(4):481-4, A10.

275. Miller D, Farah MG, Liner A, Fox K, Schluchter M, Hoit BD. The relation between quantitative right ventricular ejection fraction and indices of tricuspid annular motion and myocardial performance. J Am Soc Echocardiogr. 2004 May;17(5):443-7.

276. Lopez-Candales A, Rajagopalan N, Saxena N, Gulyasy B, Edelman K, Bazaz R. Right ventricular systolic function is not the sole determinant of tricuspid annular motion. Am J Cardiol. 2006 Oct 1;98(7):973-7.

277. Hsiao SH, Lin SK, Wang WC, Yang SH, Gin PL, Liu CP. Severe tricuspid regurgitation shows significant impact in the relationship among peak systolic tricuspid annular velocity, tricuspid annular plane systolic excursion, and right ventricular ejection fraction. J Am Soc Echocardiogr. 2006 Jul;19(7):902-10.

278. Yeo TC, Dujardin KS, Tei C, Mahoney DW, McGoon MD, Seward JB. Value of a Doppler-derived index combining systolic and diastolic time intervals in predicting outcome in primary pulmonary hypertension. Am J Cardiol. 1998 May 1;81(9):1157-61.

279. Ghio S, Pazzano AS, Klersy C, Scelsi L, Raineri C, Camporotondo R, et al. Clinical and prognostic relevance of echocardiographic evaluation of right ventricular geometry in patients with idiopathic pulmonary arterial hypertension. Am J Cardiol. 2011 Feb 15;107(4):628-32.

280. Lopez-Candales A, Dohi K, Rajagopalan N, Suffoletto M, Murali S, Gorcsan J, et al. Right ventricular dyssynchrony in patients with pulmonary hypertension is associated with disease severity and functional class. Cardiovasc Ultrasound. 2005;3:23.

281. Hinderliter AL, Willis PWt, Barst RJ, Rich S, Rubin LJ, Badesch DB, et al. Effects of long-term infusion of prostacyclin (epoprostenol) on echocardiographic measures of right ventricular structure and function in primary pulmonary hypertension. Primary Pulmonary Hypertension Study Group. Circulation. 1997 Mar 18;95(6):1479-86.

282. Galie N, Hinderliter AL, Torbicki A, Fourme T, Simonneau G, Pulido T, et al. Effects of the oral endothelin-receptor antagonist bosentan on echocardiographic and doppler measures in patients with pulmonary arterial hypertension. J Am Coll Cardiol. 2003 Apr 16;41(8):1380-6.

283. Nickel N, Golpon H, Greer M, Knudsen L, Olsson K, Westerkamp V, et al. The prognostic impact of follow-up assessments in patients with idiopathic pulmonary arterial hypertension. Eur Respir J. 2011 Sep 1.

284. Saouti N, Westerhof N, Helderman F, Marcus JT, Boonstra A, Postmus PE, et al. Right ventricular oscillatory power is a constant fraction of total power irrespective of pulmonary artery pressure. Am J Respir Crit Care Med. 2010 Nov 15;182(10):1315-20.

285. Mahapatra S, Nishimura RA, Sorajja P, Cha S, McGoon MD. Relationship of pulmonary arterial capacitance and mortality in idiopathic pulmonary arterial hypertension. J Am Coll Cardiol. 2006 Feb 21;47(4):799-803.

286. Sitbon O, Humbert M, Nunes H, Parent F, Garcia G, Herve P, et al. Long-term intravenous epoprostenol infusion in primary pulmonary hypertension: prognostic factors and survival. J Am Coll Cardiol. 2002 Aug 21;40(4):780-8.

287. McLaughlin VV, Shillington A, Rich S. Survival in primary pulmonary hypertension: the impact of epoprostenol therapy. Circulation. 2002 Sep 17;106(12):1477-82.

288. van de Veerdonk MC, Kind T, Marcus JT, Mauritz GJ, Heymans MW, Bogaard HJ, et al. Progressive right ventricular dysfunction in patients with pulmonary arterial hypertension responding to therapy. J Am Coll Cardiol. 2011 Dec 6;58(24):2511-9.

289. Hoeper MM, Lee SH, Voswinckel R, Palazzini M, Jais X, Marinelli A, et al. Complications of right heart catheterization procedures in patients with pulmonary hypertension in experienced centers. J Am Coll Cardiol. 2006 Dec 19;48(12):2546-52.

290. Miyamoto S, Nagaya N, Satoh T, Kyotani S, Sakamaki F, Fujita M, et al. Clinical correlates and prognostic significance of six-minute walk test in patients

with primary pulmonary hypertension. Comparison with cardiopulmonary exercise testing. Am J Respir Crit Care Med. 2000 Feb;161(2 Pt 1):487-92.

291. Gabler NB, French B, Strom BL, Palevsky HI, Taichman DB, Kawut SM, et al. Validation of 6-minute walk distance as a surrogate end point in pulmonary arterial hypertension trials. Circulation. 2012 Jul 17;126(3):349-56.

292. Deboeck G, Scoditti C, Huez S, Vachiery JL, Lamotte M, Sharples L, et al. Exercise testing to predict outcome in idiopathic versus associated pulmonary arterial hypertension. Eur Respir J. 2012 Dec;40(6):1410-9.

293. Lee WT, Peacock AJ, Johnson MK. The role of per cent predicted 6-min walk distance in pulmonary arterial hypertension. Eur Respir J. 2010 Dec;36(6):1294-301.

294. Mereles D, Ehlken N, Kreuscher S, Ghofrani S, Hoeper MM, Halank M, et al. Exercise and respiratory training improve exercise capacity and quality of life in patients with severe chronic pulmonary hypertension. Circulation. 2006 Oct 3;114(14):1482-9.

295. Degano B, Sitbon O, Savale L, Garcia G, O'Callaghan DS, Jais X, et al. Characterization of pulmonary arterial hypertension patients walking more than 450 m in 6 min at diagnosis. Chest. 2010 Jun;137(6):1297-303.

296. Yap LB, Mukerjee D, Timms PM, Ashrafian H, Coghlan JG. Natriuretic peptides, respiratory disease, and the right heart. Chest. 2004 Oct;126(4):1330-6.

297. Blyth KG, Groenning BA, Mark PB, Martin TN, Foster JE, Steedman T, et al. NT-proBNP can be used to detect right ventricular systolic dysfunction in pulmonary hypertension. European Respiratory Journal. 2007;29(4):737-44.

298. Nagaya N, Nishikimi T, Okano Y, Uematsu M, Satoh T, Kyotani S, et al. Plasma brain natriuretic peptide levels increase in proportion to the extent of right ventricular dysfunction in pulmonary hypertension. J Am Coll Cardiol. 1998 Jan;31(1):202-8.

299. Nagaya N, Nishikimi T, Uematsu M, Satoh T, Kyotani S, Sakamaki F, et al. Plasma brain natriuretic peptide as a prognostic indicator in patients with primary pulmonary hypertension. Circulation. 2000 Aug 22;102(8):865-70.

300. Fijalkowska A, Kurzyna M, Torbicki A, Szewczyk G, Florczyk M, Pruszczyk P, et al. Serum N-terminal brain natriuretic peptide as a prognostic parameter in patients with pulmonary hypertension. Chest. 2006 May;129(5):1313-21.

301. Mauritz GJ, Rizopoulos D, Groepenhoff H, Tiede H, Felix J, Eilers P, et al. Usefulness of serial N-terminal pro-B-type natriuretic peptide measurements for determining prognosis in patients with pulmonary arterial hypertension. Am J Cardiol. 2011 Dec 1;108(11):1645-50.

302. Roeleveld RJ, Vonk-Noordegraaf A, Marcus JT, Bronzwaer JG, Marques KM, Postmus PE, et al. Effects of epoprostenol on right ventricular hypertrophy and dilatation in pulmonary hypertension. Chest. 2004 Feb;125(2):572-9.

303. Hoeper MM, Tongers J, Leppert A, Baus S, Maier R, Lotz J. Evaluation of right ventricular performance with a right ventricular ejection fraction thermodilution catheter and MRI in patients with pulmonary hypertension. Chest. 2001 Aug;120(2):502-7.

304. Marcus JT, Noordegraaf AV, Roeleveld RJ, Postmus PE, Heethaar RM, Van Rossum AC, et al. Impaired left ventricular filling due to right ventricular pressure overload in primary pulmonary hypertension - Noninvasive monitoring using MRI. Chest. 2001;119(6):1761-5.

305. Mauritz GJ, Kind T, Marcus JT, Bogaard HJ, van de Veerdonk M, Postmus PE, et al. Progressive changes in right ventricular geometric shortening and long-term survival in pulmonary arterial hypertension. Chest. 2012 Apr;141(4):935-43.

306. Mauritz GJ, Marcus JT, Boonstra A, Postmus PE, Westerhof N, Vonk-Noordegraaf A. Non-invasive stroke volume assessment in patients with pulmonary arterial hypertension: left-sided data mandatory. Journal of Cardiovascular Magnetic Resonance. 2008;10.

307. Kondo C, Caputo GR, Masui T, Foster E, O'Sullivan M, Stulbarg MS, et al. Pulmonary hypertension: pulmonary flow quantification and flow profile analysis with velocity-encoded cine MR imaging. Radiology. 1992 Jun;183(3):751-8.

308. Ley S, Mereles D, Puderbach M, Gruenig E, Schock H, Eichinger M, et al. Value of MR phase-contrast flow measurements for functional assessment of pulmonary arterial hypertension. Eur Radiol. 2007 Jul;17(7):1892-7.

309. Sanz J, Kuschnir P, Rius T, Salguero R, Sulica R, Einstein AJ, et al. Pulmonary arterial hypertension: noninvasive detection with phase-contrast MR imaging. Radiology. 2007 Apr;243(1):70-9.

310. Sanz J, Kariisa M, Dellegrottaglie S, Prat-Gonzalez S, Garcia MJ, Fuster V, et al. Evaluation of pulmonary artery stiffness in pulmonary hypertension with cardiac magnetic resonance. JACC Cardiovasc Imaging. 2009 Mar;2(3):286-95.

311. Kawasaki T, Sasayama S, Yagi S, Asakawa T, Hirai T. Non-invasive assessment of the age related changes in stiffness of major branches of the human arteries. Cardiovasc Res. 1987 Sep;21(9):678-87.

312. Bogren HG, Klipstein RH, Mohiaddin RH, Firmin DN, Underwood SR, Rees RS, et al. Pulmonary artery distensibility and blood flow patterns: a magnetic resonance study of normal subjects and of patients with pulmonary arterial hypertension. Am Heart J. 1989 Nov;118(5 Pt 1):990-9.

313. Paz R, Mohiaddin RH, Longmore DB. Magnetic resonance assessment of the pulmonary arterial trunk anatomy, flow, pulsatility and distensibility. Eur Heart J. 1993 Nov;14(11):1524-30.

314. Gan CT, Lankhaar JW, Westerhof N, Marcus JT, Becker A, Twisk JW, et al. Noninvasively assessed pulmonary artery stiffness predicts mortality in pulmonary arterial hypertension. Chest. 2007 Dec;132(6):1906-12.

315. Kang KW, Chang HJ, Kim YJ, Choi BW, Lee HS, Yang WI, et al. Cardiac magnetic resonance imaging-derived pulmonary artery distensibility index correlates with pulmonary artery stiffness and predicts functional capacity in patients with pulmonary arterial hypertension. Circ J. 2011 Aug 25;75(9):2244-51.

316. McAllister DA, Maclay JD, Mills NL, Mair G, Miller J, Anderson D, et al. Arterial stiffness is independently associated with emphysema severity in patients with chronic obstructive pulmonary disease. Am J Respir Crit Care Med. 2007 Dec 15;176(12):1208-14.

317. Roeleveld RJ, Marcus JT, Faes TJ, Gan TJ, Boonstra A, Postmus PE, et al. Interventricular septal configuration at mr imaging and pulmonary arterial pressure in pulmonary hypertension. Radiology. 2005 Mar;234(3):710-7.

318. Saba TS, Foster J, Cockburn M, Cowan M, Peacock AJ. Ventricular mass index using magnetic, resonance imaging accurately estimates pulmonary artery pressure. European Respiratory Journal. 2002;20(6):1519-24.

319. Laffon E, Vallet C, Bernard V, Montaudon M, Ducassou D, Laurent F, et al. A computed method for noninvasive MRI assessment of pulmonary arterial hypertension. J Appl Physiol (1985). 2004 Feb;96(2):463-8.

320. Roeleveld RJ, Marcus JT, Boonstra A, Postmus PE, Marques KM, Bronzwaer JGF, et al. A comparison of noninvasive MRI-based methods of estimating pulmonary artery pressure in pulmonary hypertension. Journal of Magnetic Resonance Imaging. 2005;22(1):67-72.

321. Moulton MJ, Creswell LL, Ungacta FF, Downing SW, Szabo BA, Pasque MK. Magnetic resonance imaging provides evidence for remodeling of the right ventricle after single-lung transplantation for pulmonary hypertension. Circulation. 1996 Nov 1;94(9 Suppl):II312-9.

322. Mohiaddin RH, Paz R, Theodoropoulos S, Firmin DN, Longmore DB, Yacoub MH. Magnetic resonance characterization of pulmonary arterial blood flow after single lung transplantation. J Thorac Cardiovasc Surg. 1991 Jun;101(6):1016-23.

323. Kreitner KF, Ley S, Kauczor HU, Mayer E, Kramm T, Pitton MB, et al. Chronic thromboembolic pulmonary hypertension: pre- and postoperative assessment with breath-hold MR imaging techniques. Radiology. 2004 Aug;232(2):535-43.

324. Michelakis ED, Tymchak W, Noga M, Webster L, Wu XC, Lien D, et al. Long-term treatment with oral sildenafil is safe and improves functional capacity and hemodynamics in patients with pulmonary arterial hypertension. Circulation. 2003 Oct 28;108(17):2066-9.

325. Wilkins MR, Paul GA, Strange JW, Tunariu N, Gin-Sing W, Banya WA, et al. Sildenafil versus endothelin receptor antagonist for pulmonary hypertension (SERAPH) study. Am J Respir Crit Care Med. 2005;171(11):1292-7.

326. Chin KM, Kingman M, de Lemos JA, Warner JJ, Reimold S, Peshock R, et al. Changes in right ventricular structure and function assessed using cardiac magnetic resonance imaging in bosentan-treated patients with pulmonary arterial hypertension. American Journal of Cardiology. 2008 Jun;101(11):1669-72.

327. Blalock SE, Matulevicius S, Mitchell LC, Reimold S, Warner J, Peshock R, et al. Long-term outcomes with ambrisentan monotherapy in pulmonary arterial hypertension. J Card Fail. 2010 Feb;16(2):121-7.

328. Allanore Y, Meune C, Vignaux O, Weber S, Legmann P, Kahan A. Bosentan increases myocardial perfusion and function in systemic sclerosis: a magnetic resonance imaging and Tissue-Doppler echography study. J Rheumatol. 2006 Dec;33(12):2464-9.

329. van Wolferen SA, Boonstra A, Marcus JT, Marques KMJ, Bronzwaer JGF, Postmus PE, et al. Right ventricular reverse remodelling after sildenafil in pulmonary arterial hypertension. Heart. 2006;92(12):1860-1.

330. van Wolferen SA, van de Veerdonk MC, Mauritz GJ, Jacobs W, Marcus JT, Marques KM, et al. Clinically significant change in stroke volume in pulmonary hypertension. Chest. 2011 May;139(5):1003-9.

331. Handoko ML, de Man FS, Allaart CP, Paulus WJ, Westerhof N, Vonk-Noordegraaf A. Perspectives on novel therapeutic strategies for right heart failure in pulmonary arterial hypertension: lessons from the left heart. Eur Respir Rev. 2010 Mar;19(115):72-82.

332. Galie N, Hoeper MM, Humbert M, Torbicki A, Vachiery JL, Barbera JA, et al. Guidelines for the diagnosis and treatment of pulmonary hypertension. European Respiratory Journal. 2009;34(6):1219-63.

333. Burrows B, Kettel LJ, Niden AH, Rabinowitz M, Diener CF. Patterns of cardiovascular dysfunction in chronic obstructive lung disease. N Engl J Med. 1972 Apr 27;286(17):912-8.

334. Oswald-Mammosser M, Apprill M, Bachez P, Ehrhart M, Weitzenblum E. Pulmonary hemodynamics in chronic obstructive pulmonary disease of the emphysematous type. Respiration. 1991;58(5-6):304-10.

335. Weitzenblum E, Hirth C, Ducolone A, Mirhom R, Rasaholinjanahary J, Ehrhart M. Prognostic value of pulmonary artery pressure in chronic obstructive pulmonary disease. Thorax. 1981 Oct;36(10):752-8.

336. Vonk-Noordegraaf A, Marcus JT, Holverda S, Roseboom B, Postmus PE. EArly changes of cardiac structure and function in copd patients with mild hypoxemia*. CHEST Journal. 2005;127(6):1898-903.

337. MacNee W, Wathen CG, Flenley DC, Muir AD. The effects of controlled oxygen therapy on ventricular function in patients with stable and decompensated cor pulmonale. Am Rev Respir Dis. 1988 Jun;137(6):1289-95.

338. Timms RM, Khaja FU, Williams GW. Hemodynamic response to oxygen therapy in chronic obstructive pulmonary disease. Ann Intern Med. 1985 Jan;102(1):29-36.

339. Holverda S, Rietema H, Westerhof N, Marcus JT, Gan CT, Postmus PE, et al. Stroke volume increase to exercise in chronic obstructive pulmonary disease is limited by increased pulmonary artery pressure. Heart. 2009 Feb;95(2):137-41.

340. Rietema H, Holverda S, Bogaard HJ, Marcus JT, Smit HJ, Westerhof N, et al. Sildenafil treatment in COPD does not affect stroke volume or exercise capacity. Eur Respir J. 2008 Apr;31(4):759-64.

341. Dernaika TA, Beavin M, Kinasewitz GT. Iloprost improves gas exchange and exercise tolerance in patients with pulmonary hypertension and chronic obstructive pulmonary disease. Respiration. 2010;79(5):377-82.

342. Stolz D, Rasch H, Linka A, Di Valentino M, Meyer A, Brutsche M, et al. A randomised, controlled trial of bosentan in severe COPD. Eur Respir J. 2008 Sep;32(3):619-28.

343. Blanco I, Gimeno E, Munoz PA, Pizarro S, Gistau C, Rodriguez-Roisin R, et al. Hemodynamic and gas exchange effects of sildenafil in patients with chronic obstructive pulmonary disease and pulmonary hypertension. Am J Respir Crit Care Med. 2010 Feb 1;181(3):270-8.

344. Boeck L, Tamm M, Grendelmeier P, Stolz D. Acute effects of aerosolized iloprost in COPD related pulmonary hypertension - a randomized controlled crossover trial. PLoS One. 2012;7(12):e52248.

345. Alp S, Skrygan M, Schmidt WE, Bastian A. Sildenafil improves hemodynamic parameters in COPD--an investigation of six patients. Pulm Pharmacol Ther. 2006;19(6):386-90.

346. Light RW, Mintz HM, Linden GS, Brown SE. Hemodynamics of patients with severe chronic obstructive pulmonary disease during progressive upright exercise. Am Rev Respir Dis. 1984 Sep;130(3):391-5.

347. Stewart RI, Lewis CM. Cardiac output during exercise in patients with COPD. Chest. 1986 Feb;89(2):199-205.

348. Holverda S, Rietema H, Bogaard HJ, Westerhof N, Postmus PE, Boonstra A, et al. Acute effects of sildenafil on exercise pulmonary hemodynamics and capacity in patients with COPD. Pulm Pharmacol Ther. 2008;21(3):558-64.

349. Blanco I, Santos S, Gea J, Guell R, Torres F, Gimeno-Santos E, et al. Sildenafil to improve respiratory rehabilitation outcomes in COPD: a controlled trial. Eur Respir J. 2013 Oct;42(4):982-92.

350. King TE, Jr., Behr J, Brown KK, du Bois RM, Lancaster L, de Andrade JA, et al. BUILD-1: a randomized placebo-controlled trial of bosentan in idiopathic pulmonary fibrosis. Am J Respir Crit Care Med. 2008 Jan 1;177(1):75-81.

351. Raghu G, Behr J, Brown KK, Egan JJ, Kawut SM, Flaherty KR, et al. Treatment of idiopathic pulmonary fibrosis with ambrisentan: a parallel, randomized trial. Ann Intern Med. 2013 May 7;158(9):641-9.

352. Corte TJ, Keir GJ, Dimopoulos K, Howard L, Corris PA, Parfitt L, et al. Bosentan in pulmonary hypertension associated with fibrotic idiopathic interstitial pneumonia. Am J Respir Crit Care Med. 2014 Jul 15;190(2):208-17.

353. Collard HR, Anstrom KJ, Schwarz MI, Zisman DA. Sildenafil improves walk distance in idiopathic pulmonary fibrosis. Chest. 2007 Mar;131(3):897-9.

354. Hoeper MM, Halank M, Wilkens H, Gunther A, Weimann G, Gebert I, et al. Riociguat for interstitial lung disease and pulmonary hypertension: a pilot trial. Eur Respir J. 2013 Apr;41(4):853-60.

355. Valerio G, Bracciale P, Grazia D'Agostino A. Effect of bosentan upon pulmonary hypertension in chronic obstructive pulmonary disease. Ther Adv Respir Dis. 2009 Feb;3(1):15-21.

356. Hurdman J, Condliffe R, Elliot CA, Swift A, Rajaram S, Davies C, et al. Pulmonary hypertension in COPD: results from the ASPIRE registry. Eur Respir J. 2012 Sep 27.

357. Calverley PM, Howatson R, Flenley DC, Lamb D. Clinicopathological correlations in cor pulmonale. Thorax. 1992 Jul;47(7):494-8.

358. Zvezdin B, Milutinov S, Kojicic M, Hadnadjev M, Hromis S, Markovic M, et al. A postmortem analysis of major causes of early death in patients hospitalized with COPD exacerbation. Chest. 2009 Aug;136(2):376-80.

359. Marcus JT, Noordegraaf AV, De Vries P, Van Rossum AC, Roseboom B, Heethaar RM, et al. MRI evaluation of right ventricular pressure overload in chronic obstructive pulmonary disease. Journal of Magnetic Resonance Imaging. 1998;8(5):999-1005.

360. Gao Y, Du X, Qin W, Li K. Assessment of the right ventricular function in patients with chronic obstructive pulmonary disease using MRI. Acta Radiol. 2011 Sep 01;52(7):711-5.

361. Hilde JM, Skjorten I, Grotta OJ, Hansteen V, Melsom MN, Hisdal J, et al. Right ventricular dysfunction and remodeling in chronic obstructive pulmonary disease without pulmonary hypertension. J Am Coll Cardiol. 2013 Sep 17;62(12):1103-11.

362. Raeside DA, Brown A, Patel KR, Welsh D, Peacock AJ. Ambulatory pulmonary artery pressure monitoring during sleep and exercise in normal individuals and patients with COPD. Thorax. 2002 Dec;57(12):1050-3.

363. Biernacki W, Flenley DC, Muir AL, MacNee W. Pulmonary hypertension and right ventricular function in patients with COPD. Chest. 1988 Dec;94(6):1169-75.

364. Turnbull LW, Ridgway JP, Biernacki W, McRitchie H, Muir AL, Best JJ, et al. Assessment of the right ventricle by magnetic resonance imaging in chronic obstructive lung disease. Thorax. 1990 Aug;45(8):597-601.

365. Chang CL, Robinson SC, Mills GD, Sullivan GD, Karalus NC, McLachlan JD, et al. Biochemical markers of cardiac dysfunction predict mortality in acute exacerbations of COPD. Thorax. 2011 Sep;66(9):764-8.

366. Hoiseth AD, Omland T, Hagve TA, Brekke PH, Soyseth V. NT-proBNP independently predicts long term mortality after acute exacerbation of COPD - a prospective cohort study. Respir Res. 2012;13:97.

367. Leuchte HH, Baumgartner RA, Nounou ME, Vogeser M, Neurohr C, Trautnitz M, et al. Brain natriuretic peptide is a prognostic parameter in chronic lung disease. Am J Respir Crit Care Med. 2006 Apr 1;173(7):744-50.

368. Inoue Y, Kawayama T, Iwanaga T, Aizawa H. High plasma brain natriuretic peptide levels in stable COPD without pulmonary hypertension or cor pulmonale. Intern Med. 2009;48(7):503-12.

369. Stolz D, Breidthardt T, Christ-Crain M, Bingisser R, Miedinger D, Leuppi J, et al. Use of B-type natriuretic peptide in the risk stratification of acute exacerbations of COPD. Chest. 2008 May;133(5):1088-94.

370. Andersen CU, Mellemkjaer S, Nielsen-Kudsk JE, Sonderskov LD, Laursen BE, Simonsen U, et al. Echocardiographic screening for pulmonary hypertension in stable COPD out-patients and NT-proBNP as a rule-out test. COPD. 2012 Aug;9(5):505-12.

371. Gale CP, White JE, Hunter A, Owen J, Allen J, Watson J, et al. Predicting mortality and hospital admission in patients with COPD: significance of NT pro-BNP, clinical and echocardiographic assessment. J Cardiovasc Med (Hagerstown). 2011 Sep;12(9):613-8.

372. Khanna D, Gladue H, Channick R, Chung L, Distler O, Furst DE, et al. Recommendations for screening and detection of connective tissue disease-associated pulmonary arterial hypertension. Arthritis Rheum. 2013 Dec;65(12):3194-201.

373. Peacock AJ, Crawley S, McLure L, Blyth K, Vizza CD, Poscia R, et al. Changes in right ventricular function measured by cardiac magnetic resonance imaging in patients receiving pulmonary arterial hypertension-targeted therapy: the EURO-MR study. Circ Cardiovasc Imaging. 2014 Jan;7(1):107-14.

374. National Institute for Clinical Excellence. Management of chronic obstructive pulmonary disease in adults in primary and secondary care, CG101. 2010.

375. Adir Y, Shachner R, Amir O, Humbert M. Severe pulmonary hypertension associated with emphysema: a new phenotype? Chest. 2012 Dec;142(6):1654-8.

376. Bishop JM, Cross KW. Use of other physiological variables to predict pulmonary arterial pressure in patients with chronic respiratory disease. Multicentre study. Eur Heart J. 1981 Dec;2(6):509-17.

377. Zisman DA, Ross DJ, Belperio JA, Saggar R, Lynch JP, 3rd, Ardehali A, et al. Prediction of pulmonary hypertension in idiopathic pulmonary fibrosis. Respiratory Medicine. 2007 Oct;101(10):2153-9.

378. Boerrigter BG, Bogaard HJ, Trip P, Groepenhoff H, Rietema H, Holverda S, et al. Ventilatory and cardiocirculatory exercise profiles in COPD: the role of pulmonary hypertension. Chest. 2012 Nov;142(5):1166-74.

379. Fradley MG, Larson MG, Cheng S, McCabe E, Coglianese E, Shah RV, et al. Reference limits for N-terminal-pro-B-type natriuretic peptide in healthy individuals (from the Framingham Heart Study). Am J Cardiol. 2011 Nov 1;108(9):1341-5.

380. Burgess MI, Mogulkoc N, Bright-Thomas RJ, Bishop P, Egan JJ, Ray SG. Comparison of echocardiographic markers of right ventricular function in determining prognosis in chronic pulmonary disease. J Am Soc Echocardiogr. 2002 Jun;15(6):633-9.

381. Bach DS, Curtis JL, Christensen PJ, Iannettoni MD, Whyte RI, Kazerooni EA, et al. Preoperative echocardiographic evaluation of patients referred for lung volume reduction surgery. Chest. 1998 Oct;114(4):972-80.

382. Tramarin R, Torbicki A, Marchandise B, Laaban JP, Morpurgo M. Doppler echocardiographic evaluation of pulmonary artery pressure in chronic obstructive pulmonary disease. A European multicentre study. Working Group on Noninvasive Evaluation of Pulmonary Artery Pressure. European Office of the World Health Organization, Copenhagen. Eur Heart J. 1991 Feb;12(2):103-11.

383. Laaban JP, Diebold B, Zelinski R, Lafay M, Raffoul H, Rochemaure J. Noninvasive estimation of systolic pulmonary artery pressure using Doppler echocardiography in patients with chronic obstructive pulmonary disease. Chest. 1989 Dec;96(6):1258-62.

384. Fisher MR, Criner GJ, Fishman AP, Hassoun PM, Minai OA, Scharf SM, et al. Estimating pulmonary artery pressures by echocardiography in patients with emphysema. Eur Respir J. 2007 Nov;30(5):914-21.

385. Keller R, Ragaz A, Borer P. Predictors for early mortality in patients with long-term oxygen home therapy. Respiration. 1985;48(3):216-21.

386. Dubois P, Machiels J, Smeets F, Delwiche JP, Lulling J. CO transfer capacity as a determining factor of survival for severe hypoxaemic COPD patients under long-term oxygen therapy. Eur Respir J. 1990 Oct;3(9):1042-7.

387. Skwarski K, MacNee W, Wraith PK, Sliwinski P, Zielinski J. Predictors of survival in patients with chronic obstructive pulmonary disease treated with long-term oxygen therapy. Chest. 1991 Dec;100(6):1522-7.

388. Sabit R, Bolton CE, Fraser AG, Edwards JM, Edwards PH, Ionescu AA, et al. Sub-clinical left and right ventricular dysfunction in patients with COPD. Respir Med. 2010 Aug;104(8):1171-8.

389. Mills NL, Miller JJ, Anand A, Robinson SD, Frazer GA, Anderson D, et al. Increased arterial stiffness in patients with chronic obstructive pulmonary disease: a mechanism for increased cardiovascular risk. Thorax. 2008 Apr;63(4):306-11.

390. Maclay JD, McAllister DA, Mills NL, Paterson FP, Ludlam CA, Drost EM, et al. Vascular dysfunction in chronic obstructive pulmonary disease. Am J Respir Crit Care Med. 2009 Sep 15;180(6):513-20.

391. Mahmud A, Feely J. Effect of smoking on arterial stiffness and pulse pressure amplification. Hypertension. 2003 Jan;41(1):183-7.

392. Giacomin E, Palmerini E, Ballo P, Zaca V, Bova G, Mondillo S. Acute effects of caffeine and cigarette smoking on ventricular long-axis function in healthy subjects. Cardiovasc Ultrasound. 2008;6:9.

393. Abroug F, Ouanes-Besbes L, Nciri N, Sellami N, Addad F, Hamda KB, et al. Association of left-heart dysfunction with severe exacerbation of chronic obstructive pulmonary disease: diagnostic performance of cardiac biomarkers. Am J Respir Crit Care Med. 2006 Nov 1;174(9):990-6.

394. Ouanes I, Jalloul F, Ayed S, Dachraoui F, Ouanes-Besbes L, Fekih Hassen M, et al. N-terminal proB-type natriuretic peptide levels aid the diagnosis of left ventricular dysfunction in patients with severe acute exacerbations of chronic obstructive pulmonary disease and renal dysfunction. Respirology. 2012 May;17(4):660-6.

395. Humbert M, Sitbon O, Yaici A, Montani D, O'Callaghan DS, Jais X, et al. Survival in incident and prevalent cohorts of patients with pulmonary arterial hypertension. European Respiratory Journal. 2010;36(3):549-55.

396. Naeije R. Assessment of right ventricular function in pulmonary hypertension. Curr Hypertens Rep. 2015 May;17(5):35.

397. Goto Y, Slinker BK, LeWinter MM. Similar normalized Emax and O2 consumption-pressure-volume area relation in rabbit and dog. The American journal of physiology. 1988 Aug;255(2 Pt 2):H366-74.

398. Suga H, Sagawa K, Shoukas AA. Load independence of the instantaneous pressure-volume ratio of the canine left ventricle and effects of epinephrine and heart rate on the ratio. Circ Res. 1973 Mar;32(3):314-22.

399. Redington AN, Rigby ML, Shinebourne EA, Oldershaw PJ. Changes in the pressure-volume relation of the right ventricle when its loading conditions are modified. Br Heart J. 1990 Jan;63(1):45-9.

400. Sanz J, Garcia-Alvarez A, Fernandez-Friera L, Nair A, Mirelis JG, Sawit ST, et al. Right ventriculo-arterial coupling in pulmonary hypertension: a magnetic resonance study. Heart. 2011 Sep 13.

401. Wauthy P, Pagnamenta A, Vassalli F, Naeije R, Brimioulle S. Right ventricular adaptation to pulmonary hypertension: an interspecies comparison. Am J Physiol Heart Circ Physiol. 2004 Apr;286(4):H1441-7.

402. Kerbaul F, Rondelet B, Motte S, Fesler P, Hubloue I, Ewalenko P, et al. Isoflurane and desflurane impair right ventricular-pulmonary arterial coupling in dogs. Anesthesiology. 2004 Dec;101(6):1357-62.

403. Rex S, Missant C, Segers P, Rossaint R, Wouters PF. Epoprostenol treatment of acute pulmonary hypertension is associated with a paradoxical decrease in right ventricular contractility. Intensive Care Med. 2008 Jan;34(1):179-89.

404. Lambermont B, Ghuysen A, Kolh P, Tchana-Sato V, Segers P, Gerard P, et al. Effects of endotoxic shock on right ventricular systolic function and mechanical efficiency. Cardiovasc Res. 2003 Aug 01;59(2):412-8.

405. de Man FS, Handoko ML, van Ballegoij JJ, Schalij I, Bogaards SJ, Postmus PE, et al. Bisoprolol delays progression towards right heart failure in experimental pulmonary hypertension. Circ Heart Fail. 2012 Jan;5(1):97-105.

406. Gomez-Arroyo JG, Farkas L, Alhussaini AA, Farkas D, Kraskauskas D, Voelkel NF, et al. The monocrotaline model of pulmonary hypertension in perspective. Am J Physiol Lung Cell Mol Physiol. 2012 Feb 15;302(4):L363-9.

407. Dewachter C, Dewachter L, Rondelet B, Fesler P, Brimioulle S, Kerbaul F, et al. Activation of apoptotic pathways in experimental acute afterload-induced right ventricular failure. Crit Care Med. 2010 Jun;38(6):1405-13.

408. Rondelet B, Dewachter C, Kerbaul F, Kang X, Fesler P, Brimioulle S, et al. Prolonged overcirculation-induced pulmonary arterial hypertension as a cause of right ventricular failure. Eur Heart J. 2012 Apr;33(8):1017-26.

409. Belhaj A, Dewachter L, Kerbaul F, Brimioulle S, Dewachter C, Naeije R, et al. Heme oxygenase-1 and inflammation in experimental right ventricular failure on prolonged overcirculation-induced pulmonary hypertension. PLoS One. 2013;8(7):e69470.

410. Rondelet B, Kerbaul F, Motte S, van Beneden R, Remmelink M, Brimioulle S, et al. Bosentan for the prevention of overcirculation-induced experimental pulmonary arterial hypertension. Circulation. 2003 Mar 11;107(9):1329-35.

411. Pagnamenta A, Dewachter C, McEntee K, Fesler P, Brimioulle S, Naeije R. Early right ventriculo-arterial uncoupling in borderline pulmonary hypertension on experimental heart failure. J Appl Physiol. 2010 Oct;109(4):1080-5.

412. Kuehne T, Yilmaz S, Steendijk P, Moore P, Groenink M, Saaed M, et al. Magnetic resonance imaging analysis of right ventricular pressure-volume loops: in vivo validation and clinical application in patients with pulmonary hypertension. Circulation. [Evaluation Studies]. 2004 Oct 5;110(14):2010-6.

413. Tedford RJ, Mudd JO, Girgis RE, Mathai SC, Zaiman AL, Housten-Harris T, et al. Right ventricular dysfunction in systemic sclerosis-associated pulmonary arterial hypertension. Circ Heart Fail. 2013 Sep 1;6(5):953-63.

414. Kass DA, Beyar R, Lankford E, Heard M, Maughan WL, Sagawa K. Influence of contractile state on curvilinearity of in situ end-systolic pressure-volume relations. Circulation. 1989 Jan;79(1):167-78.

415. Vanderpool RR, Pinsky MR, Naeije R, Deible C, Kosaraju V, Bunner C, et al. RV-pulmonary arterial coupling predicts outcome in patients referred for pulmonary hypertension. Heart. 2014 Sep 11.

416. Trip P, Rain S, Handoko ML, van der Bruggen C, Bogaard HJ, Marcus JT, et al. Clinical relevance of right ventricular diastolic stiffness in pulmonary hypertension. Eur Respir J. 2015 Jun;45(6):1603-12.

417. Mathai SC, Bueso M, Hummers LK, Boyce D, Lechtzin N, Le Pavec J, et al. Disproportionate elevation of N-terminal pro-brain natriuretic peptide in scleroderma-related pulmonary hypertension. Eur Respir J. 2010 Jan;35(1):95-104.

418. Chung L, Liu J, Parsons L, Hassoun PM, McGoon M, Badesch DB, et al. Characterization of connective tissue disease-associated pulmonary arterial

hypertension from REVEAL: identifying systemic sclerosis as a unique phenotype. Chest. 2010 Dec;138(6):1383-94.

419. Spruijt OA, de Man FS, Groepenhoff H, Oosterveer F, Westerhof N, Vonk-Noordegraaf A, et al. The effects of exercise on right ventricular contractility and right ventricular-arterial coupling in pulmonary hypertension. Am J Respir Crit Care Med. 2015 May 01;191(9):1050-7.

420. Vanderpool RR, Rischard F, Naeije R, Hunter K, Simon MA. Simple functional imaging of the right ventricle in pulmonary hypertension: Can right ventricular ejection fraction be improved? Int J Cardiol. 2016 Nov 15;223:93-4.

421. Bellofiore A, Chesler NC. Methods for measuring right ventricular function and hemodynamic coupling with the pulmonary vasculature. Ann Biomed Eng. 2013 Jul;41(7):1384-98.

422. Forfia PR, Vachiery JL. Echocardiography in pulmonary arterial hypertension. Am J Cardiol. 2012 Sep 15;110(6 Suppl):16S-24S.

423. Kerbaul F, Rondelet B, Motte S, Fesler P, Hubloue I, Ewalenko P, et al. Effects of norepinephrine and dobutamine on pressure load-induced right ventricular failure. Crit Care Med. 2004 Apr;32(4):1035-40.

424. Kerbaul F, Rondelet B, Demester JP, Fesler P, Huez S, Naeije R, et al. Effects of levosimendan versus dobutamine on pressure load-induced right ventricular failure. Crit Care Med. 2006 Nov;34(11):2814-9.

425. Missant C, Rex S, Segers P, Wouters PF. Levosimendan improves right ventriculovascular coupling in a porcine model of right ventricular dysfunction. Crit Care Med. 2007 Mar;35(3):707-15.

426. Wauthy P, Abdel Kafi S, Mooi WJ, Naeije R, Brimioulle S. Inhaled nitric oxide versus prostacyclin in chronic shunt-induced pulmonary hypertension. J Thorac Cardiovasc Surg. 2003 Nov;126(5):1434-41.

427. Kerbaul F, Brimioulle S, Rondelet B, Dewachter C, Hubloue I, Naeije R. How prostacyclin improves cardiac output in right heart failure in conjunction with pulmonary hypertension. Am J Respir Crit Care Med. 2007 Apr 15;175(8):846-50.

428. Fesler P, Pagnamenta A, Rondelet B, Kerbaul F, Naeije R. Effects of sildenafil on hypoxic pulmonary vascular function in dogs. J Appl Physiol (1985). 2006 Oct;101(4):1085-90.

429. Borgdorff MA, Bartelds B, Dickinson MG, Boersma B, Weij M, Zandvoort A, et al. Sildenafil enhances systolic adaptation, but does not prevent diastolic

dysfunction, in the pressure-loaded right ventricle. Eur J Heart Fail. 2012 Sep;14(9):1067-74.

430. Macchia A, Marchioli R, Tognoni G, Scarano M, Marfisi R, Tavazzi L, et al. Systematic review of trials using vasodilators in pulmonary arterial hypertension: why a new approach is needed. Am Heart J. 2010 Feb;159(2):245-57.

431. Gan CT, McCann GP, Marcus JT, van Wolferen SA, Twisk JW, Boonstra A, et al. NT-proBNP reflects right ventricular structure and function in pulmonary hypertension. European Respiratory Journal. 2006;28(6):1190-4.

432. Galie N, Humbert M, Vachiery JL, Gibbs S, Lang I, Torbicki A, et al. 2015 ESC/ERS Guidelines for the diagnosis and treatment of pulmonary hypertension: The Joint Task Force for the Diagnosis and Treatment of Pulmonary Hypertension of the European Society of Cardiology (ESC) and the European Respiratory Society (ERS): Endorsed by: Association for European Paediatric and Congenital Cardiology (AEPC), International Society for Heart and Lung Transplantation (ISHLT). Eur Respir J. 2015 Oct;46(4):903-75.

433. Bradlow WM, Hughes ML, Keenan NG, Bucciarelli-Ducci C, Assomull R, Gibbs JSR, et al. Measuring the Heart in Pulmonary Arterial Hypertension (PAH): Implications for Trial Study Size. Journal of Magnetic Resonance Imaging. 2010 Jan;31(1):117-24.

434. Stevens GR, Lala A, Sanz J, Garcia MJ, Fuster V, Pinney S. Exercise performance in patients with pulmonary hypertension linked to cardiac magnetic resonance measures. J Heart Lung Transplant. 2009 Sep;28(9):899-905.

435. Paciocco G, Martinez FJ, Bossone E, Pielsticker E, Gillespie B, Rubenfire M. Oxygen desaturation on the six-minute walk test and mortality in untreated primary pulmonary hypertension. Eur Respir J. 2001 Apr;17(4):647-52.

436. Macchia A, Marchioli R, Marfisi R, Scarano M, Levantesi G, Tavazzi L, et al. A meta-analysis of trials of pulmonary hypertension: a clinical condition looking for drugs and research methodology. Am Heart J. 2007 Jun;153(6):1037-47.

437. Ghio S, Klersy C, Magrini G, D'Armini AM, Scelsi L, Raineri C, et al. Prognostic relevance of the echocardiographic assessment of right ventricular function in patients with idiopathic pulmonary arterial hypertension. Int J Cardiol. 2010 Apr 30;140(3):272-8.

438. Jurcut R, Giusca S, La Gerche A, Vasile S, Ginghina C, Voigt JU. The echocardiographic assessment of the right ventricle: what to do in 2010? Eur J Echocardiogr. 2010 Mar;11(2):81-96.

439. Voelkel NF, Quaife RA, Leinwand LA, Barst RJ, McGoon MD, Meldrum DR, et al. Right ventricular function and failure: report of a National Heart, Lung, and Blood Institute working group on cellular and molecular mechanisms of right heart failure. Circulation. 2006 Oct 24;114(17):1883-91.

440. Galie N, Barbera JA, Frost AE, Ghofrani HA, Hoeper MM, McLaughlin VV, et al. Initial Use of Ambrisentan plus Tadalafil in Pulmonary Arterial Hypertension. N Engl J Med. 2015 Aug 27;373(9):834-44.